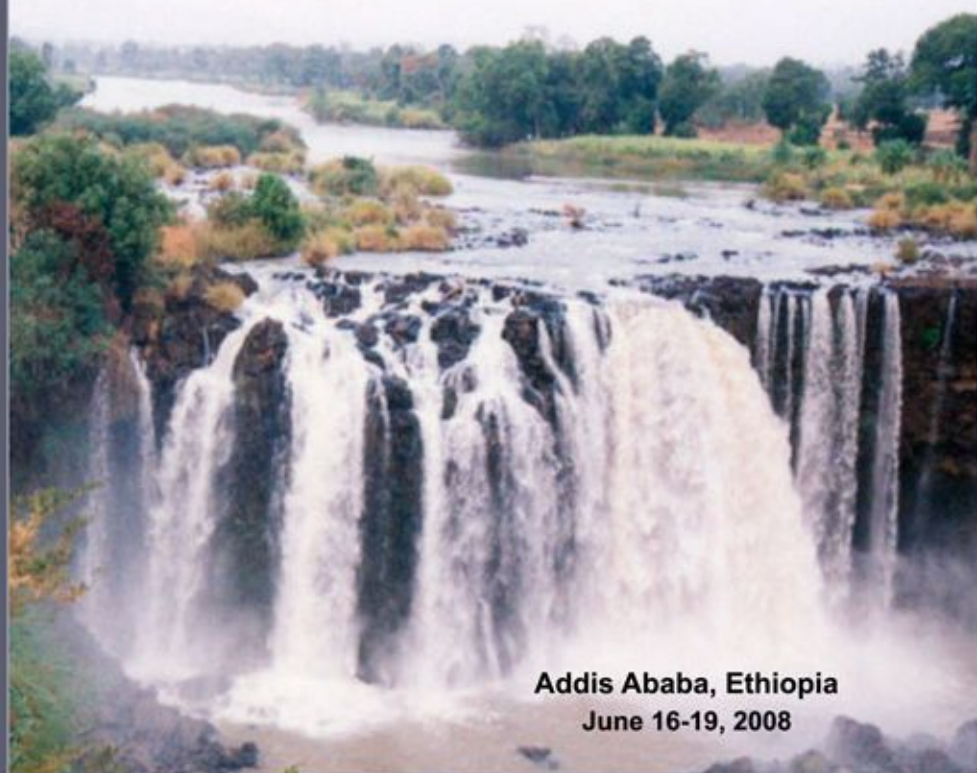Proceedings of the Workshop on

Hydrology and Ecology
of the Nile River Basin
under Extreme Conditions

Edited by:

Wossenu Abtew and Assefa M. Melesse

Addis Ababa, Ethiopia
June 16-19, 2008

Proceedings of the Workshop on
Hydrology and Ecology of the Nile River Basin under Extreme Conditions

This workshop is funded by the
Office of International Science and Engineering
National Science Foundation
USA

Editors: Wossenu Abtew & Assefa M. Melesse

For more information please contact

Assefa M. Melesse, Ph. D., P.E., D.WRE
Assistant Professor
Department of Environmental Studies, ECS 339
Florida International University
11200 SW 8th Street
Miami, FL 33199, USA
Tel. (305) 348-6518
Fax (305) 348-6137
E-mail: melessea@fiu.edu

Workshop Scientific Steering Committee Members

Assefa Mekonnen Melesse, Ph. D., P.E., D.WRE

Dr. Assefa M. Melesse is an Assistant Professor of Water Resources Engineering at the Department of Environmental Studies, Florida International University. His research encompasses the application of spatial analysis and remote sensing data from various sensors and electromagnetic spectra for understanding of water and energy fluxes at watershed and regional scales. His research activities are spanning over five countries with the goal of understanding and modeling the land-water interactions and fluxes of water, sediment and contaminant to coastal waters, river restoration and response to land-use and climate changes and also soil moisture-river flow-climate change linkages.

Giday WoldeGabriel, Ph. D

Dr. Giday WoldeGabriel is a senior research geologist at the Earth Environmental Sciences Division of the Los Alamos National Laboratory in New Mexico, USA. Dr. WoldeGabriel was a Lecturer at Addis Ababa University before he moved to the United States to work on his advanced degree in geology, studying the Main Ethiopian Rift. He has conducted a variety of earth-science research at Los Alamos, including alternative energy sources such as geothermal and oil shale, sequestration of CO_2 in deep geologic formations to alleviate global warming, and geologic disposal of spent nuclear fuel from commercial reactors. Dr. WoldeGabriel is also actively involved in determining geological context and ancient climatic and environmental conditions of human origins in Ethiopia. He has authored and co-authored several technical papers, including more than 15 Nature and Science publications. Dr. WoldeGabriel has actively worked to raise the awareness of serious hydrological, environmental, ecological, and climatic issues in the Nile River Basin since 1998. He has given a number of public lectures at Los Alamos National Laboratory and at the USAID office for Africa in Washington D. C.

Gabriel Senay, Ph. D., P.E.

Dr. Gabriel Senay is a principal scientist with SAIC, contractor to the US Geological Survey (USGS) Earth Resources Observation and Science (EROS) Center and an adjunct professor at the Geographic Information Science Center of Excellence (GIScCE), South Dakota State University. He teaches remote sensing of water resources and conducts agro-hydrologic research on water use, crop performance monitoring and production assessment using satellite-derived data and hydrologic simulation models.

Gerald "Gary" Geernaert, Ph. D

Dr. Gerald "Gary" Geernaert is director of the Institute of Geophysics and Planetary Physics (IGPP), at Los Alamos National Laboratory (LANL). In this position, he is responsible for strategic investments in the astrophysical, space, geophysical, and climate sciences, that involve external collaborations. Between 1994 and 2002, Geernaert was Director of the Department of Atmospheric Environment, at the National Environmental Research Institute, located near Copenhagen, Denmark; in this capacity, he was responsible for the technical component of the air quality monitoring and forecasting network for Denmark and Greenland; promoting joint ventures together with industry; and managing research in the basic and applied sciences and engineering. He was the founder and subsequent president of the Danish Atmospheric Research Society that began in 1998. Prior to 1994, he was a program manager for marine meteorology and remote sensing, at the US Office of Naval Research, in Arlington, USA.

J. Phillip King, P.E., Ph.D., M.B.A.

Associate Professor and Associate Department Head
Department of Civil Engineering
New Mexico State University
Box 30001, MSC 3CE
Las Cruces, NM 88003-0001
Tel. 505-646-5377 (office), 505-646-6049 (fax)
E-mail: jpking@nmsu.edu (primary)

Preface

Impacts of the changing climate on fresh water resources coupled with the human-induced activities that accelerate undesirable hydrologic alterations have become a challenge to meeting the freshwater needs of growing global populations. The effort to meet the freshwater demands of the Nile basin countries for various purposes will benefit from the ecohydrology knowledgebase of regions and river basins as well as focused and goal-oriented scientific research. This regional workshop has the goal of developing and strengthening collaborations with key partners from the Nile Basin countries, identifying research and education thrust areas and forming working groups for a follow up formulation of research and educational plans. Outcomes of the workshop discussion will help launch an integrated national and basin scale collaborative research program that will provide the scientific and technological bases for transboundary policy development and management. Scientific papers addressing climate change, land-use dynamics and hydrology of the Nile River Basin are presented in four different general topics: Climate change, land-use dynamics and hydrology of the Nile River basin, Hydrological modeling and simulations of Nile hydrology, Hydrometrological Analysis and River basin management and Water use issues. Special thanks go to the authors who provided high quality papers and abstracts. We believe such a workshop creates a forum for discussion and collaboration between regional and international scientists on the key research questions of the basin. Understanding the ecohydrological issues of the basin is the key for a sustainable environment and advanced water resource management to meet the ever increasing challenges.

Editors:
Wossenu Abtew, Ph.D., P.E., D.WRE
Principal Engineer, South Florida Water Management District

Assefa M. Melesse, Ph.D., P.E., D.WRE
Assistant Professor, Department of Environmental Studies
Florida International University

Wossenu Abtew, Ph.D., P.E., D.WRE

Dr. Wossenu Abtew is a Principal Engineer at the South Florida Water Management District in Florida, USA. Dr. Abtew is a civil engineer, agricultural engineer and a hydrologist. He has worked on various aspects of regional water management systems and environmental restorations for the last 18 years. He has authored technical papers on variety of subjects including wind, evapotranspiration, constructed wetlands design and operation, synthetic data generation and application, droughts, hurricanes, hydrology and hydraulics, sampling methods, monitoring network design, hydro-meteorological monitoring and data quality control, water quality monitoring, best management practices, the South Florida Water Management System and etc.

Assefa Mekonnen Melesse, Ph. D., P.E., D.WRE

Dr. Assefa M. Melesse is an Assistant Professor of Water Resources Engineering at the Department of Environmental Studies, Florida International University. His research encompasses the application of spatial analysis and remote sensing data from various sensors and electromagnetic spectra for understanding of water and energy fluxes at watershed and regional scales. His research activities are spanning over five countries with the goal of understanding and modeling the land-water interactions and fluxes of water, sediment and contaminant to coastal waters, river restoration and response to land-use and climate changes and also soil moisture-river flow-climate change linkages.

*Contents*_

Plenary Session

Climate Change, Land-use Dynamics and Hydrology of the Nile River Basin

Hydrological Simulations and Modeling of Nile Hydrology

Hydrometrological Analysis

River Basin Management and Water Use Issues (Part I)

River Basin Management and Water Use Issues (Part II)

ECOHYDROLOGY AND CLIMATE CHANGE SCIENCE: A CHALLENGE AND OPPORTUNITY IN UNDERSTANDING THE NILE BASIN SYSTEM

[1]Assefa M. Melesse, [2]Wossenu Abtew and [3]Gabriel Senay

[1]Florida International University, USA.
[2]South Florida Water Management District
[3]USGS/EROS-SDSU

ABSTRACT

The Nile River system is regarded as one of the most important ecohydrological systems of the world. Although the freshwater carried by Nile accounts a very small fraction of the volume of water compared to Amazon (2%), Mississippi (15%) and Mekong (20%) Rivers, its diverse ecological richness, history, mosaiced landscape and land-cover makes it unique and a valuable resource to the basin countries. The basin is the home of over 160 million people in 10 countries providing basic livelihoods for the agriculture, fishing, tourism, recreation, power generation and domestic water supply. Despite the rich resources, the basin is also characterized by limited knowledge on the ecohydrology of the basin. Studies have shown that, the river system has shown a fluctuation of seasonal and annual flows and in some watersheds a decline in dry season flows across the basin. This is mainly driven by impacts of the erratic and unpredicted changes in climate variables, undesirable changes in land-use on hydrologically and hydraulically sensitive segments of the river system. Ecological stress on the natural resources such as vegetation, soil and water is significant from the ever increasing demand for tillable land by the increasing population and also from lack of watershed management. Given the trend in demand for resources (water, land and soil), extreme climatic events and climate change will make sustenance challenging. Some predict the worst is yet to come, unless we take active measures and adapt to the changes.

Taking active measures to understand the ecohydrological system of the Nile Basin and the impacts of natural climate variations and climate change land-water system of the Nile will require a sustained study. The land-use and climate changes are the major drivers that lead to the decline and variability of river flows. Although these changes alter the hydrology in many ways, they are also interrelated and influence one

anther in a fashion poorly understood. Partitioning the changes in water fluxes attributed to changes in land-use and climate shift is not yet fully explored.

The interactions of the hydrology, ecology and the dynamic climate are one important aspect of the bigger picture worth researching. Eco-hydro-climatology is an approach to understand the interaction of the three fields of science for better mapping of fluxes, response of vegetation to fluxes, impacts of climatic variables on the hydrology and vegetation patterning and vice versa. This approach will be unique in that it addresses the underlying problems surrounding the interaction and causation. This effort will require systematically gathered scientific data on the landscape cover, biotic resources and also well monitored hydrometrological data of the basin.

Despite its contribution to the Nile flow system, the Blue Nile River basin suffers from little or incomplete data covering the hydrologic and hydraulic aspects of the river and streams. Studies are either limited to large scale flow analysis or incomplete. Scattered information on hydrology of tributaries and other water bodies, which are equally important for flow sustenance, is also limited. The resilience of the systems to shocks of land use alterations, precipitation variability in timing and volume, changes in air temperature, sediment fluxes to Lake Tana are not understood. Programs that promote sustainable water and land use practices are not perceivable. Watershed management and water use policies that encourage community participation, promote environmental education, and empower regional offices to monitor, protect and manage water resources and support scientific studies are vital. On the science front, understanding of the upper portion of the basin is an effort long overdue.

Another challenge is the scale mismatch among the ecology, hydrology and climate science. The close interaction and relationship of the three fields in shaping the hydrological and ecological landscapes of the basin will necessitate exploring the possible interactions and correlation at different spatial and temporal scales. Understanding the water flux of the basin at a river basin scale will require upscaling field/ecological scale processes and downscaling climatic process which are at regional scale or higher. Aggregation and disaggregation of parameters on the other hand suffer from uncertainty and can also result in error propagation.

The opportunities in the eco-hydro-climatological approach are the ability of remote sensing tools in providing various information at different spatial and temporal scales. Although the role of current remote sensing techniques decrease as we go from regional to field or from climatological to ecological scales, various techniques of down and upscaling techniques have proven to provide reliable information. In the Nile basin this approach will suffer from the absence of field scale experiments and research undertakings that help understand the fundamental processes which govern the movement of water and nutrients in the atmosphere-soil-water interface.

SCIENTIFIC AND TECHNOLOGICAL INTERVENTIONS TO ALLEVIATE TRANSBOUNDARY WATER CONCERNS IN THE NILE RIVER BASIN

Giday WoldeGabriel
EES-9/MS D462
Earth Environmental Sciences Division
Los Alamos National laboratory

EXTENDED ABSTRACT

Protracted environmental and climatic stresses exacerbated by persistent cycles of severe droughts, flooding, excessive deforestation, erosion, unproductive agricultural practices, desertification, population growth, etc., have been greatly impacting the Nile River basin. However, potentially serious water supply concerns in transboundary drainage basins are not unique to the Nile River Basin. In fact, there are approximately 261 international drainage systems and a larger number of transboundary aquifers, covering about half of the global land surface that is home to 40% of the world population (Wolf, 1999). Nevertheless, the Nile River Basin transboundary water resources issues demand immediate attention given the persistent drought history of the region. The rain-fed Nile River waters mostly come from the Ethiopian Highlands with additional input from the Lakes Region of east-central equatorial Africa. The Nile River crosses several unique hydroclimatic zones that range from equatorial rainforests to hot and dry desert environments before it trickles into the Mediterranean Sea.

Ongoing efforts since the last decade have created conducive opportunities for dialogue and cooperation among the Nile River Basin riparian nations to collectively prepare policy guidelines for strategic action plan on the sustainability of the finite water resources and environmental conditions of the basin (Nile-COM, 1999). The Nile Basin Initiative (NBI) strategic action program covers general principles, rights and obligations, institutional structure, subsidiary institutions, and other provisions. Scientific and technological investigations outlined in the cooperative framework are crucial because without such interventions, the major factors that have drastically impacted the quality and quantity of the Nile River will not be properly addressed.

Lack of current and accurate integrated and transparent local and regional climatic, hydrological, hydrometeorological, and hydrological data and models in most of the basin countries has greatly contributed to the transboundary water resources concerns. However, systematic and timely scientific investigations could facilitate historical data processing and new data acquisition and integration for climatic, basin hydrology, rainfall, stream flow and flooding, reservoir operations, irrigation, erosion, sedimentation, etc., evaluations and modeling. Such information could be ultimately fed to decision support systems to develop multiple solutions to address ongoing concerns related to the Nile River water problems and the unpredictable climatic conditions. Most Nile Basin countries lack the resources and expertise to tackle the major factors that threaten the region on their own. There is a need for genuine material support and expert participations from the developed countries in order to apply scientific and technological advances for evaluating and reversing the ongoing hydrological, environmental, and ecological problems in the basin. For example, the following fundamental items could be addressed through such collaborative efforts.

1. Develop regional climatic models to determine major source of moisture flux for rains that feed the major tributaries of the Nile River.
2. Adopt new technologies (remote sensing and Geographic Information Systems) for water resources applications, climatic monitoring, and drainage management
3. Encourage and establish regional climatic and meteorological data collection, repository, processing, and sharing opportunities.
4. Establish modern short and long-term, basin-wide hydrometeorological forecasting capabilities.
5. Develop modeling capabilities for critical infrastructure, environmental/ecological conditions, and the social basis for instabilities as part of the Nile River Basin Initiative.

Such collaborative scientific engagements among scientists from the Nile basin countries and their peers from the developed countries could lead to long-term productive interactions to address pressing issues of the day such as those listed below.

1. Develop and test complex decision support systems that deal with the assessment of potential transboundary water conflicts and social unrests as climatic conditions fluctuate, water supplies tighten, food security threatened, and environmental and ecosystems degrade.
2. Transboundary freshwater disputes are critical global issues; the Nile River basin template could be applied to international watersheds and countless aquifers covering about half of the land surface of the globe that is inhabited by 40% of world population.
3. Because of its unique geographic location, the Nile River basin provides an important test bed for new science and technological applications in the areas of remote sensing, GIS applications, ground truthing, and complex and multidisciplinary regional modeling for drainage basins, climate, and ecology.

In conclusion, genuine and balanced long-term engagements of the U.S. and its allies with the Nile Basin riparian countries could greatly contribute to lasting and effective regional sociopolitical and economic stabilities and growth.

REFERENCES

Wolf, A. T., 1999, The transboundary fresh water dispute database project, Water International, vol. 24, No. 2, 160-163.

Nile River basin Cooperative Framework Panel of Experts, 1999 Draft of the Cooperative framework, Rev. 2, Entebbe, Uganda, 22 p.

SECURING WATER FOR THE ENVIRONMENT IN THE MARA RIVER OF LAKE VICTORIA CATCHMENT, KENYA AND TANZANIA

Michael McClain[1], Joseph Ayieko[2], Assefa Melesse[1], Praxedis Ndomba[3], Jay O'Keeffe[4], Leah Onyango[5], Rashid Tamatamah[3] and D. Victor Wasonga[6]

[1] Florida International University, Miami USA
[2] Egerton University, Egerton Kenya
[3] University of Dar es Salaam, Dar es Salaam Tanzania
[4] UNESCO-IHE, Deft Netherlands
[5] Maseno University, Kisumu Kenya
[6] National Museums of Kenya, Nairobi Kenya

EXTENDED ABSTRACT

The Mara River basin encompasses some of the world's most unique ecosystems and human communities, tightly linked by their dependence on water from the Mara River. From its headwaters in Kenya, the Mara River flows through a mosaic of forests, tea fields, and croplands before entering Maasai pastoral lands. In this semi-arid landscape, human demands for water – especially for livestock and agriculture – run high and surface flows of the Mara River system are essential to meeting demands.

Downstream of these burgeoning human communities lay two of the world's most important wildlife refuges, the Masai Mara National Reserve and the Serengeti National Park. Together these protected areas host nature's largest annual migration of land animals, when more than two million wildebeest, zebra, gazelle, and other animals migrate to the Mara River each dry season. The Mara River is the only perennial source of water for these animals. Both they and the river's aquatic organisms are dependent on the quantity and quality of its flows.

Water demands further downstream continue to be high where the river feeds into the Mosirori wetlands and Lake Victoria. The lake and its adjoining wetlands have long been recognized among the world's most bio-diverse freshwater systems. Hundreds of fish species inhabit the lake and wetlands at the mouth of the Mara River, and fisheries

provide a primary source of income for the thousands of people living along the wetlands and Lake Victoria coast.

Meeting human water needs while minimizing adverse effects on ecosystems and wildlife is a fundamental tenet of Integrated Water Resources Management (IWRM), and the specification of environmental flow allocations (EFAs) is a widely recognized mechanism to ensure minimal ecosystem water needs are met. Protection of EFAs is mandated in the Kenyan Water Act of 2002 and the Tanzanian National Water Policy of 2002, and more detailed rules and strategies for implementation have since been drafted in each country. Responsibility for determining and enforcing EFAs is assigned to the Kenyan and Tanzanian ministries of water.

With these political and institutional enabling conditions in place, the Global Water for Sustainability (GLOWS) Program, with financial assistance from USAID East Africa, is supporting the efforts of the Ministry of Water and Irrigation (Kenya) and the Ministry of Water (Tanzania) to implement the new rules and strategies for water resources management, including the specification of EFAs for the Mara River.

GLOWS is facilitating and coordinating a full-scale environmental flow assessment in the Mara River Basin in close collaboration with the local water offices. Presently there are more than 200 methodologies used worldwide for estimating environmental flow needs. The GLOWS Project has elected to apply the Building Block Methodology (BBM), which was developed in South Africa during the 1990s and has been widely utilized.

The BBM is carried out over a period of eight to twelve months by a team of experts representing the disciplines of hydraulic engineering, geomorphology, hydrology, aquatic ecology, riparian ecology, water quality, and social science. The assessment was launched with a five-day training course in May, 2006. Three sites were selected for detailed studies and filed visits were made during March and July of 2007. The experts reconvened in October of 2007 to discuss the findings of each specialist and to reach consensus among the experts on the required environmental flows. A coordinator oversaw the entire assessment and facilitated the individual actions of the experts. Representatives from the water offices and other local authorities are also participated in the effort.

The assessment is emphasized the environmental flow needs of the Masai Mara National Reserve and the Serengeti National Park during the dry season. This includes meeting the drinking water needs of the millions of migrating ungulates and other animals as well as providing for the critical aquatic habitat needs of hippos, crocodiles, fish, and for riparian vegetation. These efforts were made more urgent by the intense drought the Mara River basin experienced during late 2005 and early 2006, when the river fell to its lowest levels in many years. The impacts on humans, livestock, and wildlife were severe, and as a consequence local stakeholders and institutions are acutely aware of the importance of quantifying and protecting the highest priority flows for basic human needs and the environment.

It is not enough to make recommendations of flows for the environment. Environmental flow allocations must become binding and be enforced. GLOWS is continuing to support the water offices in both Kenya and Tanzania to implement the EFA recommendations.

WATER RESOURCES OF THE NILE BASIN - EXTREME EVENTS, CLIMATE CHANGE, AND REGIONAL SECURITY

G. L. Geernaert
Los Alamos National Laboratory

EXTENDED ABSTRACT

Many river basins world-wide are experiencing increasing pressures on water resources, due in most part to ambitious economic goals, population growth and climate change. To assist in measuring societal stress caused (in part) by water, indicators such as "carrying capacity" have been introduced; sustainability has been used in a generic sense; and diversification of the economic base has been pursued. When the carrying capacity is exceeded by some degree, one of the possible societal responses is to migrate; and in some cases migrations are less than welcome. The Nile Basin is a classic example of a Basin undergoing increasing societal stress, due to increased pressure on water supplies.

The Nile River basin drains about 3.3 million km^2 of terrain that includes 81,500 km^2 lakes and 70,000 km^2 swamps in the 10 riparian nations of Burundi, DR Congo, Egypt, Eritrea, Ethiopia, Kenya, Rwanda, Sudan, Tanzania, and Uganda. The mean annual rainfall is estimated at 2,000 billion m^3, resulting in an annual flow of about 84 billion m^3 at Aswan Dam in southern Egypt. Very little Nile River water ever reaches the Mediterranean Sea; and there is tremendous interannual variability in rainfall amounts. In each of the riparian states, there are ambitious economic growth targets, populations are rapidly growing, and agricultural production is accelerating to feed the increasing populations. The Nile Basin, like many other river basins, is being strained economically and politically, due to increasing pressure on resources that do not adequately support the growing population.

A unique and complicated feature of the Nile Basin is that water is managed by decades-old treaties, and each of the dominant countries has uniquely different economic and political goals. For example, Egypt's livelihood relies upon water flowing down the Nile; Sudan relies on Nile River water both for its agricultural and energy production needs; and Ethiopia has a rapidly growing population in need of

agricultural production and economic growth. The NBI has explored basin-wide initiatives to create common goals and agendas, so that each of the nations can coordinate and manage water, particularly during lean precipitation years.

A unique feature of the Nile Basin during recent decades is the prevalence of extended droughts, interrupted by occasional floods. Management of water during extreme events has become challenging, insofar that today's reserves often don't support even the average year. However, little is known of the overall water budget of the Basin, thus the reason for this workshop. Our goal is to build a better understanding of Nile Basin water budgets and sectoral needs: overall input of rain water to the basin, subsurface water and recharge rates within the basin, utilization by society (agriculture, urban, energy, etc), new technologies to consider to advance efficiency, and emerging challenges.

There are a number of scientific challenges to pursue:
- identify the water budget components of the Nile Basin for both average precipitation years and during extreme drought years, where one combines rainfall potential, surface water reserves, aquifer reserves and recharge rates, etc.;
- Determine where the water losses are in the urban and rural collection, storage, and delivery systems, in order to assess which technologies are needed to improve efficiencies;
- Identify the agricultural needs for water and how water is managed during extreme events (droughts and flood); and
- Document the more confident predictions of climate change and how such changes will alter future precipitation and evapotranspiration patterns of the Nile Basin, including the looming issue of how climate change will affect the frequency of occurrence and severity of droughts and flood.

Each of these challenges requires that one taps into a world-wide brain trust, since the challenges are beyond the capacity of any one university, agency, nation, or continent. All river basins share these challenges, where lessons learned from one river basin experience can be considered when addressing another river basin.

SIGNIFICANCE OF PAST CLIMATIC RECORDS IN TERRESTRIAL SEDIMENTS FOR ASSESSING CURRENT AND FUTURE CONDITIONS

Giday WoldeGabriel
Earth Environmental Sciences Division
Los Alamos National Laboratory
Los Alamos, NM 87545 USA

EXTENDED ABSTRACT

Since the 1970s, the Nile River Basin has been subjected to multiple catastrophic drought and flooding conditions that greatly impacted millions of people and the environment. With increased population and degraded ecological conditions, there is a greater need today to learn more about paleoclimatic records in order to evaluate current and future climatic changes and to mitigate their potential impacts on Nile Basin communities and the environment they live in. Pleistocene sediments deposited in rift valleys, lakes, and other depositional settings within the Nile River drainage system preserve robust paleoclimatic and paleohydrologic records. In addition to past climatic and hydrologic archives, these sedimentary deposits provide information about variations in sediment supply, types of sediments, sedimentation rates, and the tectonic history of the depositional environments. In the Nile drainage basin, natural forces related to climatic changes and tectonic uplift mostly control sediment supply. However, anthropogenic effects (e.g., deforestation and primitive farming practices) in the last several centuries have also greatly contributed to the amount of sediment load in rivers mostly from the upper riparian highlands.

Given the widespread occurrences of long-lived, rift- and plateau-bound lakes and other depositional environments (e.g., swaps and wetlands and volcanic depressions) throughout the Nile River drainage system, it is imperative to investigate and temporally constrain the nature and impacts of past climate and climate-induced hydrological changes and the recent dramatic anthropogenic effects in the basin. The latest international drilling project in Lake Malawi is a testimony to the importance of terrestrial lake sediments in the study of continuous records of past climate change in the southern tropics of East Africa (Johnson et al., 2005). However, low-cost small-scale shallow drilling of

lake sediments could also provide equally important data relevant for investigating and documenting past local and regional climatic and environmental conditions. For example, excellent core recoveries from recent exploratory shallow (80 m) drilling within the dry floor of the 1.2 Ma Valles caldera in the southwestern United States penetrated volcaniclastic mud, silts, silty clays, gravel, and thin layers of interbedded basal late Pleistocene (0.55 Ma) primary and reworked ash layers (Fawcett et al., 2007; WoldeGabriel et al., 2007). Five glacial and interglacial cycles of late Pleistocene age (0.40-0.52 Ma) that are consistent with climatic records reported from Lake Baikal, Antarctica, and marine sediments were identified (Fawcett et al., 2007). Work is in progress to determine the sedimentological, volcanic, and climatic records in the shallow core samples.

Paleoclimatic and paleohydrological investigations of a shallow core (10.6 m) from Lake Albert, a rift-bound lake in northwestern Uganda indicate at least three periods of reduced inflow to the Nile in the late Pleistocene (30,000 years) because of drier conditions (Beuning et al., 1997). Sediments from two shallow lakes in Ethiopia outside but close to the Nile River drainage divide also provide information about Holocene climatic conditions in eastern Africa. An investigation of a shallow (~16 m) core from a lake located above 3000 m in the southeastern highlands (Bale Mountains) of Ethiopia revealed the presence of a retreating high-altitude glacier at about 17,000 years ago with ice melting ending between 12,600 and 11,800 years (Tiercelin et al., 2007, in press). A similar study of a shallow core (12.6 m) from a rift-bound saline-alkaline lake indicated a glacial-interglacial transition at about 12,700-12,000 calibrated years before present (Chalié and Gasse, 2002). This observation is temporally consistent with glacier melting and retreating reported from lake sediments in the nearby Bale Mountains located to the east of the rift floor (Tiercelin et al., 2007, in press). The lake sediments from the rift-bound Lake Abiyata also indicate early to middle Holocene wet episode (12,000-5,400 calibrated years before present) in the region (Chalié and Gasse, 2002).

Despite different elevations and geographic locations, results from the three shallow cores of lake sediments from eastern Africa provide consistent local and regional climatic records. Similar studies of shallow sedimentary cores from Lake Tana in Ethiopia, the Lake region of eastern central Africa, the Sudd in southern Sudan, the Nile Delta, and other depocenters in between could provide more detailed and more

complete basin-wide paleoclimatic and paleohydrological data for the Nile River. Such basin-wide effort could engender broader cooperation among concerned scientists of the Nile River Basin and their colleagues from the developed world.

REFERENCES

Beuning, K. R. M., Talbot, M. R., Kelts, K., A revised 30,000-year paleoclimatic and paleohydrologic history of Lake Albert, East Africa, Palaeogeography, Palaeoclimatology, Palaeoecology, v. 136, 3-4, p. 259-279, 1997.

Chalié, F., and Gasse, F., Late glacial-Holocene diatom record of water chemistry and lake level change from the tropical East African Lake Abiyata (Ethiopia), Palaeogeography, Palaeoclimatology, Palaeoecology, v. 187, 3-4, p. 259-283, 2002.

Fawcett, P., Heikoop, J., Goff, F., Anderson, S. R., Donohoo-Hurley, L., Geissman, J. W., WoldeGabriel, G., Allen, C. D., Johnson, C. M., Smith, S. J, and Fessenden-Rahn, J, Two middle Pleistocene glacial-interglacial cycles from the Valles caldera, Jemez Mountains, northern New Mexico, New Mexico Geological Society, 58th Conference Guidebook, p. 409-417, 2007.

Johnson, T. C., Scholz, C. A., King, J., and Cohen, A., Preliminary results of the Lake Malawi drilling program, Abstracts with Programs - Geological Society of America, vol. 37, no. 7, pp.544, Oct 2005.

Tiercelin, J.-J., Gibert, E., Umer, M., Bonnefille, R., Disnar, J.-R., Lézine, A.-M., Hureau-Mazaudier, D., Travi, Y., Keravis, D., and Lamb, H. F., High- resolution sedimentary record of the last deglaciation from a high-altitude lake in Ethiopia, Quaternary Science reviews, 2007 (in press)

WoldeGabriel, G., Heikoop, J., Goff, F., Counce, D., Fawcett, P., and Fessenden-Rahn, J., Appraisal of post-South Mountain volcanism lacustrine sedimentation in the valles caldera using tephra studies, New Mexico Geological Society, 58th Conference Guidebook, p. 83-85, 2007.

ANALYSIS OF HYDROLOGY AND WATER RESOURCES OF THE UPPER BLUE NILE RIVER BASIN UNDER CLIMATE CHANGE

Ungtae Kim[1] and Jagath Kaluarachchi[2]

[1] Research Associate, Utah State University, Logan, Utah, USA;
utkim@cc.usu.edu
[2] Associate Dean, Utah State University, Logan, Utah, USA;
jkalu@engineering.usu.edu

ABSTRACT

This study aims to evaluate the climate change impacts on both hydrologic regimes and water resources of the upper Blue Nile River Basin in Ethiopia where hydrologic data are limited. The downstream countries of the Nile River Basin are sensitive to the variability of runoff from the part of Nile Basin located in Ethiopia. Climate change affects water availability and the conditions will be worsened with increasing water demands. To analyze and evaluate the future changes in hydrology and water resources of the study area, data-parsimonious, yet reliable, methodologies and models are required. This study presents three steps for analyzing climate change impacts. The first is the construction of climate change scenarios using the conditional generation method and the outcomes of multiple general circulation models. The second is the simulation of runoff using the proposed hydrologic model under different climate scenarios. Parameter regionalization for ungauged basins is an important task given the limited data. Finally, the results from previous analyses are integrated to evaluate climate change impacts on hydrology and water resources through a set of indices. The impacts of dam operations for hydropower generation under climate change scenarios on downstream countries are also assessed. The major findings of this study suggested that (1) climate would be wetter and warmer in the 2050s; (2) flow regimes would be enhanced, especially for low flows; and (3) the proposed dam operations would not affect the water availability to downstream countries.

INTRODUCTION

Water is the most important natural resource required for the survival of all living species. Since the available amount of water is limited, scarce, and not spatially distributed in relation to the population needs, proper management of water resources is essential to satisfy the current demands as well as to maintain sustainability. Water resources planning and management in the 21st century is becoming difficult due to the conflicting demands from various stakeholder groups, increasing population, rapid urbanization, climate change producing shifts in hydrologic cycles, the use of high-yielding but toxic chemicals in various land use activities, and the increasing incidences of natural disasters. Among these difficulties, climate change impacts due to recent global warming increasing greenhouse gases on water resources are emerging concerns to decision-makers. The alteration of climate in a region drives the changes in hydrologic regimes (typically, rainfall-runoff relationship) and thus produces the unexpected fluctuation and timing of streamflow.

In most international river basins, upstream runoff variability has been an acute issue to water-reliant downstream countries. A typical example is the Nile River Basin which consists of White Nile and Blue Nile. It has been found that most regions within the Nile Basin are sensitive to climatic variations (Conway and Hulme, 1996; Yates and Strzepek, 1998a, b; Conway, 2005). The Blue Nile River Basin annually contributes about 60% of the flows to the Nile River with its 10% areal occupancy (Waterbury, 1979; Yates and Strzepek, 1998b; Sutcliffe and Parks, 1999; UNESCO, 2004; Conway, 2005). Thus, runoff variability from upstream countries is of great importance to the sustainable development of downstream countries such as Sudan and Egypt which use most of the Nile waters in accordance with the 1959 Agreement (Yates and Strzepek,1998a; Tafesse, 2001; Conway, 2005). Considering the increasing water demand of upstream countries in the Nile Basin, the impacts of climate change can worsen the availability of water resources in the basin.

Many studies have been performed to analyze the impacts of climate change on water resources of the Nile Basin (e.g., Gleick, 1991; Conway and Hulme, 1993, 1996; Strzepek and Yates, 1996; Yates and Strzepek, 1996, 1998a, b; Sene et al., 2001; Conway, 2005). However, most previous studies have focused mainly on the changes in mean annual runoff volume and their consequent effects on the economy of

downstream countries. However, climate change can affect various aspects of water resources, e.g., quantity and quality, extreme events (both low- and high-flow), timing, temperature, groundwater recharge, etc. Therefore, future decision criteria for water allocation, structure design, and water resources operations should be revised with the changes in climate-driven variables.

The upper Blue Nile River Basin considered here typically experiences severe famine due to recurrent drought and the lack of advanced water infrastructure. The end result is the vulnerability to the variability of precipitation, soil moisture, and stream flows (Degefu, 1987). In addition, impacts of climate change and potential dam operations on those water resources are emerging issues in the entire Nile River Basin system.

Since 1999, a multilateral effort called the Nile Basin Initiative has been underway to promote cooperation for maximizing the benefits of Nile waters through the cooperative development and management of the Nile River Basin system (Whittington et al., 2005). Ethiopia can be endowed with economic benefits because of the tremendous potential for hydropower generation and irrigation owing to its geographical advantages. Although several studies identifying the feasibility of hydropower projects were conducted (e.g., USBR, 1964; WAPCOS, 1990; MOWR, 1998; Block, 2007), there is a great discrepancy in the number of the selected hydropower sites and available power potential. Moreover, there are no detailed studies providing information on these proposed dam projects and the possible effects of operation of these dams on water resources under climate change.

There is a growing need for an integrated analysis that can quantify the impacts of climate change on various aspects of water resources such as precipitation, hydrologic regimes, drought, dam operations, etc. Therefore, the overall goal of this study is to assess the future variability of hydrologic regimes and water resources of the upper Blue Nile River Basin under both climate change and water resources operations, and to assess the potential impacts on the study area and its downstream countries.

STUDY AREA AND DATA

Physical Description

The upper Blue Nile River Basin is located in the Ethiopian Highlands and has a drainage area of about 176,000 km^2 measured at El Deim (Figure 1). The Blue Nile River runs from its origin, Lake Tana, to the Sudanese border and eventually meets the White Nile River at Khartoum, Sudan.

The climate of the study area varies from humid to semiarid. Most precipitation occurs in the wet season called Kiremt (June through September), and the remaining precipitation occurs in the dry season called Bega (October through January or February) and in the mild season called Belg (February or March through May). The annual precipitation has an increasing trend from northeast to southwest. The estimated annual precipitation ranges from 1200 mm to 1600 mm depending on the method and the period used in previous studies (e.g., Gamachu, 1977; Conway, 1997, 2000; Tafesse, 2001; UNESCO, 2004; Kim et al., 2007). The mean annual temperature from 1961 to 1990 was estimated at about 18.3 °C with a seasonal variation of less than 2 °C and the annual potential evapotranspiration was estimated at about 1100 mm (Kim et al., 2007).

Due to the summer Monsoon, more than 80% of annual flow is concentrated in July through October and is directly drained to downstream countries due to the absence of storage capacity. Small tributaries in the mountainous region experience large fluctuations of streamflow due to the seasonal variation of precipitation (UNESCO, 2004). Monthly discharge data at Roseires/El Deim between 1921 and 1990 (National Center for Atmospheric Research (NCAR), http://dss.ucar.edu/datasets/, March, 2006) produce a mean annual discharge of 49 km^3 and the annual discharge ranges from a minimum 31 km^3 (1972 and 1984) to a maximum 70 km^3 (1929). Based on the same data set, the 30-year mean annual discharge ranges from 38 km^3 (1978 to 1987) to 56 km^3 (1955 to 1964). Previous Nile studies estimated the mean annual discharge as 46 km^3 to 54 km^3.
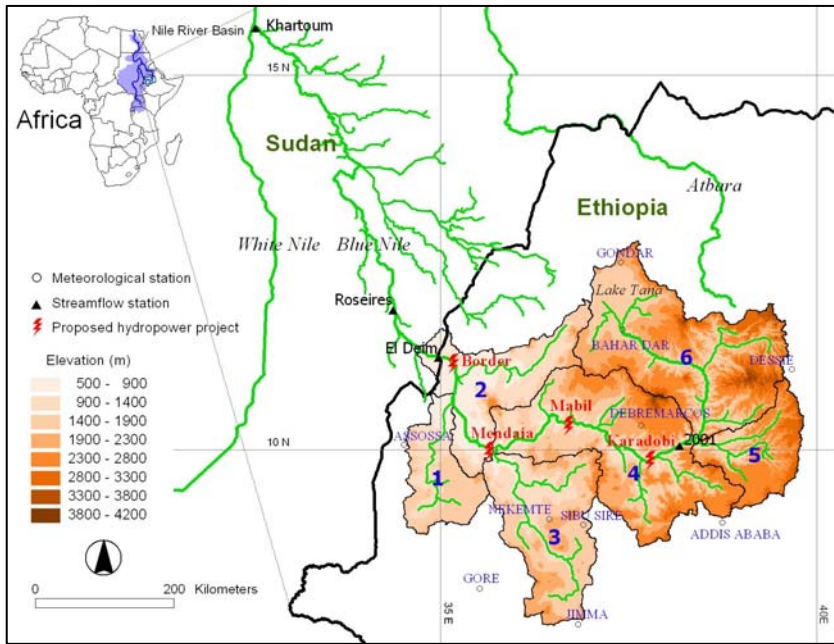
Figure 1. Physical layout of the upper Blue Nile River Basin. Six subbasins are presented in bold numbers. Digital maps were collected from the U.S. Geological Survey's EROS Data Center available at http://edc.usgs.gov/products/elevation/gtopo30/hydro/africa.html (March, 2006) and the MOWR (personal communication, April, 2006).

Data

There are few reliable meteorological or hydrologic stations located in the basin due to inaccessibility, remoteness, and economic limitations. Most hydrologic observations started in the early 1960s by the National Meteorological Service Agency (NMSA) and the MOWR of Ethiopia (Conway, 2000). Monthly data of precipitation, temperature, and discharge have relatively longer observed periods than hourly or daily data.

Monthly precipitation data of 10 selected stations (Figure 1) were collected from the Global Historical Climatology Network (GHCN, ftp://ftp.ncdc.noaa.gov/pub/data/ghcn/v2/, March, 2006). These 10 stations have been used in most previous Blue Nile studies as well, e.g.,

Johnson and Curtis (1994), Conway (1997, 2000), Kim et al. (2007), and Kim and Kaluarachchi (2007a, b). Monthly temperature data for the same period at eight of the 10 stations (Figure 1, excluding Bahar Dar and Sibu Sire) were also collected from the GHCN. Kim et al. (2007) and Kim and Kaluarachchi (2007a) filled the missing data using statistical methods. These climatic variables were spatially averaged by the Thiessen method. Monthly discharge data for Station 2001(with a drainage area of about 66,000 km^2) and El Deim were collected from the MOWR (personal communication, April, 2006) and the NCAR, respectively. Monthly discharge data of small basins located in six subbasins were also collected from the MOWR (personal communication, April, 2006) for parameter regionalization.

CLIMATE CHANGE SCENARIOS

Baseline Climate Scenario

The baseline climate scenario represents current climate conditions, typically precipitation and temperature patterns. As in most climate change studies, this study used monthly precipitation and temperature from 1961 to 1990 to represent the current climatic conditions of the study area.

For the baseline climate scenario, 100-year monthly precipitation and temperature data for the 10 stations (8 for temperature) have been successfully generated using the conditional generation method (CGM) (Kim et al., 2007; Kim and Kaluarachchi, 2007b). The CGM, which reproduces the similar spatio-temporal correlation structure to the observed, is driven from data without parameterizing or smoothing. More details of the computational scheme of the CGM are available from the original study. The baseline potential evapotranspiration scenario was then computed by the Thornthwaite method (Palmer and Havens, 1958) using the baseline temperature scenario.

Climate Change Scenarios for the 2050s

High uncertainty is expected in climate change impacts studies when selecting the outcomes of a single general circulation model (GCM) (IPCC, 1999). This study used six GCMs for the 2050s under the A2 emission scenario (IPCC Data Distribution Center, http://ipcc-ddc.cru.uea.ac.uk/, April, 2006) and their outcomes were spatially

downscaled to each meteorological station and weighted based on their accuracy to simulate the current climate patterns (1961 to 1990) of the study area (Table 1). This weighted scenario can therefore suggest a plausible change among these six GCMs. Future climate variables were constructed by perturbing the baseline scenario. This perturbation method that assumes the current temporal and spatial correlation structures of precipitation and temperature will be preserved over time and has been widely used in previous climate change studies (e.g., Conway and Hulme, 1996; Yates and Strzepek, 1998b; Xu, 2000; Fowler et al., 2003; Kim et al., 2004; Drogue et al., 2004; Wurbs et al., 2005). This study has seven future climate change scenarios, six GCMs and one weighted scenario.

Table 1. Description of the six GCMs used in this study.

GCM[a]	County	Resolution[b]	Sensitivity	Grids	Weight[c] (%) P	T
CCSR/NIES	Japan	5.625, 5.533	3.5	4	19	2
CGCM2	Canada	3.750, 3.709	3.5	9	7	20
CSIRO	Australia	3.625, 3.184	4.3	6	25	4
ECHAM4	Germany	2.813, 2.789	2.6	9	10	18
GFDL-R30	U.S.A.	3.750, 2.235	4.0	9	6	4
HADCM3	U.K.	3.750, 2.500	2.5	9	33	52

[a] From the IPCC DDC. Each GCM represents Center for Climate System Research and National Institute for Environmental Studies, Canadian Global Coupled Model 2, Commonwealth Scientific and Industrial Research Organization, European Centre Hamburg Model 4, Geophysical Fluid Dynamics Laboratory's Rhomboidal 30 truncation, and Hadley centre Climate Model 3, respectively.
[b] Average resolution of each GCM (Longitude, Latitude).
[c] Weights for precipitation (P) and temperature (T) computed by Kim et al. (2007) and Kim and Kaluarachchi (2007b), respectively.

RUNOFF GENERATION

Hydrologic Model

This study used a two-layer water balance model. This model has been successfully applied to simulate the monthly runoff dynamics of the study area by Kim and Kaluarachchi (2007a, 2007b). As shown in Figure 2, the proposed model translates monthly precipitation into monthly runoff of a basin by accounting soil moisture with evapotranspiration at each monthly time step. The six subbasins of the study area (Figure 1) are not gauged and therefore traditional model calibration is not applicable. It was determined that the volume fraction calibration approach proposed by Kim and Kaluarachchi (2007a) is suitable for simulating the monthly runoff hydrographs of these six ungauged subbasins. More details of the hydrologic model and parameter regionalization are available from the original studies.
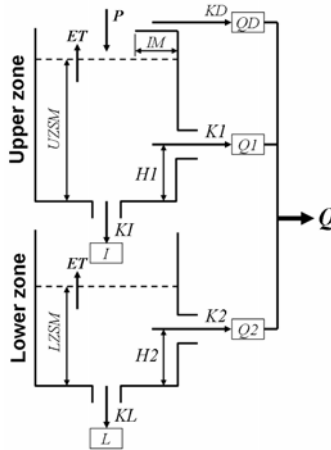
Figure 2. A schematic of the two-layer water balance model used in this study. The parameters KD, K1, K2, KI, and KL are the coefficients for direct runoff (QD), surface runoff (Q1), base runoff (Q2), infiltration (I), and percolation (L), respectively.

The parameters, H1 and H2, are the heights of runoff orifices in the upper and lower zone, respectively. The parameter IM is the fraction of impervious area. UZSM and LZSM represent upper and lower zone soil moisture, respectively. The parameters IM and KD were not used in this study.

This study assumed the model parameters calibrated and validated under current climate conditions do not vary with time because it is not practically feasible to calibrate the model parameters to various future climate conditions. The changes in land use were not also considered for the same reason. Due to these difficulties, previous similar studies also fixed their model parameters with time (e.g., Conway and Hulme, 1996; Yates and Strzepek, 1996, 1998b, Kim et al., 2004). The water balance model was run for each climate scenario (the baseline scenario, six GCMs scenarios, and the weighted scenario) using the model parameters calibrated and regionalized for the six subbasins.

IMPACTS OF CLIMATE CHANGE

Hydrology

Table 2 shows that the changes in climatic variables and runoff for the 2050s are diverse depending on each GCM. The changes in mean annual precipitation are from -11% by CSIRO to 44% by CCSR with a plausible change of 11%. On the other hand, the changes in mean annual temperature range from 1.4 °C by CCSR to 2.6 °C by HADCM with a plausible change of 2.3 °C. Potential evapotranspiration shows an increasing trend for all GCMs due to increased temperature and the changes are from 9% by CCSR to 19% by HADCM with a plausible change of 16%. The changes in mean annual runoff are from -32% by CSIRO to 80% by CCSR with a plausible change of 4%. As observed in Yates and Strzepek (1998a, b), the changes in runoff of the basin are controlled not only by precipitation but also by temperature and potential evapotranspiration. For example, the percent changes in runoff using the outcomes of GFDL and HADCM show decreases even for increased precipitation due to increased temperature (thus increased PET).

When compared to the results of previous studies for the same area, the plausible changes simulated in this study can be classified as mild increases. The relationship between the changes of runoff and the changes of precipitation and temperature was developed by regression using the simulation results of the six subbasins, and is given as:

Table 2. Changes in climatic variables and runoff for the 2050s.

GCM	ΔP (%)	ΔT (°C)	ΔPET (%)	ΔQ (%)
Weight	**11**	**2.3**	**16**	**4**
CCSR	44	1.4	9	80
CGCM	-3	1.7	11	-14
CSIRO	-11	2.1	14	-32
ECHAM	33	2.4	17	64
GFDL	1	1.7	11	-13
HADCM	6	2.6	19	-11

$$\Delta Q = 2.2 \times \Delta P - 7.5 \times \Delta T \qquad\qquad (1)$$

where ΔQ is the percent change in mean annual runoff; ΔP is the percent change in mean annual precipitation; ΔT is the °C change in mean annual temperature; and the coefficient of determination of this equation is 0.97.

This relationship is useful to predict the mean changes in runoff of the study area due to climate change. For validation purposes, Eq. (1) was applied to previous studies. Although not presented here, ΔQ (%) predicted by Eq. (1) show a good agreement with those by previous studies (a correlation coefficient of about 0.99). However, Eq. (1) may produce non feasible results, when applying to small catchments located within subbasins, because this relationship was driven from the hydrologic responses at subbasin scales. Different hydrologic responses at different basin scales have been discussed by Kim and Kaluarachchi (2007a) for the study area.

Compared to the southwest of the study area, although not shown here, the northeast showed a more increasing trend in precipitation and a less increasing trend in temperature thus less potential evapotranspiration. These trends resulted in a noticeable increase of runoff in the northeast compared to the southeast (Figure 3b). The northeast includes the Amahara region, one of the most populated and agricultural regions of Ethiopia. It is also noted that subbasin 1 in which the Dabus swamps are located showed a large decrease in runoff due to increased temperature and potential evapotranspiration in this region.

Flow regimes in a basin can be quantified using flow statistics from the flow duration curve. Flow statistics that represent high, median, and low flows were extracted from the flow duration curves of the six subbasins and the basin outlet. These flow statistics are termed Q_{10}, Q_{50}, and Q_{90} and define the flow exceedance at 10, 50, and 90% of the time, respectively. The mean flow, Q_m, was also computed because the hydropower generation capacity is a function of the mean flow at a given hydraulic head. In addition, the periods (the number of months) above Q_{10} and below Q_{50}, Q_{90}, and Q_m, which are termed D_{10}, D_{50}, D_{90}, and D_m, respectively, were computed to investigate how frequently these flows occur. The changes in flow regimes of outflows from the proposed dams (Karadobi and Border) were also evaluated using the potential dam operation policies that will be described next.

As observed in Figure 3, while Q_{10} and Q_{50} show a similar range of percent changes (-15% to 20%), Q_{90} shows a wider range (-25% to 60%). This result can be explained by runoff in low-flow seasons (March to April), which is usually more sensitive to the changes in potential evapotranspiration than high-flow seasons. Also because a low flow value is sensitive to the denominator when computing a relative percent change compared to a high flow value. In addition, Kim and Kaluarachchi (2007b) found that the larger percent changes of precipitation for the 2050s in Bega than those of other seasons strongly dominate the percent changes of low-flows.
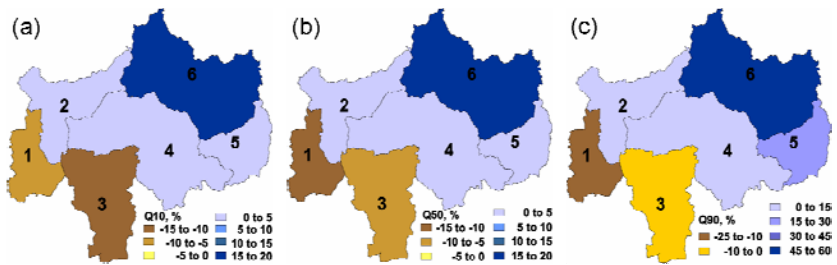
Figure 3. Spatial distribution of the percent changes in flow statistics under scenario for the 2050s.

Drought

Precipitation is the most important source of water for agriculture in the study. Therefore, precipitation variability, droughts, and their consequences greatly affect food security of the study area. The probability of precipitation for any time scale will be useful to understand the potential drought scenarios of the study area. Among many drought indices, the SPI (McKee et al., 1993) has been widely used in drought monitoring. Guttman (1998) and Hayes et al. (1999) found that the SPI has advantages of statistical consistency and the ability to describe both short- and long-term drought impacts through different time scales of precipitation anomalies.

In this study, SPI values for 1-, 3-, 6-, 9-, and 12-month time scales were computed for the period of 1961 to 1990 and SPI6 was found to be more informative to investigate the prolonged characteristics of drought in the study area. The percent changes in SPI6 values less than -1.5 (severe drought, McKee et al. (1993)) were computed for future precipitation scenarios, relative to those from the baseline precipitation scenario. As a result, the percent changes in severe drought events show diversity depending on the GCM. Based on the weighted precipitation scenario, the percent changes of severe drought events showed about -90% for subbasins 5 and 6, about -70% subbasins 2 and 4, and about -40% for subbasins 1and 3. Although the SPI is a probabilistic representation of only precipitation, a decreased trend of severe drought is generally observed across the study area due to increased precipitation for the 2050s.

Water Resources Reliability

A quantitative measure of performance of water resources systems is useful in assessing the operational strategies of the proposed dam projects. Hashimoto et al. (1982) suggested the use of indices, reliability, resiliency, and vulnerability, for classifying and assessing the performance of water resources systems. Based on Hashimoto et al. (1982), Maier et al. (2001), and Fowler et al. (2003), these indices are generally defined that reliability is a measure of the frequency or probability that a system is in a satisfactory state meeting a given criterion; resiliency generally indicates a measure of how quickly a system recovers from failure once failure has occurred; and vulnerability can be (1) the maximum duration of system failure and (2) the

cumulative maximum magnitude of water shortage in system failure. The computational scheme for these indices is similar to that of Hashimoto et al. (1982) and Fowler et al. (2003), except using a monthly time step and a different criterion.

Defining a criterion (C) is the minimum required runoff from a water resources system (river or dam outflow), the monthly runoff (X_t) at time t can be classified as a satisfactory state (S) or a failure state (F) as

$$\text{If} \quad X_t \geq C \quad \text{then} \quad X_t \in S \quad \text{and} \quad Z_t = 1$$
$$\text{else} \quad X_t \in F \quad \text{and} \quad Z_t = 0 \tag{2}$$

where Z_t is a generic indicator variable. The mean monthly runoff distribution of the baseline runoff scenario was used as a criterion and thus system failure occurs when runoff or outflow is below the criterion at any given month. Another indicator, W_t, which represents a transition from F to S, is defined as

$$W_t = \begin{cases} 1, & \text{if} \quad X_t \in F \quad \text{and} \quad X_{t+1} \in S \\ 0, & \text{otherwise} \end{cases} \tag{3}$$

If the periods of X_t in F are defined as $U_1, U_2, \ldots, U_N$ where N is the number of F periods, then reliability, resilience, and vulnerability indices during the total time period (T) can be defined as

$$\text{Reliability} \quad = \frac{\sum_{t=1}^{T} Z_t}{T} \tag{4}$$

$$\text{Resiliency} \quad = \frac{\sum_{t=1}^{T} W_t}{T - \sum_{t=1}^{T} Z_t} \tag{5}$$

$$\text{Vulnerability}_{\text{Time}} = \max\{U_1, U_2, \ldots, U_N\} \tag{6}$$

$$\text{Vulnerability}_{\text{Volume}} = \max\left\{\sum_{t \in U_i} (C - X_t), \quad i = 1, 2, \ldots, N\right\} \tag{7}$$

These indices were previously used to evaluate reservoir operations; evaluate water distribution systems; manage water quality of a river; and assess climate change impacts on water resources systems. This study assessed the percent changes in these indices computed for future runoff scenarios associated with different dam operation policies, relative to those computed for the baseline runoff scenario. Therefore, these percent changes can suggest the impacts of both climate change and dam operation on the robustness of water supply.

The reliability and resiliency under the weighted runoff scenario for the 2050s suggest that there is an increasing trend toward the northeast (Figures 4a and 4b). The improved water supply capability in this region, therefore, results in the decreased frequency of system failure and the increase of system flexibility recovering from a failure state. Although the increased runoff generally improves water supply reliability, the vulnerability of streamflows can be dominated by the timing and duration of runoff. In the case of subbasin 5, the vulnerability in maximum failure time is not decreased in spite of its increased runoff. Increased vulnerability (Figures 4c and 4d) as well as decreased reliability and resiliency (Figures 4a and 4b) is expected in the southwest region, subbasins 1and 3, due to the reduced runoff (Figure 3b). Particularly, more than a 50% increase in maximum water shortage in a failure period (Figure 4d) can cause a severe water supply problem in those subbasins.
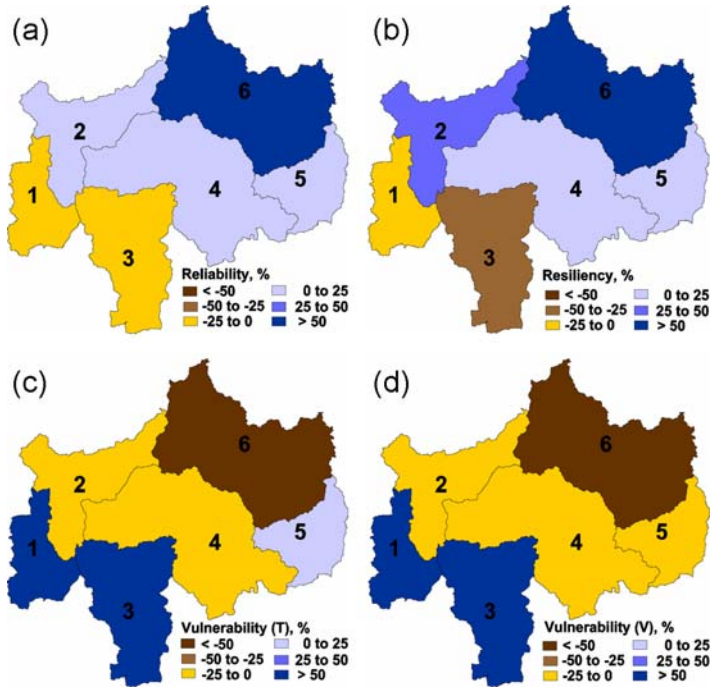
Figure 4. Spatial distribution of the percent changes in water resources assessment indices of streamflows under the weighted runoff scenario for the 2050s.

However, runoff from the entire basin (at Border) generally shows an improved capability of water supply to downstream countries. Although showing a range of changes dependent on a specific GCM, overall increased reliability and resiliency of flows are beneficial to both the study area and the downstream countries. These improved indices indicate that hydropower generation in the study area is more stable and the likelihood of water supply failure to downstream countries could be reduced.

Potential Dam Operations

Two dam sites (Karadobi and Border) were selected from the construction priority discussed by Block (2007). Based on the information of MOWR (1998) and Block (2007), the maximum capacity of each dam was assumed as 1.6 and 0.3 times of the mean annual runoff volume of the baseline runoff scenario at Station 2001and El Deim, respectively. The initial storage of each dam for the 2050s was assumed to be 70% of its maximum capacity. The capacity of each dam was assumed slightly less than that proposed by the MOWR (1998) because the discharge data used in this study are different from those of previous studies. This underestimated capacity can provide a conservative assumption for operation of the dams under future irrigation consumption and climate variability.

The operational performance of a water resources system greatly depends on the timing and quantity of streamflow at the site of interest. The constraint functions not only prescribe how the proposed dams may be filled and the optimal allotment to irrigation, but also allow for the assessment of potential impacts on downstream countries (Block, 2007). In this study, however, the allotment of streamflow to irrigation was not considered due to the lack of reliable information. This diversion for irrigation can be easily included in a future study assuming necessary information is available.

No dam operation policies for Karadobi and Border are denoted as K0 and B0, respectively. The first dam operation policy allows 5% of annual runoff volume at Border to be impounded within the basin (at one or both dams based on single or joint operation) using the historical mean monthly runoff distribution. This first policy is denoted as K1 and B1 for Karadobi and Border sites, respectively. The first policy is revised to maintain a 5% share of annual runoff within the basin while jointly

operating with other policies (i.e., re-allocate a sharing percent to the particular dam operated by the first policy). The second operation policy denoted as K2 and B2 for Karadobi and Border sites, respectively, allows only an excess of monthly runoff above a threshold (historical mean monthly flow of each month) to be impounded in each dam. The third policy denoted as K3 and B3 for the respective sites, allows supplemental releases, when the outflow at a month is below the threshold of that month while satisfying the second policy as well. The concepts of the first and second policies were originally proposed by Block (2007) on an annual basis. In this study, all policies were programmed on a monthly basis to reasonably account for the monthly variation of runoff in a year. In addition, this study proposes the third policy to effectively mitigate the intra-annual natural runoff fluctuations (i.e., below the historical mean monthly flow) which can frequently occur in the second policy without supplemental releases. For flood control and dam safety, the inflow exceeding the maximum capacity of each dam is released during simulations.

All operation polices proposed earlier can be combined for each dam. Therefore, combinations can be one case of no dam operation (K0+B0), six cases of single dam operation (K1+B0, K2+B0, K3+B0, K0+B1, K0+B2, and K0+B3), and nine cases of joint dam operation (K1+B1, K2+B1, K3+B1, K1+B2, K2+B2, K3+B2, K1+B3, K2+B3, and K3+B3). As discussed in Block (2007), none of these policies is presently acceptable under the 1959 Agreement between Ethiopia and Sudan or Egypt.

For the no dam condition based on the weighted runoff scenario for the 2050s given in Table 3, the low-flow statistic (Q_{90}) shows a large increase thus implying wetter dry seasons for the study area. On the other hand, the slightly increased high-flow statistic (Q_{10}) indicates that the flood risk to downstream countries may become higher than current climate conditions. The mean flow (Q_m) shows a 5% increase for the 2050s while the median (Q_{50}) was simulated to be rarely changed. A slight increase in hydropower generation could be possible with the increased mean flow. The low-flow period (D_{90}) is reduced by 27%, while the high-flow period (D_{10}) is increased by 22%. On the other hand, D_{50} and D_m are rarely changed. Although the slightly increased flood risk should be handled in a timely manner, the increased low-flow or the reduced low-flow period is encouraging to improve long-term food security and ecological health of the study area.

Although not shown here for all cases, the K1+B0 and K0+B3 cases performed best among six cases of single dam operation, and the K1+B3 case performed best among nine cases of joint dam operation. In general, the results in Table 3 suggest that Border dam operation (the K0+B3 case) performs better than Karadobi dam operation (the K1+B0 case) although the K1+B0 case also shows an improvement to the baseline runoff scenario. First, the reliability and resiliency of water supply to downstream are noticeably increased by 75% and 31% (4% and 18% in the K1+B0 case), respectively. Second, the maximum water shortage and failure duration (i.e., vulnerability) are noticeably reduced by -68% and -77% (-28% and -6% in the K1+B0 case), respectively. Third, overall flow characteristics are improved. Q_{10} and D_{10} are decreased by -4% and -7% (1% and 4% increases in the K1+B0 case), respectively, and therefore the likelihood of flood risk is lower than the baseline runoff scenario and the K0+B0 case. Although the increases of Q_{90} and Q_m in the K0+B3 case are smaller than the K0+B0 case (no dam), the low-flow period (D_{90}) is significantly decreased due to the controlled releases from the Border dam during low-flow seasons. A major reason for these superior improvements of the K0+B3 case than the K1+B0 case is that the K1+B0 case is less efficient in providing stable flows to downstream countries than the K0+B3 case. Recalling the operation policies, the K1+B0 case allows 5% share of annual runoff at Border to be impounded in Karadobi regardless of intra-annual fluctuations (e.g., below the historical mean monthly runoff) while the K0+B3 case can mitigate these fluctuations by releasing supplemental outflows.

Table 3. Percent changes in water resources assessment indices and flow regimes for the 2050s.

Case	GCM	Assessment index[a] (%)				Flow (%)				Period (%)			
		REL	RES	VUL_T	VUL_V	Q_{10}	Q_{50}	Q_{90}	Q_m	D_{10}	D_{50}	D_{90}	D_m
K0+B0	Weight	25	31	-12	-14	4	-1	14	5	22	1	-27	-2
	Max[b]	102	385	424	1062	67	165	142	80	258	22	114	8
	Min[c]	-91	-84	-84	-91	-29	-28	-35	-32	-91	-44	-97	-25
K1+B0	Weight	4	18	-28	-6	1	-5	6	2	4	4	-13	-2
	Max	101	374	568	1451	64	153	127	75	237	23	123	9
	Min	-93	-86	-80	-91	-31	-31	-38	-34	-88	-42	-97	-25
K0+B3	Weight	75	31	-68	-77	-4	0	3	3	-7	5	-64	0
	Max	112	421	76	237	44	57	53	40	140	16	94	6
	Min	-55	-42	-100	-100	-10	-22	-35	-18	-37	-17	-100	-11
K1+B3	Weight	70	37	-64	-74	-4	0	3	3	-9	5	-56	0
	Max	112	421	76	247	44	55	55	40	134	17	97	6
	Min	-56	-44	-100	-100	-12	-23	-36	-18	-39	-15	-100	-11

The best-performed joint dam operation (the K1+B3 case) displays an almost similar performance with the K0+B3 case. In addition to the improved water supply capacity and flow duration as in the K0+B3 case, the K1+B3 case provides more beneficial aspects than the previous two cases. Although this case also shows a range of results depending on the GCM (Table 3), the weighted runoff scenario for the 2050s suggests that, most of all, hydropower potential will be significantly increased due to the two simultaneously operating dams.

Furthermore, the results of the K1+B3 case in Table 4 show that the mean annual water storage is larger than other two cases while the outflow ratio (total outflow/total inflow) is not disturbed but increased from the baseline runoff scenario. The mean annual storage simulated by the K1+B0, K0+B3, and K1+B3 cases show 55, 13, and 65% to the total capacity of the two dams, respectively. The K0+B3 case shows the lowest mean annual storage because of (1) supplementary releases of water during low-flow seasons and (2) the smaller capacity of the Border dam than the Karadobi dam. The K1+B3 case obviously shows the largest mean annual storage by jointly operating two dams. Another important issue that must be considered in any water management project proposed for the Nile Basin system is to assess the variability of total runoff volume from upstream countries. Under the weighted runoff scenario for the 2050s, the outflow ratios for the K0+B0 case (no dam) and the three cases (K1+B0, K0+B3, and K1+B3) are 105, 102, 103 and 103%, respectively, when using the baseline runoff scenario as the total inflow (Table 4). None of the three operation scenarios disturbs the original runoff volume (baseline runoff volume) of the study area.

Table 4. Mean annual water storages and outflow ratios simulated under the proposed operation policies for the 2050s

Case	GCM	Storage	Outflow
K0+B	Weigh	0	105
	Max	0	180
	Min	0	68
K1+B	Weigh	55	102
	Max	58	175
	Min	53	66
K0+B	Weigh	13	103
	Max	34	140
	Min	3	82
K1+B	Weigh	65	103
	Max	89	140
	Min	59	82

[a] Relative to the total capacity of two dams.
[b] Relative to the baseline runoff volume.

32

Current and future water abstractions by Ethiopia from the two reservoirs or the main stem could not be considered here because (1) these two dams were proposed for hydropower generation (MOWR 1998) and (2) it is difficult to predict the exact amount of irrigation consumption of the study area for the 2050s due to the lack of reliable information. Instead, the historical irrigation data of the Blue Nile Basin in Ethiopia surveyed by the Food and Agriculture Organization of the United Nations (FAO, 1997) were used to approximately evaluate the irrigation water consumption for the 2050s. Assuming the irrigation area will be increased five times (100,000 ha) by the 2050s from the 1989 area of about 20,000 ha, the total annual irrigation water demand for the 2050s will be 0.9 km^3. This amount is about 1.8% of the existing mean annual runoff of 49 km^3 (1921 to 1990 at El Deim). When considering return flows to the main stem, the consumptive irrigation water use for the 2050s may be about 1% of the mean annual runoff volume of the basin. Therefore, the proposed operation policies without water abstractions are acceptable for the two proposed dams.

CONCLUSIONS

This work is a step toward integrating the impacts of both climate change and water resources operations on the upper Blue Nile River Basin where water is important to its livelihood, but reliable and high resolution hydrologic data are limited. This study has developed and applied hydrologic modeling techniques to explore the impacts of climate change on the study area in terms of hydrologic regimes and water resources. Instead of using highly sophisticated hydrologic modeling approaches in the absence of reliable data, simple, yet reliable, approaches were implemented in this work.

Climate change scenarios based on the GCMs are not forecasts of future climate, but can be the possible results of future climate change. The simulation results for the 2050s can contribute to the water resources planners and decision-makers in understanding the possible range and trend of climate change and their sequential impacts. These impacts include a generally increasing trend of precipitation and runoff in the northern part (Amhara) of the study area; increased streamflow robustness (water supply capacity); and encouraging results of the proposed dam operations (hydropower only) that may not affect water availability but could enhance flow durations. Food security of the study area could be increased with the reduced probability of severe drought.

To be beneficial to both Ethiopia and downstream countries, technical cooperation between Nile riparians should be promised.

ACKNOWLEDGMENTS

REFERENCES

Block, P. J. 2007. Integrated Management of the Blue Nile Basin in Ethiopia: Hydropower and Irrigation Modeling. Discussion Paper No. 00700, International Food Policy Research Institute, Washington, DC.

Conway, D. 1997. A Water Balance Model of the Upper Blue Nile in Ethiopia. *Hydrological Science Journal* 42(2): 265-286.

Conway, D. 2000. The Climate and Hydrology of the Upper Blue Nile, Ethiopia. *The Geographical Journal* 166: 49-62.

Conway, D. 2005. From Headwater Tributaries to International River: Observing and Adapting to Climate Variability and Change in the Nile Basin. *Global Environmental Change* 15: 99-114.

Conway, D.; Hulme, M. 1993. Recent Fluctuations in Precipitation and Runoff Over the Nile Subbasins and Their Impact on Main Nile Discharge. *Climatic Change* 25: 127-151.

Conway, D.; Hulme, M. 1996. The Impacts of Climate Variability and Future Climate Change in the Nile Basin on Water Resources in Egypt. *Water Resources Development* 12(3): 277-296.

Degefu, W. 1987. Some Aspects of Meteorological Drought in Ethiopia. In Drought and Hunger in Africa: Denying Famine a Future. Edited by Glantz, M.H., Cambridge University Press, New York.

FAO (Food and agriculture organization of the United Nations). 1997. Irrigation Potential in Africa: A Basin Approach. FAO Land and Water Bulletin 4, FAO Land and Water Development Division, Rome.

Fowler, H. J.; Kilsby, C. G.; O'Connell, P. E. 2003. Modeling the Impacts of Climatic Change and Variability on the Reliability, Resilience, and Vulnerability of a Water Resource System. *Water Resources Research* 39(8): 1222.

Gamachu, D. 1977. Aspects of Climate and Water Budget in Ethiopia. Addis Ababa University Press, Addis Ababa, Ethiopia.

Gleick, P. H. 1991. The Vulnerability of Runoff in the Nile Basin to Climatic Changes. *Environmental Professional* 13: 66-73.

Guttman, N. H. 1998. Comparing the Palmer Drought Severity Index and the Standardized Precipitation Index. *Journal of the American Water Resources Association* 34(1): 113-121.

Hashimoto, T; Stedinger, J. R.; Loucks, D. P. 1982. Reliability, Resiliency, and Vulnerability Criteria for Water Resource System Performance Evaluation. *Water Resources Research* 18: 14-20.

Hayes, M. J.; Svoboda, M.; Wilhite, D. A.; Vanyarkho, O. 1999. Monitoring the 1996 Drought Using the SPI. *Bulletin of the American Meteorological Society* 80: 429-438.

IPCC (Intergovernmental Panel on Climate Change). 1999. Guidelines on the use of Scenario Data for Climate Impact and Adaptation Assessment. Version 1, Prepared by Carter TR, Hulme M, Lal M, Task Group on Scenarios for Climate Impact Assessment, IPCC, Geneva, Swiss.

Johnson, P. A.; Curtis, P. D. 1994. Water Balance of Blue Nile River Basin in Ethiopia. *Journal of Irrigation and Drainage Engineering* 120 (3): 573-560.

Kim, U.; Kaluarachchi, J. J. 2007a. Application of Parameter Estimation and Regionalization Methodologies to Ungauged Basins of the Upper Blue Nile River Basin, Ethiopia. *Journal of Hydrology* (under review).

Kim, U.; Kaluarachchi, J. J. 2007b. Assessment of Climate Change Impacts on Water Resources of the Upper Blue Nile River Basin, Ethiopia, *Water Resources Management* (under review).

Kim, U.; Kaluarachchi, J. J.; Smakhtin, V. U. 2007. Generation of Monthly Precipitation Under Climate Change for the Upper Blue Nile River Basin, Ethiopia. *Journal of American Water Resources Association* (in press).

Kim, U.; Lee, D. and Yoo, C. 2004. Effects of Climate Change on the Streamflow for the Daechung dam Watershed. *Journal of Korea Water Resources Association* 37(4): 305-314.

Maier, H. R.; Lence, B. J.; Tolson, B. A.; Foschi, R. O. 2001. First-order Reliability Method for Estimating Reliability, Vulnerability, and Resilience. *Water Resources Research* 37: 779-790.

McKee, T. B.; Doesken, N. J.; Kleist, J. 1993. The Relationship of Drought Frequency and Duration to Time Scales. In: 8th Conference on Applied Climatology, Anaheim, CA, 17-22 January, pp 179-184.

MOWR (Ministry of Water Resources). 1998. Abbay River Basin Integrated Development Mater Plan Project: Phase 2, vol. VI, Water Resources Development, part 2, Large Irrigation and Hydropower Dams. Report, Addis Ababa, Ethiopia.

Palmer, W. C.; Havens, A. V. 1958. A Graphical Technique for Determining Evapotranspiration by the Thornthwaite Method. *Monthly Weather Review* 86: 123-128.

Sene, K. J.; Tate, E. L.; Farquharson, F. A. K. 2001. Sensitivity Studies of the Impacts of Climate Change on White Nile Flows. *Climatic Change* 50: 177-208.

Strzepek, K. M.; Yates, D. N. 1996. Economic and Social Adaptation to Climate Change Impacts on Water Resources: A Case Study of Egypt. *Water Resources Development* 12: 229-244.

Sutcliffe, J. V.; Parks, Y. P. 1999. The Hydrology of the Nile. IAHS Special Publication No. 5, IAHS Press, International Association of Hydrological Sciences, Wallingford, England.

Tafesse, T. 2001. The Nile Question: Hydropolitics, Legal Wrangling, Modus Vivendi and Perspectives. LIT Verlag, London.

USBR (U.S. Bureau of Reclamation). 1964. Land and Water Resources of the Blue Nile Basin. Main Report, United States Department of Interior Bureau of Reclamation, Washington, DC.

UNESCO (United Nations Educational, Scientific, and Cultural Organization). 2004. National Water Development Report for Ethiopia. UN-WATER/WWAP/2006/7, World Water Assessment Program, Report, MOWR, Addis Ababa, Ethiopia.

WAPCOS (Water and Power Consultancy Service). 1990. Preliminary Water Resources Development Master Plan for Ethiopia. vol. VII, Annex J: Hydropower, Ethiopia Valleys Development studies Authority, Report, Addis Ababa, Ethiopia.

Waterbury, J. 1979. Hydropolitics of the Nile Valley. Syracuse University Press, New York.

Whittington, D.; Wu, X.; Sadoff, C. 2005. Water Resources Management in the Nile Basin: The Economic Value of Cooperation. *Water Policy* 7: 227-252.

Wurbs, R. A.; Muttiah, R. S.; Felden, F. 2005. Incorporation of Climate Change in Water Availability Modeling. *Journal of Hydrologic Engineering* 10(5): 375-385.

Yates, D. N.; Strzepek, K. M. 1996. Modeling Economy-wide Climate Change Impacts on Egypt: A Case for an Integrated Approach. *Environmental Modeling and Assessment* 1: 119-135.

Yates, D. N.; Strzepek, K. M. 1998a. An Assessment of Integrated Climate Change Impacts on the Agricultural Economy of Egypt. *Climatic Change* 38: 261–287.

Yates, D. N.; Strzepek, K. M. 1998b. Modeling the Nile Basin Under Climatic Change. *Journal of Hydrologic Engineering* 3(2): 98-108.

ASSESSMENT OF CLIMATE CHANGE IMPACTS ON THE HYDROLOGY OF GILGEL ABBAY CATCHMENT IN LAKE TANA BASIN, ETHIOPIA

Abdo K. S.[a], Rientjes, T.H.M.[b] and Gieske, A. S. M.[b]

[a]SNNPR Water Resources Development Bureau, Awassa,
P.O.Box 925, Ethiopia.
E-mail: abdokedir@yahoo.com
[b]Department of Water resources, ITC,
P.O.Box 6, 7500AA, Enschede, The Netherlands.

ABSTRACT

This paper presents the results of a study on downscaling large scale atmospheric variables from the HadCM3 General Circulation Model (GCM) to meteorological variables at local scale in order to investigate the hydrological impact of possible future climate change in Gilgel Abbay catchment, Ethiopia. Statistical DownScaling Model (SDSM) was employed to transform the GCM output in daily meteorological variables appropriate for hydrological impact studies. Downscaled meteorological variables are minimum temperature, maximum temperature and precipitation and were used as input to the HBV hydrological model to simulate the catchment runoff regime. The model was calibrated (R^2=0.86) and validated (R^2=0.76) as based on historical data and possible impacts of future climate changes in the catchment are assessed. The results obtained from this investigation indicate that there is significant variation in the seasonal and monthly flow. In the main rainy season (June-September) the runoff will be reduced by 12% in the 2080s. Results from synthetic incremental scenarios also indicate that the catchment is sensitive to climate change. As much as 33% of the seasonal and annual runoff will be reduced if an increment of 2°C in temperature and reduction of 20% rainfall occur simultaneously in the catchment.

Key Words: Climate change, GCM, HBV, SDSM

INTRODUCTION

Climate changes refers to a change in the state of the climate that can be identified by changes in the mean and/or the variability of its properties and that persists for an extended period, typically decade or more. Climate change may be due to internal processes and /or external forcings. Some external influences, such as changes in solar radiation and volcanism, occur naturally and contribute to the natural variability of the climate system. Other external changes, such as the change in the composition of the atmosphere that began with the industrial revolution, are the result of human activity.

Nowadays there is strong scientific evidence that the average temperature of the Earth's surface is increasing due to greenhouse gas emissions. For instance, the average global temperature has increased by about 0.6ºC since the late 19th Century. Also the latest IPCC (Intergovernmental Panel on Climate Change) scenarios project temperature rises of 1.4-5.8ºC, and sea level rises of 9-99 cm by 2100 (Houghton, 2001). Warming and precipitation are expected to vary considerably from region to region. Changes in climate average and the changes in frequency and intensity of extreme weather events are likely to have major impact on natural and human systems (Alerts & Droogers, 2004).

With respect to hydrology, climate change can cause significant impacts on water resources by resulting changes in the hydrological cycle. For instance, the changes on temperature and precipitation can have a direct consequence on the quantity of evapotranspiration and on both quality and quantity of the runoff component. Consequently, the spatial and temporal availability of water resource, or in general the water balance, can be significantly affected which in turn affects agriculture, industry and urban development.

Climate change is expected to have adverse impacts on socioeconomic development in all nations although the degree of the impact will differ. The IPCC findings indicate that developing countries such as Ethiopia will be more vulnerable to climate change. Climate Change may have far reaching implications for Ethiopia due to various reasons. The economy of the country mainly depends on agriculture, which is very sensitive to climate variations. A large part of the country

is arid and semiarid and is highly prone to desertification and drought. The country has also a fragile highland ecosystem which is currently under stress due to population pressure. Forest, water and biodiversity resources of the country are also climate sensitive. Climate change is therefore a case for concern (NMSA, 2001).

Despite the fact that the impact of climate change is forecasted at the global scale, the type and magnitude of the impact at a catchment scale is not investigated in most part of the world. Therefore it is necessary to study the effect of climate change at this scale in order to take the effect into account by the policy and decision makers when planning water resources management.

The objectives of this study are to develop and evaluate climate scenario data for maximum temperature, minimum temperature and precipitation based on a General Circulation Models and a statistical DownScaling Models and to quantify possible effects of climate change on the hydrology of Gilgel Abbay using a selected water balance based hydrological model.

STUDY AREA

Gilgel Abbay catchment is situated in the Northwest part of Ethiopia between 10º56' to11º51' N latitude and 36º44' to 37º23' E longitudes. The Gilgel Abbay River originates from a small spring located near Gish Abbay at elevation of 2900 m a.m.s.l. and drains to the Southern part of the Lake Tana. The catchment area of Gilgel Abbay River at the outlet to Lake Tana is around 4100 km^2 as it is extracted from a Shuttle Radar Topographic Mission (SRTM) digital elevation model (DEM). The river is the largest tributary of the Lake Tana basin and accounts for approximately 30% of the total area of the basin. The catchment contributes the largest inflow to the Lake.
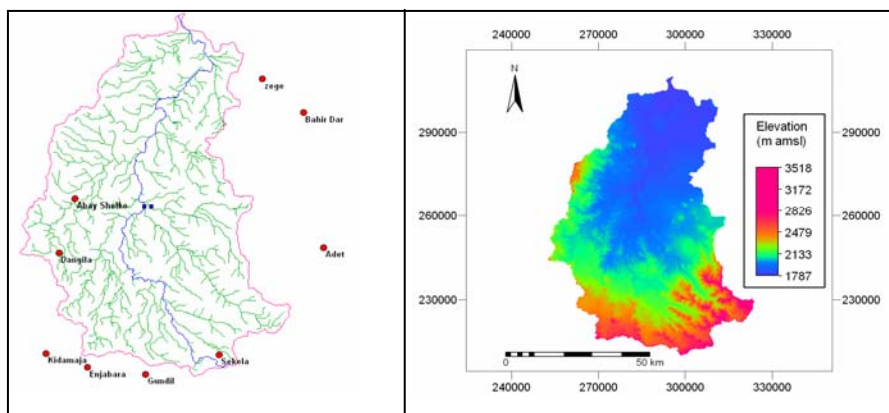
• Meteorological station   ▪ Gauging station

Figure 1. Meteorological station, Gauging station and
DEM of Gilgel Abbay catchment

With respect to topography the elevation of Gilgel Abbay catchment varies from 1787 to 3518m a.m.s.l. The higher elevation ranges are located at the Southeast corner while the remaining area is relatively uniform. From the slope map of the catchment area, around 70% of the catchment area falls in the slope range from 0-8% and 25% of the area falls in the slope range of 8-30%. The remaining 5% of the area has slope greater than 30%.
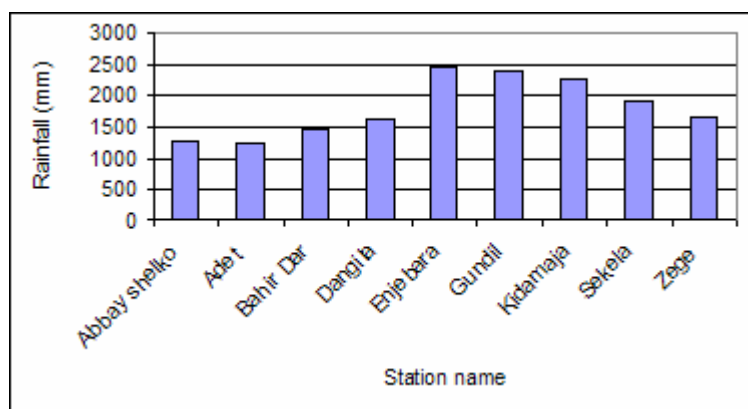
Figure 2. Mean annual rainfall from 1996-2004

There is high spatial and temporal variation of rainfall in the study area. The main rainfall season which accounts around 70-90% of the annual rainfall occurs from June to September. Small rains also occur sporadically during February/March to May. In the study area there is high diurnal change in temperature i.e. there is high variation between the daily maximum and minimum temperature. However, the seasonal variation of temperature is less compared to diurnal change. Generally the temperature of the area is highly affected by altitude where the temperature decreases with increase in altitude.

METHODOLOGY

The investigation of climate change effect on the hydrology consists of the development and use of General Circulation Models (GCMs) to provide future global climate scenarios under the effect of increasing greenhouse gases; the development and use of downscaling techniques for downscaling the GCMs output to the scales compatible with hydrological models, and the development and use of hydrological models to simulate the effects of climate change on hydrological regimes at various scale (Xu et al., 2005).

General Circulation Model (GCM)

The climate model is a mathematical description of the Earth's climate system, broken into a number of grid boxes and levels in the atmosphere, ocean and land. Each of these grid boxes serves as a model calculation unit at which equations are solved that describe the large-scale balances of the momentum, heat and moisture. In science a wide range of climate models are proposed where approaches differ with respect to the spatial resolution of the model domains and applied model algorithms and related parameterization. The relative performance of GCMs depends on the size of the region (i.e. small regions at sub-grid scale are less likely to be well described than large regions at continental scale), on its location (i.e. the level of agreement between GCM outputs varies a lot from region to region) and on the variables being analyzed (for instance, regional precipitation is more variable and more difficult to model than regional temperature) (after Carter, 2007). For this study the model output of HadCM3 GCM was employed for the A2 (Medium-High Emissions) and B2 (Medium-Low Emission) Scenarios. HadCM3 is a coupled atmospheric-ocean GCM developed at Hadley Centre for Climate Prediction and Research, UK. The atmospheric part of HadCM3

has a horizontal resolution of 2.5º latitude x 3.75º longitude, and has 19 vertical levels. The ocean component of the model has 20 vertical levels with horizontal resolution of 1.25º latitude x 1.25º longitude. HadCM3 is applied in this study because the model is widely applied in climate change impact studies and the model provides daily predictor variables with coverage over Ethiopia that can be used for the Statistical DownScaling Model.

Statistical DownScaling Models

General Circulation Models indicate that rising concentration of greenhouse gases will have significant implications for climate at global and regional scales. However, GCMs are restricted in their use for local impact studies due to the coarse resolution and inability to resolve important sub-grid scale features such as clouds and topography. As a consequence, downscaling techniques have emerged as a mean of deriving local-scale weather from regional-scale atmospheric predictor variables (Dawson & Wilby, 2007).

There are various downscaling techniques available to convert GCM outputs into daily meteorological variables that can be used in hydrological impact studies. Dibike and Coulibaly (2004) describe that it is not clear which methods provides the most reliable estimates for the future climate since effectiveness of methods also depend on the purpose of study, the area of study and data availability. Statistical downscaling has a number of advantages over the use of raw GCM output. Firstly, the stochasticity of the model facilitates the generation of ensembles of future climatic realizations that is a pre-requisite to confidence estimations. Secondly, the downscaling model may be tuned to reproduce the unique meteorological characteristics of individual stations that is a valuable asset in heterogeneous landscapes or mountainous terrain. Thirdly, such techniques are far less data intensive and computationally less demanding than dynamic methods (Leavesley et al., 1999). In situations where low-cost, rapid assessments of localized climate change impacts are required, statistical downscaling (currently) represents the more promising option (Dawson & Wilby, 2007) despite their limitation in assumption that the statistical relationships developed for the present climate also hold under the different forcing condition of the possible future climate.

One of the well recognized statistical downscaling tools which are applied widely in climate impact studies are Statistical DownScaling Models (SDSM). In this study the Statistical DownScaling Model 4.1 is used that is described as a decision support tool for assessing local climate change impacts. SDSM permits the spatial downscaling of daily predictor-predict and relationships using multiple linear regression techniques. The predictor variables provide daily information concerning the large-scale state of the atmosphere, while the predict describes conditions at the site scale.

Hydrological Model

In this study HBV-96 (see Lindstrom, 1997) is applied. HBV-96 is a water balance based mathematical model of the hydrological processes in a catchment used to simulate the runoff properties. It can be described as a semi-distributed conceptual model that allows dividing the catchment into subbasins where the subbasins can be further divided into elevation and vegetation zones. The model consists of subroutines for snow accumulation and melt, a soil accounting procedure, routines for runoff generation and a simple routing procedure. It is possible to run the model separately for several subbasins and then add the contributions to simulate runoff from the entire subbasin. Calibration as well as runoff forecasts can be for each subbasin.

The model input requirements for the HBV model are daily rainfall, temperature, estimates of potential evapotranspiration, and catchment characteristics of the area. A DEM of the catchment was prepared using SRTM with a resolution of 90 m. The DEM was processed using a DEM hydroprocessing procedure to extract drainage area, drainage network and to divide the area into different subbasins and elevation zones. The model requires daily rainfall as input. Hence rainfall data for the period of ten years (1996-2005) was prepared for nine meteorological stations in and around the catchment area. Areal rainfall in the model is computed by multiplying the rainfall by the weight of each station for the subbasin considered in the analysis. The weight of each meteorological station was computed by the inverse distance method. Potential evapotranspiration for the study area was computed by FAO Penman-Monteith method for Dangila & BahirDar stations which contain the required meteorological variables. For model development the period from 1996-2006 was used and from this the year 1996 was used as a warm up period to initialize the model before actual calibration.

The remaining nine years were divided in such a way that 2/3rd of the data (1997-2002) was used for the calibration and 1/3rd of the data (2003-2005) was used for validation. Calibration was done manually by optimizing the model parameters in each subroutine that have significant effect on the performance of the model.

In this study the analysis of the simulated stream flow for hydrological impact of climate change was carried out in three time horizons in future periods each covering non-overlapping 30 years. These period consists of 2020s (2011-2040), 2050s (2041-2070) and 2080s (2071-2099). In addition to climate model-based scenarios, synthetic incremental scenario was also used to investigate a wide range of changes in climatic variables which in turn helps to test the system sensitivity to climate change.

RESULTS AND DISCUSSION

Downscaling the GCM for Future Scenario

Climate scenarios for future periods have been developed for two emission scenarios A2 and B2 for 100 years based on the mean of 20 ensembles where further analysis was done based on three 30-year periods centered on the 2020s (2011-2040), 2050s (2041-2070) and 2080s (2071-2099).

Temperature

The downscaled minimum temperature shows an increasing trend in all future time horizons for both A2 and B2 scenarios. The average annual minimum temperature will increase by 1^oC in 2020s. In 2050s the increment will be 2.2^oC and 1.7^oC for A2 and B2 scenario respectively. For the 2080s periods the average annual minimum temperature will be increased by 3.7^oC and 2.7^oC for A2 and B2 scenario respectively. The increment for the A2 scenario is greater than the B2 scenario since the A2 scenario represents a medium high scenario which produces more CO2 concentration than the B2 scenario which represents a medium low scenario. The downscaled maximum temperature scenario also indicates that there will be an increasing trend for both A2 and B2 scenarios. The projected temperature in 2020s indicates that the maximum temperature will rise by 0.6^oC. In 2050s the increment will be 1.4^oC and 1.1^oC for A2 and B2 scenarios respectively. In 2080s the annual maximum temperature will be increased by 2.5^oC and 1.8^oC for A2 and B2 scenario respectively. The increment in maximum temperature is less than the minimum temperature.

Precipitation

Projection of rainfall did not manifest a systematic increase or decrease in all future time horizons unlike that of maximum and minimum temperature which exhibits an increasing trend for both A2 and B2 scenarios in all future time horizons. The rainfall amount generally shows a decreasing trend in the beginning of the rainy season (May and June) and shows increasing trend towards the end of the rainy reason (September and October) for both A2 & B2 scenario in all future time horizon. The rainfall will experience a decrease of 18% and 11.2% in June from the baseline period by 2080s for A2 and B2 scenarios

respectively whereas the rainfall increase by 8.5% and 5.7% in September by 2080s for A2 and B2 scenarios respectively. The rainfall will also indicate a reduction in July and August from the baseline period for the A2 scenario in all future time horizons however, for the B2 scenario there is also indication of increment in some future time horizon. In the main rainy season (June-September) the rainfall exhibits a relative decrease from the baseline period for the A2 scenario in all future time horizons whereas the B2 scenario indicates a decrease by 2020s and a slight increment by 2050s and 2080s. The mean annual rainfall variation is not significant as compared to the monthly variation. The mean annual rainfall indicates a decrease in 2020s followed by a slight increase in 2050s and 2080s.

The mean monthly rainfall distribution downscaled from SDSM shows a similar pattern with work of de Boer (2007) which describes the impact of climate change on rainfall pattern in the Ethiopian highland. As indicated in his work the mean monthly rainfall decrease in May, June and July and increase in September, October and November with respect to the baseline period.

As described in the IPCC Third Assessment Report (McCarthy et al., 2001), the projected future changes in mean seasonal rainfall in Africa are less well defined. The diversity of African climates, high rainfall variability, and a very sparse observational network make the predictions of future climate change difficult at the sub regional and local scales. Under intermediate warming scenarios, rainfall is predicted to increase in December-February and decrease in June-August in parts of East Africa. With a more rapid global warming scenario, large areas of Africa would experience changes in December-February or June-August rainfall that exceed natural variability. With reference to this study rainfall will also experience a reduction in June-August for most part of the future time horizons, however, the rainfall variation in December-February is not significant because these are the driest month which contribute less than 1% of the annual rainfall in the study area. Conway (2005) indicates that, with respect to the future climate in the Nile basin, that there is high confidence that the temperature will increase leading to increased evaporation. However, there is much less certainty about future rainfall because of the low convergence in climate model projection in the key headwater regions of the Nile. The same paper states that there is

large inter-model difference in the detail of rainfall changes over Ethiopia using the results from seven recent climate model experiments.

Hydrological Model Calibration and Validation

Calibration was done manually by optimizing the model parameters in each subroutine that have significant effect on the performance of the model. Based on this, several runs were made to select the most optimum parameter set in order to match the observed discharge with simulate discharge. The observed and simulated hydrograph using the above optimum parameter is shown in Figure 3. Visual inspection of the observed and simulated hydrograph shows that the performance of the model in simulating the baseflow, rising and recession limb of the hydrograph is good. The model simulation for high flow is satisfactory although it underestimates very high single peaks that commonly are caused by extreme high rainfall events that operate at time scales different from the model daily calculation time step.
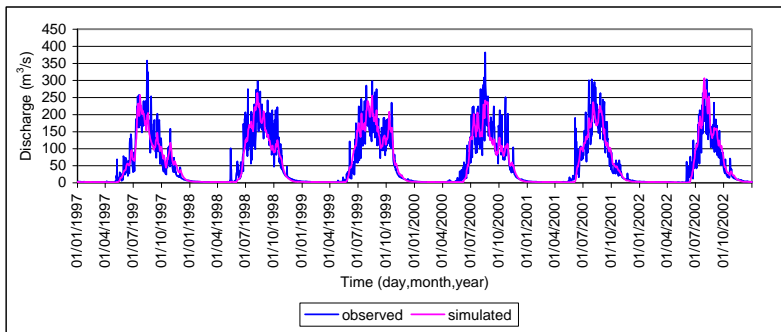
Figure 3. Daily observed and simulated hydrograph during calibration period

Table 1. List of objective function and its value
obtained during calibration

Objective function		value
Nash and Sutcliffe efficiency coefficient, R^2	$R^2 = \dfrac{\sum(Qobs - \overline{Qobs})^2 - \sum(Qsim - Qobs)^2}{\sum(Qobs - \overline{Qobs})^2}$	0.86
Correlation coefficient, r	$Corr \dfrac{\sum(Qobs - \overline{Qobs})(Qsim - \overline{Qsim})}{\sqrt{\sum(Qobs - \overline{Qobs})^2 \sum(Qsim - \overline{Qsim})^2}}$	0.92
Relative Volume error, R.V.E (%)	$R.V.E = \dfrac{\sum(Qobs - Qsim)}{\sum Qobs} \times 100$	-0.13

The objective functions which were used to evaluate the model performance are summarized in Table 1. As it is indicated in the table, the Nash and Sutcliffe efficiency criterion which is considered a generic performance indicator in the HBV model is equal to 0.86 and is considered satisfactory for this study. The model was also validated against an independent data set and the model performs reasonably well in simulating the discharge. The Nash and Sutcliffe efficiency and the correlation coefficient during the validation period are 0.76 and 0.9 respectively.

Hydrological Impact of Future Climate Change Scenario

The ultimate objective of the downscaling is to generate an estimate of meteorological variables for a given scenario that characterizes a future climate so that these meteorological variables will be used as a basis for hydrological impact assessment. Therefore, after calibrating the hydrological models with the historical record, the next step is the simulation of river flows in the catchment by using the downscaled precipitation and temperature and evapotranspiration as input to hydrological models. The evapotranspiration is computed based on the downscaled minimum and maximum temperature for each time horizon. Subsequently the hydrological model was used to identify possible trends in the simulated river flow. The present condition in the hydrological model is represented by taking the average of the longest possible records available in study area. These include at least ten years data for all station used in the analysis.

Simulation results for three future time horizons are summarized in Table 2 and Figure 4. As it is shown in the table the variation in mean annual runoff is moderate. The mean annual runoff will be reduced by 2.6% and 2.9% in 2080s for the A2 and B2 scenarios respectively. However, there is significant variation in the seasonal and monthly flow. In the main rainy season (June-Sep) the runoff will be reduced by 11.6% and 10.1% in 2080s for A2 and B2 scenario respectively. With respect to individual months, there will be large reduction in June where the mean monthly flow will reduce by 66% and 59% in 2080s for the A2 and B2 scenarios respectively. July also exhibit a reduction in mean monthly flow where the flow will be reduced by 20% and 16% in the 2080s for the A2 and B2 scenarios. In August, with the exception of B2 scenario at the 2050s, there is reduction in mean monthly flow as well. The mean monthly flow of the river will start to increase afterwards. In September there will be mixed sign where the flow will start to decrease in 2020s and increase in 2050s and 2080s for both scenarios. The mean monthly flow of October will be increased by 33% and 15% in 2080s for both A2 and B2 scenarios in all future time horizons. There will also be a reduction in November for both A2 and B2 scenarios in all future time horizons.
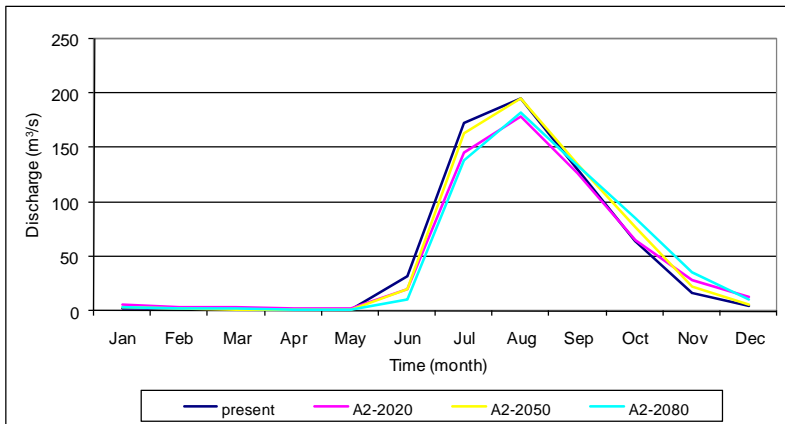
Figure 4. Mean monthly flow for A2 scenario

Table 2. Average increase/decrease of runoff (%)
from the present condition

Time	A2-2020	A2-2050	A2-2080	B2-2020	B2-2050	B2-2080
Seasonal runoff (Jun-Sep)	-11.6	-3.5	-12.2	-13.3	-1.4	-10.1
Annual runoff	-5.4	0.2	-2.6	-6.8	0.4	-2.9

In terms of volume of flow, maximum reduction exhibit in the months of July where the mean monthly runoff will be reduced by 91.6 MCM. There will be maximum increment in October where the mean monthly runoff will be increased by 56.2 MCM. Generally speaking, in those months which account for more than 90% of annual runoff there will be a shift in mean monthly runoff distribution where the flow will show a reduction sign in June, July and August and increment in September, October and November.

Uncertainties and Sensitivity Analysis

Hydrological climate change impact assessment involves recognizing three key aspects of uncertainty. Firstly there are uncertainties linked to General Circulation Models (GCMs), secondly there are uncertainties in the representation of climatology at regional and local scales that also include differences between dynamic and statistical downscaling methods and thirdly there are parameter and structural uncertainties in hydrological models used for impact assessment

The uncertainties of climate scenarios and GCM outputs are large. Although the GCM's ability to reproduce the current climate has increased, direct outputs from GCM simulations are inadequate for assessing hydrological impact of climate change at regional and local scales. It is true that different hydrological models can give different values of stream flow for a given input, but the large uncertainties in the effect of climate on stream flow arise from uncertainties in climate change scenarios as long as a conceptually sound hydrological models are used (Xu et al., 2005). In order to deal with the GCM inadequacies, the delta-change method, i.e. the computation of difference between the current and future simulations and addition of these changes to observed time-series, is widely used and also applied in this study. This assumes that the GCMs more reliably simulate relative changes rather than absolute values.

Given the deficiencies of GCM predictions and downscaling techniques, the use of synthetic incremental scenario as input to catchment-scale hydrological models is widely used in addition to climate model-based scenarios. Incremental scenarios are based on reasonable but arbitrary changes in climatic variables such as temperature and precipitation are made often according to qualitative interpretation of climate model prediction or analysis of changes in climatic characteristics that occurred in the past. Incremental scenarios are used to investigate a wide range of changes in climatic variables which in turn helps to test the system sensitivity. Based on this, ten types of incremental scenarios were developed for the Gilgel Abbay catchment and seasonal and annual runoff changes were analyzed. The result from incremental scenario indicates that an increase in temperature of $2^{o}C$ without rainfall change decreases the seasonal and annual runoff by 1.7% and 2% respectively. If the change in temperature is $4^{o}C$, the seasonal and annual runoff would be decreased by 3.3% and 4% respectively. However, if the increase in $2^{o}C$ temperature will occur simultaneously with a rainfall reduction of 10%, the seasonal and annual runoff will be decreased by 17.7%. If the reduction of rainfall is 20% and the temperature will rise by $2^{o}C$, the seasonal and annual runoff will be reduced by 33%. From this analysis it is possible to conclude that the Gilgel Abbay catchment is sensitive to climate change and it is more sensitive to change in rainfall than change in temperature.

CONCLUSION AND RECCOMENDATION

The tremendous importance of water in both society and nature underscores the necessity of understanding how a change in global climate could affect the availability and reliability of water resources at a catchment scale. However, this is complicated by the fact that the climate change information required for impact studies is of a spatial scale much finer than that provided by General Circulation Models. This mismatch is partly resolved by downscaling techniques even though the procedure of downscaling also must be associated with uncertainty. In this study the problem was exacerbated by the lack of good quality data for a significantly long period for the study area. Despite this, maximum effort was made to investigate the likely future of hydrological impact of climate change and the following conclusion and recommendation are drawn from this study.

Conclusion

The results from the applied statistical downscaling model indicates that both the minimum and maximum temperature show an increasing trend in all future time horizons for both A2 and B2 scenarios. Climate change scenarios for Africa, based on the results from several General Circulation Models using the data collated by the Intergovernmental Panel on Climate Change Data Distribution Centre (IPCC-DDC) indicate that future warming across Africa with ranges from 2°C (low scenario) to 5°C (high scenario) by 2100. Result obtained from SDSM in this study fall within the range of IPCC temperature change recommendations.

The result of downscaled precipitation reveals that precipitation does not manifest a systematic increase or decrease in all future time horizons for both A2 and B2 scenarios unlike that of minimum and maximum temperature. However, in the main rainy season which accounts 75-90% of annual rainfall of the area, the mean monthly rainfall indicates a decreasing trend in the beginning of the rainy season (May & June) and an increasing trend towards the end of the rainy season (September & October) for both A2 and B2 scenarios in all future time horizons.

The result of hydrological model calibration and validation indicates that the HBV model simulates the runoff considerably good for the study area. The model performance criterion which is used to evaluate the model result indicates that the Nash and Sutcliffe efficiency criteria (R^2) are 0.86 and 0.76 during calibration and validation periods respectively.

The hydrological impact of future change scenarios indicates that there will be high seasonal and monthly variation of runoff compared to the annual variation. In the main rainy season (June-September) the runoff volume will reduce by 11.6% and 10.1% for A2 and B2 scenarios respectively in 2080s.

Results from synthetic incremental scenarios indicate that the catchment is sensitive to climate change especially to changes in rainfall. An increase of 2°C temperature without changes in rainfall decreases the seasonal and annual runoff by 1.7% and 2%. However, if change in

temperature is accompanied by 20% rainfall reduction, seasonal and annual runoff will be reduced by 33%.

Recommendation

There are many sources of uncertainty in the hydrological impact scenarios that are in the climate modeling, the method used for transferring the climate signal to meteorological stations, and in the hydrological modeling. The model simulations have not considered land use changes explicitly although, it is likely that changes in land use may interact with climate leading to different projections of future hydrological conditions. Therefore the result of this study should be taken with care and be considered as indication of likely future changes rather than an actual prediction.

The outcome of this study is based on single GCMs and two emission scenarios. However, it is often recommended to apply different GCMs and emission scenarios so as to make comparison between different models as well as to explore a wide range of climate change scenarios that would result in different hydrological impacts. Hence this work should be extended in the future by including different GCMs and emission scenarios.

REFERENCES

Aerts, J. C. H. & Droogers, P. (2004). Climate change in contrasting river basin: adaptation strategies for water, food and environment. Wallingford: CABI.

Allen, R. G., Pereria, L. S., Raes, D. & Smith, M. (1998). Crop Evapotranspiration: Guidelines for computing crop water requirements. FAO, Rome.

Carter, T.R. (2007). General Guidelines on the use of scenario data for Climate Impact and Adaptation Assessment. Finnish Environmental Institute, Helsinki, Finland.

Conway, D. (2005). From headwater tributaries to international river: Observing and adapting to climate variability and change in the Nile basin. Global Environmental Change, 15, 99-114.

Dawson, C. W. & Wilby, R. L. (2007). Statistical Downscaling Model SDSM, version 4.1. Department of Geography, Lancaster University, UK.

deBoer, B. (2007). Climate change and impacts on the extreme rainfall over the Blue Nile Region. KNMI, Royal Netherlands Meteorological Institute, De Bilt, Netherlands.

Dibike, Y. B & Coulibaly, P. (2004). Downscaling of Global Climate Model output for flood Frequency Analysis in the Saguenay River System. Project no. S02-15-01, Department of Civil Engineering, McMaster University, Canada.

Houghton, J.T. (2001). Climate change 2001: the scientific basis: contribution of working group I to the third assessment report of the intergovernmental panel on climate change (Houghton, J. T., Ed.). Cambridge University Press.

Leavesley, G. H., Wilby, R. L. & Hay, L. E. (1999). A comparison of downscaled and raw GCM output: implication for climate change scenarios in the San Juan River basin, Colorado. Journal of Hydrology, 225(1-2), 67-91.

Lindstrom, G., Johansson, B., Persson, M., Gardelin, M., & Bergstrom, S. (1997). Development and test of the distributed HBV-96 hydrological model. *Journal of Hydrology, 201*, 272-288

McCarthy, J. J., Canziani, O. F., Leary, N.A., Dokken, D.J & White, K. S. (2001). Climate change 2001: Impacts, Adaptation, and Vulnerability Contribution of Working Group II to the Third Assessment Report of the Intergovernmental Panel on Climate Change.

NMSA. (2001). Initial National Communication of Ethiopia to the United Nations Framework convection on Climate Change (UNFCCC). National Meteorological Services Agency, Addis Ababa, Ethiopia.

SMHI. (2006). Integrated Hydrological Modeling System: Manual Version 5.10.

Xu, C. Y., Widen, E. & Halldin, S. (2005). Modeling Hydrological Consequence of Climate change- Progress and Challenges. Advances in Atmospheric Sciences 22(6), 789-797.

ESTIMATING ENVIRONMENTAL FLOW REQUIREMENTS DOWNSTREAM OF THE CHARA CHARA WEIR ON THE BLUE NILE RIVER

Matthew P. McCartney[1] , Abeyu Shiferaw[2] and Yilma Seleshi[3]

[1] International Water Management Institute, P.O. Box 5689, Addis Ababa, Ethiopia. m.mccartney@cgiar.org
[2] P.0.Box 31769 Addis Ababa, Ethiopia. abiyushif@yahoo.com
[3] Department of Civil Engineering, Addis Ababa University, P.O. Box 150241 Addis Ababa, Ethiopia
yilmash@ceng.aau.edu.et

ABSTRACT

Over the last decade flow in the Abay River (i.e., the Blue Nile) has been modified by operation of the Chara Chara weir and diversions to the Tis Abay hydropower stations, located downstream of the rivers source, Lake Tana. The most conspicuous impact of these human interventions has been significantly reduced flows over the Tis Issat Falls. This paper presents the findings of a hydrological study conducted to estimate environmental flow requirements downstream of the weir. The South African *desktop reserve model* was used to determine both high and low flow requirements in the reach containing the Falls. The results indicate that to maintain the basic ecological functioning in this reach requires an average annual allocation of 862 Mm^3 (i.e. equivalent to 22% of the mean annual flow). Under natural conditions there was considerable seasonal variation, but the absolute minimum mean monthly allocation, even in dry years, should not be less than approximately 10 Mm^3 (i.e. 3.7 m^{3}s^{-1}). These estimates make no allowance for maintaining the aesthetic quality of the Falls, which are popular with tourists. The study demonstrated that, in the absence of ecological information, hydrological indices can be used to provide a first estimate of environmental water requirements. However, to ensure proper management, much greater understanding of the relationships between flow and the ecological condition of the riverine ecosystem is needed.

INTRODUCTION

Water resource management is critical to development, because of its numerous links to poverty reduction, through health, agricultural productivity and industrial and energy growth. However, strategies to reduce poverty should not lead to the unsustainable degradation of water resources or ecological services (World Bank, 2003). One of the major challenges for sustainable water resource management is to assess how much water can be taken from a river before its ability to meet social, ecological and economic needs declines.

The Blue Nile (known as the Abay River in Ethiopia) is the principal tributary of the main Nile River. The river and its tributaries drain a large proportion of the central, western and south-western highlands of Ethiopia before dropping to the plains of Sudan. The river provides 62% of the flow reaching the Aswan High Dam and is a vital source of water for both Sudan and Egypt (World Bank, 2006). Despite the fact that almost all the flow is generated in the Ethiopian Highlands, currently Ethiopia utilizes very little of the Blue Nile water. To date, only two relatively minor dams have been constructed in the Abay catchment. Both are utilized for hydropower production. It is estimated that irrigation covers less than 10,000 ha. This compares to over 1 million hectares of irrigation in the Sudanese part of the Blue Nile catchment (Awulachew *et al*., 2008).

One of the dams constructed in Ethiopia, and the only one actually located on the mainstem of the Abay River, is the Chara Chara weir. This is used to regulate flow from Lake Tana, for downstream electricity production at two power stations at Tis Abay (Figure 1). An environmental impact assessment was conducted prior to construction of the weir. However, estimates of flow requirements were based largely on the aesthetic impact of different discharges over the famous Tis Issat waterfall, a major tourist attraction situated immediately downstream of the diversion to the power stations (Howard *et al*., 1997).

This paper describes a more rigorous approach to determine environmental flows downstream of the Chara Chara weir. The current study determined the impact of the weir on flows from Lake Tana and estimated environmental flow requirements in the river reach containing the Falls. These were compared with the actual flows in the river since the weir became fully operational in 2001. The study is believed to be

one of the first attempts to rigorously quantify a full range of environmental flow requirements (i.e., both high and low flows) and to assess the impact of flow regulation, anywhere on the Blue Nile River.

STUDY SITE

Lake Tana occupies a shallow depression (maximum depth 14m) in the Ethiopian highlands. The geology of the area is primarily basaltic lavas of the Aden Volcanic series. The lake is believed to have formed as a consequence of damming by lava during the Pliocene (Mohr, 1962). The surface area of the Lake is 3,156 km^2. The catchment area at the lake outlet is 15,321 km^2. The climate of the area is largely controlled by the movement of inter-tropical convergence zone, which results in a single rainy season between June and September. The mean annual rainfall over the catchment is estimated to be 1,342 mm, with slightly more rain falling in the south than in the north of the catchment (Melkamu, 2005).

The mean annual inflow to the lake is estimated to be 114 m^{3}s^{-1} (3,595 Mm^{3}y^{-1}). Mean annual evaporation and rainfall are approximately balanced and the mean annual outflow is estimated to be 120 m^{3}s^{-1} (i.e. 3,776 Mm^{3}y^{-1}) (Kebede *et al.*, 2006). The outflow equates to 257 mm over the total catchment, giving a coefficient of runoff of 18%. Under natural conditions, discharge from the lake is closely linked to rainfall and there is considerable seasonal and inter-annual variability (Kebede *et al.*, 2006).

The original power plant at Tis Abay (Tis Abay-I) was constructed by the Ethiopian Electricity Light and Power Authority (EELPA) and came on line in 1964. Located approximately 35 km downstream of the lake outlet, the station was used to provide electricity for a textile factory and for domestic supply to the city of Bahar Dar. By diverting water from upstream of the Tis Issat Falls, the power plant makes use of the natural 46 m head of the Falls. The installed capacity of the power plant is 11.4 MW and initially it relied entirely on diversion of the natural flow of the river.

The concept of building a weir to regulate the outflow from Lake Tana was first postulated in the early years of the twentieth century. However, it was not until 1977 that consideration was given to regulating the flow to provide water for a larger Tis Abay power station, which could contribute to the national grid (JICA, 1977). The scheme envisaged

the construction of a weir at the outlet of Lake Tana and a second power house located 100m downstream of the Tis Abay-I plant (Figure 1). Construction of the weir started in 1984, but was abandoned shortly afterwards (Howard *et al*., 1997). Construction was re-started in 1994, and the weir was largely completed by May 1996. Initially the weir had only two gates, each with capacity of 70 m^{3}s^{-1}, and provided sufficient regulation only to improve the power production from Tis Abay-I. An additional five gates, each also with capacity 70 m^{3}s^{-1}, were added to the weir in 2001. The second power station (Tis Abay-II), with an installed capacity of 72 MW, was also completed in 2001. Since then the weir has been operated by the Ethiopian Power Corporation (EEPCO) (the successor to the EELPA) to maximize power production from both power stations. Currently the two power stations represent 11% of the total grid-based electricity generating capacity of the country (731 MW), 90% of which is generated by hydropower (World Bank, 2006).

The Chara Chara weir regulates water storage in Lake Tana over a 3m range of water levels from 1784 masl to 1787 masl. The active storage of the lake between these levels is 9,100 Mm^3, which represents approximately 2.4 times the average annual outflow. At full supply level the total flow through the seven gates is 490m^{3}s^{-1}. Approximately 110 m^{3}s^{-1} (the total flow capacity of both Tisa Abay-I and II) can be released continuously with 95% reliability (Howard *et al*., 1997).
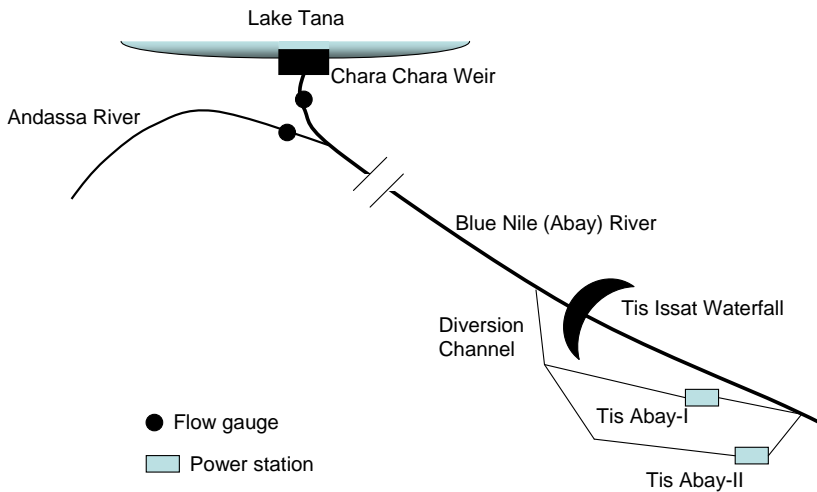
Figure 1. Schematic of the system (not to scale)

As part of the environmental impact assessment an attempt was made to estimate flow requirements over the Tis Issat Falls. The focus was on tourist needs and so this evaluation was based primarily on the appearance of the Falls under different flow regimes (Howard *et al*., 1997). The maximum flows were recommended, not for the wet season when flows would naturally be highest, but to make the Falls look most dramatic during the peak tourist season from December to February (Table 1).

Table 1. EIA recommended flow over the Tis Issat Falls
(source: Howard *et al.*, 1997)

	Jan	Feb	Mar	Apr	May	Jun	Jul	Aug	Sep	Oct	Nov	Dec	Total
Flow (m^3s^{-1})	60	60	10	10	10	10	20	20	40	40	40	60	
Volume (Mm^3)	161	146	27	26	27	26	54	54	104	107	104	161	995

METHOD

The current study comprised two elements. First, analyses of flow data to quantify the changes in the hydrological regime of the river, arising from operation of the weir and diversions to the power stations. Second, an evaluation of environmental flow requirements, derived from hydrological indices, through application of the South African Desktop Reserve Model (DRM) (Hughes and Hannart, 2003).

Change in Hydrological Regime

A gauging station, located immediately downstream of the outlet from Lake Tana, has operated continuously since 1959. The intermediate catchment between the Chara Chara weir and the diversion to the Tis Abay power stations has an area of 1,094 km^2. The principal tributary between the lake and Tis Abay is the Andassa River, which is gauged just upstream of its confluence with the Blue Nile (Figure 1). The catchment area at the gauging station (which has also operated since 1959) is 573 km^2.

Time series of monthly flow data, were obtained from the Ministry of Water Resources for both gauging stations from January 1959 to December 2006. Daily flow series were obtained for both

stations from January 1973 to December 2006. An estimate of the contribution from the ungauged portion of catchment downstream of the lake outlet was derived simply by multiplying the flow series derived from the Andassa gauge using an area-weighting. The flows downstream of Lake Tana were added to the flows from the outlet to provide an estimate of the total flow at the diversion to the power stations. Turbine discharge data for both Tis Abay-I and Tis Abay-II power stations were obtained from EEPCO and used to estimate the monthly flows diverted to produce electricity as well as the water remaining in the river to flow over the Falls.

Analyses of flows were conducted over three time periods: May 1959 to April 1996, May 1996 to December 2000 and January 2001 to December 2006. These periods correspond to different levels of regulation of the Lake Tana outflow (Table 2). Standard hydrological techniques, including flow frequency analyses and the development of flow duration curves (using the daily data) (Gustard *et al*., 1992) were used to compare the flow regimes in each of these periods.

Table 2. Periods of different flow regulation from Lake Tana.

Period	Description
May 1959 - April 1996	No regulation of outflow from Lake Tana. Diversions to the Tis Abay-I power station commenced in January 1964.
May 1996 – December 2000	Two-gate Chara Chara weir becomes operational in May 1996. Weir operated to regulate flow to the Tis-Abay-I power station.
January 2001 – December 2006	Five new gates constructed and new weir becomes operational in January 2001. Weir operated to regulate flow to both the Tis Abay-I and Tis Abay-II power stations.

Estimated Environmental Flows

Environmental flows are the water that is left in a river, or released into it (e.g., from a reservoir), in order to maintain valued features of the ecosystem (Tharme and King, 1998). In recent years, there has been a rapid proliferation of methods for estimating environmental flows, ranging from relatively simple, low-confidence, desk-top approaches, to resource-intensive, high-confidence approaches

(Tharme, 2003). The comprehensive methods are based on detailed multi-disciplinary studies, which often involve expert discussions and collection of large amounts of geo-morphological and ecological data (e.g., King and Louw, 1998). Typically they take many months, sometimes years, to complete.

A key constraint to the application of comprehensive methods, particularly in developing countries, is lack of data linking ecological conditions to specific flows. To compensate for this, several methods of estimating environmental flows have been developed that are based solely on hydrological indices derived from historical data (Tharme, 2003). Although it is recognized that a myriad of factors influence the ecology of aquatic ecosystems (e.g., temperature, water quality and turbidity), the common supposition of these approaches is that the flow regime is the primary driving force (Richter *et al*., 1997).

One such method is the DRM, which is intended to quantify environmental flow requirements in situations when a rapid appraisal is required and data availability is limited (Hughes and Hannart, 2003). The model is built on the concepts of the building block method, which was developed by South African scientists over several years (King *et al*., 2000), and is widely recognised as a scientifically legitimate approach to setting environmental flow requirements (Hughes and Hannart, 2003).

The Building Block Method is underpinned by the premise that, under natural conditions, different flows play different roles in the ecological functioning of a river. Consequently, to ensure sustainability, it is necessary to retain key elements of natural flow variation. Hence, so called Building Blocks are different components of flow which, when combined, comprise a regime that facilitates the maintenance of the river in a pre-specified condition. The flow blocks comprise low flows, as well as high flows, required for channel maintenance and differ between "normal years" and "drought years". The flow needs in normal years are referred to as "maintenance requirements" and divided between high and low flow components. The flow needs in drought years are referred to as "drought requirements" (Hughes, 2001). The DRM provides estimates of these building blocks for each month of the year.

In this study, the DRM was used to estimate environmental flow requirements in the river reach between the diversion to the Tis Abay

power stations and the point where the water is returned to the river (Figure 1). This reach includes the Tis Issat Falls. To estimate environmental flow requirements the model needs a naturalized flow series as input. Prior to the construction of the two gate Chara Chara weir (in 1996) outflows from Lake Tana were unmodified and so represent a naturalized flow series. These data were used as input to the model. For the flow over the Falls, the contribution of flow from the Andassa River and the rest of the catchment between Lake Tana and the Falls was added to the Lake Tana outflow series. Some data were missing. Single months of missing data during periods of declining flow were infilled by interpolation. However, in cases where there were consecutive months of missing data or missing data occurred during periods when flows were rising, this was not possible and so the whole year was eliminated from the analyses. A total four months were filled by interpolation and six years were eliminated. Hence, a total of 31 years of data were used as input to the model.

In South Africa, rivers are classified in relation to a desired ecological condition, and flow requirements set accordingly. Six management classes are defined, ranging from A to F. Class A rivers are largely unmodified and natural and class F rivers are extremely modified and highly degraded (DWAF, 1999). Classes E and F are deemed ecologically unsustainable so class D (i.e. largely modified) is the lowest allowed "target" for future status. This classification system is used in conjunction with the building block method and flow requirements are computed accordingly; the higher the class, the more water is allocated for ecosystem maintenance and the greater the range of flow variability preserved. In the current study, to reflect the importance of water abstractions for hydropower production, the desired ecological condition of the Blue Nile was set as C/D (i.e., moderately to largely modified). In contrast to the analyses conducted for the environmental impact assessment, no allowance was made for the aesthetic quality of flows over the Falls.

Flow variability plays a major role in determining environmental flow requirements. Within the model, the long-term variability of wet and dry season flows is based on calculating the coefficient of variation (CV) for all monthly flows for each calendar month. The average CVs for the three main months of the both the wet and the dry season are then calculated and the final CV-Index is the sum of these two season's averages (Hughes and Hannart, 2003). A limitation of the model is that

in computing CV-Index, the model assumes that the primary dry season months are January to March as occurs over much of South Africa. Within the model this cannot be altered. However, for the Blue Nile the key months are August to October and March to May for the wet and dry seasons respectively. To ensure that the model computed a flow variability index closer to reality the input time series of flows was shifted so that each year began in June rather than in October, which is the practice in South Africa. After running, the model outputs were corrected to ensure that model results were applied to the correct months.

RESULTS

Impacts of Flow Regulation

Figure 2 shows the mean monthly flow, measured immediately downstream of the Chara Chara weir, for the three periods investigated. The May 1959 to April 1996 results indicate the extreme seasonal variability in the natural flow regime, ranging from a mean of 346 m^3s^{-1} in September to just 12 m^3s^{-1} in June. On average only 12% of the natural discharge from the lake occurred in the 5 months February to June. In the period May 1996 to December 2000, both wet season flows and dry season flows were significantly higher than occurred in the previous period. The higher dry season flows were a consequence of partial flow regulation by the two-gate Chara Chara weir. The higher wet season flows were a consequence of above average rainfall in these years, particularly in 1998. Mean annual flow in 1998 (196.0 m^3s^{-1}; 6182 Mm^3) was the highest annual discharge measured in the whole 48 year record. The results for the period from January 2001 to December 2006, illustrate the much higher dry season flows and reduced wet season flows arising as a consequence of the full flow regulation by the Chara Chara weir. As a consequence of regulation there is much less variability in flow from the lake. After 2001, 43% of the discharge from the lake occurred in the 5 months February to June.

	May 1959 - Apr 1996	May 1996 - Dec 2000	Jan 2001- Dec 2006
Jan	77.4	127.4	97.6
Feb	53.2	84	98.7
Mar	33.4	57.3	109.3
Apr	20.2	69.1	109.9
May	12.9	41.4	94.3
Jun	11.5	39.1	95
Jul	34.8	75.5	116.5
Aug	168.8	184.6	127.8
Sep	345.9	449	204.4
Oct	309.7	423.8	150.8
Nov	200.7	297.4	122.6
Dec	125.6	177.7	109.3
MAF	116.3	169	119.7
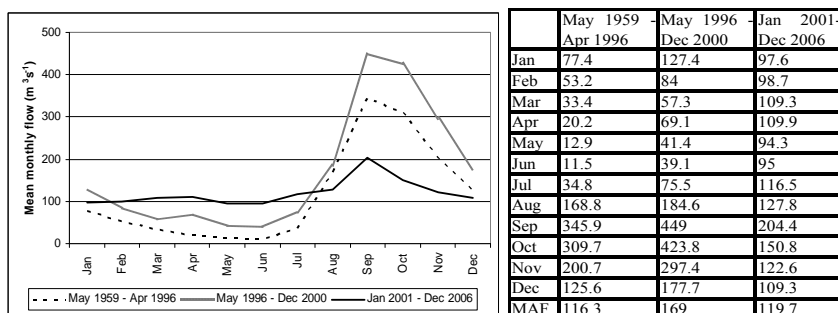
MAF = mean annual flow

Figure 2. Mean monthly flow from Lake Tana for three periods of different flow regulation

Flow duration curves, which show the percent of time that a specified discharge is equaled or exceeded, were derived for the period for which daily data were available (i.e., from January 1973 to December 2006) (Figure 3). These confirm the significant impact of the new seven-gate Chara Chara weir on flow from the lake. Since 2001, there has been a significant increase in flows lower than Q_{50} (i.e. the mean daily flow exceeded 50% of the time) and a significant decrease in flows above Q_{50}. Q_{95} and Q_{90} increased from 9.0 m^3s^{-1} and 11.9 m^3s^{-1} to 59.3 m^3s^{-1} and 64.5 m^3s^{-1} respectively. In contrast Q_{10} and Q_5 decreased from 285.8 m^3s^{-1} and 382.6 m^3s^{-1} to 195.5 m^3s^{-1} and 246.3 m^3s^{-1} respectively.

	Jan 1973 - Apr 1996	May 1996- Dec 2000	Jan 2001- Dec 2006
Q_{95}	9.0	11.3	59.3
Q_{90}	11.9	17.5	64.5
Q_{70}	21.0	49.2	79.3
Q_{50}	54.7	126.2	101.9
Q_{25}	155.1	239.3	136.6
Q_{10}	285.8	449.0	195.5
Q_5	382.6	513.0	246.3
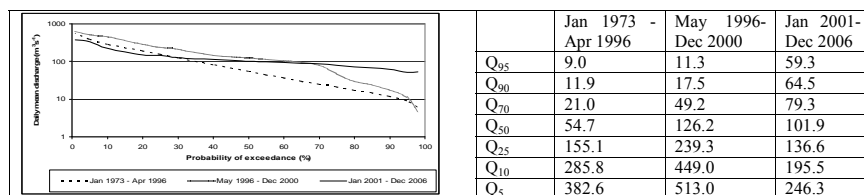
Figure 3. Flow duration curves for the Blue Nile River, at the outlet from Lake Tana. Note that flows are shown on a log scale to illustrate clearly the differences in low flows in the three different time periods

Impact of Hydropower Diversions

The data provided by EEPCO indicate that when only the Tis Abay-I power station was operational (i.e. between 1964 and 2000) average annual turbine discharge was just 192 Mm^3 (i.e. 6.1 m^3s^{-1}).

Throughout this period just 4.5% of the average annual discharge at Tis Abay (4,227 Mm^3) was diverted. Since 2001, when Tis Abay-II came on line, the average annual turbine discharge has increased to 3,090 Mm^3 (i.e. 97.9 m^{3}s^{-1}). This equates to 72% of the average annual discharge at Tis Abay (4,306 Mm^3) between 2001 and 2006.

Diversions to the original Tis Abay-I power station had very little impact on the flows over the Tis Issat waterfall. Between 1964 and 2000 average annual discharge over the Falls is estimated to have been 128 m^{3}s^{-1} (i.e. 4,040 Mm^3). By comparison, between 2001 and 2006 the average annual discharge over the Falls is estimated to have been just 41 m^{3}s^{-1} (i.e. 1,305 Mm^3), with a minimum of just 4.7 m^{3}s^{-1} (i.e. 147 Mm^3) in 2004 and less than 12m^{3}s^{-1} (i.e. 378 Mm^3) in both 2003 and 2005. Between 2001 and 2006, in many months, the mean discharge was less than 50% what it was prior to 2001 (Figure 4).
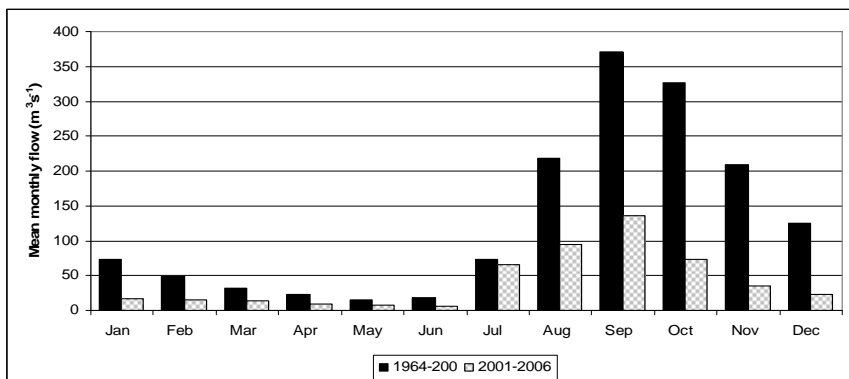
Figure 4. Comparison of flow over the Tis Issat Falls for the periods 1964-2000 and 2001-2006

Environmental Flow Requirements

Figure 5 presents a comparison of the observed time series and the DRM derived environmental flow series for the river reach including the Falls. Results from the model indicate that to maintain the river at class C/D requires an average annual environmental flow allocation of 862 Mm^3 (i.e., equivalent to 22% of the natural mean annual flow) (Table 3). This is the average annual "maintenance flow" calculated from the mean of both the maintenance low flows (i.e. 626 Mm^3) and maintenance high flows (i.e., 236 Mm^3). The drought flows correspond to 11% of the mean annual flow (i.e., 440 Mm^3).
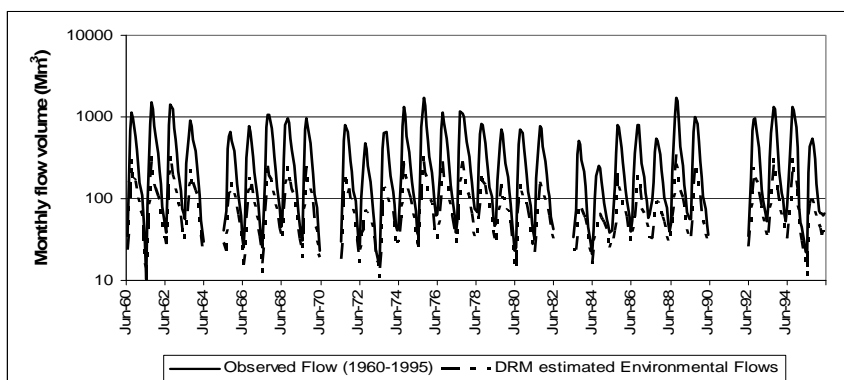
Figure 5. Time series of monthly observed flow and estimate flows
(1960-1995) for the reach of Abay River that includes the Tis Issat Falls
(log scale on the y-axis).

Table 3. Summary output from the desktop reserve model applied to the
reach of the Tis Issat Falls based on 1960-1995 monthly flow series.

Annual Flows (Mm^3 or index values)					
MAR		4017	**Total Environmental flow**	= 862 (22% MAF)	
S.D.		1293	**Maintenance Low flow**	= 626 (16% MAF)	
CV		0.322	**Drought Low flow**	= 440 (11% MAF)	
BFI		0.37	**Maintenance High flow**	= 236 (6% MAF)	
	Observed flow (Mm		**Environmental flow requirement (Mm^3)**		
			Maintenance flows		Drought flows
Month	Mean	CV	Low	High	Total	
Jan	217	0.35	68	0	68	48
Feb	135	0.34	56	0	56	39
Mar	97	0.31	42	0	42	30
Apr	58	0.29	28	0	28	20
May	42	0.35	22	0	22	16
Jun	44	0.46	20	1	21	10
Jul	180	0.43	27	11	39	20
Aug	590	0.38	51	33	83	36
Sep	946	0.39	77	115	192	54
Oct	839	0.36	84	33	117	59
Nov	526	0.33	78	31	109	55
Dec	345	0.33	74	12	86	52

For the period 2001 to 2006, average annual flows over the Falls (i.e., 1,305 Mm^3) exceeded the annual total maintenance flow requirements predicted by the model (i.e., 862 Mm^3). However, more detailed analysis shows that in most months average flows were significantly less than the environmental flow requirements predicted by the model. For several months average flows were less than 70% of the estimated requirement (Table 4). Only in months July to October (i.e., wet season months) did the average flow over the period 2001 to 2006 exceed the recommendation of the DRM (Table 4; Figure 6). This suggests that, in recent years, dry season flows have been insufficient to maintain even basic ecological functioning of this reach of the Abay River. Furthermore, even though the average over the period exceeds the DRM recommendation, in several years even the wet season flow was a lot less than recommended. For example, in September and October 2005, flows over the Falls were estimated to have been just 44 Mm^3 and 7.6 Mm^3 respectively; less than even the recommended minimum drought flows.
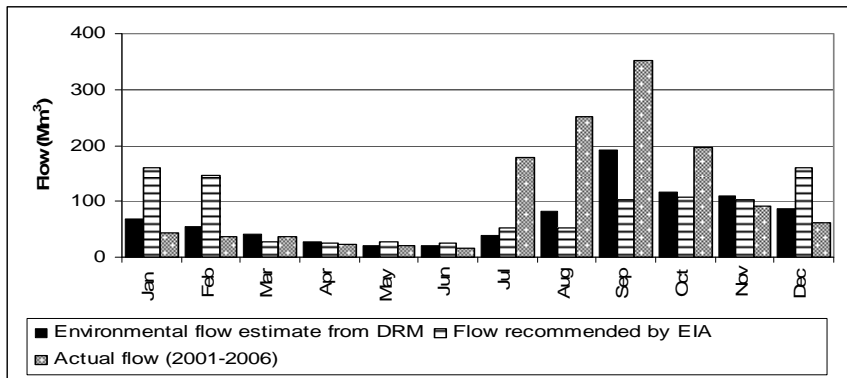
Figure 6. Comparison of mean monthly environmental flow requirement estimated using the DTM, with the recommendation of the EIA and the actual flows over the Falls.

Table 4. Comparison of environmental flow requirements computed by the DTM and observed mean monthly flows in the river reach that include the Falls, between 2001 and 2006.

Month	Over the Tis Isaat Falls		
	Total maintenance requirements	**Observed flows**	**Ratio of observed to environmental flow requirement**
	Mm³/month	**Mm³/month**	
Jan	68	44	0.64
Feb	56	36	0.64
Mar	42	36	0.85
Apr	28	22	0.81
May	23	21	0.96
Jun	21	16	0.76
Jul	39	178	4.57
Aug	83	252	3.03
Sep	192	352	1.83
Oct	117	196	1.68
Nov	109	92	0.85
Dec	86	61	0.71
Annual	862	1305	

DISCUSSION

Operation of the Chara Chara weir has altered the flow regime of the Abay River. Between the outlet from Lake Tana and Tis Abay, the regulation has significantly increased dry season, and significantly decreased wet season, flows. No ecological surveys have been conducted, but there is little doubt that the reduced inter-seasonal variability will have had an impact on the ecology of the river, benefiting those species that depend on more regular flows whilst adversely impacting those species adapted to seasonal drying. The changes in flow are likely to have affected sediment transport and altered water chemistry and temperature regimes. Although the consequences of these changes may not be apparent for many decades, it is possible that they will modify, amongst other things, channel morphology and substrate composition, as well as river biota (McCartney *et al*., 2000).

In addition to ecological impacts, the change in flow regime has also had social impacts. For instance the reduced wet season flows have resulted in less flooding. In a recent survey, local communities expressed

satisfaction at the reduction in flooding, which in the past used to destroy their crops (Gebre *et al*., 2008). Some farmers have also benefited from the higher dry season flows since they enable increased dry season irrigation. This means that they are able to produce a dry season crop, part of which is used for household consumption and part of which is sold (Shiferaw, 2007). The increased dry season flows have also benefited women who have to collect household water supplies from the river (Shiferaw, 2007). Thus riparian communities located between the weir and Tis Abay, largely perceive the weir to have brought livelihood benefits.

Since 2001, flows in the reach containing the Falls have been significantly reduced, in both the wet and dry seasons, as a consequence of diversions to the power stations. Again, although no ecological surveys have been conducted there is little doubt that the reduction in flows will have had very severe consequences for many species including aquatic macrophytes, benthic organisms and fish (Seddon 2000; Staissny 1996). The reduced flows are also very likely to have had adverse impacts on many riparian species. By changing the magnitude and extent of inundation and altering land-water interaction the change in flows may have disrupted plant reproduction. Over-time it may allow the encroachment of upland plants previously prevented by more frequent flooding (Nilsson *et al.* 1997).

The change in flows over the Falls has also had social consequences. Surprisingly the number of tourists visiting the Falls increased in recent years (Shiferaw, 2007). This is partly the result of greater numbers of tourists generally in Ethiopia and partly because the Falls are still promoted as a major tourist attraction. Many of the tourists who visit Bahar Dar are unaware that flows over the Falls have decreased. According to local people, many visitors are now unhappy with the visual spectacle and, because they are annoyed, refuse to buy locally made handicrafts. In the past the selling of these products contributed significantly to the income of many local people. Although a few people have gained employment at the power stations many have not. Consequently the loss of income from tourists has had a negative impact on the livelihoods of many local people which has not been compensated through alternative opportunities (Gebre *et al*., 2008). The local community also complain that they have no access to electricity, despite the fact that the power stations are located very close to their village. Furthermore, development opportunities (e.g. a school and

clinic) promised when Tis Abay-II was built, have not been forthcoming. Consequently, many people living in the village closest to the power station feel they have gained nothing and have in fact lost as a consequence of the construction of the weir and the power stations (Gebre *et al.*, 2008).

The DRM has been used extensively in South Africa. Its use in other countries is limited, but it has been applied in Swaziland, Zimbabwe, Mozambique (Hughes and Hannart, 2003) and Tanzania (Kashaigili *et al.* 2007). For the current study, the accuracy of the model results cannot be substantiated without further study. However, given that it is underpinned by empirical equations developed specifically for South Africa, and is only intended to be a "low-confidence" approach, the results must be treated with caution. Nonetheless, despite the limitations, in the absence of quantitative information on the relationships between flow and the ecological functioning of the river ecosystem, it is a valuable first estimate of environmental flow requirements in this reach of the river. To improve the estimate detailed studies need to be undertaken to investigate the ecological sensitivity of the river to flow modification throughout its length from the Lake Tana outlet to the Falls and, indeed, downstream of the point where the diverted flows are returned to the river. Beyond this, the social implications of altered flow regimes should be carefully evaluated. In addition, other detailed studies should be conducted at different locations on the Abay and its tributaries, and also on other rivers, to calibrate and improve the DRM for more general application on the Nile and elsewhere in Ethiopia.

With many more dams planned in Ethiopia in the near future it is essential to ensure that environmental and social safeguards are developed and implemented (Hathaway, 2008). Ethiopia would therefore benefit from a long-term program to build capacity in environmental flow assessment. As a starting point, this should be developed using the expert opinion of national ecologists, hydrologist, social scientists and others who have detailed knowledge and experience of the country's rivers. Even if the initial results are uncertain, attempting environmental flow assessment utilising an expert panel approach, would develop team building and assist interactions between different disciplines (King *et al.*, 2000). This would be a useful first step in the development of national expertise in environmental flow assessment.

CONCLUSION

In recent years the Tis Abay power stations have been vital for electricity production and have contributed significantly to the economic development of Ethiopia. However, although detailed studies have not been conducted, there is little doubt that operation of the Chara Chara weir, in conjunction with diversions to the power stations, has resulted in some negative environmental and social impacts. Although preliminary and requiring verification through further research, the results presented in this paper illustrate the viability of using the DRM to provide a scientific base for an initial assessment of water allocation to mitigate some of the negative consequences. Much more detailed hydroecological and social studies are now required to validate these findings.

Environmental flows are increasingly recognized as a critical component of sustainable water resources management. However, in Ethiopia, in common with many developing countries, their estimation and implementation is impeded by lack of data and expertise. Given the dam building program currently being planned and implemented in Ethiopia, the country would be wise to initiate a capacity building program in environmental flow assessment.

ACKNOWLEDGEMENTS

REFERENCES

Awulachew, S. B, McCartney, M., Steinhaus, T, Mohamed,A. 2008. A review of hydrology, sediment and water resources use in the Blue Nile Basin, IWMI Research Report, Forthcoming.

DWAF (Department of Water Affairs and Forestry), 1999. Resource Directed Measures for Protection of Water Resources – Volume 8: Classification System for Water Resources, DWAF, Pretoria, South Africa.

Gebre, A., Getachew, D. and McCartney, M. 2008. Stakeholder Analysis of the Chara Chara Weir, Lake Tana. International Water Management Institute, Addis Ababa, Ethiopia. 54 pp.

Gustard, A., Bullock, A. and Dixon, J.M. 1992. Low flow estimation in The United Kingdom. Institute of Hydrology Report 108. Institute of Hydrology, Wallingford.

Hathaway, T. 2008. What cost Ethiopia's Dam Boom? International Rivers Network. California, USA. 26pp.

Howard. H; Bellier, C, Kennedy, R. and Donkin. 1997. Environmental Impact Assessment, Federal Democratic Republic of Ethiopia, Ministry of Water Resources medium scale Hydropower plant study project Tis Abay II joint venture

Hughes, D.A. and Hannart, P. 2003. A desktop model used to provide an initial estimate of the ecological in-stream flow requirements of rivers in South Africa. Journal of Hydrology 270 (3-4) 167-181.

Hughes, D.A. 2001. Providing Hydrological Information and Data Analysis Tools for the Determination of the Ecological In-stream Flow Requirements for South African Rivers. Journal of Hydrology, 241 (1-2), 140-151

Hughes, D.A. and Münster, F. 2000. Hydrological information and techniques to support the determination of the water quantity component of the ecological reserve for rivers. Report to the Water Research Commission by the Institute for Water Research, Rhodes University. WRC Report No. 867/3/2000, Pretoria, South Africa.

JICA (Japanese International Corporation Agency) 1977. Feasibility Report on power development at Lake Tana Region, Ethiopia

Kashaigili, J.J., McCartney, M.P. and Mahoo, H.F. 2007. Estimation of environmental flows in the Great Ruaha River Catchment, Tanzania. Journal of Physics and Chemistry of the Earth 32, 1007-1014.

Kebede, S., Travi, Y., Alenayehu, T. and Marc, V. 2006. Water balance of Lake Tana and its sensitivity to fluctuations in rainfall, Blue Nile Basin, Ethiopia. Journal of Hydrology 316, 233-247.

King, J., Tharme, R.E. and de Villiers, M.S. 2000. Environmental flow assessments for rivers: manual for the building block methodology. Water Research Commission Technology Transfer Report No. TT 131/00, Pretoria, South Africa.

King, J. and Louw, M.D. 1998. Instream flow assessments for regulated rives in South Africa using the Building Block Methodology. Aquatic Ecosystem Health and Management, 1, 109-124.

McCartney, M.P., Sullivan, C. and Acreman, M. 1999. Ecosystem impacts of large dams. A review for IUCN 80 pp.

Melkamu, A. 2005. Reservoir operation and establishment of reservoir

rule for Lake Tana. (M.Sc.Thesis) Addis Ababa University

Mohr, P.A., 1962. The Geology of Ethiopia. University College Press, Addis Ababa 268 pp.

Nilsson C, Jansson R and Zinko U. 1997. Long-term responses of river-margin vegetation to water-level regulation. Science 276, 798-800.

Richter, B.D., Baumgartner, J.V, Wiginton, R. and Braun, D.P. 1997. How much water does a river need? Freshwater Biology 37, 231-249.

Shiferaw, A. 2007. Environmental flow assessment at the source of the Blue Nile River, Ethiopia. MSc thesis. Addis Ababa University, Ethiopia. 64 pp.

Seddon M.B. 2000. Molluscan biodiversity and the impact of large dams. IUCN, Gland.

Staissny M.L.J. 1996. An overview of freshwater biodiversity: with some lessons from African fishes. Fisheries 21, 7-13.

Tharme, R. 2003. A global perspective on environmental flow assessment: emerging trends in the development and application of environmental flow methodologies for rivers. River Research and Applications 19:397-441.

Tharme, R.E. and King, J.M. 1998. Development of the Building Block Methodology for Instream Flow Assessments and supporting research on the effects of different magnitude flows on riverine ecosystems. Water Research Commission Report No. 576/1/98.

World Bank, 2006. World Bank, 2006. Ethiopia: managing water resources to maximize sustainable growth. World Bank Agriculture and Rural Development Department. Washington D.C.

World Bank, 2003. Environmental Flows: concepts and methods. Water Resources and Environment: Technical Note C1. The World Bank Washington DC, USA.

BLUE NILE BASIN HYDROLOGY RELATIONSHIP TO CLIMATIC INDICES

Wossenu Abtew[1], Assefa M. Melesse[2] and Tibebe Dessalegne[3]

[1]Principal Engineer, South Florida Water Management District, West Palm Beach, USA; email:wabtew@sfwmd.gov
[2]Assistant Professor, Department of Environmental Studies, Florida International University
[3] Senior Engineer, BEM Systems

ABSTRACT

Climatic teleconnections to regional rainfall and stream flows have been correlated and respective predictions have become part of water management decision in regions such as South Florida in the United States. As changes in the climate is expected to have dramatic changes in temperature and precipitation, the ability to predict and make water resources management decisions is more critical than ever. For some parts of the world, these hydrologic changes may present major challenges to continue to provide for human water needs while balancing concerns about ecological integrity. Studies have shown that climatic indices associated with the prevailing climate have a very strong correlation to regional hydrology. Climatic teleconnections to the Blue Nile River Basin, Ethiopia, hydrology was evaluated using spatial average basin rainfall and Blue Nile flows at Bahir Dar. The El Niño Southern Oscillation index (ENSO) relationship using sea surface temperature (SST) anomalies in region Niño 3.4 and variation in air pressure between the western and eastern tropical pacific was used for analysis. The analysis indicates that the Upper Blue Nile Basin rainfall and flows are connected to the ENSO index. High rainfall and high flows are likely to occur during La Niña years and dry years are likely to occur during El Niño years at a confidence level of 90 to 95 percent. Extreme dry and wet years are very likely to correspond with ENSO event as given above. The great Ethiopian famine of 1888-1892 corresponds to one of the strongest El Niño years, 1888. The recent drought years of 1965, 1972, 1983, 1987 and 1997 in Ethiopia correspond to strong El Niño years. In this paper a new approach is proposed on how to classify the strength of ENSO events. A cumulative SST index value ≥ 5 and cumulative southern oscillation index value of ≤ -7 indicate strong El

Niño. A cumulative SST index value of $\leq$ -5 and cumulative southern oscillation index of $\geq$ 7 indicate strong La Niña.

Key Words: Blue Nile Basin, ENSO, El Niño, La Niña, Climate Teleconnection

INTRODUCTION

Variation in the weather in the short term and climate in the long term has been a mystery for man kind for a long time and many cultures attribute the phenomena to super natural forces. In the last century, significant progress has been made in understanding the ocean, the atmosphere and land processes, inter-relationships and regional teleconnections. Modeling of these complex systems and prediction of weather and climate has achieved significant progress with a lot more work left for more understanding of the various processes and reduction of uncertainties in weather forecasting and climatic predictions for practical applications. Weather is defined as the state of the atmosphere or meteorological conditions as temperature, humidity, atmospheric pressure, wind speed and precipitation. Weather forecasts are made up to 10 days into the future with forecasting error increasing for longer periods. Climate is the weather averaged over longer temporal and spatial domain for months to years to centuries (Garbrecht and Piechota, 2006). Prediction of hydrometeorology using global climate indices or other methods has become a necessity for water resources management in a future where water supply per capita declines and the impact of variability of the resource increase. Prediction of temporal and spatial variation of precipitation and runoff is necessity for water resource management and planning to mitigate impacts of droughts and floods.

Analysis of climate variation is evaluated from directly measured hydrometeorology data such as rainfall, stream flow, stream water level, groundwater level, and air and water temperature. Significant climatologic variation can be derived from historical events of droughts and floods. Ice cores and tree rings analysis have been used to derive long-term climatic data. Sea surface temperature variation and pressure gradient records have been correlated to regional weather and climatic variations. One of the earliest works done on global climatic relationships is by Walker and Bliss in the early 1930s (Walker and Bliss, 1930). They studied world weather and developed statistical

correlation equations to predict a weather parameter at a part of the world using different weather parameters of other parts of the globe as variables. One case is where they related Honolulu and Port Darwin atmospheric pressure, the Nile flood and Indian monsoon to air temperature in western Canada. Sun spot number was one of the variables in their studies.

The Atlantic Multidecadal Oscillation (AMO) between warm phase and cool phase is shown to explain 10 percent of the Mississippi River outflow and 40 percent of Lake Okeechobee inflow in the United States. ENSO, AMO and Pacific Decadal Oscillation have been linked to the climate of South Florida (Enfield et al., 2001, Zhang and Trimble, 1996). Not only atmospheric, oceanic and land processes affect the climate but also solar activity has link to hydrometeorology variation (Trimble et al., 1997, Soon et al., 2000). Solar sunspot activity is measured by the number of sunspots and by the magnitude of geomagnetic activity. Solar sunspot activity has an average cycle of 11 years with reversal in the sun's magnetic field between cycles. Trimble et al. (1997) have shown that the runoff inflows into Lake Okeechobee of South Florida are associated to solar activity as estimated by the number of sunspots and geomagnetic activity. Other researchers have also shown evidence in the connection between solar activity and the earth's climate (Friis-Christensen and Lassen, 1991).

Seleshi and Zanke (2004), in their analysis of recent changes of rainfall in Ethiopia, concluded that Ethiopian Highlands June-September rainfall is positively correlated to the Southern Oscillation Index and negatively correlated to the equatorial eastern pacific sea surface temperature. The variables for linear regression equations developed to forecast Ethiopian summer rains included sea surface temperature (SST) anomalies of the western Indian Ocean, the tropical eastern Indian Ocean, and Niňo3.4 SST anomalies for the preceding March, April and May rainfall (Gissila et al., 2004).

EL NIŇO-SOUTHERN OSCILLATION (ENSO) INDICES

El Niño is an ocean-atmosphere phenomenon where the cooler eastern pacific worms up once every two to seven years. The increase in eastern pacific sea surface temperature (SST) is attributed to the weakening of the easterly trade winds which results in warm water from the western pacific moving to the east. An average of $+0.4^{o}$ C deviation

from average SST for three or more consecutive months indicates ENSO event. Based on SST anomalies in Niño 3.4 region (5°N-5°S, 120° - 170°W,) periods 1951, 1953, 1957, 1958, 1963, 1965, 1966, 1969,1972, 1977, 1979, 1980, 1982, 1983, 1986, 1987, 1990-94, 1997 and 2002-2006 were El Niño years and most correspond to periods presented in Trenberth (1997). The weather impact of El Niño varies with the strength of ENSO. In South Florida there is strong correlation between dry season rainfall (November-May) and ENSO events. Rainfall is significantly higher during El Niño and drier during La Niña events. Climatic prediction based on this correlation has become part of water management decision (Obeysekera et al., 2007). Thomas (2007) developed regression equations forecasting Colorado River stream flow using climatic index as variables for application in water resource management.

Monthly climatic index as ENSO do not amplify the strength of the event. Cumulative index clearly indicate the comparative strength of a climatic phenomenon such as SST. In this study, a new approach, the use of cumulative climatic index, is presented for analysis of relationship of annual rainfall and stream flow and climatic indices. Based on historical records of ENSO events, a cumulative SST index of ≥ 5 indicates strong El Niño and a cumulative SST index of $\leq$ -5 indicates strong La Niña. SST cumulative annual index is shown in Figure 1 for Niño 3.4.

Southern Oscillation (SO) is the variation in air pressure between the western and eastern tropical pacific. The SO index (SOI) is a measure of air pressure difference between Tahiti in the east and Darwin, Australia to the west as compared to historical average of the differences. Negative differences indicate El Niño conditions as lower pressure in the eastern Pacific is associated to warmer water and weakened easterly trade winds. Positive SOI correspond to negative SST index and La Niña. The proposed ENSO event strength indicators are cumulative values of 7 and -7 for La Niña and El Niño, respectively. Figure 2 depicts cumulative annual SOI.
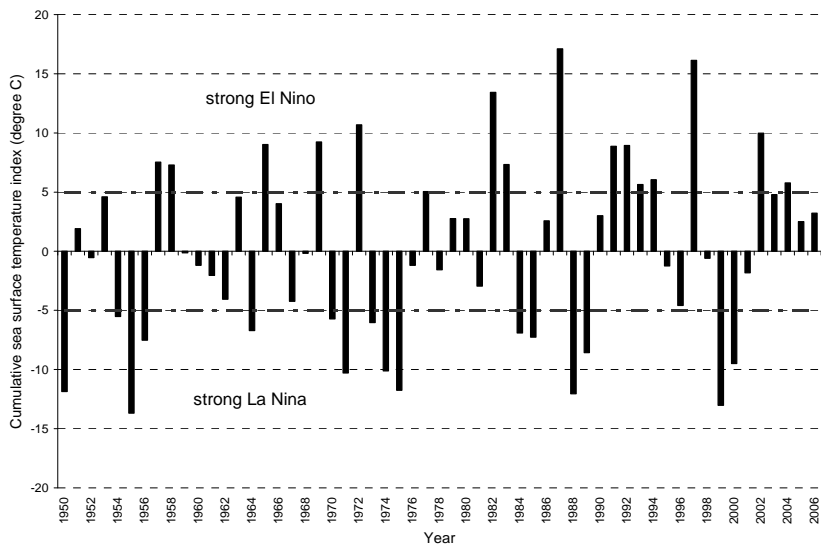
Figure 1. Cumulative annual sea surface temperature Index (Niño 3.4).
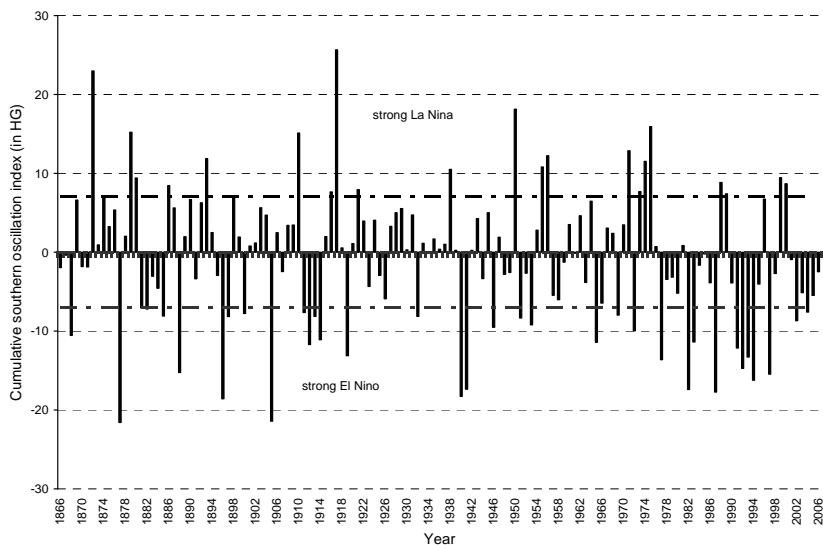
Figure 2. Cumulative annual southern oscillation index.

UPPER BLUE NILE BASIN RAINFALL

The Blue Nile River drainage basin is approximately 324,530 km^2 (Peggy and Curtis, 1994). The Upper Blue Nile River Basin (Figure 1) is 176,000 km^2 in area (Conway, 2000). The major tributaries in Ethiopia are Gilgel Abbay, Megech, Ribb, Gumera, Beshlo, Woleka, Jemma, Muger, Guder, Chemoga, Fincha, Dedessa, Angar, Dura and Beles. Figure 3 depicts the Upper Blue Nile River Basin and its tributaries in Ethiopia. The Upper Blue Nile Basin is relatively wet with annual mean rainfall of 1423 mm (1960-2002) with standard deviation of 125 mm. The rainfall statistics is based on 32 rainfall stations with varying length of record (Abtew et al., 2008). Conway (2000) reported a mean annual rainfall of 1421 mm based on 11 gauges for a period of record of 1900-1998. The Upper Blue Nile Basin annual rainfall is depicted in Figure 4. Out of the nine driest years (1984, 1962, 2002, 1986, 1982, 1965, 1995, 1961 and 1994) all occurred during El Niño years except 1984 and 1962. 1984 followed strong El Niño years of 1982-1983. Out of the 12 wettest years (1973, 1964, 1971, 1977, 1993, 1975, 1974, 1998, 1978, 1967, 1996 and 1988) ten occurred during La Niña years except in 1977 and 1993. Conway (2000) reported that dry years show a degree of association with low values of SOI (El Niño). Eldaw et al.,(2003) reported that the July to October flows of the Nile are correlated to the Pacific SST and Guinea rainfall. Other studies that relate El Nino events to Ethiopian droughts are reviewed in Gissila et al. (2004). Jury et al. (2002) have shown that African rainfall variation is related to El Niño-Southern Oscillation Indices (ENSO).
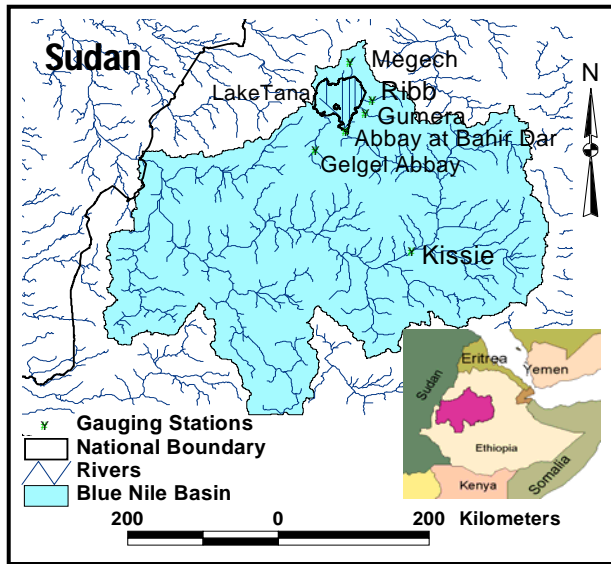
Figure 3. The Upper Blue Nile Basin in Ethiopia.
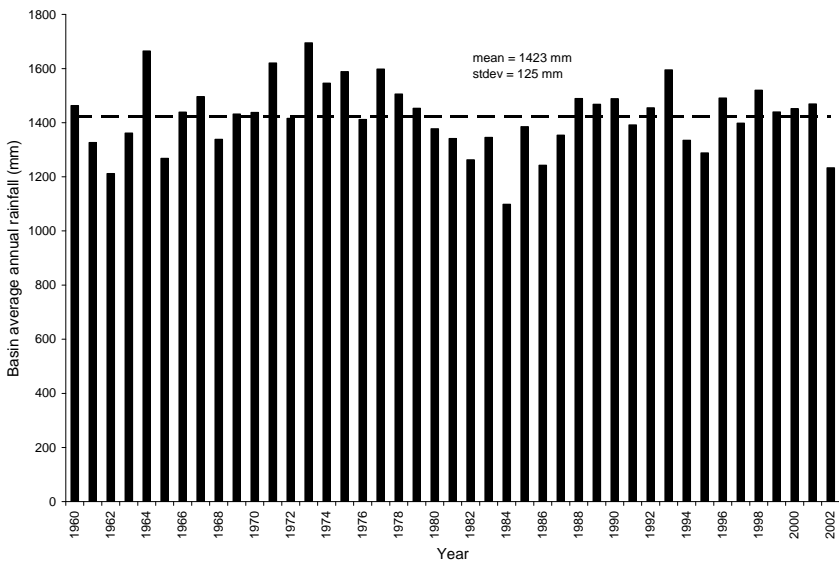
Figure 4. Upper Blue Nile Basin average annual rainfall (1960-2002).

In this study, a scatter plot of cumulative annual ENSO index and annual Upper Blue Nile Basin rainfall deviations shows that wet years are more likely to occur in La Niña years and dry years occur during El Niño years (Figure 5). In 27 years out of 42 years of record, below average rainfall corresponded with El Niño years and above average rainfall occurred during La Niña years. A test of significance of a binomial proportion can be applied to show that the events are not random (Snedecor and Cochran, 1980). With an assumed probability of 0.5 that correspondence of ENSO events to rainfall deviations in a year is a random event as the null hypothesis, Chi square (χ^2) test of goodness of fit can be performed. The following equation expresses the test (Eq. 1).

$$\chi^2 = \frac{\sum (f - F)^2}{F} = \frac{(r - np)^2}{np} + \frac{(r - np)^2}{nq} \qquad (1)$$

Where n is the number of years of analysis (42); f is observed number of years where annual rainfall deficit corresponds to ENSO event (r=27); n-r is the number of years where rainfall deficit does not correspond to ENSO event (n-r=15); F is expected frequency of random correspondence assuming a probability of 0.5 (np=21); F is also expected number of years rainfall deficit not corresponding with any ENSO events (nq=21). The computation results in $\chi^2 = 3.41$. Compared to the expected (χ^2 Table) value at 1 degree of freedom, the null hypothesis that the rainfall deficit has 50/50 chance to correspond to any ENSO event is rejected at 0.10 significant test level.
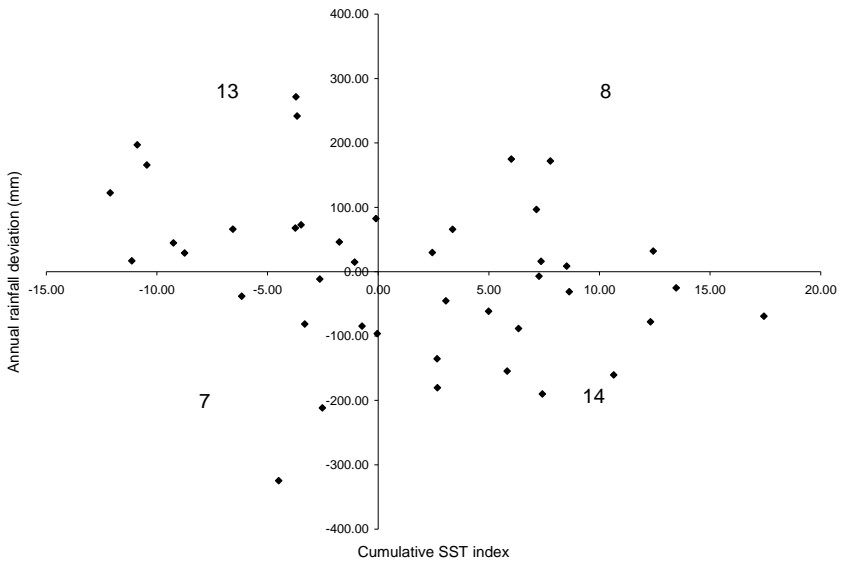
Figure 5. Relationship of cumulative annual ENSO Indices and Upper Blue Nile Basin annual rainfall deviations.

Anecdotal records of Ethiopian droughts correspond to ENSO events. The great Ethiopian famine of 1888-1892 (Pankhurst, 1966) corresponds to one of the strong El Niño years, 1888. In recent years, 1965, 1972-73, 1983-84, 1987-88 and 1997 were drought years with low agricultural production and impacts on millions of people and the environment (Seleshi and Zanke, 2004). Years 1965, 1972, 1983, 1987 and 1997 correspond to strong El Niño years. Analysis of the Nile flows at Aswan from 1872 to 1972 showed correspondence of high flows with negative SST and low flows with positive SST anomalies for the months of September, October and November (Eltahir, 1996).

BLUE NILE FLOW AT BAHIR DAR

Flow data with some missing data and few questionable data was available for the Blue Nile flow at Bahr Dar for the period 1961-2003. Questionable data and missing data were estimated by interpolation and filling with flows of similar pattern months in other years. An example of questionable data is data where the mean is less than the minimum. The annual flow ranged from a maximum of 6,489 million m^3 to a minimum of 975 million m^3. The mean annual flow is 3,850 million m^3 and the standard deviation is 1,353 million m^3. Figure 6 depicts annual flow of the Blue Nile at Bahir Dar. Seventy one percent of the flows are from July through November while 70 percent of the rainfall at Bahir Dar occurs between June and September. Seventy three percent of the Upper Blue Nile Basin areal average rainfall occurs between May and September. Comparison of annual flow deviations with cumulative Nino 3.4 sea surface temperature index shows that wet years are likely to occur during La Niña years and dry years are likely to occur during El Niño years (Figure 7). Seven of the nine highest annual flow years occurred during La Niña years (1964, 1999, 1988, 2000, 2001, 1975 and 1962). Also, seven of the driest nine years occurred during El Niño years (1964, 1999, 1988, 2000, 2001, 1975 and 1962.
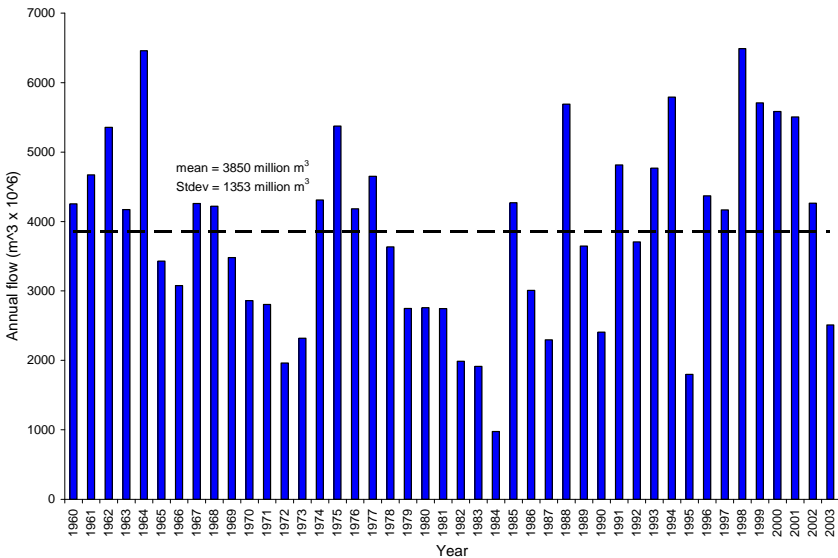
Figure 6. Blue Nile annual flows at Bahir Dar.

85

The Chi square value based on equation (1) with n, r, F values of 43, 29, 21.5 is 5.25. This test is significant at 5 percent level indicating that below average flows correspond to El Niño years and above average flows correspond to La Niña years. Figure 8 shows comparison of monthly flows of the Blue Nile at Bahir Dar with three months moving average ENSO (SST). El Niño events occur when sea surface temperature deviation is greater or equal to +0.50 ^{0}C and La Niña events occur when sea surface temperature deviation is less than or equal to -0.50 ^{0}C. Average flows during La Niña years are 25% higher than flows during El Niño and neutral years.
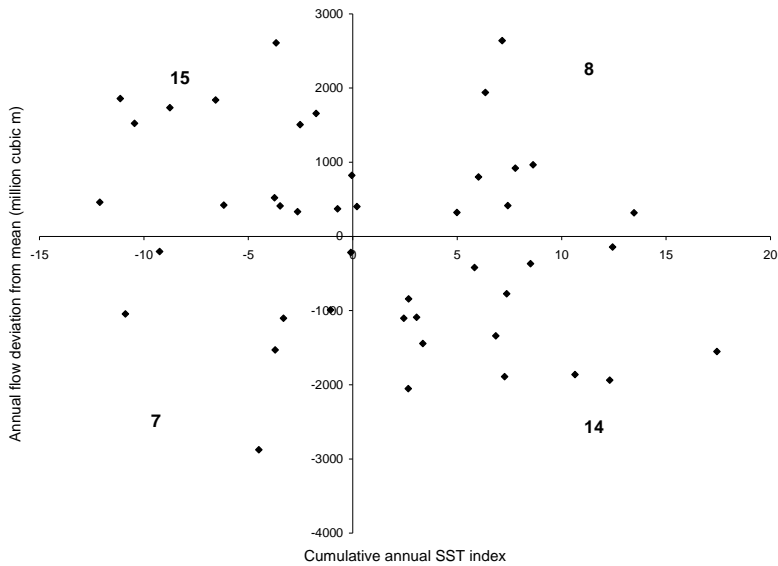
Figure 7. Relationship of cumulative annual ENSO Index and Blue Nile at Bahir Dar annual flow deviations.
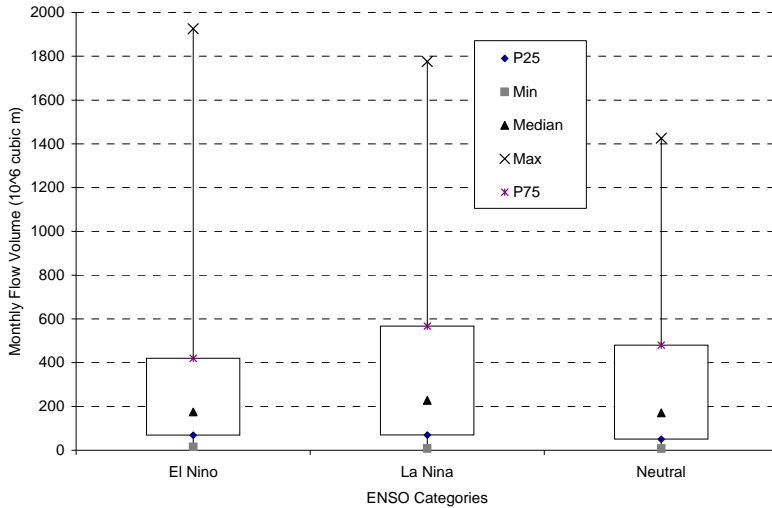
Figure 8. Relationship of month moving average ENSO (SST) index and Blue Nile at Bahir Dar monthly flow.

SUMMARY

Climatic teleconnections to the Blue Nile hydrology was evaluated using basin average rainfall and Blue Nile flows at Bahir Dar. The El Niño Southern Oscillation index (ENSO) relationship using sea surface temperature anomalies in region Niño 3.4 and variation in air pressure between the western and eastern tropical pacific was used for analysis. The analysis indicates that the Blue Nile Basin rainfall and flows are connected to the ENSO index. High rainfall and high flows are likely to occur during La Niña years and dry years are likely to occur during El Niño years. Extreme dry years are highly likely to occur during El Niño years and extreme wet years are highly likely to occur during La Niña years. The prediction of El Niño and La Niña relatively has higher certainty than predicting basin rainfall and runoff. Identifying teleconnections to a region's hydrology has practical applications for water resources management. In this paper a new approach is proposed on how to classify the strength of ENSO events. A cumulative SST index value ≥ 5 and cumulative southern oscillation index value of ≤ -7 indicate strong El Niño. A cumulative SST index value of ≤ -5 and cumulative southern oscillation index of ≥ 7 indicate strong La Niña.

REFERENCES

Abtew, W., A.M. Melesse and T. Dessalegne. 2008. Characteristics of Monthly and Annual Rainfall of the Upper Blue Nile Basin. Paper presented at the Nile Basin Hydrology and Ecology under Extreme Climatic Conditions, June 16-19, 2007, Addis Ababa, Ethiopia.

Conway, D. 2000. The Climate and Hydrology of the Upper Blue Nile River. The Geographical Journal. Vol. 166(1):49-62.

Eldaw, A.K., J.D. Salas and L.A. Garcia. Long-Range Forecasting of the Nile River Flows Using Climatic Forcing. Journal of Applied Meteorology. Vol. 42:890-904.

Eltahir, E.A.B. 1996. El Niño and the Natural variability in the Flow of the Nile River. Water Resources Research. Vol. 32(1):131-137.

Friis-Christensen, E. and K. Lassen. 1991. Length of the Solar Cycle: An Indicator of Solar Activity Closely Associated with Climate. Science. Vol. 254:698:700.

Garbrecht, J.D and T.C. Piechota. 2006. Climatic Variations, Climate Change, and Water Resources Engineering. ASCE. Reston Virginia.

Gissila, T., E. Black, D.I.F. Grimes and J.M. Slingo. 2004. Seasonal Forecasting of the Ethiopian summer Rains. International Journal of Climatology, 24:1345-1358.

Jury, M.R. and D.B. Enfield. 2002. Tropical Monsoons around Africa: Stability of El Niño-Southern Oscillation Associations and Links with Continental Climate. Journal of Geophysical Research, Vol. 107, No. C10, 3151.

Obeyesekera, J., P. Trimble, C. Neidrauer, C. Pathak, J. VanArman, T. Strowd and C. Hall. 2007. Consideration of Long-Term Climatic Variability in Regional Modeling for SFWMD Planning and Operations. G. Redfield (ed.). The 2007 South Florida Environmental Report. Chapter 2: Hydrology of the South Florida Environment. South Florida Water Management District. West Palm Beach. FL.

Pankhurst, R. 1966. The Great Ethiopian Famine of 1888-1892: a new assessment Part one. Journal of the History of Medicine and Allied Sciences XXI, 95-124.

Peggy, A.J. and D. Curtis. 1994. Water Balance of Blue Nile Basin in Ethiopia. Journal of Irrigation and Drainage Engineering. Vol 120(3):573-590.

Seleshi, Y. and U. Zanke. 2004. Recent Changes in Rainfall and Rainy
        Days in Ethiopia. International Journal of Climatology, Vol.
        24:973-983.

Snedecor, G.W. and W.G. Cochran. 1980. Statistical Methods. The Iowa
        State University Press.   Ames, Iowa.

Thomas, B.E. 2007. Climatic Fluctuations and Forecasting of
        Streamflow in the Lower Colorado River Basin. Journal of the
        American Water Resources Association Vol. 43(6):1550-1569.

Trenberth, K.E. 1997. The Definition of El Niño. Bulletin of the
        American Meteorology Society, Vol. 78(12):2771-2777.

Trimble, P., E.R. Santee and C. Neidrauer. 1997. Including the Effects of
        Solar Activity for more Efficient Water Management: An
        Application of Neural Networks. Special Report. South   Florida
        Water Management District. West Palm Beach, FL.

Walker, G.T and E.W. Bliss. 1930. World Weather IV. Vol. 3(24):81-95.

Zhang, E.Y. and P. Trimble. 1996. Forecasting Water Availability by
        Applying Neural Networks with Global and Solar Indices.
        Proceedings of the 16th Annual American Geophysical Union.
        Hydrology Days. 1-13.

CLIMATE CHANGE PREDICTIONS FOR EAST AFRICA – CERTAINTY, UNCERTAINTY, AND RECOMMENDATIONS

G. L. Geernaert
Los Alamos National Laboratory

EXTENDED ABSTRACT

During "average" years, the Nile River basin drains about 3.3 million km^2 terrain that includes 81,500 km^2 lakes and 70,000 km^2 swamps in the 10 riparian nations of Burundi, DR Congo, Egypt, Eritrea, Ethiopia, Kenya, Rwanda, Sudan, Tanzania, and Uganda. The mean annual rainfall is estimated at 2,000 billion m^3, resulting in an annual flow of about 84 billion m^3 at Aswan Dam in southern Egypt. Very little Nile River water reaches the Mediterranean Sea; and there is tremendous interannual variability in rainfall amounts.

Interannual variability is enormous. In most regions of the Nile Basin, the typical interannual rainfall variability is of order 50%; compounded with sequential dry years, the available water for agriculture, energy, and other activities is slowly diminishing and with a large interannual variability.

Climate predictions for East Africa mirror most of the rest of the world, i.e., a general warming of up to 2C in 2050 and by 5C in 2100. The warming will not be homogeneously distributed; e.g., western parts of Ethiopia are expected to warm more rapidly than the eastern part of Ethiopia; and both Sudan and Egypt are likely to experience a warming of order 2C by 2050. For precipitation, most models suggest that Sudan and northern Ethiopia will experience severe drying; these precipitation predictions, however, are based on tremendous uncertainty. Since water supplies represent the ultimate indicator of regional stability, we will attempt in this presentation to explore the dynamics governing East African precipitation variability, based on a combination of climate predictions and future changes in population pressure on water resources.

Precipitation in the horn of Africa is governed in large part by the interconnectivity of the dynamics related meteorological phenomena, e.g.:

(a) the Somali jet and sea surface temperature patterns, that in turn exhibit an ENSO correlation;
(b) the Mascarene High Pressure system over the Indian Ocean, that in turn exhibits an ENSO correlation;
(c) The African Easterly Jet, with origins in tropical southeast Asia;
(d) the South Atlantic High Pressure system (St. Helena High); and
(e) midlatitude low pressure systems that sweep towards tropical Africa.

The challenge is to build conceptual models of the drivers that affect future climate states in east Africa, e.g., ENSO, Somali jet, etc. Once the conceptual models are collectively tested in GCMs of sufficient spatial resolution will the community be capable of refining more certain statements of the future climate and impact on water resources.

APPLICATION OF A PHYSICALLY-BASED WATER BALANCE MODEL ON FOUR WATERSHEDS THROUGHOUT THE UPPER NILE BASIN IN ETHIOPIA

Collick, Amy S.[1], Easton, Zach M.[2], Adgo, Enyew[3],
Awulachew, Seleshi. B[4], Zeleke, Gete[5] and Steenhuis, Tammo S.[6]

[1]Assistant Professor, Bahir Dar University, Bahir Dar, Ethiopia,
asc38@cornell.edu
[2]Research Associate, Cornell University, Ithaca, NY USA,
zme2@cornell.edu
[3]Director Natural Resources, ARARI,; Bahir Dar Ethiopia Currently,
Professor, Bahir Dar University, enyewadgo@yahoo.com
[4]IWMI Regional Representative, Sub-regional Officer for Nile Basin &
Eastern Africa, Addis Ababa, Ethiopia, s.bekele@cgiar.org
[5] Coordinator, Rural-Urban Linkages Thematic Research Area of the
Global Mountain Program, Addis Ababa, Ethiopia, g.zeleke@cgiar.org
[6]Professor, Cornell University, Ithaca NY USA, tss1@cornell.edu

ABSTRACT

Local hydrological knowledge is important because of the lack of long duration, continuous hydrological data at a small watershed scale and the extensive variability in rainfall and resulting runoff over the Ethiopian landscape. A better understanding of the local hydrological characteristics of different watersheds in the headwaters of the Nile River is of considerable importance because of the collective interest in the access to its water resources and the need to improve and augment development and management activities of these resources. A simple hydrological model for watersheds in varying locales at daily and weekly time scales was developed to gain insight into the hydrologic conditions of the larger Nile River basin. This model appears to be useful as a tool for planning watershed management and conservation activities. The water balance model was based on the Thornthwaite and Mather procedure, using rainfall and evaporation as major inputs, available water storage and contributing area as partitioning factors within the watershed. Discharge data from three SRCP watersheds and one near Sekota were used for calibration of the storage coefficient. The Nash-Sutcliffe efficiencies along with other comparison statistics showed that model performed well compared to other water balances of the upper Nile Basin done with a monthly time step. The model was able to represent daily

discharge values well. Despite the large distance between the test watersheds, the input parameter values were remarkably similar. Good quality data, even for short durations, were key to the effective modeling of runoff in the highland watersheds.

INTRODUCTION

A better understanding of the hydrological characteristics of different watersheds in the headwaters of the Nile River is of considerable importance because of the international interest in the utilization of its water resources, the need to improve and augment development and management activities of these resources, and the potential for negative impacts of climate change in the future. Conflicting views of water resource utilization and ownership has been challenging the development of appropriate management of the Nile River Basin for the countries most dependent on its resources including Egypt, Sudan, and Ethiopia. Egypt's agricultural production and domestic requirements depends primarily (99%) on the waters of the Nile River, withdrawing up to 55.5 billion cubic meters per year (Geith and Sultan, 2002); Sudan's agriculture also relies heavily on these waters; while Ethiopia, at the Nile's headwaters, is interested in further developing the water resources to meet development needs and attain "water security" through equitable sharing among the Nile countries (Yacob Arseno and Imeru Tamrat, 2005). Only 5% of Ethiopia's surface water (0.6% of the Nile Basin's water resource) is being currently utilized by Ethiopia while cyclical droughts cause food shortages and intermittent famine (Yacob Arseno and Imeru Tamrat, 2005). The Ethiopian highlands are the origin, or source, of much of the river flow reaching the Nile River, contributing greater than 60% of Nile flow (Ibrahim, 1984 and Conway and Hulme, 1993) possibly increasing to 95% during the rainy season (Ibrahim, 1984).

Since the Nile River discharge is highly dependent on the flow generated in the Ethiopian highlands, increases in utilization of water resources and management activities which alter discharge levels in Ethiopia may have a significant effect on overall flow of the Nile, and consequently become a considerable concern for populations in the regions downstream in Sudan and Egypt. Thus, a better understanding of flow characteristics throughout the upper Nile River's basins in Ethiopia accounting for seasonal differences and different time and spatial scales is necessary. There have been limited studies on basin characteristics,

climate conditions, and hydrology of the Upper Nile Basin in Ethiopia (Antar et al., 2006; Mishra and Hata, 2006; Johnson and Curtis, 1994; and Conway, 1997) with very few published hydrological data from the Blue Nile and its tributaries (Conway, 2000; Mishra et al., 2003). To remedy these data gaps, several hydrological models of the Blue Nile basin that simulate the hydrological responses of extreme climate and environmental changes have been developed, including the work by Conway (1997), Deksyos Tarekegn and Abebe Tadege (2005), Johnson and Curtis (1994), Kebede et al. (2006), and others. A water balance was clearly the model format of choice for these studies owing to its simplicity and effectiveness even with limited data inputs. Both Mishra et al. (2004) and Conway (1997) developed grid-based water balance models for the Blue Nile Basin using monthly discharge data from the El Diem Station in Sudan, near the Ethiopian border, in order to study the spatial variability of flow parameters and the sensitivity of runoff to changes in climate, respectively. The El Diem Station collected discharge data from the whole Blue Nile Basin in Ethiopia from the 1960s to the present. The data provide limited insight into spatial variability and distribution of flow within the basin itself. As an alternative to large-scale basin modeling, hydrological modeling of watersheds is also relevant, especially to gain insight into the particular hydrological conditions throughout the larger basin and how these conditions affect the important agricultural practices of many Ethiopian communities. Johnson and Curtis (1994) used short-duration (<4 years) discharge data from several smaller basins or watersheds throughout the Blue Nile Basin for the development of a monthly water balance to better understand the rainfall-runoff relationship for forecasting purposes and to develop a method for calibrating water balance coefficients for those small basins lacking any available data. Very few other examples of small scale water balance modeling in the Blue Nile Basin have been published.

The development of a simple but robust hydrological model for small watersheds in varying locales at short time scales (daily and weekly) can provide insight into the hydrologic conditions of the different watersheds composing a larger river basin and be useful as a tool for watershed management planning and conservation activities. This study offers a simple water balance model developed on daily and weekly time steps for watersheds in and around the Blue Nile Basin using daily precipitation and evaporation and continuous and intermittent

manually-gauged discharge data. The hydrological characteristics of the watersheds and the quality of the data are assessed.

DESCRIPTION OF WATERSHEDS

Soil Conservation Research Programme (SCRP) Research Sites

With the support of the Swiss Agency for Development and Cooperation, the SCRP was established in 1981 aiding the Ethiopian government in their efforts to improve the soil and water conservation activities employed to counteract land degradation (SCRP, 2000a). Environmental, climatic, and social data were collected at SCRP research sites established throughout Ethiopia. Three monitoring sites were selected for this study: Anjeni, Andit Tid, and Maybar. Table 1 summarizes the geographical location, description, and data used in the model from these three sites, and a map in Figure 1 illustrates their location in Ethiopia. The three catchments were well above 2,000 meters above sea level (masl) but under 500ha in area.

Table 1. Location, description, and data used in the model from the three SCRP research sites (SCRP, 2000a, b, c)

Research site	Location (Region)	Area (ha)	Elevation (masl)	Data type	Length of data
Andit Tid	39º43'E, 9º48'N (Shewa)	477.3	3,040 – 3,548	RF, ET, Q (daily)	1987 -1998 (1995 – 96 incomplete)
Anjeni	37º31'E, 10º40'N (Gojam)	113.4	2,407 - 2507	RF, ET, Q (daily)	1988 - 1997
Maybar	37º31'E, 10º40'N (South Wollo)	112.8	2,530 – 2,858	RF, ET, Q (daily)	1988 -2001 (1990 – 91 incomplete)

Yeku Watershed

The Yeku Watershed lies between 12°30'46" and 12°32'14" North and 39°03'10" and 39°04'28" East, approximately 15 km south of the small town of Sekota in the eastern section of the national regional state of Amhara in Northern Ethiopia, or more specifically, in the Sekota Woreda in the Wag-Himra zone of Amhara region (Figure 1). With elevations from approximately 2000 to 2400 meters above sea level (masl), the watershed immediately drains into the Yeku and Weleh Rivers, eventually to the Tekeze River, one of the tributaries to the Atbara River in northern Ethiopia which flows to the Nile River in the Sudan, north of the confluence of the Blue and White Niles. Settlements, moderately to intensely cultivated fields, bush and shrub areas, grassland, and rock outcrops compose the landscape. The water flows of the Yeku River that runs through the watershed were measured daily and during storm events. Rainfall, pan evaporation, and various soil characteristics were measured as part of a hydrological assessment in collaboration with Amhara Micro-Enterprise Development, Agricultural and Research Extension, and Watershed Management (AMAREW) project. The Yeku Watershed serves as an example of the community-based integrated watershed resource management facilitated by the AMAREW project and in cooperation with several national and international collaborators.
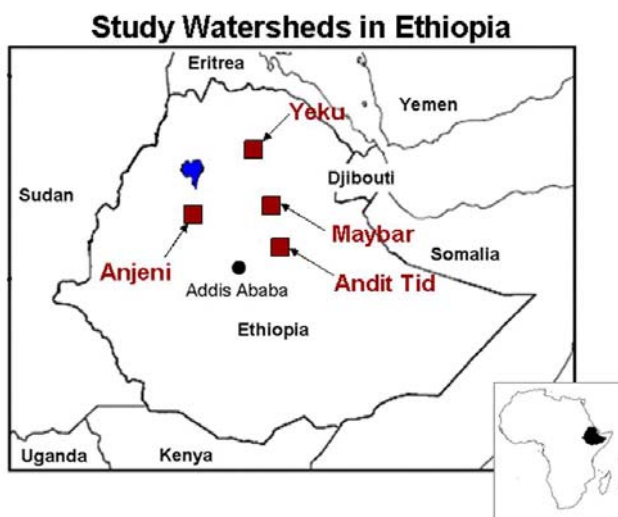
Figure 1. Map of the four watersheds, including the SCRP sites and Yeku.

96

MODEL DEVELOPMENT

A simple water balance model was developed to investigate the runoff contribution from a semi-arid highland watershed. The model was developed for daily, weekly, and monthly time steps using data from different areas of the upper Nile Basin in Ethiopia. The model estimates the moisture storage, *S,* (mm), of the topmost layer of the soil using precipitation, *P,* (mm/day), potential evapotranspiration, *PET,* (mm/day), *R* (mm/day) saturation excess runoff at the watershed outlet, percolation to the subsoil, *Perc* (mm/day), and previous time step storage, $S_{t-\Delta t}$, (mm), as inputs. The basic water balance for the catchment area for a time step of Δt is:

$$S = S_{t-\Delta t} + (P - AET - R - Perc)\Delta t \qquad \text{Equation 1}$$

Daily *P* measured by both automatic rainfall gauges and manual gauges was compared to daily *PET* values, either observed (pan evaporation) or estimated using the Penman-Monteith evaporation as available data dictated.

During wet periods when either the rainfall exceeds evapotranspiration (i.e., P > PET) or the moisture content is above field capacity, the moisture storage, S_t, is determined from the addition of the previous day's moisture $S_{t-\Delta t}$ (mm), to the difference between precipitation, *P*, and potential evapotranspiration, PET, during the time step. Conversely, when evaporation exceeds rainfall (i.e., P < PET) and the moisture content of the soil is at or below field capacity (dry conditions), actual evapotranspiration, *AET*, (mm), decreases linearly from the potential rate at field capacity to zero at the wilting point (Thornthwaite and Mather, 1955; Steenhuis and van der Molen 1986):

$$AET = PET\left(\frac{S_t}{AWC}\right) \qquad \textit{Equation 2}$$

The available soil storage capacity per unit area, AWC, (mm) is defined as the difference between soil storage at wilting point and at field capacity and varies according to soil characteristics (e.g., porosity, bulk density). Based on Equation 2, the soil surface storage at time step Δt can be written as an exponential function:

$$S_t = S_{t-\Delta t}\left[\exp\left(\frac{P-PET}{AWC}\right)\right] \quad \text{when } P < PET \qquad\qquad \text{Equation 3}$$

When rain exceeds evaporation and fully saturates the soil, any moisture above field capacity runs off, and can be determined by adding the change in soil moisture from the previous time step ($S_{t-\Delta t}$) to the difference between precipitation and actual evapotranspiration $S_{t-\Delta t} + P - AET$.

The AWC can be considered uniform across the watershed when the water balance is applied in temperate climates (Steenhuis and van der Molen, 1986). In monsoon climates, this assumption is not valid because the watershed dries out differentially, and runoff occurs only when the soil saturates, so that AWC is not uniform across the watershed. In the modeling framework, this means that various parts of the watershed will start to contribute to runoff at different times. In other words, there is a "threshold" effect in which the effective storage of an area must be satisfied before runoff is created, and these thresholds may vary within the watershed (i.e., from lowest to highest effective storage). Thus, in the model, we break the watersheds up into a series of regions. In each region, there is a "tipping bucket" that must be filled before runoff from a particular area is generated. Total runoff during a storm event is the sum of the runoff contributed by each of these sections of watershed.

We assumed that above field capacity the excess moisture is partitioned between percolation and runoff. Percolation, *Perc*, (mm d^{-1}) is added to a baseflow reservoir, RS, (mm d^{-1}) at each time step (Easton et al., 2007):

$$RS_t = RS_{t-\Delta t} + \left(Perc_t - BF_{t-\Delta t}\right)\Delta t \qquad\qquad \text{Equation 4}$$

where *BF* is the modeled baseflow (mm d^{-1}). Baseflow is modeled using a linear reservoir method as:

$$BF_t = RS_t \frac{[1- \exp\ (-a\ \Delta t)\,]}{\Delta t} \qquad\qquad \text{Equation 5}$$

where *a* (d^{-1}) is the recession coefficient, a property of the aquifer, and can be calibrated from the baseflow recession curve, and *Δt* is the time step.

DATA INPUTS

Rainfall and evaporation were key input data for modeling all the watersheds. Each watershed was also broken up into a series of contributing areas with different AWC, or effective soil moisture storage. This storage must be filled before runoff is created. Two base flow parameters—base flow recession and fraction of the water in excess of AWC being lost to percolation—were also applied. The models are most sensitive to rainfall data. The rainfall data and other model inputs and parameters from each of the watersheds are described in the following sections.

SCRP Research Sites

Daily and weekly hydrology data, including rainfall (P), evaporation (ET), and discharge (Q) from three research sites (Maybar, Anjeni, and Andit Tid) in the Nile basin were used to calibrate and validate the model. Hydrological data were collected from 1982 to 1993 with overlap for all three stations from 1985 to 1992. The SCRP watersheds all receive >1000mm of rainfall per year, which is sufficient for sustainable crop production. Annual rainfall in both Andit Tid and Maybar watersheds commonly occurs in a bimodal distribution, with short rains between March and May contributing only 20.1 and 19.3% of the total rainfall. In the Anjeni watershed, annual rainfall mostly occurred between May and October in a unimodal distribution. The major rainfall during the recognized main rainy season between June and September accounts for 60.7, 74.8, and 66.9% of the total annual rainfall in Andit Tid, Anjeni, and Maybar watersheds, respectively. Table 2 provides a summary of the hydrological data for the three SCRP monitoring sites. Anjeni has the highest rainfall (P) and highest potential evapotranspiration (PET) of the three catchments. However, discharge was slightly less than discharge at Andit Tid. Andit Tid has a humid climate with the lowest average daily temperature of the sites, but the greatest average annual discharge. Along with the lowest rainfall, Maybar also produced the lowest annual runoff (430.4mm). The annual runoff coefficients from the data for Maybar, Anjeni, and Andit Tid are 29.8, 42.0, and 48.9%, respectively.

Table 2. Annual hydrological data for the SCRP monitoring sites

	°C	P (mm)	PET (mm)	Q (mm)
Andit Tid	12.6	1,478.4	1,158.9	722.5
Anjeni	16.0	1,661.9	1,554.7	699.6
Maybar	16.4	1,443.5	1,177.5	430.4

Yeku Watershed

In the Yeku watershed, daily rainfall and evaporation data collected from June, 2003 to May, 2004 were used in addition to daily and storm event flows. During the hydrological assessment, daily rainfall was measured using both automatic and manual rain gauges. Potential evaporation rates were determined from pan evaporation values adjusted with a pan coefficient of 0.75. Runoff was gauged manually. Daily flow and storm events were measured near the terminus of two small rivers (Weleh tributary and Yeku) flowing through the watershed and totaled into weekly discharge volumes.

The Yeku Watershed is characterized by low rainfall and high evaporation compared to the other data sets in this study. Annual rainfall of 625mm and annual evaporation of 1954.2mm (average 5.1mm day-1) from June 2003 to May 2004 with nearly half (48.1%) falling in the month of August 2003. The annual rainfall amount was relatively low considering an average annual rainfall of 800mm was previously mentioned (Kindu Mekonnen et al., 1999). However, we have been unable to locate reliable hydrological data from studies other than from the current research. Nevertheless, rainfall is very erratic and varies spatially and temporally over the watershed and throughout the region. As with rainfall, flow in the Yeku River is limited to the rainy season and persists at a very low rate after the rains have ended. Interflow is responsible for the extended flow as the excess water stored in the watershed is released, but this flow averaged only 0.06mm per day until it ended in October. Since base flow was so limited, both base flow parameters (fraction to percolation and recession coefficient) were both zero.

CALIBRATION AND VALIDATION

The data were divided to provide data sets for both calibration and validation: SCRP watersheds from 1988 to 1989 (Maybar has substantial missing data during 1990 and 1991) and from 1992 to 1996 for validation. The selection of the data sets for calibration and validation was based on the availability of continuous data. Because flow data for the Yeku watershed only were available for one season, these data were used to test the potential of the model only. Better calibration and validation is contingent on the availability of further data from Yeku. Available water content (AWC) and contributing area (percent of total area) of each of the watershed sections were key parameters used to calibrate the model.

Besides AWC, the parameters affecting baseflow were also varied if flow was known to persist well beyond the end of the rainy season. For example, in the Yeku River, baseflow was nearly nonexistent after October; so the recession coefficients described in Equation 6 and the baseflow reservoir (R_s) in Equation 5 were zero. The fraction of the water in excess of AWC being lost to percolation varied between the different watersheds, ranging from 0.4 in Yeku to as high as 0.8 in the SCRP watersheds. Table 3 summarizes the parameters applied in the model and provides the range of rainfall (P), potential evapotranspiration (PET), and discharge (Q obs) observed in the watershed for the time step (daily, weekly, or monthly) of the available data. Because most of the available data began in January, well into the dry season, the initial soil moisture was considered to be zero. Streams completely dried up in Yeku, but not in the SCRP watersheds, which at least maintained flow of >1 mm during each month.

By running model simulations varying AWC for each section of the watershed with varying contributing areas, percolation fraction, and recession coefficient, a model efficiency coefficient (E) commonly used to assess the predictive power of hydrological models developed by Nash and Sutcliffe (1970) was optimized. For each watershed, an efficiency coefficient closest to one was sought because it indicated a good match between modeled and observed data. The performance of the model during the calibration and validation period was evaluated using the efficiency coefficient (E), the root mean squared error (RMSE), and the normalized root mean squared error (RMSE%), or the RMSE divided by the range of the observed data. Means, standard deviations, minimums,

and maximums of the model input parameters, including precipitation, evaporation, and discharge, were also calculated.

MODEL RESULTS

Available precipitation, potential evapotranspiration, and daily, weekly, or monthly discharge data of the eight watersheds were incorporated into the model in several Microsoft Excel spreadsheets. The water balance model developed in this study was tested with data from different areas of Ethiopia with varying time steps. The model generated discharge from existing precipitation (P) and evaporation (E) data using available water content as a storage threshold within subdivided areas of a watershed. For each time step, an example of the model and the value of each of the parameters used for the different watersheds will be presented.

Table 3. Description of the parameters and range of values for the parameters for the different study watersheds.

		Andit Tid	Anjeni	Maybar	Yeku
	Time Step	Daily	Daily	Daily	Weekly
Adjusted P (mm)					
maximum		101.7	87.0	71.4	143.0
minimum		0.0	0.0	0.0	0.0
mean		4.1	4.5	3.8	12.0
PET (mm)					
maximum		7.0	7.0	7.0	66.8
minimum		0.0	0.3	0.0	18.0
mean		3.2	4.2	3.2	37.1
Q (mm)					
maximum		60.8	29.3	37.9	27.6
minimum		0.0	0.1	0.0	0.0
mean		2.4	1.9	1.1	3.3
Watershed partitions					
Available water content (mm)		20 – 700	100 – 4,000	150 – 4,000	10 - 700
Initial Soil Moisture (mm)		0.0	0.0	0.0	0.0
Baseflow estimation					
Fraction of excess to percolation		0.8	0.8	0.8	0.4
Recession coefficient		0.2	0.1	0.1	0.0

SCRP Watersheds: Daily Time Step

The Soil Conservation Research Programme (SCRP) monitoring watersheds provided the most comprehensive data compared, and the modelled period for this time step extended from 1988 to 1996. These watersheds are also small in area, all less than 500ha. Figures 3 A – C

presents comparisons of the modelled discharge and the actual measured discharge (observed) data for Andit Tid (A), Anjeni (B), and Maybar (C) watersheds for daily values.

The model often underestimates discharge generated from rainfall events greater than 50mm d^{-1}. The comparison of observed and predicted data in includes the calibration and validation periods, and in the case of Anjeni, the validation period was decreased to two years (1992 – 1994) because there were missing data in 1995 and 1996. However, validation periods for Andit Tid and Maybar extended from 1992 to 1996. The calibration period for all three SCRP sites was the same (1988 – 1989). The Anjeni was divided into four separate areas with AWC ranging from 100 to 4000 mm and area contributions from 15 – 40%. The AWC and area were optimized for each watershed. Although located several hundred kilometers apart, the three watersheds' parameters were nearly identical except one value for the Andit Tid watershed. While Anjeni and Maybar tended to have higher AWC values, Andit Tid required a very low value of AWC in place of the highest value (4000 m with an area contribution of 20%) of Anjeni and Maybar. This was necessary to increase the area of shallow storage to compensate for the steep slopes and subsequent higher runoff coefficient in Andit Tid, and the lower AWC in 85% of this watershed's area allows for less storage and the generation of high runoff. A summary of the AWC and area contributions for the three SCRP sites is available in Table 4. The shallow storage in over half the area of the watersheds simulated the higher runoff response producing more runoff while the deeper storage capacity in 35% of Anjeni and Maybar may be necessary to offset shallower slopes and lower runoff coefficient in these watersheds.
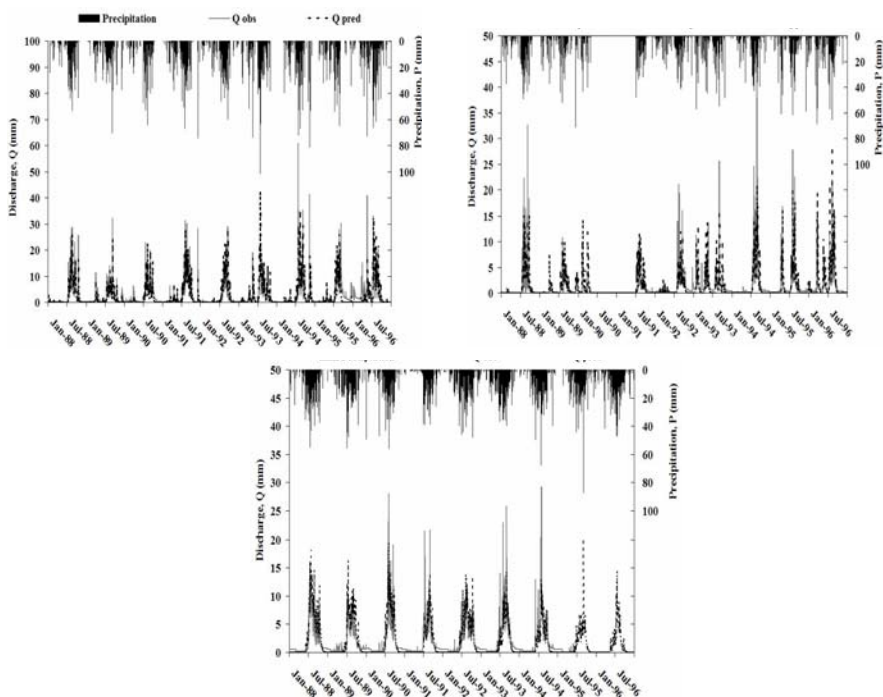
Figure 3. Comparison of observed and predicted river discharge, Q, and rainfall from 1988 to 1996 in the A) Andit Tid Watershed, B) Anjeni Watershed, and C) Maybar Watershed. Observed discharge data was lacking from 1995 and 1996 for Anjeni, precipitation and observed discharge data was lacking from 1990 to 1991 for Maybar.

Table 4. Available water content and the area contribution of the different areas in the SCRP watershed sites.

SCRP Monitoring Sites						
	Andit Tid		Anjeni		Maybar	
	AWC, mm	% area	AWC, mm	% area	AWC, mm	% area
Area 1	100	40	100	40	100	40
Area 2	400	25	400	25	400	25
Area 3	10	20	4000	20	4000	20
Area 4	700	15	700	15	700	15

Yeku Watershed: Weekly Time Step

Modeling the Yeku Watershed proved to be the most difficult because continuous data were lacking and the only available data were collected manually at variable time intervals (<1 minute to 30 minutes) during storm events and daily (normal flow) when flow persisted. The Yeku River did not flow from approximately late October until July depending on the amount of rain and duration of the rainy season. Although some storm discharge events were missed especially during the later part of the rainy season (late August 2003) and full hydrographs of each event were not complete, the water balance model did adequately simulate the heavy discharge in late July and early August 2003 (See Figure 4) when data on discharge were adequate.

The AWC were low for the Yeku Watershed with 85% of the area with less than 400 mm of storage (40% of 10 mm AWC, 25% of 400 mm, and 20% of 300 mm), and only 15% at 700 mm. Most of the watershed was intensely cultivated, making it prone to runoff. Furthermore, the ridges of the gullies dissecting the watershed landscape are highly degraded and their soils have hardened severely which amplifies runoff. On the contrary, the high, steep slopes along the boundary of the watershed cover a small area, and these soils have high infiltration capacity, delaying any flow from these areas. Consequently, the storage on these slopes is higher than in other areas of the landscape.

Figure 4. Comparison of observed and predicted discharge from the Yeku River for the 2003 rainy season.

Model Analysis

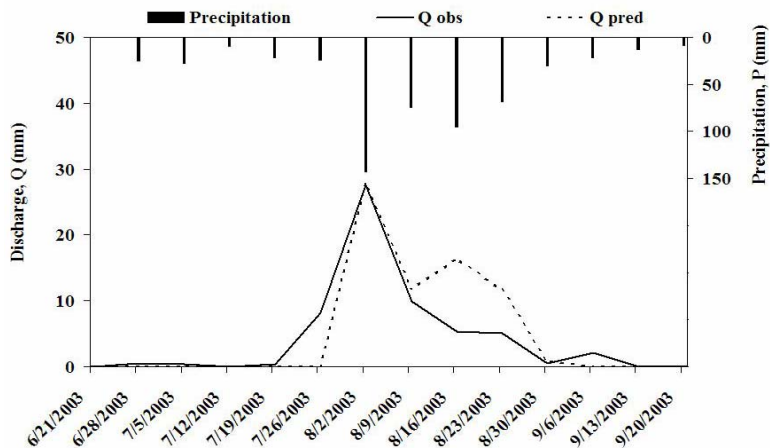Parameterization of the model was based on optimizing the Nash-Sutcliffe efficiency coefficient (E) since it considers how well the fluctuations in modeled discharge coincide with those of the observed data and how well the model predictions agree with the observed data. The root mean squared error (RMSE) and the normalized root mean squared error (RMSE%) indicate the degree to which the model predictions deviate from the observed data. The RMSE has limitations because different time steps were used in the simulations of different watersheds which will affect the RMSE. For example, daily RMSE will be much lower than monthly RMSE because the actual data points represent cumulative discharge over an individual time step. Therefore, RMSE% was used because it considers the error over the range of the data. Together the E and RMSE (%) provide insight into the performance of the model. Table 5A – B provides the statistical analyses of the model performance for all eight watersheds studied (A. SCRP watersheds and B. Yeku Watershed).

The efficiency of the model is quite good in the watersheds, ranging in efficiency from 0.56 to 0.86 in either calibration or validation periods. However, a relatively high efficiency does not always indicate good model performance, as in the case of the Yeku Watershed (Table 5B). Since the single large peak discharge was effectively modeled, the efficiency was relatively high (E = 0.77). However, the RMSE% is very high at 48.3%, and this indicates there is low confidence in the predictive ability of the model results for this watershed due to the pronounced differences between observed and modeled data points. On the contrary, the Maybar watershed has relatively low RMSE (2.5mm and 2.2mm) and RMSE% values (7.7% and 5.8%) indicating confidence in the model; however, the efficiency is low relative to the other watersheds (Table 5A). The efficiency in the Maybar model was strongly influenced by a particular outlier in the difference between the observed and modeled data.

Although the efficiencies were optimized during the calibration period, the model actually resulted in higher efficiencies during the validation period in several cases. Two of the three model performances, which involved calibration and validation periods, resulted on average 10% higher E during validation, ranging from 0.63 – 0.75 for validation and 0.58 – 0.82 for calibration.

The RMSE% values (Calibration, 7.7 – 16.2% and validation, 5.8 – 10.3%) were all higher during the calibration period further supporting the stronger confidence in the model during the validation period of most of the watersheds.

Table 5. Statistical comparison of the modeled and observed discharge data from the four t watersheds

A: SCRP Watershed

	Mean Q (mm)		Std Deviation Q (mm)				
	Observed	Modeled	Observed	Modeled	E *	RMSE (mm)	RMSE%
ANJENI							
Calibration (1988 - 1989)	1.9	2.1	2.6	3.7	0.67	2.6	16.2
Validation (1992 - 1996)	2.1	1.6	3.0	3.1	0.75	3.0	10.3
ADIT TID							
Calibration (1988 - 1989)	1.9	2.1	4.1	4.3	0.82	4.3	13.4
Validation (1992 - 1994)	2.6	2.4	5.5	4.6	0.56	4.6	7.6
MAYBAR							
Calibration (1988 - 1989)	0.8	1.0	2.5	2.2	0.58	2.5	7.7
Validation (1992 - 1996)	1.3	1.2	2.8	2.5	0.63	2.2	5.8

B: Yeku Watershed

	Mean Q (mm)		Std Deviation Q (mm)				
	Observed	Modeled	Observed	Modeled	E * (mm)	RMSE (mm)	RMSE%
Yeku Watershed	4.5	5.3	7.7	8.9	0.77	13.3	48.3

DISCUSSION

Modeling the hydrology of Ethiopian watersheds is challenging because reliable long-term data are not available and our understanding of hydrological responses to precipitation and rainfall is limited. Furthermore, the mechanisms that determine runoff in humid to semi-arid watersheds and waterways are complex. For a model to be of use in promoting development and equitable water allocation, these challenges must be overcome. The model developed in this study depends primarily on the precipitation and evaporation of the watershed area with additional inputs of available water content of various sections of known area within the watershed and particular baseflow coefficients (Easton et al., 2007). Finally, knowledge of discharge is necessary for calibration and parameterization. This model performed as well as other water balance models of the Blue Nile Basin in Conway (1997), Johnson and

Curtis (1994), and Conway and Hulme (1996). Our model has the advantage in being applicable to variable time steps and can be used to predict water balances from smaller watersheds rather than only the behavior of the entire basin collected at the outlet to Sudan. Even though the data requirements are few compared to extensive climate models and land use models requiring GIS capabilities and extensive data sets, good quality input and calibration data are essential for robust model predictions. For example, in the Yeku Watershed, the model producing realistic discharge data using adequate weekly precipitation and weekly evaporation data from a single year (Figure 4). However, missing data and use of insensitive measurement techniques negatively affected calibration and parameterization of the model affecting the reliability of model predictions (Table 5B). On the contrary, input and comparison data from the SCRP watersheds were of good quality, and the model performed well. Legesse et al. (2003) concluded that the input data (precipitation and evaporation) is quite sensitive to error but may be corrected through effective parameterization. In conclusion, long-term historical data may not be absolutely necessary because parameterization and calibration can be successfully achieved with short duration (>1 year, single rainy season, etc.), but good quality input and calibration data.

Data from at least one year provides some insight into the watershed's runoff response and indicates the inherent runoff and flow mechanisms throughout the landscape. Rains in the highlands of Ethiopia are often heavy and intense, producing an immediate response of overland flow and runoff. Immediately following the dry season, when soils have hardened and water barely penetrates the surface, infiltration excess explained the initial flushes of runoff during the first intense storms of the season on degraded soils nearest the gullies and waterways (Dunne and Leopold, 1978). However, as the season progresses, saturation excess likely dominates (Liu et al. 2008). Martinez-Mena et al. (1998) determined these same runoff generation processes (infiltration and saturation excess) were working in watersheds in the semi-arid region of Spain, near the Mediterranean Sea. On less degraded soils, the relationship between total rainfall and the runoff response confirmed the role of saturation excess because after a certain amount of rainfall, the thin soil surface became saturated and runoff was generated (Martinez-Mena et al., 1998; Liu et al. 2008). As the rains continued, the area in which soils were saturated would expand, generating runoff, and thereby increasing the area of the watershed

contributing to runoff.   Consequently, this also increases the runoff
coefficient (runoff to rainfall ratio) of the watershed.   As the watershed
soils continued to saturate, interflow began to influence discharge and
could be seen as an increase in baseflow (or normal flow after a storm
event had fully receded). The interflow and the subsequently enhanced
baseflow would persist for a month or so after the rains had ended in
small, shallow-soil watersheds or for several months in large watersheds
with greater storage capacity. The baseflow parameters (Table 3)
controlled the generation of interflow and baseflow in the model
depending on the flow distribution of the studied stream. The baseflow
parameters (fraction to percolation and recession coefficient) in the
SCRP watersheds having baseflow were quite high at 0.8 to simulate
more water percolating into the soil and available to flow on days
without rainfall. On the contrary, the Yeku River has very minimal
baseflow, and the fraction to percolation was only 0.4 while the recession
coefficient was not used.

Saturation excess is the runoff mechanism inherent in the water
balance based on the Thornthwaite-Mather procedure used for this study
(Thornthwaite and Mather, 1955; Steenhuis and van der Molden, 1986).
Rainfall and evaporation were the primary input parameters. The
available water content (AWC) or storage capacity throughout the
watershed and the extent of their area (% area) determined the amount of
accumulating rain necessary to fill the capacity after which runoff would
be generated. Although the water balance does not incorporate
infiltration excess, the very shallow storage (<10mm) in the different
watersheds may help to include infiltration excess because these storages
are filled and rapidly produce runoff line in those areas with degraded,
hardened soils. However, in the case of the SCRP sites, when rainfall
exceeds 60mm d^{-1}, the model grossly underestimates discharge (Figure
3A - C). This may be caused by the underestimation of infiltration
excess at the onset of the rains on the particularly shallow, degraded soils
of the watershed, the inability of the model to account for 100% runoff
contribution by the watershed after the steady state of the rains (rainfall =
flow) has been reached, or not accounting for the influence of rapid
interflow generation.

Varying the available water content (AWC) allows the effective
rainfall (rainfall minus evaporation) to be partitioned throughout the
watershed and the area (% area) in which they encompass helps to fine
tune the level of contribution from these areas of the watershed. In the

interest of modeling runoff in different watersheds throughout Ethiopia with very limited, but good quality data, the particular time step, area, and similar hydrological conditions, runoff response in particular, indicate the extent of partitioning and fine tuning of runoff response necessary. For example, the three SCRP watersheds were generally similar hydrologically (rainfall amount, runoff response, evaporation, extent of baseflow), covered relatively similar land area, and the time step of the hydrological data was the same. Therefore, the partitioning and fine tuning of modeled runoff in these watersheds were nearly identical (Table 4). Only in Andit Tid, where the response was slightly more rapid, there was a modification to one area of the watershed (Area 3: 10mm with an area of 20%) in order to enhance runoff. Potentially, the approach to determining water balance described in this study could be used with existing data available for watersheds throughout the highland Ethiopia and grouped with other ungauged watersheds of similar physical and hydrological characteristics and likely to require the same partitioning according to runoff response and contributing area throughout the watershed landscape. For example, the Yeku Watershed was the only watershed studied in the low rainfall regime of Northern Amhara with data available for this study. With more data from similar watersheds, a good performing model could be developed for watersheds of similar condition.

REFERENCES

Allen, R. G., L. S. Pereira, D. Raes, and M. Smith (1998), Chapter 2 - FAO penman-monteith equation, in *Crop Evapotranspiration - Guidelines for Computing Crop Water Requirements* Anonymous, FAO, Rome, Italy.

Antar, M. A., I. Elassiouti, and M. N. Allam (2006), Rainfall-runoff modeling using artificial neural networks technique: a Blue Nile catchment case study*, Hydrological Processes, 20*, 1201-1216.

Area of Andit Tid, Shewa, Ethiopia: Long-term monitoring of the agricultural environment 1982 – 1994 (2000)*, Soil Erosion and Conservation Database, Soil Conservation Research Programme (SCRP)*.

Area of Anjeni, Gojam, Ethiopia: Long-term monitoring of the agricultural environment 1984 – 1994 (2000), *Soil Erosion and Conservation Database, Soil Conservation Research Programme*.

Area of Maybar, Wello, Ethiopia: Long-term monitoring of the agricultural environment 1981 – 1994 (2000)*, Soil Erosion and Conservation Database, Soil Conservation Research Programme (SCRP)*.

Conway, D. (1997), A water balance model of the upper Blue Nile in Ethiopia*, Hydrological Sciences, 42*, 265-282.

Conway, D. (2000), The climate and hydrology of the Upper Blue Nile River*, The Geographical Journal, 166*, 49-62.

Conway, D. and M. Hulme (1993), Recent fluctuations in precipitation and runoff over the Nile sub-basins and their impact on main Nile discharge*, Climatic Change, 25*, 127-151.

Conway, D. and M. 1. Hulme (1996), The impacts of climate variability and future climate change in the Nile Basin on water resources in Egypt*, Water Resources Development, 12*, 277-296.

Deksyos Tarekegn and Abebe Tadege (2006), Assessing the impact of climate change on the water resources of the Lake Tana sub-basin using the WATBAL model*, CEEPA Discussion Paper No. 30, Centre for Environmental Economics and Policy in Africa, University of Pretoria*.

Dunne, T. and L. B. Leopold (1978)*, Water in Environmental Planning*, 818 pp., W.H. Freeman, San Francisco, California.

Easton, Z. M., P. Gerard-Marchant, M. T. Walter, A. M. Petrovic, and T. S. Steenhuis (2007), Hydrologic assessment of an urban variable source watershed in the northeast United States*, Water Resources Research, 43*.

Gheith, H. and M. Sultan (2002), Construction of a hydrologic model for estimating *wadi* runoff and groundwater recharge in the eastern desert, Egypt*, Journal of Hydrology, 263*, 36-55.

Ibrahim, A. M. (1984), The Nile – Description, hydrology, control and utilization*, Hydrobiologia, 110*, 1-13.

Johnson, P. A. and P. D. Curtis (1994), Water balance of Blue Nile River Basin in Ethiopia*, Journal of Irrigation and Drainage Engineering – ASCE, 120*, 573-590.

Kebede, S., Y. Travi, T. Alemayehu, and V. Marc (2006), Water balance of Lake Tana and its sensitivity to fluctuations in rainfall, Blue Nile basin, Ethiopia*, Journal of Hydrology, 316*, 233-247.

Kindu Mekonnen, Solomon Gizaw, and Lakew Desta (1999), Yeku Integrated Watershed Development Project: Feasibility Study Report.

Legesse, D., C. Vallet-Coulomb, and F. Gasse (2003), Hydrological response of a catchment to climate and lane use changes in

tropical Africa: Case study south central Ethiopia, *Journal of Hydrology, 275*, 67-85.

Liu, B.M, Yitayew Abebe, O.V. McHugh , A. S. Collick Brhane Gebrekidan and T.S. Steenhuis. 2008. Overcoming limited information through participatory watershed management: Case study in Amhara, Ethiopia. Physics and Chemistry of the Earth 33: 13–21

Martinez-Mena, M., J. Albaladejo, and V. M. Castillo (1998), Factors influencing surface runoff generation in a Mediterranean semi-arid environment: Chicamo watershed, SE Spain, *Hydrological Processes, 12*, 741-754.

Mishra, A. and T. Hata (2006), A grid-based runoff generation and flow routing model for the upper Blue Nile Basin, *Hydrological Sciences Journal, 51*, 191-206.

Mishra, A., T. Hata, and A. W. Abdelhadi (2004), Models for recession flows in the upper Blue Nile River, *Hydrological Processes, 18*, 2773-2786.

Mishra, A., T. Hata, A. W. Abdelhadi, A. Tada, and H. Tanakamaru (2003), Recession flow analysis of the Blue Nile River, *Hydrological Processes, 17*, 2825-2835.

Nash, J. E. and J. V. Sutcliffe (1970), River flow forecasting through conceptual models part I: A discussion of principles, *Journal of Hydrology, 10*, 282-290.

Steenhuis, T. S. and Van der Molen, W.H. (1986), The Thornthwaite-Mather procedure as a simple engineering method to predict recharge, *Journal of Hydrology, 84*, 221-229.

Thornthwaite, C. W. and J. R. Mather (1955), The Water Balance, *Publication #8*.

Yacob Arsano and Imeru Tamrat (2005), Ethiopia and the Eastern Nile Basin, *Aquatic Sciences, 16*, 15- 27.

FLOW ANALYSIS AND CHARACTERIZATION OF THE BLUE NILE RIVER BASIN SYSTEM

[1]Assefa M. Melesse, [2]Wossenu Abtew and [3]Tibebe Dessalegne

[1]Assistant Professor, Department of Environmental Studies, Florida International University, Miami, USA; email:melessea@fiu.edu
[2]Principal Engineer, South Florida Water Management District
[3]Senior Engineer, BEM systems

ABSTRACT

The flow characteristic of the Blue Nile River (BNR) basin is presented. The study presents low and high flow, flow duration curve (FDC) and trend analysis of the BNR and its major tributaries. Different probability density functions were fitted to better describe the low and high flow of BNR at Bahir Dar. Flow duration curves were developed and low flow (below 50% exceedance) and high flow (over 75% exceedance) of the curves were analyzed and compared. The Gravity Recovery and Climate Experiment (GRACE) satellite-based maps of monthly changes in gravity converted to water equivalents from 2003-2006 for February, May and September showed an increase in the moisture influx in the BNR basin for the month of September and loss of moisture in February and May. It was also shown that 2004 and 2005 were drier with less moisture influx compared to 2003 and 2006. Based on the Kolmogorov-Smirnov, Anderson-Darling and Chi-square tests goodness of fit, Gen. Pareto and Gen. Extreme Value and Gumbel Max distributions best describe the low and high flows within the BNR basin. This will be beneficial in developing flow hydrographs for similar ungauged watersheds within the BNR basin. The below 50% and above 75% exceedance on the FDC for five major rivers in addition to BNR showed different characteristics depending on size, land cover, topography and other factors. The low flow frequency analysis at BNR@ Bahir Dar showed 0.55 m^3/s as the monthly low flow with recurrence interval of 10 years.

Key Words: Blue Nile River, low and high flow, PDF, GRACE, flow duration curve, trend analysis

INTRODUCTION

Spanning over ten countries, the Nile River basin (White and Blue Nile Rivers) is the home of over 160 million people. Though Nile River is the longest river in the world, the total volume of water in the Nile River system is much smaller than Amazon and Mississippi Rivers. But the river is historically important and is the livelihood of many people is dependent on it. The basin is characterized as one of the most degraded mainly due to rapid population growth, poverty, political instability, poor watershed management, poor or absence of effective water use policy and frequent natural disasters.

Contributing over 57% of the Nile flow, the Blue Nile River (BNR) is one of the most ecologically, economically and environmentally important rivers of Ethiopia. Regardless of its large volume of water contribution to the Nile River system, the hydrological and other geomorphologic characterization studies are little. Only a few studies of this portion of the watershed have been conducted and the information available on the hydrology of the river and the basin is incomplete (Gamachu, 1977; Conway, 1997, 2000; Bewket and Sterk, 2004; Mishra et al., 2004). The population pressure in the highlands covering the upper basin of BNR, the land-use changes mainly for agriculture and the climate change impact on the hydrology of the region have contributed to the reduction of the flow from the river in recent years. Hydrometeorologic studies of the basin will benefit efforts to manage water and ecological resources of the basin.

Issues Related To Hydrologic Alterations

Water resources of the BNR basin is facing multifaceted problems ranging from destruction of critical forest reserves which maintain the dry season flows to poor water use and watershed management policy, which can lead to watershed and water resources degradation and pollution and also unsustainable utilization of water resources.

Land Clearing/Deforestation

High population growth, limited alternative livelihood opportunities and the slow pace of rural development are inducing deforestation, overgrazing, land degradation and declining in agricultural

114

productivity. The absence of alternative sources of energy other than biomass, has put the available forest resource at risk. Forest clearing in hydrological sensitive areas like that of the head waters can lead to low dry season flows and reduction in recharge.

Siltation/Soil Degradation

Blue Nile River and its tributaries erode the top fertile soils of the highlands and transport thousands of tons of alluvial soil to receiving water bodies and lower basin countries. Sediment from watershed erosion is deposited in Lake Tana, source of BNR. Soil erosion has been the main problem in the reduction of agricultural productivity, poor water quality, loss of biodiversity and water level fluctuation in the basin.

Eucalyptus

Since its introduction over 100 of years ago from Australia, eucalyptus tree has been the main source of fuel wood, timber and construction in Ethiopia. Despite its popularity due to its fast growth even under moisture stress condition, its complex multi-dimensional impacts on soil moisture and ground water, on the soil fertility, on other plant life and on soil fauna undermine potential of land for biological productivity has been criticized. Poore and Fries (1985) indicated the strong surface roots compete vigorously with ground vegetation and with neighboring crops in situations where water is in short supply and largely displace original ecosystems. Van Lill et al. (1980) and Scott and Lesch, (1997) reported that afforestation of grassland (with Eucalyptus grandis and Pinus patula) reduced annual flows at Mokobulaan, Transvaal, South Africa. Zhou et al. (2002) found in Southern China that the water table level in a watershed planted with eucalypts (Eucalyptus exserta) was 80 cm lower than that under a bare watershed, whereas while it was only 30 cm lower in another watershed under mixed forest.

The recent replacement of agricultural fields along the main roads in northwestern Gojjam and at other places with eucalyptus plantation has been going at an alarming rate. It has been found that it is a good source of cash and shown to have more return than agricultural crops. If this practice is continuing, the ecological, hydrological and socioeconomic implications can be higher.

Poor Watershed Management

Land degradation, soil erosion and eventual deposition to surface waters have been attributed to poor watershed management. The need for diverting more water to irrigation canals and construction of dams without proper engineering design addressing location, size and improved watershed management has been a practice in some cases in the region. History has shown that most dam and irrigation project failures are associated with siltation resulting from little or no watershed management activities.

Poor Water and Watershed Management Policy

Land and water use policies which do not result in improved land and water use management and promote the conservation and protection of sensitive water resources, wetlands and recharge areas will contribute to the degradation of watersheds and water resources. Empowering local and national institutions to coordinate and implement appropriate water monitoring, protection and water use activities, lead and coordinate community participation and educate and train water users on the integrated water resources management are important actions yet to be taken.

Poor Headwater and Wetland Protection

Headwaters and wetlands are important parts of the any hydrological systems and their protection is vital for maintaining stream flow and groundwater recharge. Encroaching of these sensitive ecosystems for grazing land and agricultural practice has put the wetlands in danger and led to their shrinkage. Such practice can lead to irregular flows and reduces the minimum flow during the dry season.

Lack of Baseline Data/Information

Unlike part of the Nile basin in the lower basin, the upper Blue Nile River basin in Ethiopia has little baseline information on its biological resources, hydrological and hydraulic characteristics of the river. Information on soils, land cover and other socio-economic settings are limited and scattered. Sediment and water quality data and detailed biodiversity information is not available. Any future effort to plan and

implement sustainable water and land resources management should have this information.

The major objective of this study is to characterize the BNR system based on the historical low and high flow records and understands the trend of the critical flow (dry season low flow).

STUDY AREA AND DATASETS

Study Area Description

Originating from Lake Tana (1830 m amsl) in north western part of Ethiopia (Figure 1), the BNR is a major source of water for the economy of lower basin countries. With drainage area of approximately 324,530 km^2, the upper Blue Nile basin covering mainly parts of the highlands in Ethiopia has been characterized as one of the most degraded with natural and human-induced processes. The basin faces environmental and natural resources degradation attributed to anthropogenic (forest degradation, poor or no watershed management practices, overgrazing, poor agricultural water and soil conservation practices and others) and climate change-induced (droughts, unpredictability of rainfall volume and distribution, increased temperature leading to alterations in ecosystem structure). About 66% of the area of this densely populated basin falls in the highlands and hence receives fairly high levels of rainfall (800 to 2,200 mm). This volume of rainfall has a higher spatiotemporal variability leading to higher moisture stress and complete crop failures in some years. Figure 2 shows the mean monthly basin-wide rainfall for the BNR basin.
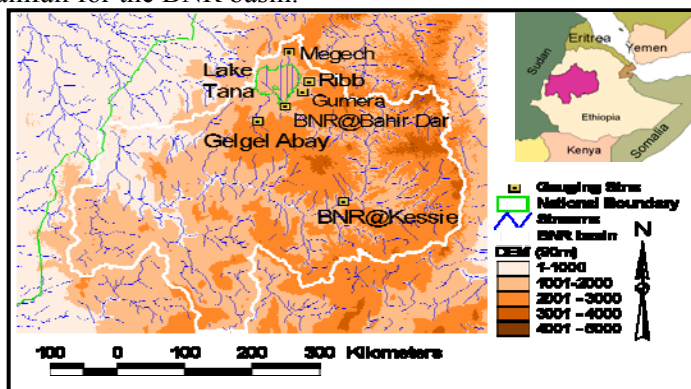
Figure 1. Location of stations and the BNR Basin as it exits Ethiopia.

117

Dataset

For this study, hydrometeorological data (rainfall and flow) and Gravity Recovery and Climate Experiment (GRACE) satellite data were acquired and processed. Daily rainfall data for selected stations in the basin beginning 1950 were acquired from the Ethiopian Metrological Agency. Similarly, monthly flow values for the six major gauging stations (Blue Nile at Bahir Dar, Gelegel Abay, Chemoga, Kessie, Gumera and Ribb) were acquired and processed for the analysis.
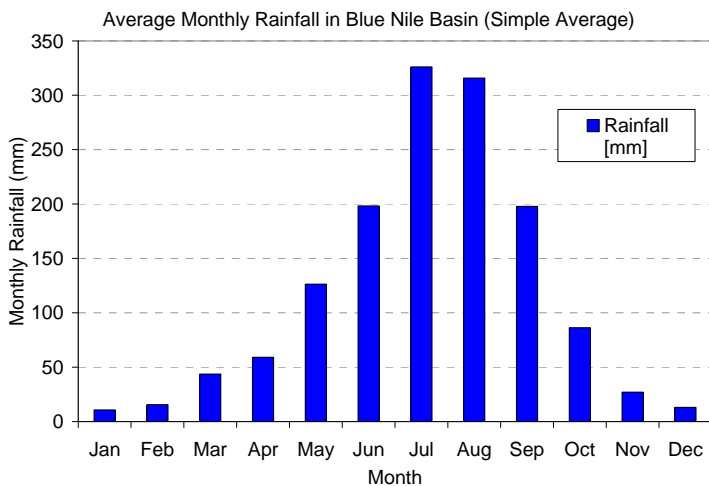
Figure 2. Mean monthly rainfall of the BNR Basin.

METHODOLOGY

GRACE Data

Gravity Recovery and Climate Experiment (GRACE) (http://www.csr.utexas.edu/grace/), twin satellites were launched in March 2002 to make detailed measurements of Earth's gravity field which will lead to discoveries about gravity and Earth's natural systems. The changes in gravity can be due to changes in runoff and ground water storage and fluxes on land masses (http://www.csr.utexas.edu/grace/). In this study, monthly changes in gravity converted to equivalent of water derived from the GRACE Stateline data for the period of 2003-2006 for the months of February, May and September were used to

understand the seasonal and annual changes in the basin's water resources. The method for converting the change sin earth's gravity to water equivalent is shown in Wahr et al. (1998).

Probability Density Frequency Curves and Goodness-of-Fit Tests

In order to understand the probability distribution of the river flow (low and high flows), over 40 distributions were evaluated using three most commonly used goodness-of-fit tests: Kolmogorov-Smirnov (K-S), the Anderson-Darling test and chi-square test. The Kolmogorov-Smirnov test (Chakravart et al., 1967) is used to evaluate if a sample comes from a population with a specific distribution. The K-S test statistic itself does not depend on the underlying cumulative distribution function being tested. It is also an exact test (the chi-square goodness-of-fit test depends on an adequate sample size for the approximations to be valid).

The Anderson-Darling test (Stephens, 1974) is a modification of the Kolmogorov-Smirnov (K-S) test and gives more weight to the tails than does the K-S test.

The chi-square test (Snedecor and Cochran, 1989) is an alternative to the Anderson-Darling and Kolmogorov-Smirnov goodness-of-fit tests. The chi-square goodness-of-fit test can be applied to discrete distributions such as the binomial and the Poisson. The Kolmogorov-Smirnov and Anderson-Darling tests are restricted to continuous distributions.

Flow Duration Curve (FDC) and Low-Flow Frequency Analysis

Flow duration curve shows the percentage of time that a given flow rate is equaled or exceeded. Constructed from flow data of fixed time period (eg., daily, monthly, annual), the shape of the FDC can indicate the hydrogeological characteristics of a watershed (Smakhtin, 2001). Flow duration curves from the mean monthly flow data of the BNR and four other major tributaries were constructed to understand the low and high flow end of the rivers and also characterize the rivers based on the slopes of the two end of the curve. High slopes in the low flow tail (<50%) will indicate a less sustained low flow during the dry seasons than a low slope FDC. This indicated less and/or variable base flow in

the dry seasons. Similarly, high slopes in the high flow end of the FDC indicates less contribution from natural storages like groundwater.

A Low-flow frequency analysis shows the number of years when a low-flow rate is exceeded. This depicts the recurrence interval, the average interval (in years) that the river discharge falls below a given rate, and can also be used to represent base flow conditions. The curve is generated from the series of annual minimum flow values extracted from the stream monitoring data. High slope of the low-flow curve can be taken as indicator of variable low flow.

RESULTS AND DISCUSSIONS

GRACE Water Equivalent Maps

The GRACE water equivalent maps (Figure 3) show the monthly change in water storage in the basin (cm) for the months of February, May and September from 2003-2006. The months were selected to represent different levels seasons and rainfall volumes.

Seasonal Comparison

It is shown that the months of February and May have shown a deficit in the water equivalent (negative value) due to loss of water from the BNR basin. On the other hand, September has shown a consistent gain in water (positive value) resulting from the wet season flows.

Annual Comparison

Comparison of the changes in moisture or water storage in the BNR basin from 2003- 2006 from GRACE maps (Figure 3) shows that 2004 was drier than the rest of the years for the month of September. This can be driven mainly by the amount of precipitation. On the other hand, the February changes in water storage in the BNR basin was less in 2003 than the rest of the years. This indicates during the dry season water loss due to evapotranspiration will be the dominant mechanism. The change in water storage for May has a similar trend that 2003 has less change in storage than the period of 2004-2006. The month of May is considered to receive some rainfall in the basin (Figure 2) and is also characterized as one of the months with high temperatures.

Probability Density Frequency Curves

The probability distribution curves for the minimum and maximum flows of the Blue Nile at Bahir Dar gauging station was constructed and based on the goodness-of-fit test, the and General Pareto and Generalized Extreme Value distributions best describe the maximum minimum flows, respectively. Figure 4 shows the PDFs.

Flow Duration Curves

The FDC curves from the six major stations in the BNR basin is shown in Figure 5. The FDC curves show that the flows at Kessie and BNR at Bahir Dar have a large and sustained flow than the other stations with a relatively flatter slope in the high flow tails of the curves. The flow at Gelegel Abay has also a much sustained dry season flow like that of the Kessie and BNRat Bahir Dar but with relatively smaller discharge.

Flow from the tributaries of the BNR (Ribb, Gumera and Megech) are relatively smaller and the high flow tail end of the FDC from these rivers show a less sustained flow as shown by higher slopes of the curve in Figure 5. The base flow from these rivers during the dry seasons can be small as they tend to have high slope FDC curve on the high flow tail.

Low Flow Analysis

The low flow frequency curve shows the recurrence intervals of a particular selected low flow for the river system. Figure 6 shows the recurrence interval of the low flows from the BNR at Bahir Dar. It is shown that assuming the low flow occurring every 10 years, the monthly average low flow was found to be 0.55 m^3/sec for BNR at Bahir Dar.

Maximum and Minimum Flow Trend

Temporal trend of the maximum and minimum monthly flows at two selected stations were analyzed and shown in Figure 7. The historical maximum monthly flow of the Gelegel Abay has shown little variation over the period of time. On the other hand the mean monthly minimum flow indicated a decline beginning early 1990s. Similarly the Chemoga average monthly flow showed little visible variation but the minimum monthly flow has shown a declining trend since 1994.
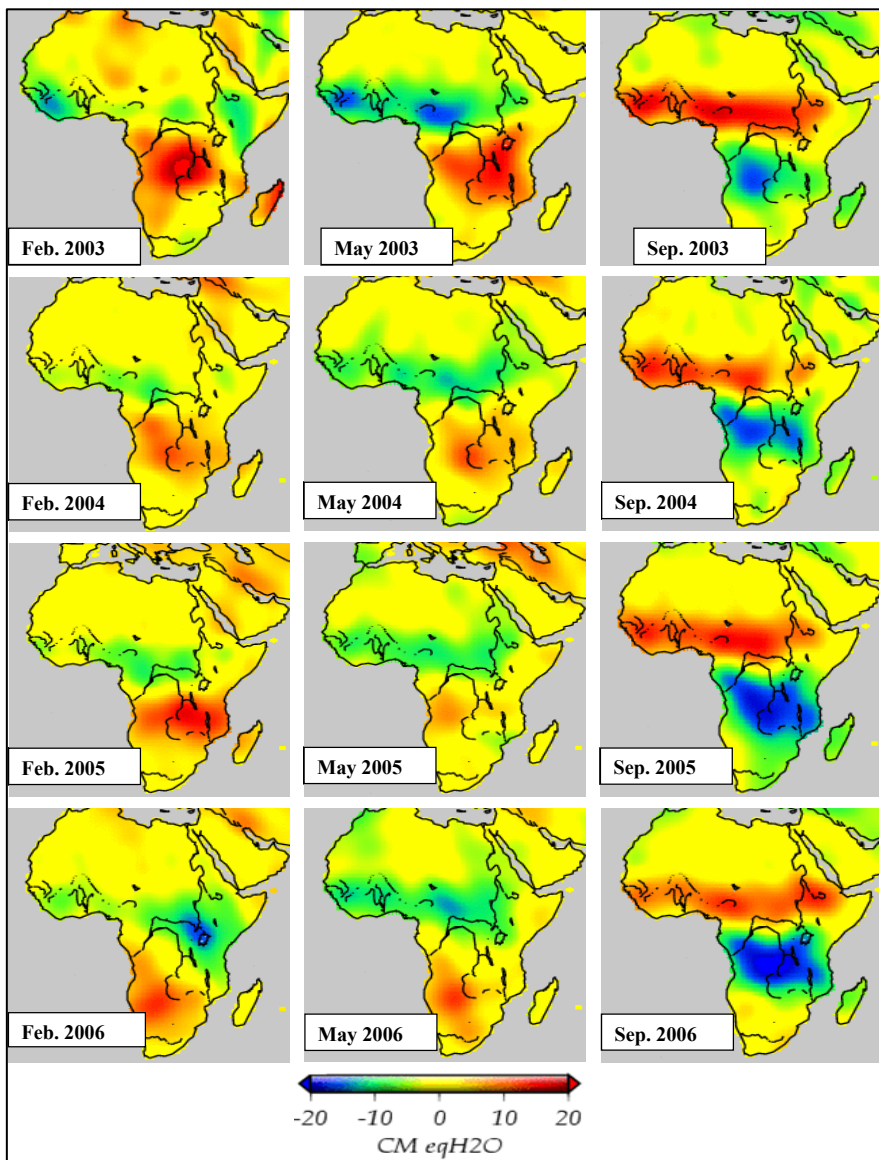
Figure 3. GRACE maps of monthly changes in water equivalent for Africa.
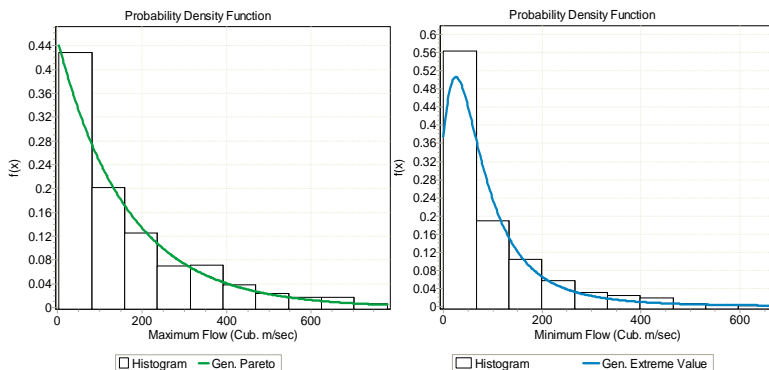
Figure 4. Probability Density Function curves of the monthly Blue Nile River flow at Bahir Dar, a) Maximum flow, b) Minimum flow.
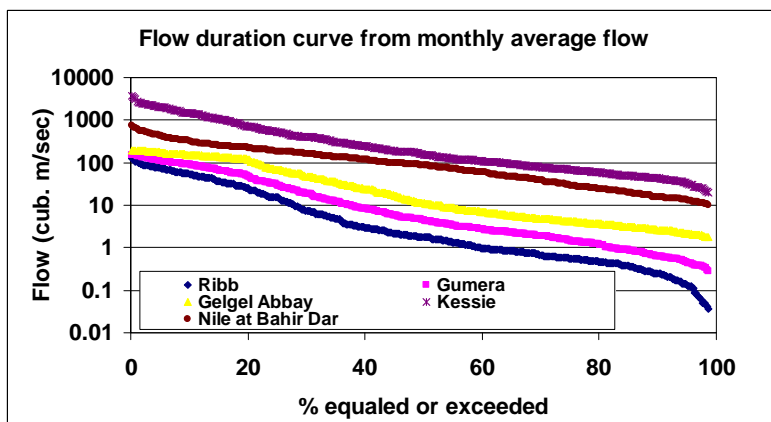

Figure 5. Flow duration curves of the BNR and its tributaries.
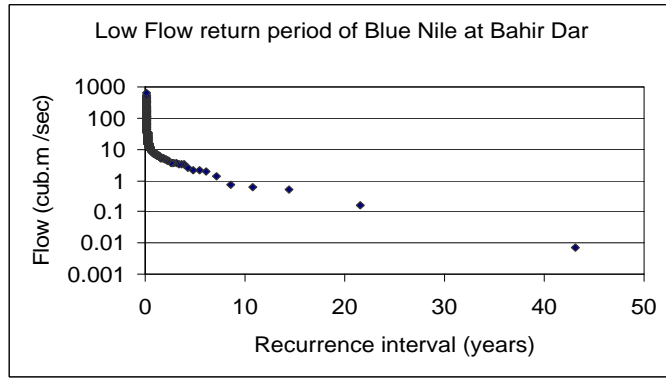
Figure 6. Low flow return period for the Blue Nile River Flow at Bahir Dar.
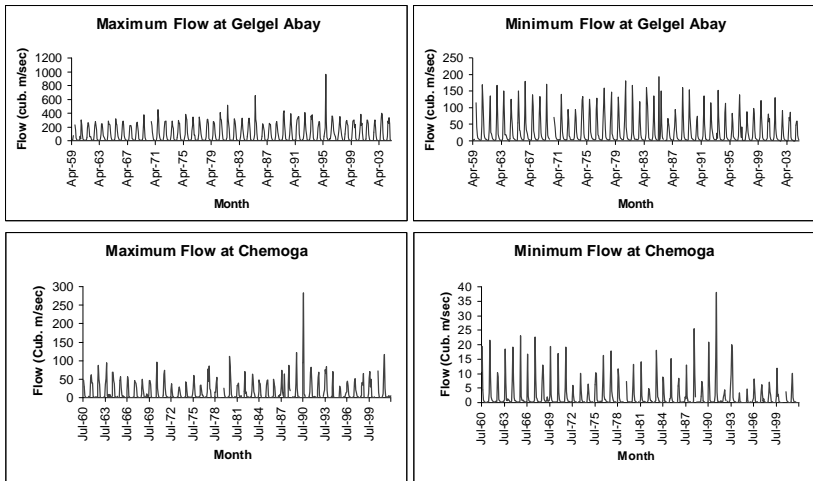
Figure 7. Average maximum and minimum flows at Gelegl Abay and Chemoga stations.

SUMMARY

Despite the large volume of water contribution to the Nile River System, presence of major hydrological issues that require scientific studies, monitoring and analysis, the technical information and research pertinent to the hydrology of the basin is very limited. In this analysis, Hydrometrological analysis is conducted. Monthly flow characterization and analysis were conducted for the BNR and its major tributaries. Using GRACE satellite water equivalent monthly deviation, seasonal and annual variation in the water fluxes of the BNR was studied.

From the flow analysis, flows at Kessie and BNR at Bahir Dar has shown a sustained flows with a relatively flatter slope of the FDC at both ends. Flows from the other rivers with the exception of the Gelgel Abay, has very low base flow contribution as shown from the stepper sloes of the FDC in the high flow tail end. The Low flow analysis of the BNR at Bahir Dar also shows a 10-year recurrence of 0.55 m^3/sec monthly average flow. Tend analysis of flow two stations shows a recent decline in the low flow compared to a no significant change in the high flow values.

The GRACE satellite based monthly changes in water equivalent values indicated the seasonality and also annual variability of the moisture fluxes in the basin. The analysis shows a moisture deficit in the months of February and May and a gain in moisture in September mainly driven by the wet season rainfall.

ACKNOWLEDGEMENTS

REFERENCES

Bewket, W and G. Sterk, 2004, Dynamics in land cover and its effect on stream flow in the Chemoga watershed, Blue Nile basin, Ethiopia, Hydrol. Process. Vol. 19(2): 445-458.

Chakravarti, L., and Roy. 1967. *Handbook of Methods of Applied Statistics, Volume I*, John Wiley and Sons, pp. 392-394.

Conway, D. 1997. A water balance model of the Upper Blue Nile in Ethiopia. Hydrological Sciences Journal. Vol. 42: 265-286.

Conway, D. 2000. The climate and hydrology of the Upper Blue Nile River. The Geographical Journal. Vol. 166: 49-62

Gamachu, D. 1977. Aspects of Climate and Water Budget in Ethiopia. Addis Ababa University Press: Addis Ababa.

Mishra, A., T. Hata , A. W. Abdelhadi, 2004. Models for recession flows in the upper Blue Nile River, Hydrol. Process. Vol. 18, 2773–2786.

Poore, M.E.D and C. Fries, 1985. The Ecological Effects of Eucalyptus, FAO Forestry Paper No. 59, FAO, Rome, pp 54-55.

Scott, D.F and W. Lesch. 1997. Streamflow responses to afforestation with Eucalyptus grandis and Pinus patula and to felling in the Mokobulaan experimental catchments, South Africa. Journal of Hydrology. Vol. 199: 360–377.

Smakhtin, V.Y, 2001. Low flow hydrology: a review. Journal of Hydrology. Vol. 240:147-186.

Snedecor, G.W. and W.G. Cochran. 1989. *Statistical Methods, Eighth Edition*, Iowa State University Press.

Stephens, M. A. 1974. *EDF Statistics for Goodness of Fit and Some Comparisons*, Journal of the American Statistical Association, Vol. 69, pp. 730-737.

Van Lill, W.S, F.G. Kruger and D.B. Van Wyk. 1980. The effects of afforestation with Eucalyptus grandis Hill ex Maiden and Pinus patula Schlecht. Et Cham. on streamflow from experimental catchments at Mokobulaan, Transvaal. Journal of Hydrology. Vol. 48: 107–118.

Wahr, J., M. Molenaar, and F. Bryan, 1998. Time-variability of the Earth's gravity field: Hydrological and oceanic effects and their possible detection using GRACE, J. Geophys. Res., 103, 32,205–30,229.

Zhou, G.Y., J.D. Morris, J.H. Yan, Z.Y. Yu, S.L. Peng. 2002. Hydrological impacts of reafforestation with eucalypts and indigenous species: a case study in southern China. Forest Ecology and Management 167: 209–222.

NON-LINEAR PARAMETERIZATION OF LAKE TANA'S FLOW SYSTEM

Ambro Gieske[1], Abeyou W. W.[2], Getachew H.A.[3],
Alemseged T.H.[1] and Tom Rientjes[1]

[1]ITC, Water Resources Division, Enschede, The Netherlands,
gieske@itc.nl
[2]University of Bahirdar, Ethiopia
[3]Water Resources, Mines and Energy Bureau, Mekele, Tigray, Ethiopia

ABSTRACT

Lake Tana is a high altitude lake in the source area of the Blue Nile River with an area of around 3000 km^2, lying approximately 1786 m above sea level. Its flow system is governed by four main components: the inflow from surrounding rivers into the lake, the outflow at Bahirdar through the Blue Nile, the direct rainfall on the lake and the direct evaporation from the lake.

Several water balance models have recently been made in which model parameters are usually determined by calibrating simulated lake levels against observed levels. These models are operating at monthly and daily time steps. Solute mass balances were recently included in the modeling.

In this paper a study is made of the lake's flow system parameters by modeling average lake level fluctuations on a daily basis, using the observed inflow and outflow components together with the lake rainfall and evaporation. The parameterized level-outflow curves provide a good strategy for filling gaps in incomplete records and allow precise modeling of the lake level changes not only during the peak of the rainy season, but also during the period of recession before the new rainy season.

The modeling therefore gives a better insight into the natural behavior of the lake during periods of both maximum and minimum levels. Moreover, as a result of the modeling an estimate can be made of the so-called ungauged river flows. Finally, the system response to external forcing can be studied, such as for example, natural variations in

climate, peak rainfall periods, changes in outflow by man made structures

INTRODUCTION

The hydrology of the Nile Basin has lately received much attention. Two main aspects can be distinguished: first, there is the problem of optimizing the use of the available water resources for all countries along the Nile, and second there is the question how the Nile Basin is responding to climate changes. An excellent introduction into these aspects was recently given by Kebede et al. (2006). Earlier work on the Nile may be found in many textbooks, for example, Sutcliffe and Parks (1999).

Whereas the hydrology of the White Nile with its many tributaries, lakes and swamps, has been well documented, the hydrology of the Blue Nile has received less attention in scientific literature, although the flow of the Blue Nile exceeds that of the White Nile by far. Lake Tana is situated on the head waters of the Blue Nile and its outflow contributes about 8% of the total Blue Nile flow.

The first detailed hydrological description of Lake Tana and its environment (Figure 1) was made after the Lake Tana Mission from 1920-1924 (Grabham and Clark, 1925, Shahin, 1985, Hurst et al., 1959, Sutcliffe and Parks, 1999). The second study was made by an Italian team in 1937 as described in "Missione di Studio al Lago Tana" (Morandini, 1940). A first bathymetric survey of the lake was made during this study. The author also reported on some of the older lake reconnaissances in the 19th and early 20th century. Later the bathymetric survey was repeated by Pietrangeli (1990). Essayas (2007) conducted a third bathymetric survey with sonar and GPS. As mentioned above, Kebede et al. (2006) carried out a study of the water balance in the period from 1960-1992 and developed a preliminary hydrological model at monthly time steps. This modelling exercise was repeated by SMEC (2007) basically for the same time period and also at monthly time steps. Abeyou (2008) studied the problem of determining the contribution of the ungauged flow into the lake by regionalization of the river catchments in the Lake Tana Basin. He then developed a daily lake mass balance model for the period 1995 to 2003 (reported elsewhere in this workshop). Finally, Getachew (2008) included the solute mass balance in the average lake water balance.

In this paper a study is made of the lake's water balance during the period 1992-2003 at daily time steps. The aim was to try and obtain an independent view of the lake's natural response characteristics to climatic forcing. However, as is clear from the outflow records, the construction of the regulator weir at Chara Chara has played an increasingly important role from 1996 onwards. It is clear that the situation will change even more after the completion of the Tana-Beles Hydropower Scheme and after the completion of the newly planned reservoirs in Lake Tana's Basin. With these developments in mind, it becomes even more important to improve our understanding of the lake's response characteristics and increase the current river and lake monitoring activities.
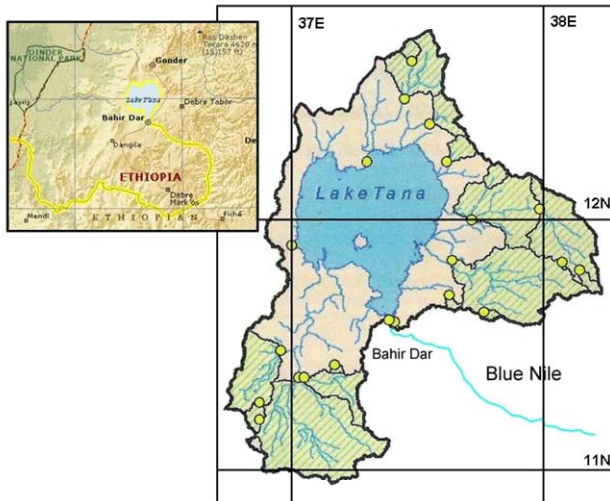
Figure 1. The figure shows the location of Lake Tana and the Blue Nile in the Ethiopian Highlands.
The yellow dots mark the river gauging stations.

RELATION BETWEEN LAKE LEVEL AND OUTFLOW

Kebede et al. (2006) showed that the lake's outflow is related to the levels by the empirical formula due to Klemes (1978) and further discussed by Sene (1998):

$$q_{out} = a\left(h - h_{base}\right)^b \tag{1}$$

where h=lake level, h_{base}=zero reference level (1785.52 m), and a and b are empirical parameters. Based on the monthly flow data from 1960 until 1992, the values for parameters a and b were found to be 0.0156 and 3.25 respectively, when q_{out} is given in mm/month.

Normally the value of b should be between 1.5 and 2. However, in the case of the Blue Nile, there are large differences in flow control features during low and high flows. Hurst et al. (1959) report that the cataracts in the upper reefs at Chara Chara (see Figure 2) are the controlling feature at low flows whereas the channels around Debre Mariam Island control the high flows. Compound section characteristics such as these may lead to high powers (Rantz, 1983). The hydraulic situation after the construction of the Chara Chara regulator weir seems unclear at present.
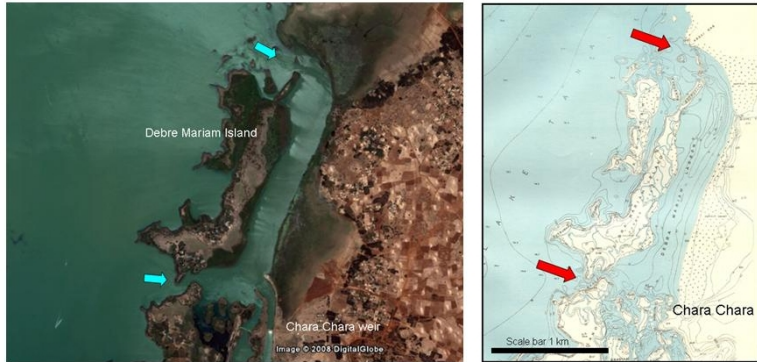
Figure 2. The left picture is captured from Google Earth (2008). The map on the right originates from the 1920-1924 Lake Tana Mission by Grabham and Black (1925) as published by Hurst et al. (1959).

In this study a set of daily data is considered for the period from January 1, 1992 until December 31, 2003. Figure 3 shows that the discharge during the rising lake stage is higher than the discharge during the falling stage. This phenomenon is called a "looped rating curve" or "hysteresis'' (Rantz, 1983). It is thought that this might occur under natural circumstances due to back-water effects in the Blue Nile near the lake's outlet near Bahir Dar. The early stage-discharge curves reported by Grabham and Black (1925) showed a much smaller loop presumably due to vegetation growth in the channel.

It should be noted that the situation has changed after 1996 when the Chara Chara weir was completed. The following model was developed to simulate this effect prior to 1996. Instead of (1) we write

$$q_{out} = a(h - h_{base} - z)^b \tag{2}$$

The variable z is a small stage correction depending recursively on q_{out} as

$$\frac{dz}{dt} = -\frac{z}{\gamma} + \frac{q_{out}}{\alpha} \tag{3}$$

where γ is a decay constant and α an effective backwater area. Parameter γ is found to be about 50 days and α about 90,000 m^2. Hence, the correction z goes to zero after a couple of months in the dry season and re-appears again after the start of the rainy season. Its maximum size is limited to about 18 cm. When q_{out} is given in m^3 s^{-1} then a=52 m^{3}s^{-1}, b=3.2 and h_{base}=1785.0 m.

There are two reasons for developing the empirical lake level-outflow relation:

- It was noted that the 1994 outflow is a copy of the 1993 outflow record, presumably due to a gap in the records. The empirical model provides a better strategy for filling the 1994 gap in the records.
- The model allows extrapolation of the natural lake levels in the absence of the Chara Chara weir and any other structures (dams, hydropower)
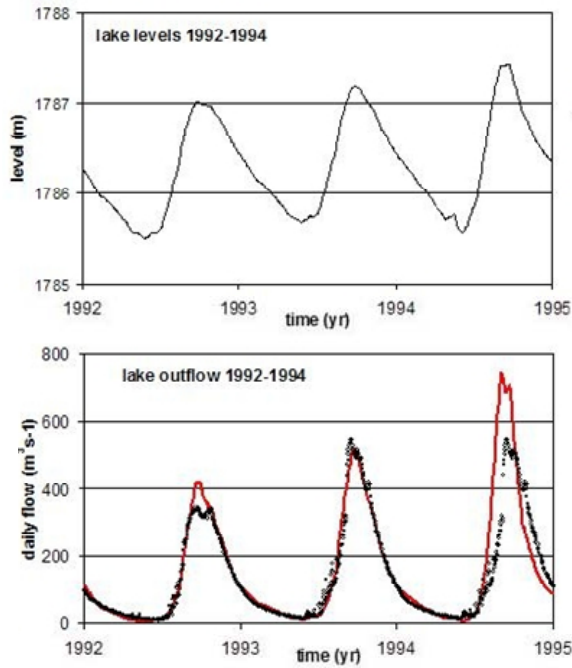
Figure 3. The left diagram shows lake levels 1992-1994, whereas the diagram on the right shows the observed outflows (black dots) and the modeled outflows (red line). Note that the 1993 and 1994 observations are identical, presumably because of a gap in the data. The 1994 data has been replaced by data according to the red line.
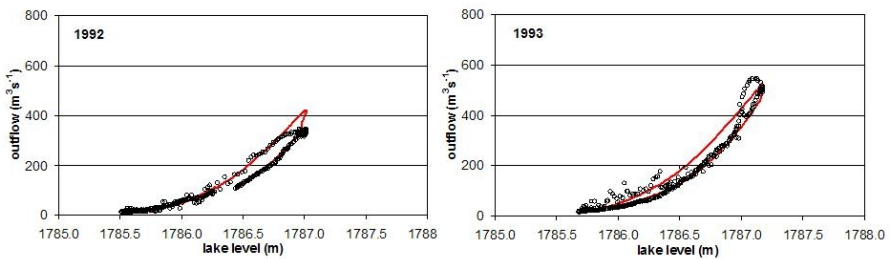
Figure 4. Looped rating curves for 1992 and 1993. Note the deviations in the peak flow periods.

MODIS IMAGE PROCESSING

Use was made of the public domain TERRA/MODIS Reflectance Product (MOD09Q1) which is delivered as tiles in the Integerized Sine Projection (ISP). In this case tile h21v7 was used with 8 day composite reflectances (band 2) where pixels are 250 m in size. A number of images were ordered from the public domain MODIS LPDAAC website for a period in 2001 when lake levels were high and a period in 2003 when the lake levels were very low because of the large outflow through the newly constructed Chara Chara weir at the lake outlet near Bahir Dar. The dates of these images are given in Table 1. Figure 5 shows how the temporal selection of the images was made with regard to lake levels. Nine images were processed for the high lake levels in 2001 and 9 images for the low levels in 2003. The images were converted with MODIS Reprojection Software (MRT) from ISP to a UTM projection. After a final adjustment of the image georeferences, reflection values were calculated and outliers removed. Because the resulting images were still rather noisy because of cloud and shade remnants, it was decided to stack and average them to increase the signal to noise ratio. The difference between land (red) and water (blue) was made on the base of the bimodal distributions in the histograms. A reflectance value of 0.1 was taken as the separation between land and water.

Table 1. MODIS MOD09Q1 8-day composite image selection.

2001	DoY	level (m)	2003	DoY	level (m)
	241	1787.35		145	1784.82
	249	1787.49		153	1784.76
	257	1787.61		161	1784.70
	265	1787.70		169	1784.69
	273	1787.54		177	1784.66
	281	1787.48		185	1784.74
	289	1787.45		193	1784.94
	297	1787.41		201	1785.25
	305	1787.32		209	1785.25

Table 2. Lake areas and water levels for 2001 (high) and 2003 (low).

year	Lake km^2	Est. Isl km^2	Dega Isl. km^2	Water km^2	Level m
2001	3071.82	26.39	1.19	3044.24	1787.48
2003	2940.73	29.68	1.26	2909.79	1784.87
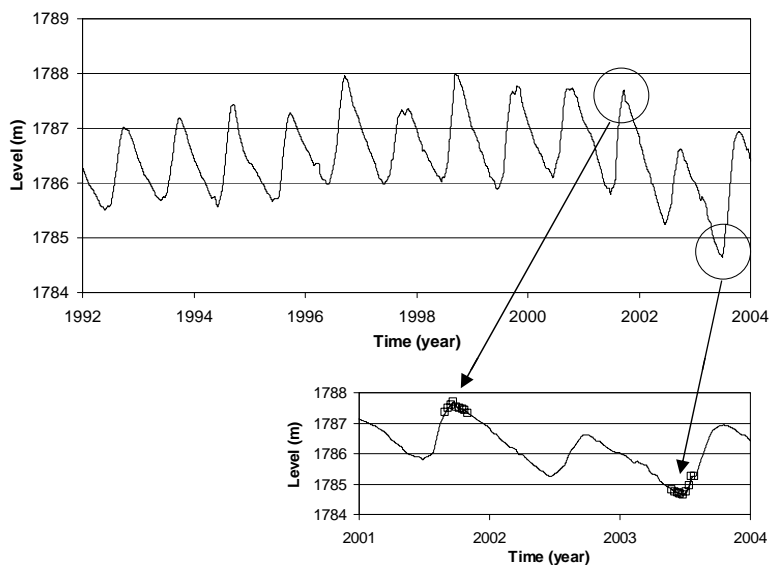
Figure 5. The top figure shows the recorded lake levels from 1992 to 2004 (Essayas, 2007) while the enlarged figure shows the MODIS temporal selection of 8-day composite MOD09Q1 reflectances

134
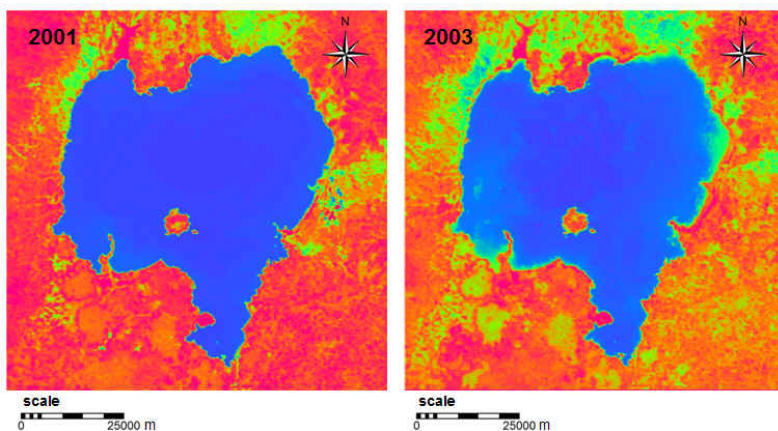
Figure 6. The average of 9 reflection MODIS images (band2) for high levels in 2001(left) and low levels in 2003(right) according to Table 1 and Figure 5.
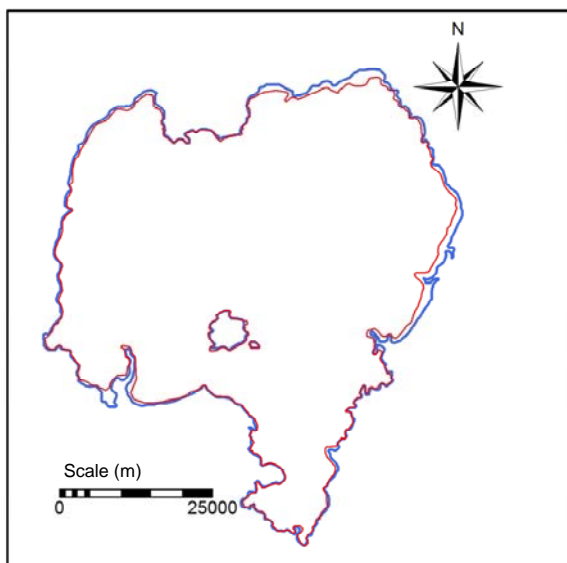
Figure 7. Coast outline for high lake levels (blue line) in 2001 and low lake levels (red line) in 2003.

The results of the analysis are summarized in Table 2. Figure 6 shows the results for 2001 (left image) and 2003 (right image). Figure 7 shows the difference between the lake areas in 2001 and 2003 respectively. The difference between the red and blue lines is greater in the east near the Fugera floodplain, as a result of the low surface gradients in this area. The same happens in the southern part near the long deltaic arm of the Gilgel Abbay and in the north along the shore of the Dembia floodplain. The average high level during the sequence of images in 2001 was 1787.48 m with an average lake area of 3071 km^2, while the average level in 2003 was 1784.87 m with an area of 2941 km^2.

RELATION BETWEEN AREA, DEPTH AND VOLUME

When the inflow components are combined into a single parameter, the net basin supply N, can be written as

$$N = P - E + \frac{q_{in}}{A_0} \tag{4}$$

where A_0 is the lake area which is approximately constant here. According to Sene (1998) the average net basin supply N_0 can be set equal to

$$N_0 = \frac{q_{out,0}}{A_0} \tag{5}$$

where A_0 is the lake area at level h_0, $q_{out,0}$ the annual average outflow. An equilibrium level h_0 can then be defined by inserting (5) into equation (2) taking $z=0$ for simplicity. This yields

$$h_0 = \left(\frac{A_0 N_0}{a} \right)^{1/b} \tag{6}$$

Furthermore when introducing parameter c as the rate change of lake surface area with depth, this may be related to the lake area A as

$$A = A_0 \left(1 + c(h - h_0)/h_0 \right) \tag{7}$$

According to Sene (1998) for Lake Tana the following values may be used: A_0=3000 km^2, P_0=1290 mmyr^{-1}, E_0=1300 mmyr^{-1}, $(q_{in})_0/A_0$=1.3, $(q_{out})_0/A_0$=1.3, A_c=13750 km^2 and c=0.03.

Based on SMEC (2007) a slightly lower N_0=1.24 myr^{-1} is found. This leads to a value of h_0 of 1.30 m. Parameter c was determined traditionally by means of bathymetric surveys in combination with land topographic surveys. More recently, satellite water level information (Topex/Poseidon), Digital Elevation Maps (SRTM, ASTER) are also used. Here the results of the MODIS imagery are used. The results of Table 2 together with the results obtained here for h_0, lead to an approximate c value of 0.02, even lower therefore than the figure reported by Sene (1998).

For the lake water balance modelling the following approach is used. Again use is made of the results obtained with the MODIS images (Table 2). The lake's area A as a function of the level change Δh may be written in a first order approximation as

$$A = A_0 + \frac{dA}{dh}\Delta h \tag{8}$$

When use is made of the MODIS image results as given in Table 2, the approximate value of the derivative dA/dh is determined as 51.5 km^2 per m change of the lake level, and A_0 is taken as 2968 km^2 with h_0=1786m in accordance with the SRTM DEM values and the MODIS analysis. Kebede et al. (2006) simply took the lake area A as constant, which seems plausible in view of the low value of c mentioned above.

DAILY LAKE COMPUTER MODEL

According to Sene (1998) the lake water balance equation can be written as

$$\frac{dh}{dt} = P(t) - E(t) + \frac{q_{in}(t)}{A(h)} - \frac{q_{out}(t)}{A(h)} \tag{9}$$

where P=precipitation, E=evaporation, q_{in}=combined river inflow, q_{out}=outflow through Blue Nile and A=lake area as a function of level.

The differential equation (9) can be solved as an explicit finite difference equation, because the daily time step is small enough to avoid unstable numerical schemes. Hence there is no need for iterative schemes as in the case of Kebede et al. (2006) where monthly time steps were used. The finite difference scheme was solved with a small experimental Delphi-7 Pascal program. Daily data was available for the period 1992 to 2003.

Data Description

There is a gradient of increasing precipitation from North to South over the land surface from Gondar towards the Gilgil Abbay Catchment. However, not much is known about the rain on the lake itself. SMEC (2007), Abeyou (2008) and Getachew (2008) provide a more extensive discussion on this point. Here the precipitation P over the lake is simply taken as the average rainfall of the stations at Gondar and Bahir Dar.

The evapotranspiration was calculated with the Penman-Monteith method for several stations in the Lake area, and then adapted for open water evaporation E (see e.g. Vallet-Coulomb et al., 2001). Again the average of the stations Gondar and Bahir Dar was used. During the calculations it was found that the Hargreaves method which is based on temperature measurements only, provides good approximate values for the open water evaporation from the lake. This needs to be tested further with temperature measurements of the lake and the air immediately above.

Daily river discharge data was available for the gauging stations on eight rivers: Gilgil Abbay, Gumera, Ribb, Megetch, Koga, Gumero, Garno and Gelda. These data were visually inspected for outliers, and gaps. Some obvious errors were repaired and outliers as much as possible removed. Since part of the Lake Tana catchment is not gauged, the runoff from the ungauged part has to be estimated. Sene (2008) and Kebede et al. (2006) used a runoff coefficient of 0.22 to estimate the flow, whereas Abeyou (2008) used a regionalization technique to arrive at flow estimates. Here the inflow of the gauged catchments will be adjusted by calibration of the simulated lake levels against the observed levels, as was done recently by SMEC (2007) using a monthly time step. The difference between the gauged values and the calibrated flows then provides an estimate for the flow from the ungauged catchments. It should be noted that this approach implicitly assumes that there is no

138

leakage or loss to the groundwater below the lake. The solute mass balance as reported by Getachew (2008) appears to indicate that the lake's mass balance is closed. However, much more work on chemical monitoring has to be done before definite conclusions can be drawn.

The daily data of the outflow through the Blue Nile presented a rather complex picture (see Figure 8). The 1994 outflow data were a copy of the 1993 outflow data and these flow data were replaced by making use of the lake level-outflow relation as explained in the previous section (see Figure 3). The flow data seemed to be increasingly influenced by the construction activities at Chara Chara regulator weir from 1995 onwards. The outflow appeared to stabilize around 100 m^3s^{-1} around 2002. However, there are very many jumps in the data in the period from 1995 to 2001 and it is not a priori clear whether the data contain errors or whether the jumps in the flow rates are due to real physical events, for example closing and opening of the regulator gates. The weir itself controls the flow accurately, so operational monitoring results should allow better modelling of the lake's mass balance. However, regrettably, detailed operational data were not available to us at this stage.
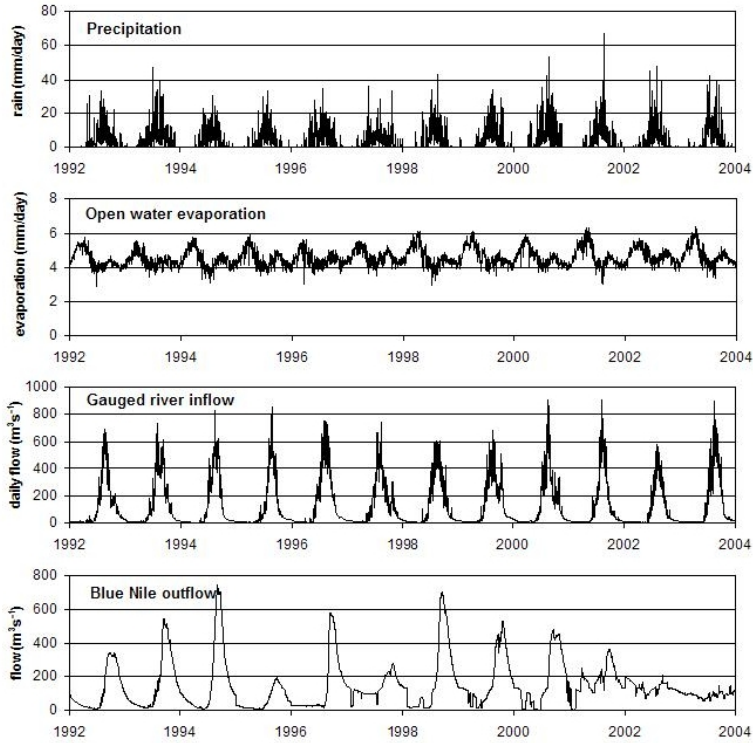
Figure 8. Input data set for the daily lake mass balance model: Precipitation, Evaporation, Gauged river inflow and Blue Nile outflow.

Modelling Results

Figure 9 shows the modeled versus the simulated water levels in the twelve year period from 1992 to 2003. The model parameters were manually calibrated during the calibration process. The final root mean square error was 0.15 m. The bottom diagram shows the difference between observed and simulated levels as a residual graph. It was found during the calibration process that differences can be traced back to effects not only caused by errors in inflow but probably also by errors in outflow records. Because the outflow lags the inflow from both rain and rivers, the effect of changing inflow has a different effect on the residual graph compared to the effect caused by changes in the outflow. Hence it proved possible to adjust records of specific years upwards or downwards. The difference between river inflow and rainfall is much

140

more difficult to detect in the residual graph. It is clear from the residual graph in Figure 9 that peaks are related to the rainy season where large local rainfall events may cause runoff that is not present in the records of Bahir Dar and Gondar.
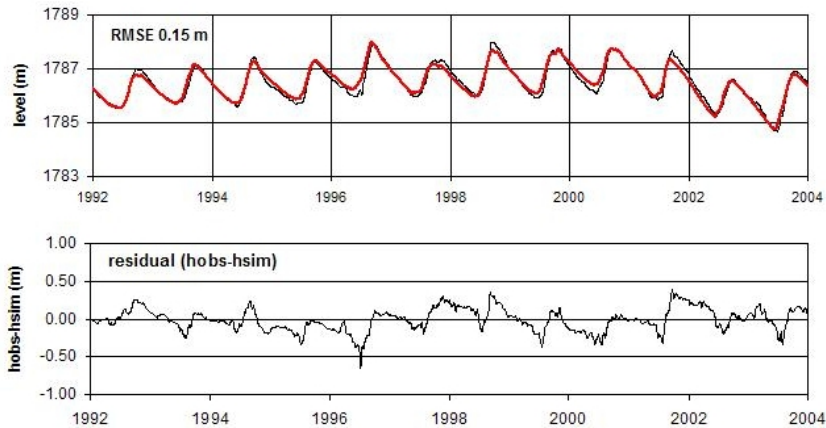
Figure 9. The top diagram shows both the observed lake levels (black line) and the simulated levels (red line). The bottom diagram shows the difference between observed and simulated levels as the residual

The close fit between observed and modeled lake levels between 1996 and 2003 indicates that the outflow record is basically correct. However, it seems advisable to obtain more detailed operational records in the future.

No effect of area changes as a function of height could be found. The error in the four input components (*P, E, inflow, outflow*) appears to be larger than the effect of changing area with height. Therefore the lake's area may be taken as constant when modelling with the present set of input data.

Table 3. Lake water balance resulting from mass balance model (1992-2003).

	Input data (mm/yr)	Calibrated Values (mm/yr)
Lake Evaporation	1671	1671
Precipitation	1255	1255
Gauged river inflow	1297	1770
Blue Nile outflow	1525	1348
Balance	-644	6

The results of the model are summarized in Table 3. All figures are in mm/yr over the lake area. The Blue Nile outflow was reduced from 1525 to 1348 mm/yr. This difference is probably due to difficulties in converting river levels into accurate flow rates during peak flow periods. The gauged river flows increased from 1297 to 1770 mm/yr. This difference may be attributed to both the ungauged river flow and the unrecorded peak flow from the gauged river catchments. Thus the present modelling shows that this ungauged flow may be in the order of 473 mm/yr. However, it should be noted, as mentioned before, that it is assumed that there is no loss to the groundwater below the lake. Moreover, part of the 473 mm/yr may also be due to high rainfall over the lake, although there is no firm evidence to support this. The difference between input and output terms is 6 mm, as a result of slightly different lake levels at the beginning and the end of the modelling period.

DISCUSSION

An empirical lake level-outflow relation has been developed to be able to replace the suspect part in the 1993 Blue Nile outflow record. This model can perhaps also be used in the future to simulate the natural lake levels in the absence of dams, weirs and hydropower schemes.

The analysis also showed the existence of looped rating curves in 1992 and 1993. The Chara Chara regulator weir construction activities and weir operations after 1994, changed the natural outflow pattern of the lake. It is not clear whether this will also lead to changes in channel sedimentation around Debre Mariam Island.

MODIS public domain images made it possible to develop a relation between lake level and area. No bathymetric relations are required for the type of modelling in this paper, although they are essential of course for lake sedimentation analysis. The area-level relation was implemented in the modelling. However, no significant difference was observed between the modelling with constant and variable lake area. The large errors and fluctuations in the input data obscure this second order effect. Therefore the lake area may be taken as constant for practical modelling purposes.

A daily lake mass balance model has been developed in which the simulated daily lake levels were calibrated against the observed levels with a Root Mean Square Error (RMSE) of 0.15m.

The calibration made use of the residual graph which shows that phase differences between inflow and outflow patterns can be employed to apply corrections for individual years. This procedure can be further elaborated in future modelling work.

A few recommendations may be made for future work. Firstly, rainfall and evaporation on the lake should be studied to enable quantification of these components with higher accuracy. Secondly, the modelling in this paper assumes zero leakage from the lake to the groundwater below. Hence the ungauged flow becomes the only remaining unknown term in the lake's water balance. The alternative approach is to determine the ungauged flow independently by regionalization procedures (Abeyou, 2008). It appears important to compare and contrast both approaches. Thirdly, it seems important to incorporate the operational monitoring of the weirs and hydropower schemes into the modelling in the future. Finally, the problem of peak inflow and outflow monitoring deserves extra attention because it appears that the main deviations in the modelling occur during the peaks of the rainy season.

REFERENCES

Abeyou Wale Worqlul. 2008. Estimation of flow from ungauged catchments by regionalization procedures –Lake Tana, Ethiopia. ITC MSc Thesis.

Essayas Kaba. 2007. Validation of altimetry lake level data and its application in water resources management. MSc Thesis, ITC, Enschede, The Netherlands.

Getachew Hadush Asmerom, 2008. Groundwater contribution to the flow of the upper Blue Nile. ITC MSc Thesis.

Grabham, G.W. and R.P. Black. 1925. Report of the Mission to Lake Tana, Government Press, Cairo, Egypt.

Hurst, H.E., R.P. Black and Y.M. Simaika. 1959. The Nile Basin, Vol IX, Government Printing, Cairo Egypt, pp206.

Kebede, S., Y, Travi, T. Alemayehu and V. Marc. 2006. Water balance of Lake Tana and its sensitivity to fluctuations in rainfall, Blue Nile basin, Ethiopia. J. Hydrol., 316: 233-247.

Klemes, V. 1978. Physically based stochastic hydrologic analysis. Advances in Hydro-sciences, 11: 285-356.

Morandini, G. 1940. Missione di studio al Lago Tana, Vol. 3. Richerche Limnologiche, Parte Prima, Geografia Fisica, Reale Academia d'Italia, Roma, Italia, pp319.

Pietrangeli. 1990. Studio Pietrangeli, Hydrological Report. Government of Ethiopia. Addis Abeba.

Rantz, S.E. 1982. measurement and Computation of Streamflow: Volume 2 Computation of Discharge, Geological Survey Paper 2175, Washington, USA.

Sene , K.J. .1998. Effect of variations in net basin supply on lake levels and outflows. Hydrol. Process., 12: 559-573.

Shahin M. 1985. Hydrology of the Nile Basin. Elsevier, Amsterdam, The Netherlands, pp575.

SMEC. 2007. Hydrological Study of the Tana-Beles Sub-Basins. Draft Inception Report. Snowy Mountains Engineering Corporation, Australia.

Sutcliffe, J.V. and Y.P. Parks. 1999. The Hydrology of the Nile. IAHS Special Publication no. 5, IH, Wallingford, UK, pp179.

Vallet-Coulomb, C., Dagnachew Legesse, F. Gasse, Y. Travi, Tesfaye Chernet. 2001. Lake evaporation estimates in tropical Africa (Lake Ziway, Ethiopia). J. Hydrol., 245:1-18.

Xungang, Y. and S.E. Nicholson. 1998. The water balance of Lake Victoria. Hydrological Sciences J. 43(5): 789-811.

GROUND WATER FLOW SIMULATION OF THE LAKE TANA BASIN, ETHIOPIA

[1]Yirgalem A. Chebud and [2]Melesse, A.M.

[1]Department of Earth Sciences, Florida International University, USA
[2]Department of Environmental Studies, Florida International University, USA

ABSTRACT

With the intention to capture the groundwater contribution into Lake Tana, a case study was conducted at the Gumera River sub-basin, one of the five sub-basins that drain into Lake Tana. The Gumera sub-basin was delineated using 90-m SRTM digital elevation model (DEM) using ArcHydro tools. The sub-basin boundary and the stream outlets are used as boundary conditions acting as the divide line of the groundwater flow into and out of the other watersheds while stream networks are used as internal drainage lines. Input parameters are obtained from past studies and also based on experts' experience. Upon reviewing the basin's geological information, unconfined subsurface flow condition is considered and it was simulated using MODular three-dimensional finite-difference ground-water FLOW model (MODFLOW). The result indicates that head contours are aligned to the streams showing their relationship as a subdued form of the surface water flow which are dictated by the drainage lines. The result depicted that groundwater outflow follows the surface water outlet. The result suggested the need to account contribution from the sub-basins on to the base flow, and to estimate groundwater inflow from the floodplain separately. The contribution from the floodplain was conceptualized by steady state flows of unconfined aquifer justified by the slow changes of groundwater level in the floodplain. The result has shown that 0.1 Billion Cubic Meter (BCM) is flowing annually across the perimeter of the Lake Tana. Four wells in the low and mid-altitudes were used to calibrate the head distribution. The study has given clues to further validate for inverse methods of parametric and flow estimation.

Key Words: Lake Tana, groundwater, modeling, Blue Nile, MODFLOW

INTRODUCTION

The Tana basin constitutes 3.1 million ha fresh water body that receives subsurface flow from the 16,500 km^2 drainage area (Kebede, 2005), (Figure 1). The lake serves for fishery, navigation and hydropower purposes. The downstream side of it is breeding places of the fish species which makes it sensitive to any intervention that affects the subsurface flow in any way. Despite its ecological and economical importance, little is known about the potential of subsurface water and its carrying capacity in the basin.

The research gaps and scarcity of monitoring data to understand the subsurface flow in the Tana Basin is reported by Kebede et al.,(2005). This has contributed to the knowledge gap on the groundwater quantification and sensitivity analysis to anthropogenic and climate-induced changes. This paper highlights the importance of identifying options to simplify and understand the process using simulation models. Given the ease of capturing geological data and conveniently measuring base flow with spatial and temporal scale of interest, it is arguable that a shift of focus is necessary to understand future possibilities of ground water parametric estimation through numerical and stochastic modeling approaches.

Unlike the physical models, numerical and stochastic models would find their way of replicability at different watersheds helping long-term calibration (Gelhar, 1993, Rubin, 2005). For this purpose, it was intended to study the capability of the MODular three-dimensional finite-difference ground-water FLOW model (MODFLOW) in subsurface flow estimation for the Lake Tana groundwater flow system.
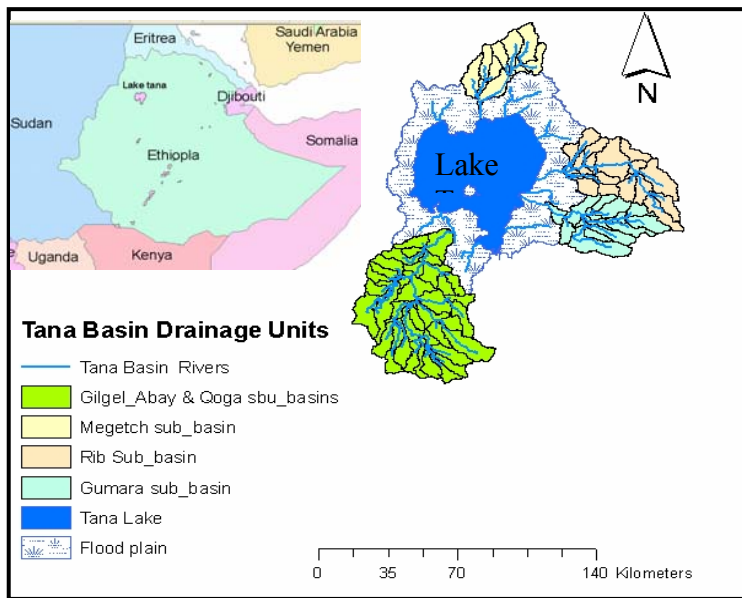
Figure 1. The Lake Tana drainage system and contributing watersheds.

The specific objectives of this study are to (a) understand regional and basin level ground water flow in the Lake Tana basin and (b) evaluate MODFLOW application for simulation of the groundwater flow in the Lake Tana basin.
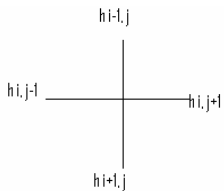
Review

Physical models in combination with geochemical tracers are traditionally used to quantify groundwater flow and analyze the flow pattern (Anderson and Wossener, 1992). The use of tracers to understand the subsurface inflow and outflow from Lake Tana has given fundamental clues of potential inflows and outflows within and out of the basin (Kebede et al. 2005). However, these traditional methods specifically, the physical models are known for their cost and less replicability. The comparability of numerical and stochastic models with physical models for parametric estimation of ground water flow is reported by Gelhar (1993), suggesting their cost effectiveness and replicability without compromising the data.

Gelhar (1993) suggests techniques to tackle the uncertainty over the simulation models through distributed hydrogeological models. Apparently, the differentiation of the distributed hydrogeological modeling units would be based on topography and aquifer type. As a case in point hydrogeologic units could have differing flow patterns identified as fracture Darcian flows (Anderson and Wossener, 1992).

For complex physical models, use of the MODFLOW, which is built on finite difference methods, is encouraging while the numerical finite difference methods could be sufficient to address unsophisticated simple physical models with sound boundary and initial conditions (Anderson and Wossener, 1992). The finite difference (finite element) is the numerical method used for subsurface flow analysis using interfaces such as Matalab. Numerical methods by Poisson's equation and the discretized format for iteration is expressed as follows (Wang and Anderson, 1982)

$$\frac{\partial^2 h}{\partial x^2} + \frac{\partial^2 h}{\partial y^2} = \frac{E}{T} \qquad \text{Steady state} \qquad (1)$$

$h_{i,j} = [h_{i+1,j} + h_{i-1,j} + h_{i,j+1} + h_{i,j-1} - E*DX^2/T]/4 \quad (2)$

$$\frac{\partial^2 h}{\partial x^2} + \frac{\partial^2 h}{\partial y^2} = \frac{S}{T}\frac{\partial h}{\partial t} + \frac{E}{T} \qquad \text{Transient} \qquad (3)$$

$h_{i,j,t} = [h_{i,j,t-\Delta t} + (T\Delta t/S) [h_{i+1,j,t-\Delta t} + h_{i-1,j,t-\Delta t} - 4 h_{i,j,t-\Delta t} + h_{i,j+1,t-\Delta t} + h_{i,j-1,t-\Delta t}] + E*DX^2/S]/4$ \hfill (4)

where h = head; T = transmissivity; E = evapotranspiration, S = storativity, DX = grid interval, t = time.

Geology of the Basin

As part of the modeling framework, the knowledge on the structural geology, hydrogeology, and geomorphology of the basin remains a key factor for parameterization of inputs and also identify assumptions. Lake Tana basin is a junction point of three grabens centering Lake Tana which were active in the mid tertiary and quaternary and run from Gondar, Dengel Ber and Debre Tabor (Chorowicz et al., 1998). The lake is dammed by dyke swarms that run NW-SE, NE-SW, ESE –WNW (Hautot et al., 2005) and a 50 km lava flow cutoff at the outlet of the Blue Nile River to a possible depth of 100m (Chorowicz et al., 1998). Quaternary lacustrine sediments and alluvial deposits are evident at the head and toes of the basin namely Chilga, Debretabor and Fogera plains overlain on the flood basalts. The simplified geological cross-section by Hautot, et al., (2006) shows that the underlying formations beneath the 250m thick basaltic grabens are Adigrat and Nile Gorge sand stones and Ashengi, Aiba and Tarma Ber formations that go 1-2 km deep.

The underlying basaltic graben serves as a cutoff against seepage loss from the lake as it is confirmed upon the absence of geochemical mixing outside of the basin (Kebede et al., 2005). On the contrary, a regional groundwater inflow is identified from a possible aquifer that extends from mount choke (South of Lake Tana basin), confirming its signature of geochemical mixing at Andasa springs. Even then with the circumscribing course of the Blue Nile River gorge the amount delivered to Lake Tana is not well known. The contribution from Guna aquifer (East of Tana basin) is found to have negligible contribution for lack of evidence of geochemical mixing within the basin (Kebede et al., 2005). The minor geochemical mixing obtained at Wanzaye, $\delta^{18}O$ (3.2%), is attributed to the mixing from the cold springs of Debretabor than the Guna aquifers (Kebede et al., 2005). In summary these evidences help to assume that major subsurface inflow to Lake Tana is from the basin itself.

The inflow within the basin is characterized by quick hydrological response through the fractures of the faulted blocks dipping towards the Lake Tana from all directions with strike NNE, SSW (Kebede et al., 2005). This is observable from the normal and lateral slip faults of the structural geologic map (Figure 2) by Chorowicz et al., (1998) which are confirmed from satellite images. Looking at the

geological structures and topography of the Tana basin quick response of the subsurface flow within the basin is evident.
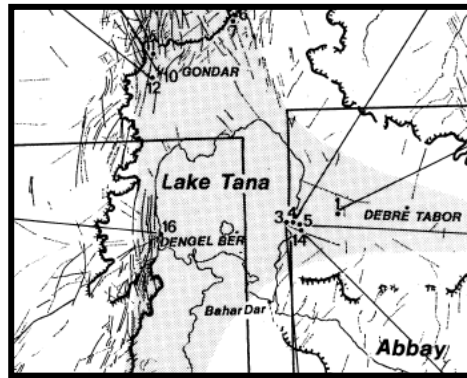
Figure 2. Normal and lateral slip faults in the Tana basin from Chorowicz et al., 1998.

METHODOLOGY

Two modeling exercises were conducted: one at a representing sub-basin called Gumera and the other at Lake Tana floodplains. For the Gumara Sub-basin, a one dimensional flow profile is simulated on the MATLAB interface based on analytic solutions (Wang and Anderson, 1982). The digital elevation model (DEM) was used as a guiding line to observe the topographic profile and hence model the ground water as a subdued form of it. A separate 2-D flow simulation on the floodplains was also designed using finite difference method which involved iteration techniques. The 2-D flow model was simulated using MODFLOW software. In all the cases, steady state flow patterns are simulated.

Model Set Up

The model set up for the two dimensional sub-basin model with MODFLOW was conducted by setting the watershed boundary as no flow zones, and the streams as internal drainage lines. The outlet is represented by a pumping well with equal discharge amount as the stream flow as shown in Figure 3a. Secondary data of input variables collected from BECOM and reported in Kebede et al., (2005) is applied on grid basis

(Figure 3b). This includes transmissivity determined from pumping test by BECOM. Quoting form BECOM, Kebede et al., (2005) stated that the transmssivity of the Tana grabens and alluvial deposits are 100 to 200 m^2/day and 700m^2/d, respectively while on the back side of the western Tana escarpments it is only $1m^2$/day. The evapotranspiration was estimated using Penman's method (Ward, 1995). Leakance to the confined aquifer is assumed 5% of the precipitation with conservative expert judgment and incorporated in the evapotranspiration parameters (as a loss). Hydraulic head data from two shallow wells developed in year 2006 by the district were used for calibration.
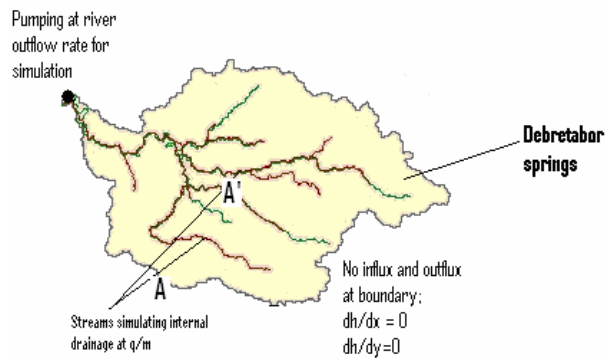
Figure 3a. Boundary conditions and internal drainage.
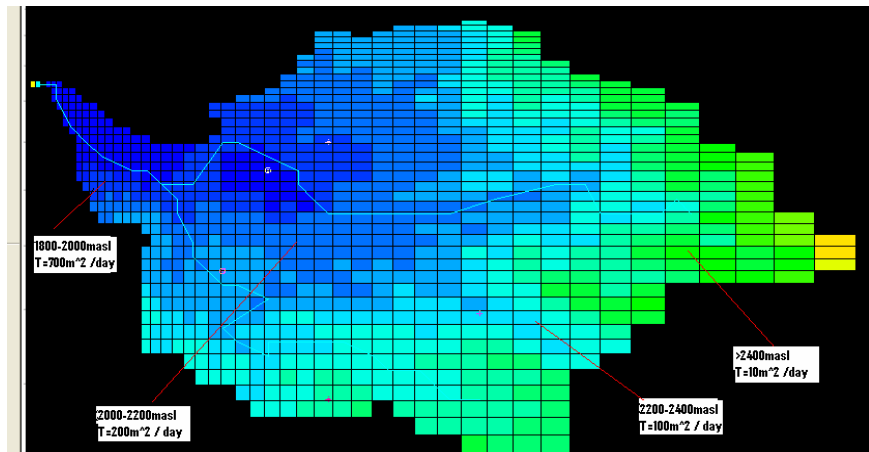
Figure 3b. Distributed inputs of transmissivity and elevation for the Gumera sub-basin.

151

Analysis

The Shuttle Radar Terrain Mapping (SRTM) DEM data with 90m resolution from U.S Geological Survey (USGS) (USGS, 2007) is used to delineate the Tana basin. Watershed analysis tools of ArcHydro (Maidment, 2002) were used to process the raw data, fill sinks, and generate stream network and watersheds. Four sub-basins namely Rib, Gumera, Megech, and the Gilgel Abay-Koga were delineated. This has helped to do analysis on separate sub-basins and also capture the Tana plain separately from the other sub-basins. A GIS layer of Gumara sub-basin was developed that MODFLOW uses as flow boundary condition and the streamlines were used as 'drains'.

RESULTS AND DISCUSSION

Subsurface Flow from Gumara Sub-Basin

Vertical Cross Section Analysis

A radiometrically corrected Landsat Enhanced Thematic Mapper Plus (ETM+) imagery of the study area was enhanced by a high pass filter (HFF) to identify fractures. The results were in agreement with the structural maps developed by Chorowicz et al.,(1998). Based on these evidences of fracture flow dominance over the sub-basin, a one dimensional overview of the flow profile was simulated using finite difference methods with Matlab interface to look at the flow cross-section in one dimension. Based on the topographic profile map from the DEM that indicates 3 rising shelves at a regular contour interval of 200 m from the 1820 to 2400 m amsl (Figure 3b) the simulation was done across the A-A` shelve. For this purpose, a simplified form of the Poisson's equation (Wang and Anderson, 1982) (1) is reduced to Laplace equation taking the form

$$\frac{\partial^2 h}{\partial x^2} + \frac{\partial^2 h}{\partial y^2} = 0 \qquad (5)$$

Based on observations on the morphology, stream network and slope classifications from the DEM, both linear as well as the sinusoidal fitting of the groundwater level as a replica of the topography was tested. And the sinusoidal subdue of the groundwater is found fitting to the internal

drainage conditions. This is in agreement with the BECOM hypothesis that (quoted in Kebede et al., 2005) the ground water could be in a perched form with high water table and flux around streams.

The sinusoidal head variation is captured through Toth solutions (Wang and Anderson, 1982) and applied with a constant head at the two boundaries setting the foot of the valley bottom at zero, and the streams at their own elevation from DEM. Based on one year observation an annual average head of 20m at the upstream (A) is considered. The model is run with Matlab interface whose outcome is a sub-basin head profile (Figure 4) and the flow pattern (Figure 5). The head profile is on a 30m thick unconfined aquifer with head at 20m on the upstream. The head is at 1m interval while the topographic relief is at 10 meters vertical interval. The horizontal grid follows the topographic interval of 100m.
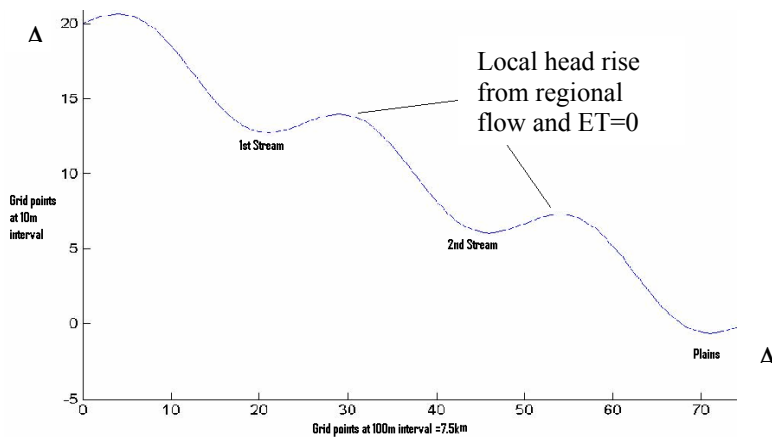
Figure 4. Regional flow model for the cross section of A-A` of Figure 3a on the sub-basin.

A flow-net analysis estimates an interception of 65% of the groundwater as base flow by the streams (Figure 4). Also, the local watershed and sub-basin flow mix on stream lines is noticeable from the flow profile (Figure 5). Even the remaining 35% should diverge with other influxes from other areas and recur in the downstream. In other words the subsurface flow contributes to Lake Tana as the base flow than as direct subsurface flow into the lake. To confirm the result, the ideal solution could be use of tracers (Fetter, 1988), however, in the absence of such experiments, 2D modeling with calibration of wells is opted.
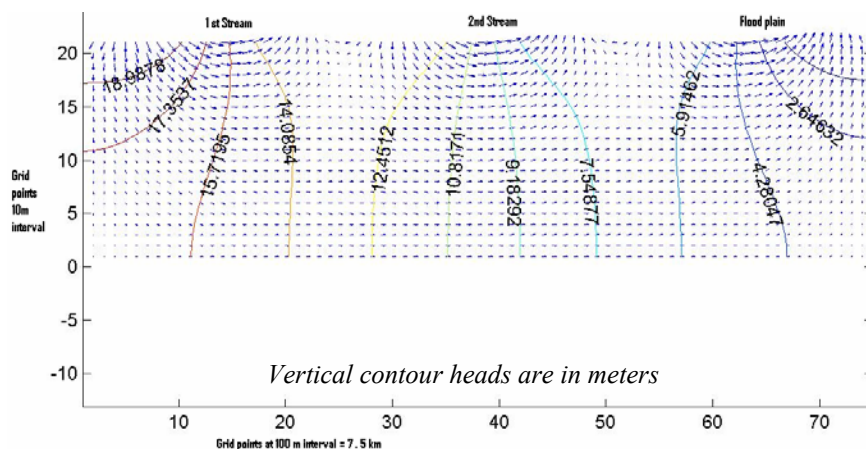
Figure 5. A vertical cross-section sub-basin level flow
on cross-section A-A.

Two Dimensional Flow Analysis of Gumara Sub-Basin

With the intention to confirm the overall head distribution in the sub-basin, a 2D flow analysis was modeled using MODFLOW. The watershed boundary of the sub-basin was used as the boundary conditions of the model considering the watershed boundary as no flow zones, streams as drains, and watershed outlets as siphoning out wells at equal discharge as the stream outflow. In this analysis, both precipitation and evapotranpiration were considered as sources and sinks (recharge and out fluxes) and Poisson's equation was applied.

This hydrogeological simulation through forced boundary condition has shown that in both the dry and wet season the hydraulic head (Figure 6) is concentrated near the streams showing that the flow is a subdued form of the watershed drainage line into stream courses. Given the fact that the steam flow line is perpendicular to the contour lines, it proves that most of the groundwater flow is draining into the streams (Figure 6). This is in conformity with the 1D model indicating alignment of head distributions with the streams. Nevertheless, no local rise of heads is observed which might be attributable to the consideration of evapotranspiration and leakance.
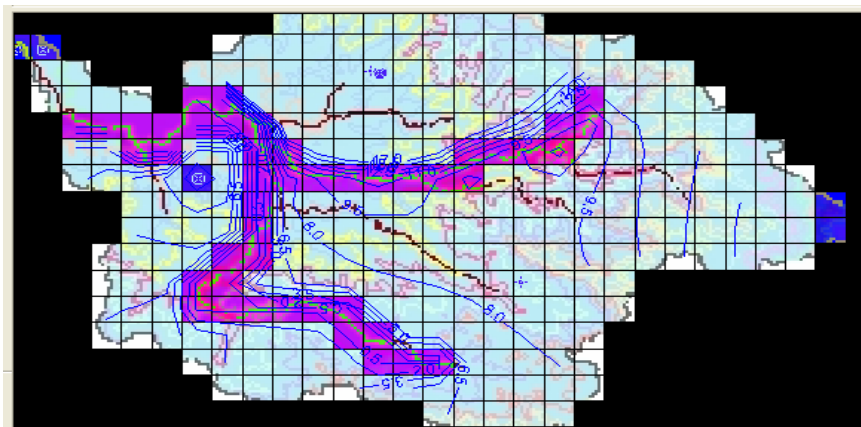
Figure 6. Head contour (blue lines) for Gumera sub-basin
aligning with stream lines.

The model is run with two constant head calibrating wells. The
analysis indicated that ground water input from the watershed could be
captured from the base flow of the stream plus the flow through the thin
unconfined section. Also this study confirms the facts established by
Kebede et al.,(2005) that quick response of groundwater outflow and less
retention due to the high fracture garben calling it "perched aquifer".

Subsurface Flow in the Floodplain

The major outcome of the 2D study on Gumara sub-basin is that,
while the groundwater inflow could be taken into account by the base
flow, a separate contribution is identified from the floodplain that is
flooded for months to its surface during the rainy season and starts to
yield into the lake during the dry seasons. This contribution is from a 20
km section of floodplain which carves as a concentric circle centering
Lake Tana (Figure 7). The flow from the plain across the perimeter is
estimated using Poisson's equation of steady state flow for unconfined
condition. A finite difference model set up at the floodplain involved two
major rivers, Rib and Gumara at 10 km apart, and the Lake Tana (20 km
from the head).
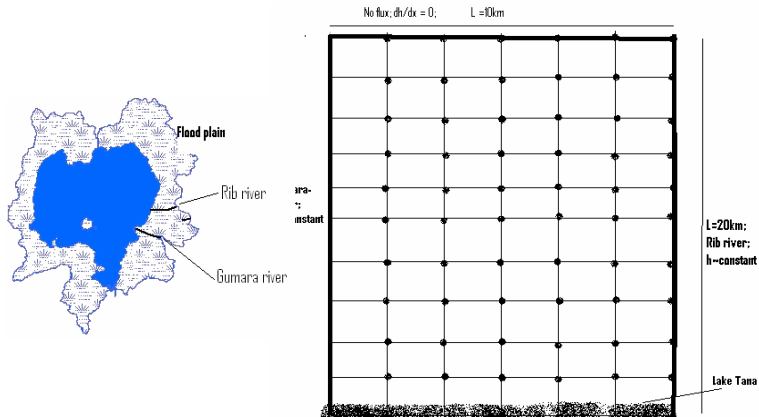
Figure 7. Model setup for the floodplains and grid points are for finite differences estimate.

The hydraulic head distribution from the simulation (Figure 8) for the dry and wet seasons indicate that subsurface flow is from the rivers towards the floodplains, higher heads near the rivers with decreasing gradient towards the main land. It is also found out that the floodplain receives about 0.16 billion cubic meters (BCM) from base flow of the rivers, while the flood itself contributes 0.1BCM to Lake Tana. The difference (6 millions m^3) is being stored in the floodplain. The hydraulic head is calibrated against shallow wells in the floodplain.

A 1D transient flow simulation for the wet season indicates the reversal of the head distribution. Apparently the recharge from precipitation played a significant role to reverse it.
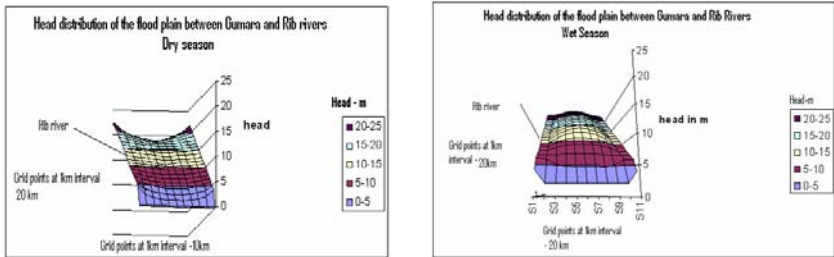
Figure 8. Simulated and calibrated head distribution for floodplain.

CONCLUSION

The main purpose of this study was to understand the ground water flow system of Lake Tana and quantify the flow. From the past studies, the hydrogeology of the basin and watershed analysis of the study area using ArcHydro, the boundary conditions were identified. This has enabled an understanding of the different hydrogeologic units and subsequently facilitates the model setup. The model setup for the Gumera sub-basin was made on MODFLOW 2002. The analysis depicted the alignment of the groundwater from sub-basins along the streams suggesting the need for separate analysis for floodplains. The subsurface flow from the floodplains is done using finite difference methods. Finally, the contribution of groundwater was accounted from the subsurface flows of the floodplains and the base flow from the sub-basins.

The simulation has improved the understanding of the groundwater flow system of the Lake Tana Basin both in upper catchments and the floodplains. This is achieved with the employment of MODFLOW whose advantages were found three fold: (1) Its capability of working with the GIS shape files and take up DEM data, (2) its simulation of the irregular boundaries of the sub-basin and (3) the utilities that simulate groundwater wells, internal drainage streams etc., which are vital for distributed hydrogeological modeling. Moreover, the utilities of MODFLOW such as PEST (parametric estimators) for forward and inverse modeling approach makes it inviting. The simplicity, flexibility and control of calibration points were an advantage.

157

ACKNOWLEDGEMENTS

REFERENCES

Anderson M.P., W.Wossener, 1992, Applied Groundwater Modeling: Simulation of Flow and Advective Transport, Academic Press, USA.

Chorowicz U., B.Collet, F.F.Bonavia, P.Mohr, J.F.Parrot, T. Korme, 1998, The Tana basin, Ethiopia: intra-plateau uplift, rifting and subsidence, Tectonphysics, 295 351-367, ELSEVIER

Fetter, C.W., 1988, Applied Hydrogeology, 2nd Edition, Merrill publishing Co., Columbus, Ohio, 592 p.

Richard H, V Paul, Coombes, H Michael, Marshall, M Umer, J. Sarah , E Dejen, 2006, Late Pleistocene Desiccation of Lake Tana, source of the Blue Nile

Gelhar, L W. 1993, Stochastic subsurface hydrology, Printice hall, USA

Rubin Y., S.S Hubbard , 2005, Hydrogeophysics, Springer, Netherlands

Kebede S, Y Travi, T Alemayehu, T Ayenew, 2005, Groundwater Recharge, circulation and geochemical evolution in the source region of the Blue Nile River, Ethiopia

Hautot S, K Whaler, W Gebru, M Desissa, 2006, The Structure of a Mesozoic Basin Beneath the Lake Tana area, Ethiopia, revealed by mangetotelluric imaging, The African Earth Sciences, 331-338.

Maidment D, 2002, ARC Hydro, GIS for Water Resources, ESRI press, California, USA

Wang, H.F, and M.P. Anderson, 1982, Introduction to Ground Water Modeling; Finite Difference and Finite Element Methods, W.H. Freeman, 256 p.

USGS, 2007. SRTM topographic data, http://srtm.usgs.gov/ (accessed on Dec,, 2007).

Ward A and W Elliot, 1995, Environmental hydrology, LEWIS Publishers, USA

HYDROLOGICAL BALANCE OF LAKE TANA, UPPER BLUE NILE BASIN, ETHIOPIA

Wale A.[a], Rientjes T.H.M.[b], Dost R.J.J.[b], Gieske A.[b]

[a]Bahir Dar University, Water Resource Engineering Department, Ethiopia. E-mail: abeyou_wale@yahoo.com
[b]Department of Water Resources, ITC, Enschede

ABSTRACT

In recent studies by Kebede et al. (2006) and SMEC (2007) closure of Lake Tana water balance is obtained by runoff from ungauged catchments that cover a large part of the Lake Tana basin. Since both studies applied simple pragmatic approaches to estimate runoff from ungauged catchments, in this study emphasis is on more advanced approaches as based on regionalisation and spatial proximity principles. In this work also a simple *ad-hoc* procedure on area comparison is used to estimate runoff.

In the regionalisation approach model parameters of the conceptual HBV rainfall-runoff model of gauged catchments is transferred to ungauged catchments to allow runoff simulation. For such, a regional model is developed through regression analysis where system characteristics are related to model parameters. In the proximity procedure model parameters from neighboring gauged catchment models are directly transferred while in the third procure runoff estimations are simply based on parameter transfer based on catchment size comparison.

Criteria for selection of gauged catchments to be used in the procedures are the relative volume error and Nash-Sutcliffe coefficient that, respectively should be less than +5% or -5% and be greater than 0.6. Following this procedure, results indicate that flows from ungauged catchments are estimated as large as 42%, 47% and 46% of the total river inflow for the three respective procedures.

Lake areal rainfall is estimated by inverse distance interpolation, open water evaporation is estimated by the Penman-combination equation while observed inflows from gauged catchments and outflow data are directly used in the lake water balance. The water balance

closure term was established by comparing measured to calculated lake levels where data of a recent bathymetric survey is used to establish volume-area and volume-level relations.

Daily lake level simulation with inflows from ungauged catchments by regionalisation shows a good performance with a relative volume error of 1.6% and a Nash-Sutcliffe coefficient of 0.9. Results show that runoff from ungauged catchment is around 880mm per year for the simulation period 1995 to 2001.

Key Words: Regionalisation, Lake Tana, Bathymetry, Water balance, HBV

INTRODUCTION

The river Nile is one of the longest rivers in the world and the basin area covers approximately 10% of the African continent. According to the World Bank, the Nile River Basin is home to an estimated 229 million people in the year 1995 while the basin can be characterized by poverty, instability, rapid population growth and environmental degradation. Lake Tana as the source of the Blue Nile contributes more than 8% of the Nile's supply of freshwater to the Northern countries Sudan and Egypt originating from Ethiopian highlands (Conway, 1997).

Regarding the water resource there is increasing water utilization across the transboundary Nile Basin further straining the limited resources. Also in Ethiopia an increased demand is identified by irrigation and hydropower development (Kebede et al. 2006) while at the same time the country experiences a number of problems such as rapid population growth, environmental degradation and poverty. Also by climate and land use changes, recurrent droughts may further effect agricultural production and food supply in Ethiopia. For efficient use of available water resources with balanced attention to maximize economic, social, and environmental benefits, it is necessary to have effective integrated water resources assessments and planning.

Recent assessments of the hydrologic system of Lake Tana basin show uncertainties with respect to major lake water balance terms. The main source of uncertainty is by (unknown) inflows from ungauged

catchments as shown in Kebede et al. (2006) and SMEC (2007) who, moreover, indicate significantly different inflows. In this study, for estimation of lake balance terms such as rainfall, evaporation, runoff from gauged catchments and lake outflow observed data are used for water balance calculation that is at a daily time step.

For simulation of daily lake level fluctuations, data from a bathymetric survey of Lake Tana in 2006 by the Institute for Geoinformation Science and Earth Observation (ITC) is used. By this survey lake volume – lake area and lake volume – lake level relations are established that served for assessing the water balance closure term.

STUDY AREA

Lake Tana (1786 m.a.s.l.) is the source of Blue Nile River and has a total drainage area of approximately 15,000 km^2, of which the lake covers around 3,000 km^2. The lake is located in the north-western highlands at 12°00'N and 37°15'E and more than 40 rivers drain into the lake. Major rivers feeding the lake are Gilgel Abay from the south, Ribb and Gumara from the east and Magetch River from the north while at the western side of the lake only small rivers systems are present (see Figure 1). According to Kebede et al. (2006) these four major rivers contribute 93% of the inflow and only 7% of the lake inflow is from ungauged catchments. SMEC (2007) indicates that some 29% of the lake inflow is from ungauged catchments where, contrary to Kebede et al. (2006), Koga River is considered gauged with some 4% of the total river inflow.
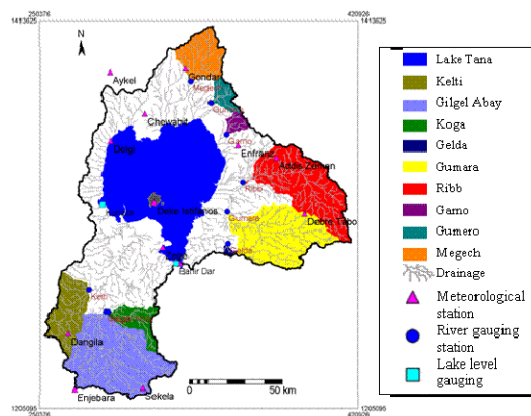
Figure 5. Lake Tana Basin area

161

By its large storage capacity, the lake is a slow responding system with annual lake level fluctuations of approximately 1.6m. Lake level fluctuations primarily respond to seasonal influences by the rainy and dry season and reaches maxima around September and minima around June with historic maximum and minimum water levels of 1,788.02m (September 21, 1998) and 1,784.46m (June 30, 2003). The only river that drains Lake Tana is the Blue Nile River (Abay River) with a natural outflow that ranges from a minimum 1075 Mm^3 (1984) to a maximum of 6181 Mm^3 (1964). For the period 1976-2006 the average outflow is estimated to be 3732 Mm^3.

WATER BALANCE TERMS FROM OBSERVED DATA

In this study the Lake Tana water balance is solved for the period 1995 till 2001 on a daily base. In the Lake balance equation Eq. [1] observation time series are available for rainfall (5 stations), evaporation (2 stations) and runoff from gauged catchments (5 catchments). For both rainfall and evaporation area averaged estimates are made by simple interpolation while, after screening, runoff time series are directly used. Outflow from Lake Tana through the Blue Nile River is also based on observation time series that also have been screened for consistency. For the selected simulation period, observations indicate that outflow of the lake was hardly affected by construction works of the Chara Chara weir and as such observations could directly be used.

$$\frac{\Delta S}{\Delta T} = P - E_{vap} + Q_{gauged} + Q_{ungauged} - Q_{BNR} \quad\quad [1]$$

Where$\Delta S/\Delta T$ denotes the change in storage over time [Mm^3 day^{-1}], P is Lake areal rainfall [Mm^3 day^{-1}], E_{vap} is open water evaporation [Mm^3 day^{-1}], Q_{gauged} is Gauged river inflow [Mm^3 day^{-1}], $Q_{ungauged}$ is Ungauged river inflow [Mm^3 day^{-1}] and Q_{BNR}: Blue Nile River outflow [Mm^3 day^{-1}]

Runoff from ungauged catchment is estimated by three procedures that are further described in section 4. Following SMEC (2007) in this study it is also assumed that the groundwater system basically is decoupled from the lake and any lake leakage may be ignored in the balance. In this respect however it must be noted that Kebede et al. (2006) estimate lake leakage to be some 7% of the total

annual lake budget. Obviously, our assumption on lake leakage may be wrong and possibly accounts for an error in the established lake balance.

Meteorologic Balance Terms

Daily lake rainfall has been estimated through few procedures that are the inverse distance squared interpolation, inverse distance linear interpolation and Thiessen polygons. For interpolation, data for the period 1992-2003 from Bahir Dar, Chawhit, Zege, Deke Estifanos and Delgi station (see Figure 1) are used. The Thiessen method shows long-term average of 1229 mm/year, Inverse distance with power 1 and 2 shows 1254mm/year and 1290mm/year respectively. In this study we adapt the latter value since in this procedure a higher weight is assigned to the station on the lake island.

For estimating lake evaporation the Penman-combination equation (see Maidment, 1993) is selected that has wide application as a standard method in hydrologic engineering. In this equation the energy balance is combined with a water vapour transfer method and results in an equation to compute the evaporation from open water surface using standard climatological records of daily sunshine hours, temperature, humidity and wind speed. The Penman-combination equation for open water evaporation reads:

$$E_P = \frac{\Delta}{\Delta + \gamma} * (R_n + A_h) + \frac{\gamma}{\Delta + \gamma} * \frac{6.43 * (1 + 0.536 U_2) * D}{\lambda} \qquad [2]$$

Where E_p is potential evaporation that occurs from free water surface [mm day^{-1}], Rn is net radiation exchange for the free water surface [mm day^{-1}], Ah is energy advected to the water body [mm day^{-1}], U_2 is wind speed measured at 2m [m s^{-1}], D: is average vapor pressure deficit, [kPa], λ is latent heat of vaporization [MJ kg^{-1}], γ is psychrometric constant [kPa °C^{-1}], Δ is slope of saturation vapor pressure curve at air temperature [kPa °C^{-1}].

Lake water evaporation is estimated using the observed daily meteorological data values at Bahir Dar and Gonder stations. Albedo of the lake is estimated from Landsat ETM+. The result shows that in the lake area the Albedo ranges from 0.05 to 0.062 with an average of 0.058. This value is used for calculation of open water evaporation and is close to the Albedo value 0.06 as used at Lake Ziway, Ethiopia (Vallet-

Coulomb et al. 2001). Calculated daily averaged evaporation shows an average value of 4.6 mm/day for the period 1992 - 2003 and a long-term averaged annual evaporation of 1690 mm/year.

Runoff From Gauged Catchments

In the Lake Tana catchment area nine gauged subcatchments have daily runoff records for the period 1992 - 2003. By a SRTM digital elevation model (DEM) of 90 meter resolution the area gauged covers for some 39% of the total basin area. Runoff time series data are analyzed for consistency and analysis indicated that some records are unreliable. By simple statistics and by simple hydrologic reasoning some observation records are rejected. Poor reliability was also indicated in the procedures where runoff from ungauged catchments is estimated (section 4.2). As a consequence, we consider observation records of only five catchments (Table 1) reliable and time series from these catchments have directly been used in the water balance and lake level simulations. The area gauged as such now only covers for some 32% of the Lake Tana catchment area.

Table 1. Catchment area and long-term average annual flow (1992 - 2003) of the major gauged tributaries of Lake Tana

River	Gilgel Abay	Gumara	Ribb	Megech	Kilti
Gauged Area Km^2	1656.2	1283.4	1302.6	513.5	606.6
Mean annual river flow in MCm	1753.5	1229.5	510.4	195.2	283.8

Lake Tana Outflow by the Blue Nile River

Outflow from Lake Tana is by the Blue Nile River that originates from the lake. For the lake level simulation period that covers from 1995 – 2001, daily observation records on runoff discharges are available and are directly used in the water balance and lake level simulation.

164

RUNOFF FROM UNGAUGED CATCHMENTS

Runoff from ungauged catchments is estimated by three procedures that are of different complexity. The first procedure applies a regionalisation procedure where a regional model (see Booij et al. 2007; Merz and Blöschl, 2004, among others) is established between catchment characteristics and model parameters that as such are used for ungauged catchment modeling. A second procedure simply transfers model parameters from neighboring or (very) nearby catchments to ungauged catchments to allow for runoff simulation. The third procedure parameter sets of gauged catchments are transferred to ungauged catchments by a simple area comparison. In all three procedures the HBV-IHMS model (see IHMS, 2006) is selected for simulation of catchment runoff.

HBV-IHMS

The HBV is a conceptual rainfall-runoff model for continuous simulation of catchment runoff. The model consists of subroutines for precipitation and snow accumulation, soil moisture accounting, actual evaporation and uses simple transformation functions and routing procedures. Soil moisture accounting is governed by two simple relations that are parameterized by FC is the maximum soil moisture storage (mm) in the model, LP that is a limit for potential evapotranspiration and Beta that controls the contribution of soil moisture storage, SM, to the response function ΔQ/ΔP.

$$\frac{\Delta Q}{\Delta P} = \left(\frac{SM}{FC} \right)^{Beta} \qquad [3]$$

Q Denotes discharge and P denotes precipitation while ΔQ/ΔP is to be interpreted as a runoff coefficient. Actual evapotranspiration, EA, which is controlled by a soil moisture routine is linearly related to the potential evapotranspiration, EP, and reads:

$$EA = EP \ \min\left(\frac{SM}{LP*FC}, \ 1 \right) \qquad [4]$$

In HBV-IHMS the runoff routine comprises two reservoirs that distribute generated runoff over time to obtain the quick and slow parts of a catchment runoff hydrograph. Runoff generated from the upper reservoir

represents quick runoff discharges while runoff from the lower reservoir represents groundwater discharges.

$$Q_o = K * UZ^{(1+Alfa)}$$

[5]

Where Qo is direct runoff from upper reservoir, parameters UZ and KHQ are the upper reservoir storage and the quick flow recession coefficient while Alfa is a measure for the non-linearity of the flow. The lower reservoir is a simple linear reservoir that simulates base flow contributions by percolation from the upper reservoir.

$$Q_1 = K_4 * LZ$$

[6]

Q_1 denotes the outflow from the lower reservoir, LZ is the lower reservoir storage while K_4 is a recession coefficient. Obviously the combination of the parameters controls runoff contributions over time that affect the shape of hydrograph. During model simulation the water balance is maintained over all simulation calculation time steps. For a full description on the model approach reference is made to Lindstrom et al. (1997) and IHMS (2006).

Model Calibration

In this study model calibration is by 'Trial & Error' where model parameters are manually changed to optimize model performance. Model performance is evaluated by two objective functions that are the Relative Volume error (RV_E) and the Nash-Sutcliffe coefficient R^2. The RV_E can vary between ∞ and $-\infty$ but performs best when a value of 0 is generated since an accumulated difference between simulated, $Q_{sim(i)}$, and observed, $Q_{obs(i)}$, discharges is zero.

$$RV_E = \left(\frac{\sum_{i=1}^{n} Q_{sim(i)} - \sum_{i=1}^{n} Q_{obs(i)}}{\sum_{i=1}^{n} Q_{obs(i)}} \right) * 100$$

[7]

A relative volume error between +5% or −5% indicates that a model performs well while relative volume errors between +5% and +10% and −5% and −10% indicate a model with reasonable performance.

Nash-Sutcliffe coefficient (R^2) is a measure of efficiency that relates the goodness-of-fit of the model to the variance of the measured data:

$$R^2 = 1 - \frac{\sum_{i=1}^{n}\left(Q_{sim(i)} - Q_{obs(i)}\right)^2}{\sum_{i=1}^{n}\left(Q_{obs(i)} - \overline{Q_{obs}}\right)^2}$$

[8]

Where $\overline{Q_{obs}}$ is the average of observed flow

R^2 can range from −∞ to 1 and an efficiency of 1 indicates a perfect match between observed and simulated discharges. R^2 values between 0.9 and 1 indicate that the model performs extremely well. Values between 0.8 and 0.9 indicate that the model performs very well while values between 0.6 and 0.8 indicate that the model performs reasonably well.

Regionalisation

Regionalisation is commonly referred to as parameter transfer based by catchment characteristics and relates hydrological phenomena to physical and climatic characteristics of a catchment, or region (after Young, 2005). The approach has five distinct steps:

- Selection of representative gauged catchments and catchment characteristics
- Modeling of the gauged catchments
- Establishing statistical relationships between optimized parameters and physical catchment characteristics. The ensemble of statistical relationships makes up the so called regional model
- Validation of regional model
- Estimation of model parameters and predicting discharge at the ungauged catchments.

Selection of Representative Catchments and Catchment Characteristics

In the Lake Tana basin there are 17 gauged catchments that cover 47% of the catchment area as established by SRTM DEM analysis. From this ensemble, at first 9 gauged catchments with spatial basin coverage of 39% are selected by availability of daily flow records from 1992 to 2003.

Physical catchment characteristics (PCCs) are classified into five major groups that are Climate, Geography and physiography, Geology, Soil and Land cover condition. In this study a total of 23 PCCs are selected and are derived from SRTM DEM analysis, geological maps, land cover maps and soil maps and meteorological data as collected from the Ethiopian Ministry of Water Resources and the Ethiopian Meteorological Agency. A listing of the PPCs used in this study is shown in Table 2 where a number of PCCs are reclassified for a specific catchment characteristic. The selection is based on research by Seibert (1999), Yaday (2007), Merz and Blöschl, 2004, Booij et al. 2007,Young, 2005 and Heuvelmans (2006).

Table 2. Selected catchment characteristics

Catchment characteristics	Description
Climate index	Is the ratio of long-term averaged precipitation to long-term averaged potential evapotranspiration
Catchment area	Reflects the volume of water that can be generated from rainfall
Length of longest flow path	Distance from the catchment's outlet to the most distant source on the catchment boundary
Hypsometric integral	Describes the distribution of elevation across the catchment area.
Average altitude	Average elevation of the catchment from SRTM DEM
Average slope of catchment	Calculated from digital elevation model SRTM DEM pixel by pixel
Drainage density	Is the total stream length for the basin divided by catchment area
Slope class as per FAO	%level: Level to undulation /level/, dominant slopes ranging between 0 to 8% %hilly: Rolling to hilly /hilly/, dominant slopes ranging between 8 to 30% %steeply: Steeply dissected to mountainous /steeply/, dominant slopes over 30%
Basin Shape	Circularity index: is the ratio of perimeter square to the area of the catchment. Elongation ratio: is the ratio of length of longest drainage to diameter of a circle which has the same area as the basin
Land cover	%forest,%grassland,%cropland, %bare land, %urban and built-up, %woody savannah
Soil	%luvisols, %leptosols, %nitisols, %vertisols and %fluvisols

Modeling of the Gauged Catchments

Any approach of regionalisation for prediction of runoff from ungauged catchments requires relationships between PCCs and the sensitive parameters of a selected rainfall-runoff model. In our research the HBV-IHMS model is selected for simulation of the rainfall-runoff relation from gauged catchment. This model approach has wide application in hydrology and in regionalisation studies has been applied by Seibert, (1999), Merz and Blöschl, (2004) and Booij et al. (2007), among others.

Moreover, by its small number of parameters, the approach may be classified as parsimonious that is favourable as compared to more complex models such as the Sacramento SMA (Burnash et al. 1973) and SWAT (USDA-ARS) approaches (see Gupta et al. 1998). At first, the HBV model is calibrated for each of the nine catchments against observed daily discharges and best-fit parameter sets are selected. Calibration objective functions selected are RV_E and R^2 from Eq's [7] and [8]. For selection of catchments to be used for establishing the regional model, values for RV_E should be smaller than $+5\%$ or -5% while R^2 should be greater than 0.6. In the simulations, the runoff data from 1992 to 2003 is divided in three, the first to warm-up the model (1992), the second to calibrate the model (1993 to 2000) and the third to validate the model (2001 to 2003).

Table 3. Result of model calibration for selected gauged catchments (1993 to 2000)

Parameter	Ribb	Gumara	Gilgel Abay	Koga	Megech	Kilti	Gelda	Gumero	Garno
R^2 [-]	0.76	0.72	0.85	0.56	0.64	0.68	0.38	0.19	0.09
RV_E [%]	2	-4.55	-1.2	-6.74	2.54	3.9	-17.01	14.01	18

Model calibration results as shown in Table 3 indicate that model performance of Ribb, Gumara, Gilgel Abay, Megech and Kilti is satisfactory while for catchments with a relatively small area such as Koga (299.8 km^2), Gumero (164.9 km^2), Garno (98.1 km^2) and Gelda (26.8 km^2) the result of calibration was not satisfactory. As such we assumed that runoff time series of those catchments cannot be considered trustworthy and that model parameters of those catchments cannot be used for regionalisation. We assume that river gauging stations, as such,

are not placed at the catchment outlet but at some location upstream that has easy road assess. Time of concentration defined as the length of time it takes for water to travel from hydrologically most remote point to the outlet was calculated and Time of concentration is 6.4 hrs, 9.5 hr, 8.2 hr and 4.6 hr respectively. This explains while quick runoff responses are not well shown in the observation records.

For model validation the period 2000 to 2003 has been selected and results are shown in Table 4.

Table 4. Model Validation from year 2001 to 2003

Catchments	Ribb	Gumara	Gilgel Abay	Megech	Kilti
Nash R^2 [-]	0.81	0.8	0.77	0.62	0.66
RV_E [%]	1.5	-5.1	-8.4	2.54	-8.76

Model validation shows better performance for Ribb and Gumara catchments as compared to model calibration while a lower performance is shown for the remaining three catchments. The overall assessment of the validation shows a R^2 greater than 0.6 in all catchments and a RV_E smaller than +10% or −10%.

In rainfall-runoff modeling it is often not possible to find one unique best parameter set and different parameter sets may give similar good results (see Beven and Binley,1992; among others). In order to reduce uncertainty and to establish a reliable parameter set a sensitivity analysis is required. In HBV-IHMS there are 7 parameters controlling the total volume and shape of the hydrograph. Sensitivity analysis of each of the parameters is done by arbitrary dividing parameter space into a number of classes for which model performance is assessed. By the sequential change of parameter values highly sensitive parameters are identified and prior parameter space is narrowed. Sensitivity analysis of model parameter was done on the Gilgel Abay catchment only.

Table 5. Summery of sensitivity analysis of model parameters

Parameter	Parameter space	Sensitivity of parameter by change from min to max value
Alfa	Narrow	Negligible change in RV_E and R^2
Beta	Moderate	RV_E less than 10 % and negligible change in R^2
FC	Wide	RV_E change less than 25% and negligible change in R^2
K_4	Narrow	Negligible change in RV_E and R^2
KHQ	Moderate	RV_E change less than 15% and high R^2 change
LP	Narrow	RV_E change less than 20% and negligible change in R^2
Perc	Moderate	Negligible RV_E with smaller R2 change

Parameters FC, LP and KHQ are classified as highly sensitive, parameters Perc and Beta are classified as sensitive while K4 and Alfa are classified as non-sensitive parameters.

Establishing the Regional Model

Relations between model parameters and PCCs are established by simple and multiple linear regression. By a correlation matrix, significant dependency is indicated for 11 combinations of model parameters and catchment characteristics out of a total of 200 (see Table 6). Significant correlations are in bold and are tested in establishing the regional model.

Multiple linear regression analysis is applied to improve on the simple linear relation by adding PCCs using forward selection or backward elimination method.

The model for a multiple regression reads:

$$Y' = \beta_0 + \beta_1 X_1 + \beta_2 X_2 + \beta_3 X_3 + \dots \beta_n X_n \qquad [9]$$

Where: β_1, β_3 …β_n are regression coefficients, X_1, X_2, X_3 …X_n are independent variable (catchment characteristics), Y' is the dependant variable (model parameter) and ß0 is an intercept of the regression line.

Table 6. Correlation between catchment characteristics and model parameters of gauged catchments

Catchment Characteristics	Model paramter							
	Alfa	Beta	FC	K4	KHQ	LP	Perc	Hq
Area km^2	-0.32	**0.81**[*]	**-0.88**[*]	0.67	-0.52	**0.88**[*]	0.61	0.44
Length of longest flow path km	-0.64	0.57	**-0.83**[*]	0.31	-0.26	0.68	0.54	0.04
Drainage density (m/km^2)	0.18	0.65	-0.14	-0.14	-0.14	0.12	0.37	0.02
Hypsometric Integral	0.48	-0.43	**0.81**[*]	-0.67	0.7	-0.69	0	-0.2
Average slope of catchment %	-0.49	0.51	-0.71	0.35	**-0.82**[*]	0.45	-0.28	-0.16
Percentage of level	0.49	0.23	0.34	-0.31	0.3	-0.2	0.37	0.11
Percentage of hilly	-0.61	-0.32	-0.45	0.48	-0.08	0.4	-0.05	0.11
Percentage of steeply	-0.28	-0.09	-0.16	0.06	-0.49	-0.05	-0.68	-0.33
Circularity index	-0.73	0.12	-0.5	-0.11	0.2	0.3	0.43	-0.28
Percentage of luvisols	-0.05	-0.13	0	0.07	0.67	0.21	**0.82**[*]	0.36
Percentage of leptosols	0.19	0.14	0.03	0.07	-0.67	-0.15	-0.74	-0.17
Percentage of nitisols	0.33	-0.28	0.37	-0.03	-0.27	-0.37	-0.72	-0.1
Percentage of vertisols	0.54	-0.6	**0.81**[*]	-0.41	**0.81**[*]	-0.56	0.13	0.1
Percentage of fluvisols	-0.71	0.29	-0.47	-0.31	-0.33	0.06	-0.24	-0.7
Elongation ration	-0.63	0	-0.24	-0.39	0.3	0.01	0.24	-0.49
Climate index	0.26	0.69	-0.23	0.17	-0.14	0.35	0.59	0.35
Average altitude m asl	-0.75	0.56	**-0.94**[*]	0.42	-0.55	0.71	0.22	-0.05
Percentage of bare land	-0.65	0.05	-0.22	-0.55	-0.03	-0.18	-0.24	**-0.81**[*]
Percentage of crop land	0.21	-0.32	0.29	0.03	-0.24	-0.29	-0.67	-0.08
Percentage of forest	0.36	0.17	0.06	0.23	-0.64	-0.06	-0.59	0.08
Percentage of grass land	-0.57	0.09	-0.46	0.11	-0.56	0.15	-0.52	-0.4
Percentage of woody savannah	0.24	0.1	0.13	-0.05	0.49	0.08	0.7	0.33
Percentage of urban and built-up	0.23	-0.41	0.4	-0.12	-0.16	-0.43	-0.75	-0.19

A number of regional models have been established by considering all parameters. When establishing a regional model it is essential that the regional model should statistically be significant but also that the model is plausible from a hydrological point of view.

In this work a number of relations for the HBV– IHMS model parameters are established. Alfa, through backward elimination, is related to the average altitude and percentage of bare land with correlation coefficient r^2 of 87% and also Alfa is related to percentage of bare land and percentage of hilly with r^2 of 85%.

Alfa = 13.83 – 3.85 log (average altitude) – 0.23 log (% of bare land)[10]

Alfa = 1.65 - 0.26 (% of bare land) -0.02 (% of hilly)   [11]

Beta, through backward elimination, is related to area with percentage of hilly or percentage of luvisols indicates two potential strong relations with r2 of 84% and 75% respectively.

Beta = 1.17 + 0.000808 (Area) – 0.014 (% of hilly)   [12]

Beta = 0.68 + 0.0008 (Area) -0.0041(% of luvisols)   [13]

FC by forward entry method shows a significant relation with catchment area and percentage of hilly with a statistically strong correlation r^2 of 96%.

FC = 2142.81 – 0.803 (Area) – 17.33 (% of hilly)   [14]

K4 optimization of the simple relation is done by backward elimination, statistically strong relations is established with r^2 of 98% with hypsometric Integral, percentage of nitisols and percentage of fluvisols.

K4 = 0.049 – 0.057 (hypsometric integral) – 0.001 (% of nitisols) – 0.001 (% of fluvisols)   [15]

KHQ optimization is done by backward elimination; the result shows a statistical strong relation with area and percentage of luvisols with r^2 of 91%.

KHQ = 0.114 -0.000036 (Area) + 0.00060 (% of luvisols)   [16]

The correlation table shows a significant relation between LP and catchment area, optimization with Percentage of bare land results a statically strong relation with r^2 of 83%.

173

LP = 0.06 + 0.0006 (Area) – 0.12 (%of bare land)   [17]

To estimate the value of Hq a regression is made by forward entry method starting with the only significant relation percentage of bare land, after optimizing the relation by catchment area the result shows statistically strong relation r^2 of 90%.

Hq = 4.64 + 0.0019(Area) – 2.34 (% of bare land)   [18]

The ensamble of the regression equations make up the so called regional model. For some HBV parameters default values are used and reference is made to (Wale, 2008).

Validation of Regional Model

        By the purpose of regionalisation to estimate model parameters of ungauged catchments the performance of the regionalisation must be assessed by comparing the predicted and observed response characteristics for gauged test catchments. Since in this study the number of gauged catchments is limited to 5, it is not possible to carry out a formal validation process with independent catchments. In stead is validation of the regional model done by introducing a validation period from 2001 to 2003 for all 5 gauged catchments.

        The model parameters of gauged catchments are estimated based on the regional model established using PCCs of the gauged catchment. Table 7 shows model performance of the regional model parameters. The result shows a satisfactory result with R^2 greater than 0.6 and RV_E smaller than +10% or –10%.

Table 7. Validation of the regional model on gauged catchments from 2001 to 2003

	Gilgel Abay	Ribb AZ	Gumara	Megech	Kilti
R^2	0.78	0.75	0.81	0.65	0.61
RV_E %	-5.1	-8.69	-8.84	-9.85	-8.66

Prediction of Discharge at the Ungauged Catchments

In this section gauged catchments model parameters are transferred to ungauged catchments to enable runoff estimation by HBV – IHMS model. A total of 11 ungauged catchments representing 48% of the lake basin area are extracted, 5 of them are part of simulated catchments downstream of gauging station, 3 of them are catchments with unsatisfactory result including ungauged areas downstream of gauging location (see section 4.1.2) and the remaining 3 are completely ungauged (i.e. Tana west, Derama and Gabi Kura). Ungauged catchment model parameters are transferred by the regional model, spatial proximity and area ratio techniques.

Parameter Transfer by a Regional Model: the regional model developed for gauged catchments is used to estimate model parameters of ungauged catchments by respective PCCs.

Parameter transfer by spatial proximity: parameters of gauged catchments are transferred to the nearby ungauged catchment based on the assumption that catchments that are close to each other will likely have a similar runoff regime.

Parameters transfer by catchment size comparison: gauged catchment model parameter sets are transferred to ungauged catchment of comparable catchment area by assuming that catchment area is the dominate factor for a volume of water to be generated. Using the parameter estimates of the above procedures runoff from ungauged catchment is simulated by the HBV-IHMS model. The result of long-term monthly averaged flow from 1992 to 2003 shows that runoff estimates by spatial proximity is highest followed by parameter transfer by area ratio and the regional model (see Figure 2).
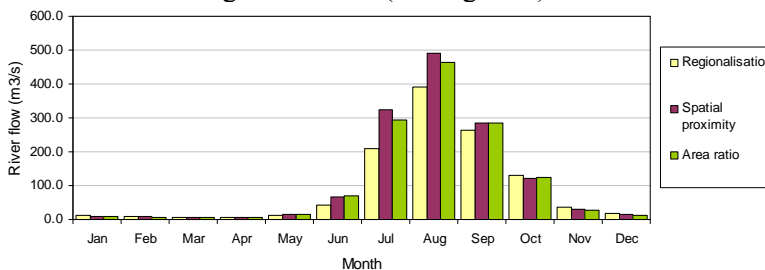
Figure 2. Comparison of long-term average monthly runoff estimates (1992 - 2003)

RESULT AND DISCUSSION

For simulation of Lake water level, bathymetry data from a survey by the Institute for Geoinformation Science and Earth Observation (ITC) 2006 has been used. During the survey data was collected at a 30 second time interval following a 5 km traverse route that covered for a total path of 835 km. By the survey a total of 4424 sample points are collected at distances of some 200 to 300m.

For establishing the bathymetric map some additional 425 sample control points along the lake and islands boundary are included as extracted from SRTM DEM. Points have elevation value of 1786.30m that is the average lake gauge level for the period 11 - 22 February 2000 when the SRTM data was collected from space. The interpolated map is sliced by ArcGIS 3D Analyst and respective volume, surface area and elevations are calculated. Eqn's [19] and [20] shows the polynomial fitted elevation-volume and area-volume relations of Lake Tana.

$$E = 1.21*10^{-13}(V)^3 - 1.02*10^{-8}(V)^2 + 6.2*10^{-4}(V) + 1774.63$$
$$R^2 = 0.999 \qquad\qquad [19]$$

$$A = 7.93*10^{-11}(V)^3 - 5.81*10^{-6}(V)^2 + 1.65*10^{-1}(V) + 1147.51$$
$$R^2 = 0.990 \qquad\qquad [20]$$

Where: A is area in Km^2, V is volume in Mm^3 and E is elevation in m.a.s.l.
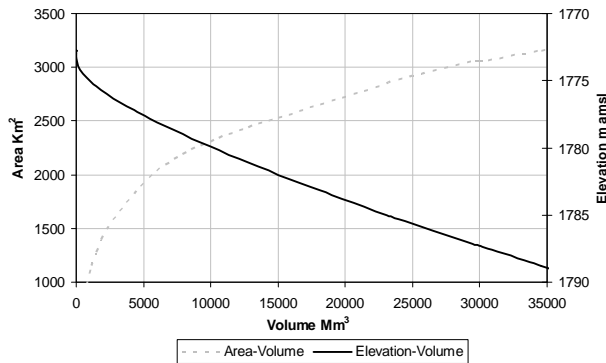
Figure 3. Elevation-Volume and Area-Volume relationship of Lake Tana

A spread sheet water balance model is developed to simulate the lake level based on Eqn's [21] and [1]. The model applies estimates of ungauged flows by the three procedures and results are shows in Figure 4.

$$V_{Lake(t)} = V_{Lake(t-1)} + \frac{\Delta S}{\Delta T}$$ [21]

Where: $V_{Lake(t)}$ is lake total volume at day t, $V_{Lake(t-1)}$ is lake volume at day t-1 and ΔS change in lake storage.
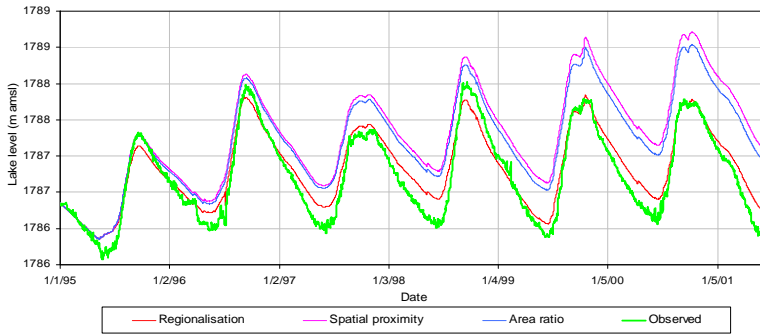
Figure 4. Comparison of lake level simulation in different ungauged flow estimation techniques

Lake level simulation using ungauged flow estimates by regionalisation shows best performance. For the spatial proximity and area ratio approaches the lake level simulation shows larger deviation from the observed lake levels as shown in Figure 4 while deviations increase over the simulation period. Table 8 shows performance indicators of lake level simulations for the three procedures.

Table 9. Performance indicators of lake level simulation (1995 - 2001)

Ungauged catchment approach	R2 [-]	RVE [%]
Regionalisation	0.90	1.6
Spatial proximity	0.003	7.07
Catchment size comparison	0.18	6.08

Lake level simulation using regionalisation shows best performance with R^2 of 0.9 and RV_E of 1.6%. Therefore only the results from regionalisation are used in Tana water balance simulations. In Table 9 respective balance terms are shown and indicate that the balance closure term is as large as 170 mm.

Table 10. Annual averaged Lake Tana water balance terms (1995 - 2001)

Water balance terms	mm	MCM
Lake areal rainfall	1220	3784
Gauged river inflow	1280	3970
Ungauged river inflow	880	2729
Lake evaporation	-1690	-5242
River outflow	-1520	-4714
Closure term	-170	-527

The closure term indicates a water balance error as large as 5% of the total lake inflow and a lake relative volumetric error of only 1.6%. We assume that errors are by the uncertain lake-groundwater interaction and some uncertainty to be associated with estimations of open water evaporation, lake areal rainfall, runoff from gauged and ungauged catchments.

CONCLUSION

Surface runoff inflow from ungauged catchments is estimated by transferring calibrated model parameters of gauged catchments. Result of parameter transfer by regionalisation, spatial proximity, and catchment size comparison indicate ungauged flows as large as 42%, 47% and 46% of the total Lake Tana river inflows. In this study show Lake rainfall is estimated at 1220mm/year, open water evaporation is estimate at 1690mm/year, lake inflow by Gilgel Abay, Megech, Gumara, Ribb and Kilti rivers is estimated at 1280mm/year and river inflow from 11 ungauged catchments is estimated at 880mm/year. River outflow is estimated at 1520mm/year and closure term is as large as 170mm/year as calculated for the period 1995 to Jan 1 2001. Simulation of lake levels show a satisfactory performance compared to the observer lake level with only 1.6% of RV_E when inflows from ungauged catchments are by regionalisation. The water balance closure is some 5% of the total annual lake inflow by rainfall and river inflows.

REFERENCE

Booij, M.J., Deckers, D.L.E.H., Rientjes, T.H.M. and Krol, M.S. (2007). Regionalisation for uncertainty reduction in flows in ungauged basins. Wallingford : IAHS, 2007. ISBN 978-1-90150278-09-1(IAHS Publication ; 313) pp. 329-337

Burnash, R.J.C, Ferral, R.L. & McGuire, R.A. (1973). A generalized streamflow simulation system. Conceptual modeling for digital computers. U.S. Department of Commerce, National Weather Service & State of California, Department of Water Resources.

Chow, V. t., D. R. Maidment, et al. (1988). Applied hydrology. New York etc., McGraw-Hill.

Conway, D. (1997). A water balance model of the Upper Blue Nile in Ethiopia. Hydrological Sciences Journal-Journal Des Sciences Hydrologiques 42(2): 265-286.

Dingman, S. L. (1994). Physical hydrology + disk for Lotus version 2 or 3. Upper Saddle River, Prentice Hall.

Gupta, H.V., Sorooshian, S., Yapo, P.O (1998). Toward improved calibration of hydrological models: multiple and non commensurable measures of information. Water resource research 34 (4), 751-763.

Heuvelmans, G., B. Muys and J. Feyen (2006). "Regionalisation of the parameters of a hydrological model: Comparison of linear

regression models with artificial neural nets." Journal of
        Hydrology 319(1-4): 245-265.

IHMS (2006). "Integrated Hydrological Modeling System
        Manual." Version 5.1.

Kebede, S., Y. Travi, et al. (2006). "Water balance of Lake Tana and its
        sensitivity to fluctuations in rainfall, Blue Nile basin, Ethiopia."
        Journal of Hydrology 316(1-4): 233-247.

Lindstrom, G., Johansson, B., Persson, M., Gardelin, M., & Bergstrom,
        S. (1997). Development and test of the distributed HBV-96
        hydrological model. Journal of Hydrology, 201, 272-288

Maidment, D. R. (1993). Handbook of Hydrology.

Merz, R. and Blöschl, G., 2004. Regionalisation of catchment model
        parameters. Journal of Hydrology, 287, 95-123.

Patricia K. (2005). From Conflict to Cooperation in the Management of
        Transboundary Waters. Linking Environment and Security –
        Conflict Prevention and Peace Making in East and Horn of
        Africa

Rientjes, T. H. M. (2007). Modeling in Hydrology. ITC, Enschede, the
        Netherlands.

Seibert, J., (1999). Regionalisation of parameters for a conceptual
        rainfall-runoff model. Agricultural and Forest Meteorology, 98-
        99, 279-293

SMEC, I. P. (2007). "Hydrological Study of The Tana-Beles Sub-
        Basins." part 1.

Vallet-Coulomb, C., D. Legesse, F. Gasse, Y. Travi and T. Chernet.
        (2001). "Lake evaporation estimates in tropical Africa (Lake
        Ziway, Ethiopia)." Journal of Hydrology, 245(1-4): 1-18.

Young, A. R. (2005). "Stream flow simulation within UK ungauged
        catchments using a daily rainfall-runoff model." Journal of
        Hydrology 320(1-2): 155-172.

Yadav, M., T. Wagener and H. Gupta (2007). "Regionalization of
        constraints on expected watershed response behavior for
        improved predictions in ungauged basins." Advances in Water
        Resources 30(8): 1756-1774.

HYDROLOGICAL WATER BALANCE OF LAKE TANA, ETHIOPIA

[1]Yirgalem A. Chebud and [2]Assefa M. Melesse

[1]Department of Earth Sciences, Florida International University, USA
[2]Department of Environmental Studies, Florida International University, USA

ABSTRACT

The level of Lake Tana fluctuates annually and seasonally following the patterns of changes in precipitation. In this study, a mass balance approach is used to estimate the hydrological balance of the lake. Water influx from five major rivers, subsurface inflow from the flood plains, precipitation, outflow from the lake constituting river discharge and evapotranspiration from the lake is analyzed on a monthly and annual basis. Spatial interpolation of precipitation using rain gage data was conducted using kriging. Outflow from the lake was identified as the evaporation from the lake surface as well as discharge at the outlet where the Blue Nile commences. Groundwater inflow is estimated using MODFLOW Software that showed an aligned flow pattern to the river channels. The groundwater outflow is considered negligible based on the secondary sources that confirmed absence of lake water geochemical mixing outside of the basin. Evaporation is estimated using Penman, Meyer's and Thornwaite's methods to compare the mass balance and energy balance approaches. Meteorological data, satellite images and temperature perturbation simulations from Global Historical Climate Network (GHCN) of NOAA are employed for estimation of evaporation input parameters. The difference of the inflow and out flow was taken as storage in depth and compared with the measured water level fluctuations. The study has shown that the monthly and annually calculated lake level replicates the observed values with RMSE value of 0.17m and 0.15m, respectively.

Key Words: Lake Tana, Blue Nile River, water balance

INTRODUCTION

Lake Tana is located in the northwestern part of Ethiopia (Figure 1) and it has a surface area of 3156 km^2, which is 20% of the 16000 km^2 drainage area. The lake receives perennial flow from four rivers: Gilgel Abay, Rib, Gumera, and Megech contributing 93% of the inflow, and at the outlet starts the Blue Nile. Very few studies that target at sensitivity of the lake level through time with changes in climatic conditions have reported that the lake is less sensitive to rainfall variations showing 10% decrease in lake level despite 50% decrease in precipitation (Kebede et al., 2005). Apparently, such studies are based on lumped mass balance approaches. Two approaches of validation seem relevant to establish the hydrological water balance of Lake Tana. The first approach by Immerzeel (2007) is validation of the water balance from distributed hydrological modeling perspective. This approach has shown that the sensitivity of the inflow to precipitation, showing 32% decrease in runoff with 10% decrease in precipitation (CEEPA, 2006). This has shown that sensitivity of the water balance against precipitation is indirect through the runoff demanding a distributed hydrological model. The significance of sensitivity of the water budget to runoff given the seasonal distribution of rainfall is reported by Conway (1997). The second approach (Moreda et al., 2006) is to validate the components on lumped water balance. This approach is set to review water balance parameters and also estimate a lumped hydrological balance of Lake Tana. The rationale is to see the room for improvement of methods on input determination even before costly distributed hydrological models is employed.
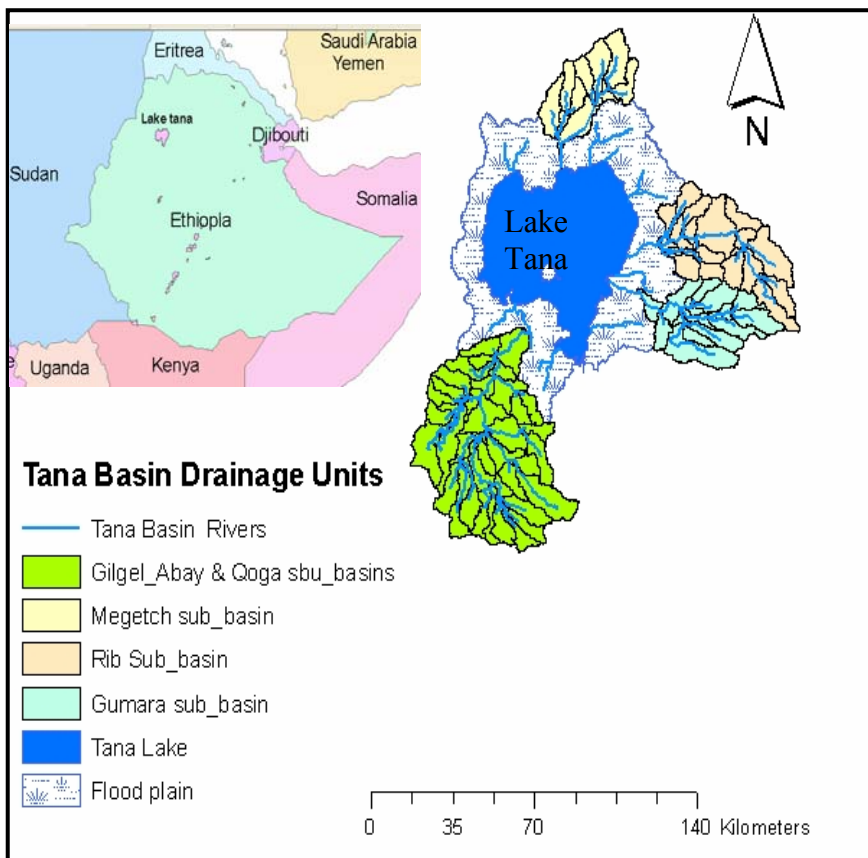
Figure 1. Tana basin, sub basins and the flood plain

Review on Water Balance Input Variables

Precipitation

Point measurement of precipitation and the increasing uncertainty on spatial distribution is a major problem for large scale hydrological studies. In recent years, the use of satellite images and estimation of perceptible water vis a vis determination of cold cloud duration index (CCD) is in the fine tuning process. Such studies conducted in the Blue Nile River basin have shown a correlation coefficient of 0.65 with the rain gauge measurements (El-Sebaie, 1997). This approach will have a significant role in understanding ungauged

watersheds. On the other hand, the use of statistical down-scaling techniques, namely Kriging appear to be preferable for its incorporation of the data to generate an ensemble and interpolate or extrapolate the spatial estimates. The spatial regression of precipitation with latitude, longitude and altitude has worked well in the upper Blue Nile basin (Conway, 1997). These methods overweigh the traditional approach of Thiesson polygon and contouring techniques.

Evapotranspiration

Evapotranspiration is often estimated with the assumption of mass and energy balances or a combination of the two. Amongst these methods, the energy budget equation is reported to be reasonably appropriate for large scale studies (Melesse et al., 2006, Lee et al., 2000). The stability of the method is determined by the Bowen Ratio (BR) of the sensible heat flux against the heat used for evaporation and simplified as follows (Lee et al., 2000).

$$BR = 0.00061P(T_0 - T_a)/(e_0 - e_a) \qquad\qquad (1)$$

Where P is barometric pressure, in millibars; T_0 is water-surface temperature, in degrees

Celsius; T_a is air temperature at 2 m above the lake in degrees Celsius; e_0 is saturation vapor pressure at the water-surface temperature in millibars; and e_a is vapor pressure at 2 m above the lake in millibars.

The ratio constrains the applicability between $0 - 1$. While the negative value would mean no evaporation, large positive values suggest inclusion of mass balance. In the case of Lake Tana, the average lake surface temperature data is about $3^{\circ}C$ above the air temperature (Kebede et al., 2005) and the energy budget equations is applicable at all seasons. However, applicability of energy budget equation could be questionable in large lakes where turbulence production could overweigh the buoyancy for certain period. In such conditions, accounting the evaporation through mass transfer budgets could be acceptable.

The applicability is constrained by Stability parameter for Mass Transfer (*SMT)*, which is proportional to the Richardson number (Lee et al., 2000)

$$SMT = (T_h - T_0)/(u_h)^2 \tag{2}$$

Where, T_h is temperature at height h, in degrees Celsius; T_o is temperature of the lake surface, in degrees Celsius; and u_h is wind speed at height h, in miles per hour.

When, *SMT* is high, the mass-transfer equation underestimates evaporation the (buoyant forces dominate) implying use of energy budget equation could be realistic. On the other hand, if SMT is low, the mass-transfer equation tends to overestimate evaporation (turbulent forces dominate). For Lake Tana, the stability will depend on the test using the meteorological data of wind speed. Given its size of 3156 sq km, the build up of turbulence (wind eddies) because of the water as a source of moisture that increases momentum flux is evident. This could be observed from two adjoining sites of the lake one a major town called Bahir Dar with wind breaks and the other a flood plain with no wind shelter. The momentum of the wind dies abruptly in both cases as it goes out of the lake indicating that the momentum flux is dependent on the moisture source than presence of the wind breaks. This suggests that evaporation estimation from the lake should differ in approach from the land surface and mass transfer would be relevant for the lake though it could be certain period of the season or day.

Pan Method is also often used to estimate evaporation from free water surface. Nevertheless its relevance is skewed to small ponds for the size, sensitivity to perturbation of temperature and reasonable accuracy of specific heat capacity of ponds (Lee, 2000).

Runoff

Water balance estimates are highly sensitive to runoff (CEEPA, 2000) and for any sensitivity analysis of the water balance against precipitation, an established relationship of runoff with precipitation in any distributed model could be important. However, in areas where paucity of data is evident little can be done in the lumped water balance modeling. Inflow to the lake from the four major rivers is taken as input to the water balance.

Ground water

In most ground water modeling exercises, models such as MODFLOW (Anderson and Woessner, 1992), and MIKESHE (Hai et al., 2007) are proven helpful. But equally, numerical methods namely iterative finite difference methods have shown simplicity without compromising accuracy of results.

A numerical method for groundwater flow representation using a Poison's equation (Wang and Anderson, 1982) is indicated as follows.

For steady state
$$\frac{\partial^2 h}{\partial x^2} + \frac{\partial^2 h}{\partial y^2} = \frac{E}{T} \tag{3}$$

For transient flows
$$\frac{\partial^2 h}{\partial x^2} + \frac{\partial^2 h}{\partial y^2} = \frac{S}{T}\frac{\partial h}{\partial t} + \frac{E}{T} \tag{4}$$

Where h = head; T = transmissivity; E = evapotranspiration, S = storativity, t = time

The choice is dependent on the level of complications. In either of the cases, use of hydrogeologic units and well representation of the boundary and initial conditions would be vital to simplify the modeling process. For complex physical models, use of the MODFLOW is encouraging while the numerical methods could be sufficient to address in flat plains with sound boundary and initial conditions. Understanding ground water flow patterns at different seasons and geological structures help to determine the physical hydrogeologic units. Leakance to an aquifer and evapotranspiration from the land surface is major inputs for the modeling exercise. Measureable variables namely, hydraulic conductivity would be obtained from secondary sources (Kebede et al., 2005) though expert judgment could still help to use it in context. Lastly availability of hydraulic head 'h' is vital for calibration of the models.

METHODOLOGY

The physical level water budgeting is done based on conservation of mass summing up components of inflows and outflows in the system. The components (identified in the water cycle) include precipitation (P), evapotranspiration (ET), river inflow/outflow, ground water recharge/discharge (G) and change in surface storage (ΔS). P +

$$\text{River Inflow} + G_{inflow} - ET - \text{River outlow} - G_{out} \pm \Delta S = 0 \qquad (5)$$

Precipitation was acquired form the rain gage information monitored by the Ethiopian Metrological Agency. Discharge data on river were acquired form the Ethiopian Ministry of Water Resources. ET was estimated based on data from satellite information acquired from U.S Geological Survey (USGS) and also metrological information from the Ethiopian Metrological Agency.

Data Analysis

Precipitation

Point measurements of precipitation are collected from secondary sources and developed to ArcGIS (ESRI, 2007) format point shape files from which Kriging was employed to interpolate and extrapolate the precipitation distribution over the lake. The farthest precipitation measurement is Debre Tabor, about 45 km from the periphery of the lake. Kriging is employed to cover the geographical variation of the rainfall. It observed that the rainfall over the lake is dominated by the northern part of the lake (Gondar). The analysis showed that contribution of the rainfall to the lake amounts to 3.78 billion cubic meter (BCM) contributing, which is 50% of the total inflow.

Lake Evaporation

The daily lake evaporation estimation is carried out using three methods: energy balance (Penman Method), mass transfer (Meyer's deterministic formula) and a simplified approach (Thornwaite Method). It is found out that the energy budget equation may not be stable for April, May, June and July as the Bowen ration is showing negative values. Similarly, the stability parameter SMT has shown small values in

September, October, November and January suggesting a comparative advantage of the two approaches in different seasons.

Penman Equation

The energy balance approach is represented by Penman Method using the equation below as

$$E_{tp} = \frac{\frac{\Delta}{\Delta + \gamma}(R_n - G) + \frac{\gamma}{\Delta + \gamma}6.43(1 + 0.53u_2)(e_s - e_d)}{\lambda} \quad (6)$$

E_{tp} = Potential evapotranspiration in mm/day, R_n = net radiation in MJ m^{-2}d^{-1}, G = heat flux density to the ground in MJ m^{-2}d^{-1}, λ = latent heat of vaporization in MJ /kg, u_2 = wind speed measured 2m above the ground in m/s, Δ = Slope of the saturation vapor pressure – temperature curve, KPa/^{o}C, γ = psychometric constant, KPa/^{o}C, e_s-e_d = vapor pressure deficit in kPa. The detailed parameters computation is shown in (Ward and Elliot, 1995)

For Penman estimation, mean monthly temperature and elevation data are collected from Ethiopian Metrological Agency while wind speed and solar insolation for Bahir Dar station are collected from World Metrological Organization.

Table 1. Meteorological data, (WMO, 2008)

Variable	Jan	Feb	Mar	Apr	May	Jun	Jul	Aug	Sep	Oct	Nov	Dec
Insolation, kWh/m²/day	5.8	6.2	6.5	6.6	6.3	5.7	5	5	5.7	5.9	6	5.7
Clearness, 0 - 1	0.7	0.7	0.6	0.6	0.6	0.6	0.5	0.5	0.6	0.6	0.7	0.7
Temperature, °C	21.1	22.4	23.5	22.5	21.4	19	17.9	17.9	18.8	20.3	20.6	20.6
Wind speed, m/s	4.1	4.3	4.1	4.1	4.1	5.1	5	4.2	3.5	3.1	3.8	4.1
Precipitation, mm	4	3	9	24	84	178	438	386	199	90	22	4
Wet days, d	2.2	2.7	3.6	5.4	8.2	11.5	12.4	14.4	10.7	5.5	2.4	1.8

Mass Transfer Approach

Meyer's approach is based on the deterministic approach derived from the general boundary layer atmospheric system. The underline assumption as stated elsewhere is that the turbulent production term overweighs the buoyancy on open water surfaces of large sizes such as lake, and big dams. Results are location independent for estimation of evapotranspiration. It is computed using the following formula (Lee et al., 2000).

$$E = C \, (e_s - e_d) \, (1 + u_{25}/10) \tag{7}$$

E = Evaporation (in/month), e_s = Saturation vapor pressure (in of Hg) of air at the water temperature 1ft deep, e_d = actual vapor pressure (inches of Hg) = $e_{s(air\,T)}$ * RH,
u_{25} = average wind velocity (mi / hr) at a height of 25 feet above the lake or surrounding land areas, C = Coefficient; 11 for small lakes and reservoirs and 15 for shallow ponds

Meyer's approach demands determination of surface temperature of the lake unlike the Penman method of air temperature for the energy budgets. For this purpose, two years lake surface temperature is estimated using 24 satellite images from 1999 & 2005 (two images for each month). The images are radiometrically corrected by converting the digital number value in Landsat thermal band (band 6-1 and band 6-2) to radiance values. Afterwards the radiance values were changed to effective temperature value according to Landsat-7 ETM handbook of NASA as validated in different studies (Bambang et al., 2001). The conversions are found as follows.

$$L_\lambda = ((LMAX_\lambda - LMIN_\lambda)/ (DNMAX - DNMIN)) * (DN - DNMIN) + LMIN_\lambda \tag{8}$$

$$T_{Landsat} = K_2 / \ln((K_1 / L_\lambda) + 1) - 273 \tag{9}$$

Where L_λ ; Spectral radiance watts/(m*m * ster * μm), DN ; Digital Number, $LMIN_\lambda$; Spectral radiance which is correlate with DNMIN watts/(m*m * ster * μm), $LMAX_\lambda$; Spectral radiance which is correlate with DNMAX watts/(m*m * ster * μm), DNMIN; Minimum value of

DN (1 (LPGS Product) or 0 (NLAPS Product)), DNMAX ; Maximum value of DN = 255, $T_{Landsat}$; Effective temperature (Celsius), K_1; 666.09 W/(m*m*ster*µm), calibration const, K_2; 1282.71 W/(m*m*ster*µm), calibration const, Value of $LMIN_\lambda$, $LMAX_\lambda$, DNMIN and DNMAX are in the header file information (meta data) that comes with the Landsat data.

Mean monthly air temperature is also derived from temperature anomaly simulation by the GHCN_NOAA. The scatter confirms that the GHCN temperature has 1:1 relationship with the meteorological data while mean lake surface temperature is 3°C above the air temperature confirming an accepted relationship (Kebede et al., 2005). The scatter diagram shows an overestimation by the satellite-based temperature estimation. This could be associated with the dominance of shallow depth of the water in most parts of the lake inflating the radiance value.
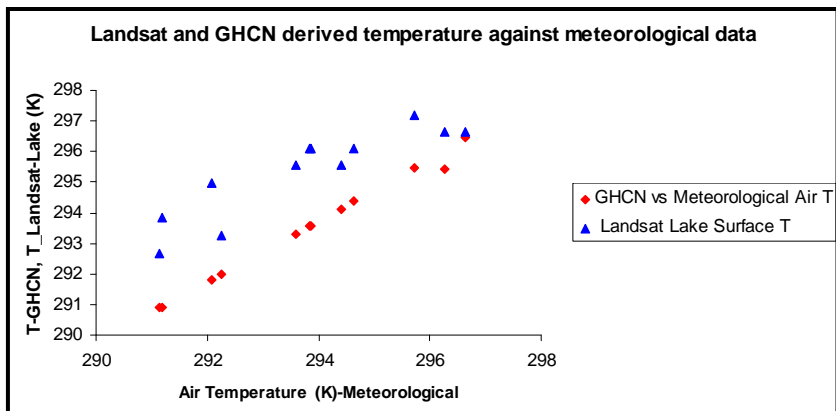
Figure 2. Lake Tana surface Temperature (°K) determined based on Landsat ETM+ correlated with GHCN and meteorological air temperature.

Temperature perturbation (anomaly) data (1972-2005) is derived from the GHCN_NOAA and compared to the mean monthly temperature of the meteorological data for the years of analysis (Figure 2).

Thornwaite Method

The Thornwaite Method is suggested for its temperature data dependence only.

$$Etp = 16\ [10T/I]^4 \tag{10}$$

Where Etp = Monthly ET in mm, T = Mean monthly temperature in $^{\circ}$C, a = location dependent coefficient described by

$$a = 6.75 \times 10^{-7}I^3 - 7.71 \times 10^{-5}I^2 + 1.792 \times 10^{-2}I + 0.49239 \tag{11}$$

where $I = \sum\limits_{j=1}^{j=12} \left[\dfrac{T_j}{5} \right]^{1.514}$

Tj is the mean monthly temperature during month j (oC)

Comparison of the three evapotranspiration estimation methods is shown in Figure 3. The energy budget and mass transfer have shown their seasonal advantages. From January to June, when the buoyancy dominates the turbulent production, Penman's method could be relevant. The turbulent production has dominated from June to October, suggesting the relevancy of the Meyer's Method. In all the cases, the Thornwaite Method has underestimated the evapotranspiration from the lake. For estimation of the monthly water budget, both the energy and mass transfer methods are used. The annual water budget is estimated using the Thornwaite method for reasonably low propagated errors from derivation of the historical temperature data whose perturbation is limited to -1.5 $^{\circ}$C up to 1.5°C.
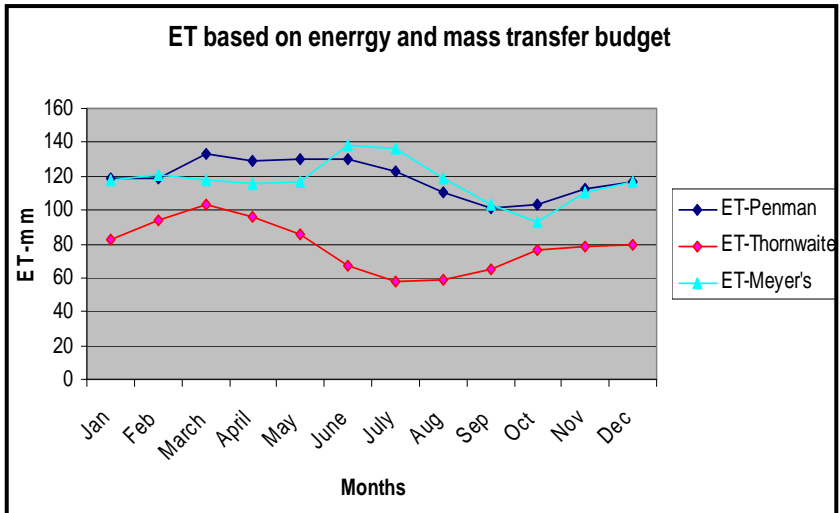
Figure 3. Monthly ET estimated for Lake Tana using the three methods.

Groundwater Flow

Preliminary analysis is first done to estimate the ground water inflow into the lake. Whereas the outflow is less significant given the less permeable basalt that dams the lake (Kebede et al., 2005). In order to understand the groundwater dynamics, one of the sub-basins namely Gumera was used to look at the flow in the sub-basin. This hydrogeological simulation through forced boundary condition has shown that in both the dry and wet season, the hydraulic head is concentrated near the streams showing that the flow is a subdued form of the watershed relief flowing across the outlet, not differing from thin section across the stream courses. This gave a clue that the ground water input from the watershed would be captured from the base flow of the stream and the flow through the thin unconfined section. A separate contribution is identified from the flood plain that is flooded for months during the rainy season and starts to yield into the lake during the dry seasons. This contribution is from a 20 km section of flood plain which carves as a concentric circle centering Lake Tana (Figure 4).
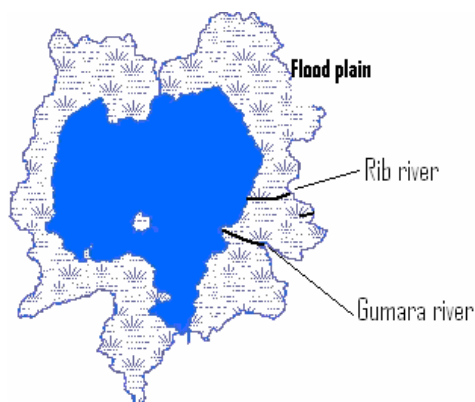
Figure 4. Lake Tana flood plain.

The hydraulic head distribution from the simulation for the dry season indicate that subsurface flow is from the rivers towards the flood plains, higher heads near the rivers with decreasing gradient towards the main land. The hydraulic head is calibrated against shallow wells in the flood plain and it is found out that the flood plain receives about 0.16 billion cubic meters (BCM) from base flow of the rivers, while the flood plain itself contributes 0.1BCM to Lake Tana. The difference (6 millions m^3) is being stored in the flood plain. A one dimensional transient flow simulation for the wet season indicates the reversal of the head distribution.

Runoff

River flow data gauged by Ethiopian Ministry of Water Resources in all the sub-basins including the outflow of Blue Nile at Bahir Dar is used in this analysis. Inflowing rivers identified are Rib, Megech, Gumera, and Gilgel Abay. The outflow is the Blue Nile river discharge just at the outlet of Lake Tana. Mean annual, mean monthly and monthly flows of 42 years data (1960 to 2003) is used to analyze the flow (Figure 5). The relationship indicates the outflow has an extended recession limb seemingly tipping the storage. The surface water inflow from the four sub-basins is about 3.5BCM making up 42% of the total inflow while the outflow at the outlet of the Blue Nile amounts to 5.3BCM.
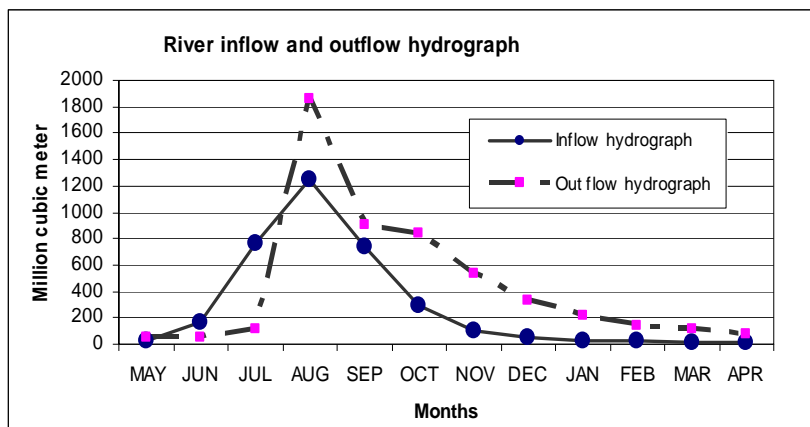
Figure 5. Inflow and outflow hydrograph of Lake Tana.

The monthly computed balance against the measured lake level shows a reasonable fit with RMSE value of 0.17m (Figure 6). The calculated lake level using different approaches of ET estimation is plotted against the measured values and it suggests no significant difference because of the distribution over months. However, on annual basis, the mass transfer method accounts to additional loss of 85mm (0.25BCM). Component wise precipitation contributes about 54% (4.26 BCM) and sub-basin level subsurface water inflow contributes about 3% (0.27BCM, dry and wet season combined). The total outflow at the outlet amounts to 5.3BCM while evapotranspiration attributes 45% of the loss (4.6 BCM). Looking at the overall balance, the inflow shows a deficit of 10% against the outflow suggesting the contributions of unaccounted inflows. The unaccounted inflows are runoff from the flood plain, regional groundwater flow, and some incurred error. In previous studies, assumptions are often held attributing 7% groundwater contribution to the inflow (Kebede et al., 2005). This is confirmed reasonable, though it should include the runoff from the flood plain.
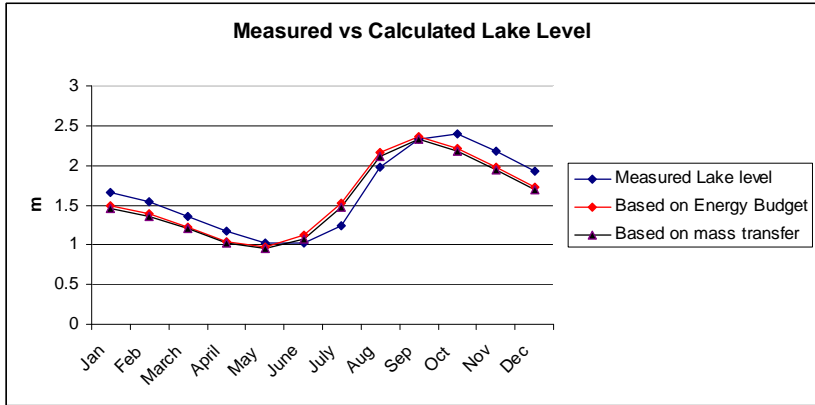
Figure 6. Measured vs. calculated average monthly Lake Tana Level using ET estimation based on energy budget and mass transfer.

The annual water budget is based on Thornwaite Method (to reduce propagated error). Historical temperature data for considerable number of years is derived from GHCN which shows a 1:1 relationship with mean monthly temperature data (Figure 2). As it is observed on Figure 7, all the computed values have underestimated the evapotranspiration. On annual basis it underestimates loss of 1.5BCM. Even then differences on annul measured and calculated lake level indicate a goodness of fit with RMS value: 0.15
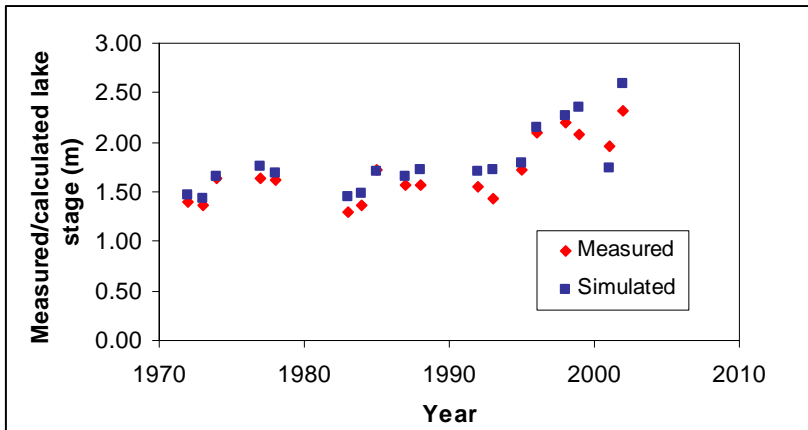
Figure 7. Mean annual stage levels of Lake Tana (1960-2003). Lake stage is referenced at 1783.5 m amsl.

CONCLUSION

At the outset the objective of this study was set to review water balance parameters and undertake lumped modeling over Lake Tana. The review is met with deeper understanding of precipitation distribution, evapotranpiration governing factors, groundwater flow patterns and runoff contribution. For Lake Tana scale point measurement of rainfall and application of kriging looks viable. However, it was discovered that except around the peripheries of the lake most of the sub-basins that have hilly topography are ungauged demanding other techniques (e.g. Satellite imagery) of precipitation measurement. Runoff measurement is also at station level and a distributed estimation has suffers from lack of temporally distributed precipitation data and spatially disaggregated measurement or estimation.

Though the result on the overall balance was not significant, it is learnt that the energy budget and mass transfer methods of ET estimation disparate seasonally in high turbulence production vs buoyancy dominating seasons. This suggests seasonal applications of the two methods especially for open water surfaces of ponds, dams and lakes. In this study, the seasonal application the two methods is seen to give better estimate than the sole use of any of the methods. With more accurate estimation of the unguaged runoff from the flood plain the balance using the combined methods of the evapotranspiration would give the best fit.

Further studies to validate the work with more data on groundwater flow, unaccounted runoff ad small streams contributions and precipitation data with good distributions of rain gages will help strengthen the results shown in this study.

ACKNOWLEDGEMENTS

REFERENCES

Anderson M., W.Wossener, 1992, Applied Groundwater Modeling: Simulation of Flow and Advective Transport, Academic Press, USA.

CEEPA, 2006, Climate Change and African Agriculture, Vulnerability of water resources of Lake Tana, Ethiopia to climate change, Policy Note No. 30, University of Pretoria, South Africa.

CONWAY D., 1997 A water balance model of the Upper Blue Nile in Ethiopia, *Hydrological Sciences-Journal-des Sciences Hydrologiques,* 42(2). pp. 265-286.

El-Sebaie I., O. El-Nawawi, Shaker I, 1997, Remote sensing applications for forecasting the amount of rainfall over the Blue Nile Basin, Journal of Environmental Hydrology, Vol 5, 1997.

ESRI, 2007. ArcGIS 9.2. Users Manual. Environmental Systems Research Institute (ESRI). Redlands, CA.

Hai L, Chen X, A.Bao, L Wang, 2007, Investigation of groundwater response to overland flow and topography using a coupled MIKE SHE/MIKE 11 Modeling system for an arid watershed, Journal of Hydrology, Vol, No.347 pp 448-449

Immerzeel, P. Droogers, 2007, "Calibration of a distributed hydrological model based on satellite Evapotranspiration", Future Water, Costerweg 1G, 6702 AA Wageningen, The Netherlands

Kebede S., Y.Travi , T.Alemayehu, V Marc, 2005, Water balance of Lake Tana and its sensitivity to fluctuationsin rainfall, Blue Nile basin, Ethiopia, **Journal of Hydrology** Volume 316, Issues 1-4, Pages 233-247

Kebede S., Y Trav, T Alemayehu, T. Ayenew, 2005, Groundwater recharge, Circulation and Ethiopia

LEE T.M, A Swancar, 2000, Influence of Evaporation, Ground Water, and Uncertainty in the Hydrologic Budget of Lake Lucerne, a Seepage Lake in Polk County, Florida, United States Geological Survey Water-Supply

Melesse A., V Nangia, X. Wang, 2006 "Hydrology and Water Balance of Devils Lake Basin: Part 1, Hydrometeorological Analysis and Lake Surface Area Mapping", Journal of spatial hydrology, Vol.6, No1, 119-132.; Part 2; Grid-Based Spatial Surface Water Balance Modeling*", Journal of spatial hydrology, vol.6, No 1. 132-145.

Moreda F, Koren V., Z. Zhang, S. Reed, Smith M, 2006, Parameterization, of distributed hydrological models: learning

from the experiences of lumped modeling, Journal of Hydrology 320 (2006) 218–237.

Trisakti B, S Sulma, S Budhiman, 2002, *Study* of Sea Surface Temperature (SST) using Landsat-7 ETM (In Comparison with Sea Surface Temperature of NOAA-12 AVHRR), the thirteen workshop of OMISAR

Wang, H.F, and M.P. Anderson, 1982, Introduction to Ground Water Modeling; Finite Difference and Finite Element Methods, W.H. Freeman, 256 p.

Ward A and W Elliot, 1995, Environmental hydrology, LEWIS Publishers, USA.

WMO, 2008. Mean monthly Metrological data. http://www.wmo.ch/pages/publications/meteoworld/_en/index_en.html (accessed January, 2008).

MODELLING EROSION AND SEDIMENTATION IN THE UPPER BLUE NILE

Steenhuis, Tammo. S.[1], Collick, Amy S.[2], Awulachew, Seleshi .B.[3], Enyew Adgo[4], Ahmed, Abdassalam Abdalla[5] and Easton, Zachary M.[6]

[1] Professor, Cornell University, Ithaca, NY USA, tss1@cornell.edu
[2] Assistant Professor, Bahir Dar University, Bahir Dar Ethiopia
[3] IWMI Regional Representative, Sub-regional Officer for Nile Basin & Eastern Africa, Addis Ababa, Ethiopia, s.bekele@cgiar.org
[4] Director Natural Resources, ARARI, Bahir Dar Ethiopia, enyewadgo@yahoo.com
Currently: Professor, Bahir Dar University, Bahir Dar Ethiopia
[5] Director, UNESCO Chair in Water Resources (UNESCO-CWR), Khartoum Sudan aaahmed55@yahoo.co.uk
[6] Research Associate, Cornell University, Ithaca, NY USA, zme2@cornell.edu

ABSTRACT

Accurate models simulating the discharge and sediment concentrations of the Nile are necessary for optimum use of the Nile water. Previous research has shown that direct runoff originates from saturated areas at the lower portions of the hillslope. For this saturation excess runoff, total runoff for a rain storm is independent of the rainfall intensity and water balance models are, therefore, appropriate for simulating river discharges. To account for the spatially distributed runoff, the landscape is divided into potential saturated areas producing overland flow and hillslopes generating interflow and baseflow. The water balance model is coupled with a simplified erosion model. The ratio of direct runoff to total flow is used to predict the sediment concentration by assuming that only the direct runoff is responsible for the sediment load in the stream. The combined model employs a minimum number of physically based parameters that can be calibrated. There is reasonable agreement between the model predictions and the ten day observed discharge and sediment concentration at the El Karo gauging station on Abay Blue Nile at the Ethiopian-Sudanese border

Key Words: Erosion, Sedimentation, Rainfall-runoff, Sediment Gauging

INTRODUCTION

The Abay Blue Nile River in Ethiopia contributes significant flow and sediment to the Nile River. Thus, a better understanding of the hydrological processes, soil loss erosion potential, and sedimentation mechanisms in the headwaters of the Nile River is of considerable importance. There is a need to improve and augment current resource management and development activities in areas with heavy degradation and low productivity, particularly in Ethiopia, where only five percent of surface water is utilized by Ethiopians. There is a particular need to develop the existing hydropower and irrigation potential of the Abay Blue Nile for socio-economic development in Ethiopia while maintaining sustainable operation of water infrastructure systems downstream in Sudan and Egypt. This paper focuses on characterizing the rainfall-runoff-sediment relationships for the Ethiopian portion of the Abay Blue Nile River. The majority of river sedimentation in the basin occurs during the early period of the rainy season and annual water runoff discharge peaks consistently lag the sediment peaks during the rainy season.

Liu et al. (2008) found that saturation excess runoff from saturated areas dominates the runoff process in several watersheds in the Ethiopian highlands. Water balance models are consistent with this type of runoff process since the runoff is related to the available watershed storage capacity and the amount of precipitation but not generally the precipitation intensity. Moreover models developed and intended for use in temperate regions (such as the USDA-SCS Curve Number method) where rainfall is generally well distributed throughout the year do not perform well in regions with monsoonal rainfall distributions (Liu et al., 2008). Therefore, water balance models, that track soil moisture levels (and saturation dynamics), often perform better than more complicated models in Ethiopia type landscapes (Johnson and Curtis, 1994; Conway, 1997; Kebede *et al.*, 2006; Liu et al., 2008).

MODEL DEVELOPMENT

A water balance type rainfall runoff model was developed and tested by Collick et al. (2008) to predict the stream flow for four relatively small watersheds in the Nile Basin. The authors reported reasonable predictions on a daily time step using nearly identical parameters for watersheds hundreds of kilometres apart. Some minor modifications were made with respect to interflow generation for

predicting the discharge of the whole Abay Blue Nile. For clarity we will present the complete watershed water balance model and add a simple erosion model. Some initial testing is done on the discharge and sediment concentration measured at the Ethiopian-Sudan border at the El Diem gauge station.

Predicting Direct Runoff, Interflow and Base Flow

The watershed is divided into two sections, the hillslopes, and the relatively flatter areas that become saturated during the rainfall season. The hillslopes have high percolation rates (McHugh, 2006) and water is generally transported subsurface as interflow (e.g. over a restrictive layer) or base flow (percolated from profile). The flatter areas that drain the surrounding hillslopes become runoff source areas when saturated (Figure 1 shows a schematic). The profile itself for the hillslopes is dived up in a root zone where the plants extract water and a bottom layer that transmit the excess water to the stream. In the saturated contributing area all excess water becomes surface runoff, and this is what we are most concerned with, we simulate only the top layer (root zone) in this application.
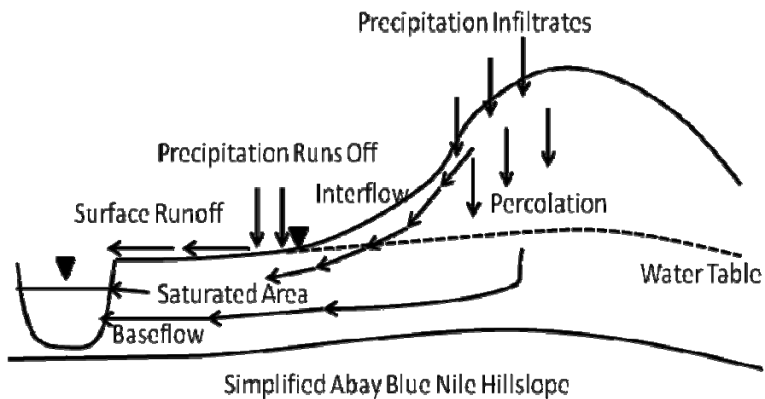
Figure 1. Schematic cross-section for the Blue Nile basin

The amount of water stored of the topmost layer of the soil, S (mm), for hillslopes and the runoff source areas were estimated separately with a water balance equation of the form:

$$S = S_{t-\Delta t} + (P - AET - R - Perc)\Delta t \qquad (1)$$

where P is precipitation, (mm d^{-1}); AET is the actual evapotranspiration; $S_{t-\Delta t}$, previous time step storage, (mm), R saturation excess runoff (mm d^{-1}), $Perc$ is percolation to the subsoil (mm d^{-1}) and Δt is the time step

During wet periods when the rainfall exceeds evapotranspiration (i.e., $P>PET$), the actual evaporation, AET, is equal to the potential evaporation, PET. Conversely, when evaporation exceeds rainfall (i.e., $P<PET$), the Thornthwaite and Mather (1955) procedure is used to calculate actual evapotranspiration, AET (Steenhuis and van der Molen, 1986). In this method AET decreases linearly with moisture content, e.g.

$$AET = PET\left(\frac{S_t}{S_{max}}\right) \qquad (2)$$

Where PET is the potential evapotranspiration (mm d^{-1}). The available soil storage capacity, S_{max}, (mm) is defined as the difference between the amount of water stored in the top soil layer at wilting point and the upper moisture content that is equal to either the field capacity for the hillslopes soils or saturation in runoff contributing areas. S_{max} varies according to soil characteristics (e.g., porosity, bulk density) and soil layer depth. Based Eq. 2 the surface soil layer storage can be written as:

$$S_t = S_{t-\Delta t}\left[\exp\left(\frac{(P - PET)\Delta t}{S_{max}}\right)\right] \qquad when\, P < PET \qquad (3)$$

In this simplified model direct runoff occurs only from the runoff contributing area when the soil moisture balance indicates that the soil is saturated. The recharge and interflow comes from the remaining hillslopes areas. There is no surface runoff from these areas. This will underestimate the runoff during major rainfall events but since our interest in weekly to monthly intervals this thought to be a major limitation.

In the saturated runoff contributing areas when rainfall exceeds evapotranspiration and fully saturates the soil, any moisture above saturation becomes runoff, and the runoff, R, can be determined by adding the change in soil moisture from the previous time step to the difference between precipitation and actual evapotranspiration, e.g.,

$$R = S_{t-\Delta t} + (P - AET)\Delta t \qquad (4a)$$

$$S_t = S_{max} \qquad (4b)$$

For the hillslopes the water flows either as interflow or baseflow to the stream. Rainfall in excess of field capacity becomes recharge and is routed to two reservoirs that produce baseflow or interflow. We assumed that the baseflow reservoir is filled first and when full the interflow reservoir starts filling. The baseflow reservoir acts as a linear reservoir and its outflow, BF, and storage, BS_t, is calculated when the storage is less than the maximum storage, BS_{max}

$$BS_t = BS_{t-\Delta t} + (Perc - BF_{t-\Delta t})\Delta t \qquad (5a)$$

$$BF_t = \frac{BS_t[1 - \exp(-\alpha \Delta t)]}{\Delta t} \qquad (5b)$$

When the maximum storage, BS_{max}, is reached then

$$BS_t = BS_{max} \qquad (6a)$$

$$BF_t = \frac{BS_{max}[1 - \exp(-\alpha \Delta t)]}{\Delta t} \qquad (6b)$$

The interflow originates from the hillslopes and with the slope of the landscape as the major driving force of the water. Under these circumstances, the flow decreases linearly (i.e., a zero order reservoir) after a recharge event. The total interflow, IF_t at time t can be obtained by superimposing the fluxes for the individual events (details are given in the Appendix):

$$IF_t = \sum_{\tau=0,1,2}^{\tau*} 2Perc_{t-\tau}^* \left(\frac{1}{\tau*} - \frac{\tau}{\tau*^2} \right) \qquad (7)$$

203

where τ^* is the duration of the period after the rainstorm until the interflow ceases, IF_t is the interflow at a time t, Perc$^*_{t-\tau}$ is the remaining percolation on t-τ days after the base flow reservoir is filled up

Predicting Sediment Concentration

The Abay Blue Nile runs through a deep gorge partly over bedrock before it reaches the Sudanese border. This means that the sediment concentration depends on the amount of suspended sediment delivered by the watersheds to this reach of the Nile. Assuming that subsurface flow does not cause erosion then all sediment is contributed by the direct surface runoff. Therefore, it is reasonable to assume that the sediment concentration in the Nile is determined by direct runoff from the contributing areas. Initially in the beginning of the rainy season the contributing areas expand and once the watershed is sufficiently saturated the contributing area does not expand further and the hillslopes begin contributing interflow. Thus, once the watershed is saturated (i.e., the hillslopes are contributing water to the stream); the sediment concentration in the water is a function of the surface runoff and interflow components. In other words, the subsurface flow dilutes the concentration of sediment delivered by the direct runoff delivered to the stream. We will call the sediment concentration in the river C^* when all saturated areas begin contributing and or the interflow is generated for the first time. The discharge is R^* at that time. For calibration purposes later we will assume that this equal to the maximum averaged 10 day concentration.

Based on the conceptual model above, we find that for the period the hillslopes are contributing interflow the sediment concentration, C, in the river is the ratio of the direct runoff and total runoff multiplied by C^*, viz:

$$C = C^* \frac{R}{R + IS + BS} \qquad (8)$$

Where R, runoff, IS, Interflow, and BS, baseflow are predicted by the water balance model, above.

Moreover, at the onset of the rainy season, when the watershed is wetting up, the contributing area increases and the discharge is smaller for any given storm than it would be later in the season. Although we do not know the exact mechanisms, it is reasonable to assume that the

concentration is equal to the ratio of predicted runoff to the maximum direct runoff, $R*$ viz:

$$C = C * \frac{R}{R*} \qquad (9)$$

Thus, the maximum concentration $C*$ and $R*$ are calibration parameters, and are set equal to the yearly maximum ten day averaged sediment concentration and the discharge during that period.

APPLICATION: THE ABAY BLUE NILE

Input Data

There is relatively little sediment concentration data available for the Abay Blue Nile. One of the most complete data sets of continuous sediment concentrations is given by Ahmed (2003) and consists of ten day averaged sediment concentrations at the El Karo gauge station at the Ethiopian-Sudan border for the period of June-October 1993. The 10 day discharge values at this station and the averaged precipitation over the entire Abay Blue Nile basin in Ethiopia are also available for the period of May 1st 1993 to April 30th 1994. To use the water balance we need the start the simulations before the rainfall period begins (and the sediment data were available), thus, we choose to start in January 1994. Consequently, we composed a year consisting of the rainfall of January 1994 to April 1994 for the first part of the simulation followed by the actual record for April-October 1993 (Figure 2).

Other parameters needed to simulate the discharge include: Potential evapotranspiration, which varies little between years and it was set at 5 mm d^{-1} during the dry season and 3.3 mm d^{-1} during the rainy season. The storages for the contributing area and hillslopes were based initially on the values from Collick et al. (2008) for three SRCP watersheds. Although the Collick et al. (2008) values gave a reasonable fit, we decided to vary them slightly to improve the agreement between observed and predicted values as the correct distribution between subsurface flow and overland flow directly determines the predicted sediment concentrations. Collick et al. (2008) assumed that 40% of the landscape had a S_{max} value of 100 mm. This represent, the contributing area in their model. For the Abay Blue Nile basin, we found a slightly better fit by reducing the contributing area to 30%. We divided the contributing area in two parts (Table 1a): 20% of the area needed little

rain to generate direct runoff (i.e., S_{max} = 10mm) and 10% needed 250 mm of effective precipitation after the dry season before generating runoff (i.e., S_{max} = 250mm). Note that that the weighted average S_{max} for the Abay Blue Nile Basin in Ethiopia compares well with the S_{max} value of 100 mm storage for two of the three SRCP watersheds (Collick et al., 2008).

Scale comes into play when simulating the hydrological dynamics of the hillslopes in the Abay Blue Nile as compared to the SRCP watersheds located in the upper reached of the basin (Collick et al., 2008). A small portion of the moisture (approximately 20% in two of three SRCP watersheds was lost to deep percolation. To simulate deep percolation, Collick et al. (2008) assumed that the S_{max} was essentially infinite (4000 mm). If we discount this storage we find that the Smax = 500 mm for the complete Nile basin (Table 1a) compares well with the values used in Collick et al. (2008).

Scale also impacts the interflow and baseflow predictions in the conveyance zone more than the storage values in the uppermost top layer. A more complicated approach was needed to adequately represent the complex landscape by using both a linear ground water reservoir and zero order hillslope reservoir. Fitted parameters are given in Table 1b.

Table 1a: Model input: S_{max} values

Portion of Watershed	Storage mm	Type
0.2	10	contributing area
0.1	250	contributing area
0.7	500	hillside

Table 1b: Model input: Other Model Parameters

SB_{max}	20	mm
t*r	140	days
c*	500	mg/l
R*	1.4	mm/day

Simulation Results

The observed rainfall and the predicted and observed discharge are given in Figure 2. The various components: Direct runoff and the sum of the interflow from the hillslopes and baseflow are shown in Figure 3. In the beginning of the rainy season almost all flow in the river is direct runoff generated from the 20% of the area that has the smallest storage. As the rainy season progresses (cumulative rainfall increases), the rest of the landscape wets up and runoff is generated from the remaining 10% of the contributing area followed by base and interflow from the hillslopes in early July 1993. Note that this corresponds to the time that the sediment concentration in the river is decreasing from the maximum (Figure 4). Less obvious but just as important is that the volumes of predicted and observed discharge in Figure 2 (i.e., areas under the curves) are equal indicating that the water balance does indeed balance with in a hydrologic cycle. In other words we can account for all precipitation that does not evaporate as stream flow in the same year. Finally, this water balance is able to explain the observed runoff coefficient of (i.e., discharge/precipitation) of approximately 20-30% during period when the majority of rainfall occurs by distributing the effective rainfall (rainfall minus potential evaporation) over saturated contributing areas that generate direct runoff - and interflow and baseflow component from the remaining 70%.
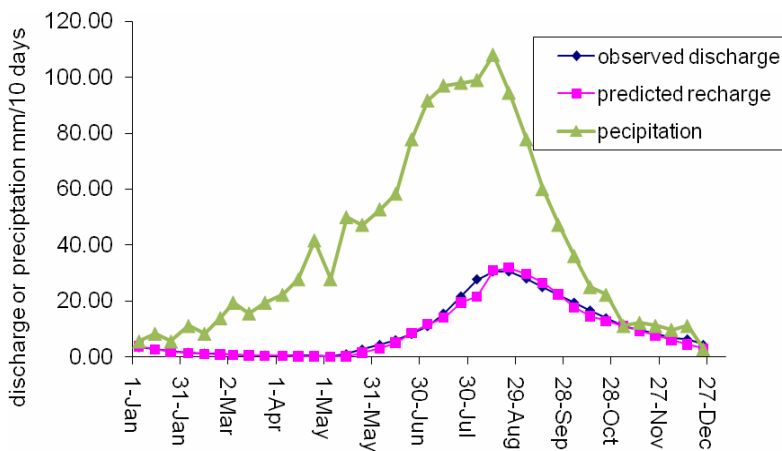
Figure 2. Precipitation predicted and observed discharge for 10 day periods in the Abay Blue Nile at El Karo.

To predict sediment concentration (Eqs. 8 and 9), the only calibration parameters is the maximum observed concentration and the flux at that time. We have set this concentration at 5000 mg/l (Table 1b). The remaining parameter values are all obtained from the water balance model presented in Figures 2 and 3. Observed and predicted sediment concentrations are shown in Figure 4. It is interesting that this simple, physically based sediment model can predict the sediment concentrations well using fluxes predicted by the water balance model. We cannot predict the sediment concentration at the end of July when the concentration suddenly drops. The model might be further improved if more processes are included. However, it should be noted that the concentrations are predicted and not the load as in other models. Loads depend on both concentration and discharge and any error in sediment concentrations.
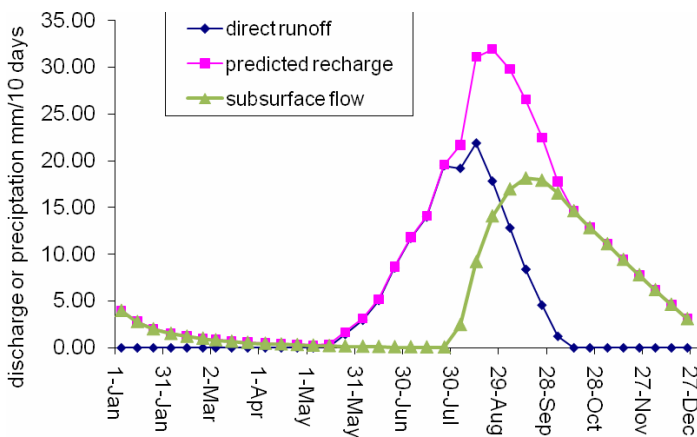
Figure 3. Predicted total discharge, direct runoff, and subsurface flow for the Abay Blue Nile at El Karo at the Ethiopian Sudanese Border.

DISCUSSION AND CONCLUSIONS

The hydrological model presented here based on direct runoff production by saturated areas, and is reasonably robust. The results of Collick et al. (2008), using a similar model applied to watersheds <500 ha, and this work reasonably reproduce the observed discharges with a

similar parameter set for root zones but slightly different subsurface routines.

We do not fully understand all of the process governing the erosion and sedimentation dynamic observed in the Abay Blue Nile, thus the sediment predictions in this paper should be considered tentative until more testing is done. It is interesting to note the decrease in observed stream concentrations before the peak runoff occurs, and that the model captures the phenomenon is important, but other, more complicated process may play a role. For instance, it could be the result of relating the sediment concentration to the time when the watershed becomes covered by vegetation. Based on watershed outflow concentrations, we cannot discriminate between these mechanisms since both signals appear at the same time because when interflow occurs the watershed is wet and vegetation begins to develop. Thus, more research is needed to elucidate erosion processes, particularly gully erosion within the watershed. We plan to do this during the summer and fall of 2008 with Cornell graduate students of the Masters Program of Integrated Management and Hydrology at Bahir Dar University and from the Ithaca campus.
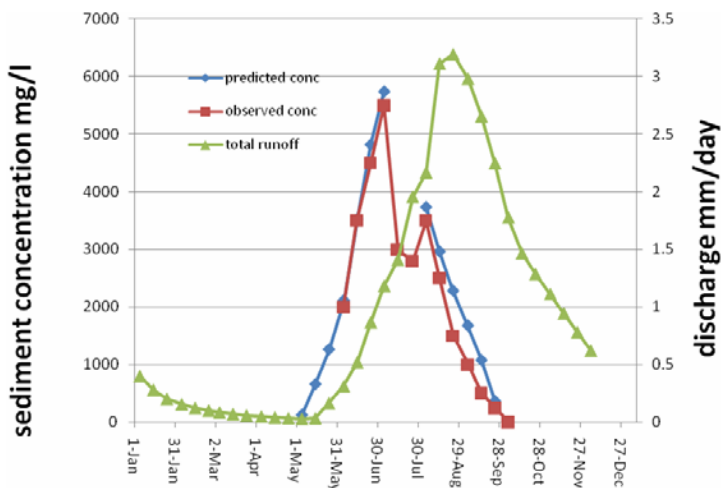
Figure 4. Predicted and observed sediment concentration in the Abay Blue Nile at El Karo.

209

APPENDIX:
DERIVATION OF INTERFLOW DISCHARGE FOR ZERO ORDER RESERVOIRS

The flux from a reservoir in generally can be expressed as a function of the flux from the aquifer (Brutsaert and Nieber, 1977)

$$\frac{dQ}{d\tau} = -aQ^b \qquad (A1)$$

Where a is a constant. For a zero order reservoir $b=0$ and a first order reservoir $b=1$;
Next the flux equation is derived as a function of the reservoir storage S. For zero order reservoir the flux from the reservoir is decreasing linearly for a single storm, i.e.

$$\frac{dQ_t}{d\tau} = -a_0 \qquad (A2)$$

Without loss of generality we can replace the time t with τ in Eq. (A1) defined as the time after the storm has occurred. In addition, we have indicated the flow Q_t is from the particular storm occurring at time t. Integrating with respect to t subject to the boundary condition that at a time $\tau*$ after the rain event the flux is zero (i.e., Q=0 at $\tau=\tau*$). Since

$$Q_t = a_0(\tau*-\tau) \qquad (A3)$$

Integrating again from $\tau=0$ to $\tau = \tau*$ we find the storage in the aquifer:

$$\int_0^{\tau*} Q_t d\tau = SI_t = \frac{1}{2}a_0\tau*^2 \qquad (A4)$$

Where Perc*$_t$ is the amount of water added to the reservoir at time t. In order to conserve mass it is obvious from Eq. A3 that:

$$a_0 = \frac{2Perc_t^*}{\tau*^2} \qquad (A5)$$

Combining Eqs. A5 and A3 results in the zero order flow equation for the discharge of the aquifer for a storm occurring at time t:

$$Q_t = 2Perc_t^*\left(\frac{1}{\tau*} - \frac{\tau}{\tau*^2}\right) \qquad (A6)$$

The total flux is equal for a daily time step

$$BI_t = \sum_{\tau=0}^{\tau^*} 2 Perc^*_{t-\tau} \left(\frac{1}{\tau^*} - \frac{\tau}{\tau^{*2}} \right) \qquad (A7)$$

REFERENCES

Ahmed A.A. 2003. "Sediment Transport and Watershed Management Blue Nile System",Friend/Nile Project report, Sudan.

Brutsaert, W. and Nieber J.L. 1977. Regionalized drought flow hydrographs from a mature glaciated plateau, *Water Resour. Res.*, *13*, 637-643.

Collick, A.S., Easton, Z.M., Adgo, E., Awulachew, S.B., and Steenhuis, T S. 2008. *In Eds.* W. Abtew and A. M. Melesse. Proceedings of the 2008 workshop on the Nile Basin hydrology and ecology under extreme climatic conditions.

Conway D. 1997. A water balance model of the Upper Blue Nile in Ethiopia. *Hydrological Sciences Journal* **42**(2): 265–286.

Johnson P.A., Curtis P.D. 1994. Water-balance of Blue Nile river basin in Ethiopia. *Journal of Irrigation and Drainage Engineering-ASCE* **120**(3):

Kebede S, Travi, Y, Alemayehu T, Marc V. 2006. Water balance of Lake Tana and its sensitivity to fluctuations in rainfall, Blue Nile basin, Ethiopia. *Journal of Hydrology* **316**: 233–247.

Lui, B.M., A.S. Collick, G. Zeleke, E. Adgo, Z.M. Easton, and T.S. Steenhuis. 2008. Monsoonal rainfall-discharge relationships. Hydrol. Proc. 22.

McHugh O.V. 2006. Integrated water resources assessment and management in a drought-prone watershed in the Ethiopian highlands. PhD dissertation, Department of Biological and Environmental Engineering. Cornell University Ithaca NY.

SEDIMENTS BUDGET OF THE NILE SYSTEM: A GEOLOGIC PERSPECTIVE

Mohamed G. Abdelsalam
Missouri S&T
Department of Geological Sciences and Engineering
1400 N. Bishop Avenue
Rolla, MO, 65401
abdelsam@mst.edu

ABSTRACT

It is estimated that ~4,000 km^3 of fertile soil was deposited within the floodplain and delta of the Egyptian Nile since the river was connected to the rest of Sub-Sahara Africa Nile ~800,000 years ago. Much of this geological material was removed from Sub-Sahara Africa to be deposited within the Egyptian Nile which is controlled by the ~6 Ma old and ~300 meters deep Eonile Canyon. This canyon is topped with ~100 meters deep fertile soil layer (erosion products of the Ethiopian Plateau) overlying medium to coarse sand and gravel (erosion products of the Precambrian Red Sea Hill rocks), and deeper marine carbonates (deposited when the Missinian Salinity Crisis forced the Mediterranean water to extend as far south as the Sudanese-Egyptian boarder). Hence, a depositional rate of ~125 m^3/km^2/year is required to build the ~40,000 km^2 Egyptian Nile floodplains and delta assuming constant deposition rate and absence of tectonic disturbances. On the other hand, it is estimated that 93,200 km^3 of geological material was removed from the 250,000 km^2 catchement area of the Blue Nile since the beginning of its incision on the NW Ethiopian Plateau ~30 Ma ago. Steady incision rate yields ~12.5 m^3/km^2/year erosion rate since the beginning of the incision of the Blue Nile on the plateau ~30 Ma ago. This rate is only one-tenth of the deposition required to build the floodplains and delta of the Egyptian Nile. Erosion rate of the Ethiopian Plateau by the Blue Nile - deduced for the geological record – is also a fraction of the present day erosion rate within the Blue Nile catchment area estimated from river sediments load to be between ~125 and 490 m^3/km^2/year. The vast discrepancy between the depositional rate along the Egyptian Nile floodplain and delta, and the erosion rate of the Ethiopian Plateau by the Blue Nile can be explained by one or more of the following reasons: (1) Dramatic acceleration of incision of the Blue Nile in the Ethiopian Plateau since ~1 Ma resulting in an increased rate of erosion; hence increased amount of

sediment flux received in Egypt. This is supported by recent studies which indicate that the incision rate of the Blue Nile on the Ethiopian Plateau has increased significantly in the past ~6 Ma. (2) The White Nile and the Tekeze-Atbara rivers might have equally been major supplier of sediments eroded from the Lake Plateau Region and the Ethiopian Plateau and deposited along the Egyptian Nile floodplains; (3) The time when the Egyptian Nile was connected to the Sub-Sahara Africa Nile is much older than the suggested ~800,000 years.

EVALUATION OF SATELLITE RAINFALL ESTIMATES AND GRIDDED RAINGAUGE PRODUCTS OVER THE UPPER NILE REGION

Tufa Dinku, Steve Connor and Pietro Ceccato

International Research Institute for Climate and Society
The Earth Institute at Columbia University; tufa@iri.columbia.edu

ABSTRACT

A dense station network over the Ethiopian highlands is used to perform an extensive validation and inter-comparisons of eleven satellite rainfall products and five gridded gauge products. The satellite products include Global Precipitation Climatology (GPCP), NOAA-CPC Merged Analysis (CMAP), the Tropical Rainfall Measuring Mission (TRMM) products 3B42 and 3B43, NOAA-CPC African Rainfall Estimation Algorithm (RFE), NOAA-CPC African Rainfall Climatology (ARC), GPCP one-degree daily (1DD), Tropical Applications of Meteorology using Satellite and other data (TAMSAT) product, the CPC morphing technique (CMORPH), Precipitation Estimation from Remotely Sensed Information using Artificial Neural Network(PERSIANN), and the Naval Research Laboratory's blended product(NRL). These products are evaluated at spatial and temporal resolutions of 2.5^o and monthly, 1.0^o and 10-daily, and 0.25^o and daily. The first and second group of products exhibited reasonably good performance. The results are not so good for comparisons of daily rainfall. The gridded monthly rainfall products include the Global Precipitation Climatology Center (GPCC), NOAA Climate Prediction Center (NOAA-CPC), and the Climate Research Unit at the University of East Anglia (UEA-CRU).   There is a very good agreement between the global products and the reference data. Correlation coefficients are about 0.95, 0.92, and 0.90 at 2.5^o, 1.0^o and 0.5^o resolutions, respectively. The performance of the products is highest during the wettest season (Jun to August), while it is relatively poor during the dry months (December, January, February). These results are very encouraging, particularly considering the complex terrain of the validation site.

INTRODUCTION

Satellite rainfall estimates are becoming very important sources for rainfall information, particularly in regions like Africa where the rain gauge distribution is very sparse. Global gridded products are also used widely in many applications. However, there has been very little validation work, particularly over Africa. In this study a relatively dense station network over the Ethiopian highlands is used to validate satellite rainfall estimates and gridded gauge products at different spatial and temporal scales. The validation region is located over Ethiopia, 5°N to 13°N, and 35°E to 40°E. It has a very complex topography with alternating valleys and mountain ranges that varies between below sea level and a highest peak of about 4620 meters.

The validation of satellite rainfall estimates was performed for three groups of products. The first group (GPCP, CMAP and 3B43) were evaluated at spatial resolution of 2.5° and monthly accumulation. The second group, which consists of NOAA-CPC African Rainfall Estimation Algorithm (RFE, Herman et al. 1997), NOAA-CPC African Rainfall Climatology (ARC, Love et al. 2004), GPCP one-degree daily (1DD, Huffman et al. 2001), the "TRMM and Other Satellites: product (3B42, Huffman et al. 2003), TAMSAT (Tropical Applications of Meteorology using Satellite data, Grimes et al. 1999, Thorne et al., 2001), and the CPC morphing technique (CMORPH, Joyce et al. 2004), were evaluated at 10-daily accumulation and 1° spatial resolution. The third group of products are evaluated at relatively high spatial (0.25°) and temporal (daily) scales. These products include RFE, 3B42, CMORPH, PERSIANN (Precipitation Estimation from Remotely Sensed Information using Artificial Neural Network, Hsu et al. 1997), and the naval research laboratory blended product (NRL, http://www.nrlmry.navy.mil/sat-bin/rain.cgi). Evaluation of five global gridded products has also been done. Three of these products come from the Global Precipitation Climatology Center (GPCC), one by the Climate Prediction Centre at the National Oceanic and Atmospheric Administration (NOAA-CPC), and another product is from the Climate Research Unit at the University of East Anglia (UEA-CRU) in UK. The three products from GPCC (Fuchs et al. 2007) are the monitoring (GPCC-mon), full-data analysis (GPCC-ful), and the 50-year climatology (GPCC-clm). The monitoring product is available at 1° and 2.5° spatial resolutions, while GPCC-ful and GPCC-clm are produced at

grid sizes of 0.5°, 1° and 2.5°. The NOAA-CPC product (Chen et al., 2002), known as PREC/L (precipitation reconstruction overland), has a spatial resolution of 2.5° while that of UEA-CRU (New et al., 2000, Mitchell and Jones, 2005) is produced at 0.5° resolution.

STUDY REGION AND DATA

The study site is a complex terrain over Ethiopia (Figure 1). The central topographic feature of the country consists of the East African Rift Valley and chain of mountains. The major rain producing feature is the Inter Tropical Convergence Zone (ITCZ); however, topography complicates the rainfall patterns significantly. The annual rainfall pattern is very complex with some areas having rainfall for ten consecutive months; others receive rainfall just for a couple of months, while still others are characterized by two distinct rainfall seasons. About 149 stations were obtained National Meteorological Agency (NMA) of Ethiopia.
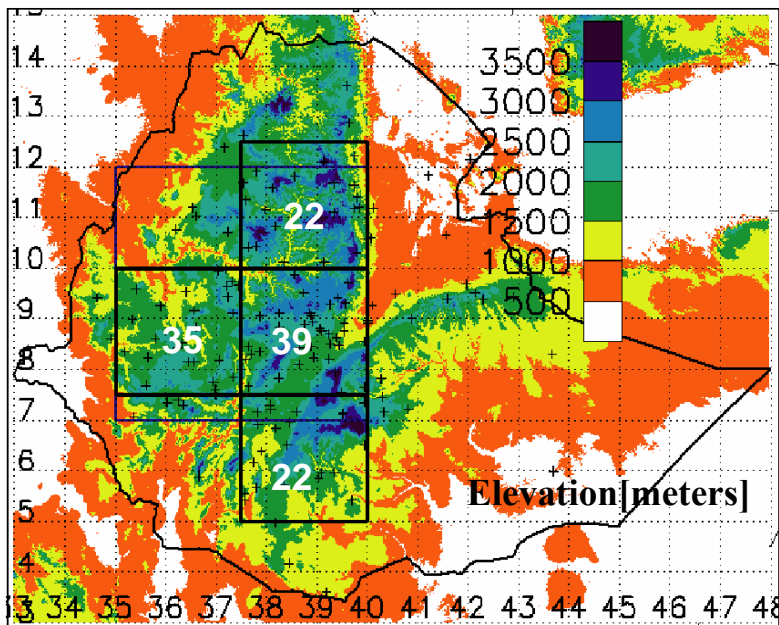
Figure 1. Topography of the study region and distributions of rain gauges; the four grid boxes (with number of gauges in each box shown) are used for evaluation at 2.5° spatial resolution.

Figure 1 shows the distribution of these stations. Most of the stations used here are a first-class station, which means that observations were taken by trained observers. The gauge data have undergone routine quality checks by NMA. Further quality checks were performed here in the context of cross validation (similar to Romero et al., 1998). The quality controlled gauge measurements are then interpolated to regular grids using climatologically aided interpolation (Willmott and Robeson 1995). All available stations were used for interpolation. However, only 2.5° with at least 20 gauges, 1° boxes with at least three gauges, and 0.25° grid boxes with at least one gauge were used for validation. Table 1a and 1b give summary of the products evaluated here with the temporal and spatial resolutions used in this study. It should be noted that the original resolution of some the products could be higher than used here.

Table 1a. The different satellite rainfall products used in this study. The products a regrouped according the three categories discussed in the text.

Product	Temporal Res.	Spatial Res.
GPCP	Monthly	2.5 deg
CMAP	Monthly	2.5 deg
TRMM-3B43	Monthly	2.5 deg
TAMSAT	10-daily	1.0 deg
GPCP-1DD	10-Daily	1.0 deg
RFE/ARC	10-Daily	1.0 deg
CMORPH	10-daily	1.0 deg
TRMM-3B42/RT	10-daily	1.0 deg
RFE	Daily	0.25 deg
CMORPH	Daily	0.25 deg
TRMM-3B42/RT	Daily	0.25 deg
NRL	Daily	0.25.deg
PERSIANN	Daily	0.25.deg

Table 1b. Summary of the global gridded rainfall Products compared here.

Product	Spatial resolution[deg]	Period
GPCC-mon	1.0, 2.5	1986-present
GPCC-ful	0.5, 1.0, 2.5	1951-2004
GPCC-clm	0.5, 1.0, 2.5	1951-2000
UEA-CRU	0.5	1901-2002
NOAA-CPC	2.5	1948-present

VALIDATION

This section presents statistics comparing the different satellites rainfall estimates and gridded global products with the reference gauge data.

Validation of Satellite Products

The following statistics are used to evaluate the products: linear correlation coefficient (CC), mean error (ME), root-mean square error (RMS), efficiency score (Eff), bias, probability of detection (POD), false alarm ratio (FAR), and critical success index (CSI).

$$ME = \frac{1}{N}\sum(S-G)$$

$$RMS = 100\frac{\sqrt{\frac{1}{N}\sum(S-G)^2}}{\bar{G}}$$

$$Eff = 1 - \frac{\sum(S-G)^2}{\sum(G-\bar{G})^2}$$

$$Bias = \frac{\sum S}{\sum G}$$

where G=gauge, $\bar{G}$ = average of gauge, S=satellite, and N=number of data pairs. ME is in millimeters [mm] and RMS in%, while Eff and Bias do not have units. The following validation statistics are based on contingency table where A, B, C and D represent hits, false alarms, misses, and correct negatives, respectively.

$$POD = \frac{A}{A+C}$$

$$FAR = \frac{B}{A+B}$$

218

$$CSI = \frac{A}{A + B + C}$$

Monthly Products at 2.5^o Spatial Resolution

In this section GPCP, CMAP and TRMM-3B43 are evaluated. The scatter plot of the three products is given in Figure 3, while Table 2 gives the error statistics. There is good agreement between gauge and the satellite products with better agreement at lower rainfall accumulations. All the three products show some underestimation at higher rainfall accumulations. CMAP and 3B43 have very similar statistics and both are slightly better than GPCP.

	GPCP	CMAP	3B43
CC	0.92	0.92	0.92
Eff	A	0.83	0.81
Bias	0.80	0.91	0.92
ME	-30	-12	-12
RMS	30	24	25
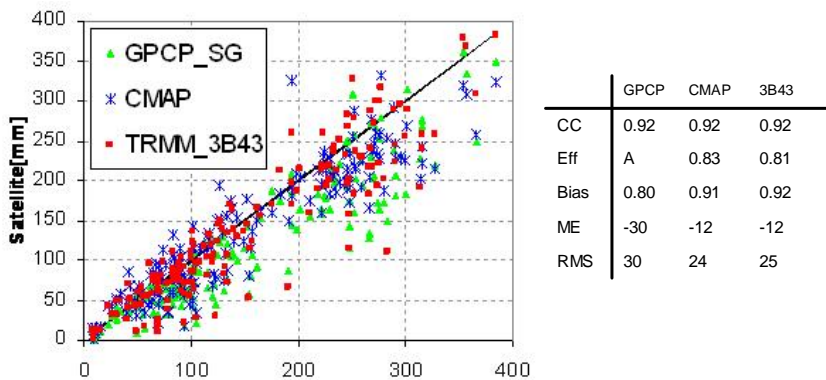
Figure 2 and Table 2. Comparison of GPCP, CMAP and TRM-3B43 with area-average gauge.

Ten-day Accumulation at 1° Spatial Resolution

RFE, ARC, 1DD, 3B42, TAMSAT and CMORPH are compared in this section. Table 3 compares the previous (RFE1) and current (RFE2) versions of the RFE algorithm. The current version suffers from significant underestimation while RFE1 overestimates high rainfall amounts. Table 3 also shows much better error statistics for RFE1. The major differences between the two algorithms are that RFE1 includes a provision for orographic warm rain process, while RFE2 incorporates

PM estimates. And it seems that accounting for warm rain process may be more important than incorporating PM estimates. Table 4 compare RFE2 with ARC. Both products show severe underestimation with very little skill, but RFE2 is slightly better. ARC does not include PM data.

The comparison of CMORPH, 1DD, 3B42 and TAMSAT is presented in Table 5 using data from the summer months of 2003 and 2004. CMORPH and TAMSAT have better statistics as compared to the others. That fact that TAMSAT, a product without PM data input and gauge adjustment, perform so well is very informative. The main advantage for this product is that it uses local calibration where the temperature threshold and regression parameters vary both spatially and temporally, while the other products are calibrated at global or regional levels.

Table 3. Comparing RFE1 and RFE2

	RFE1	RFE2
CC	0.78	0.75
Eff	0.41	-0.16
Bias	0.85	0.44
ME	-8	-30
RMS	53	74

Table 4. Comparing RFE2 and ARC

	RFE2	ARC
CC	0.66	0.66
Eff	-0.45	-0.88
Bias	0.55	0.45
ME	-30	-38
RMS	58	66

Table 5. Comparing 1DD, 3B42, TAMSAT and CMORPH at ten-daily accumulation and 1° spatial resolution.

	1DD	3B42	TAMSAT	CMORPH
CC	0.68	0.68	0.79	0.83
Eff	0.04	0.26	0.53	0.49
Bias	0.77	0.94	0.86	0.98
ME	-16	-4	-9	-1

The validation results for third group of products are given in Table 6. The statistics in Table 6 shows that all the products have poor performance in terms of pixel-by-pixel comparisons: correlation coefficients are very low and MAE values high. The bias is reasonably low for most of the products.   The exceptions are the severe underestimation by RFE2 and huge overestimation by PERSIANN. The categorical statistics (POD, FAR, CSI) show reasonable rain-no rain discrimination. The rain-no rain threshold used for the contingency table is 1 mm, which is relatively high for area-average daily rainfall. Lower thresholds would have given better categorical statistics. For instance, lowering the rain-no rain threshold to 0.1 mm would increase CSI and POD on average by 26% and 15%, respectively; and the FAR would drop by 70% to single digits. This shows that the satellite rainfall products are reasonably good at detecting the occurrence of rainfall but have problem estimating the amount of rainfall for each pixel.

Table 6. Comparing daily rainfall from different satellite rainfall productsat 0.25º spatial resolution.

	RFE	PERSIAN	NRL	3B42	3B42RT	CMORPH
CC	0.08	0.14	0.12	0.11	0.12	0.14
ME	-2.37	3.26	-0.83	-0.34	0	0.09
RMSE	10.22	18.13	12.24	11.27	13.81	10.45
Bias	0.65	1.48	0.88	0.95	1	1.01
CSI	0.62	0.57	0.51	0.6	0.54	0.68
POD	0.71	0.64	0.57	0.69	0.62	0.8
FAR	0.18	0.17	0.17	0.18	0.19	0.19

Validation of Gridded Precipitation Products

Comparison of the Global products at 2.5º Spatial Resolution

Table 7 and Figure 3 compare the performance of GPCC-clm, GPCC-ful, UEA-CRU, and NOAA-CPC relative to the reference data. The monthly rainfall totals of the products agree very well with the reference data. There are also some obvious differences. The first, though only for few pixels, is the overestimation by the two GPCC products at low and high rainfall amounts. The other discrepancy is the

over estimation of moderate rainfall amounts (100-200mm) by the UEA-CRU product.
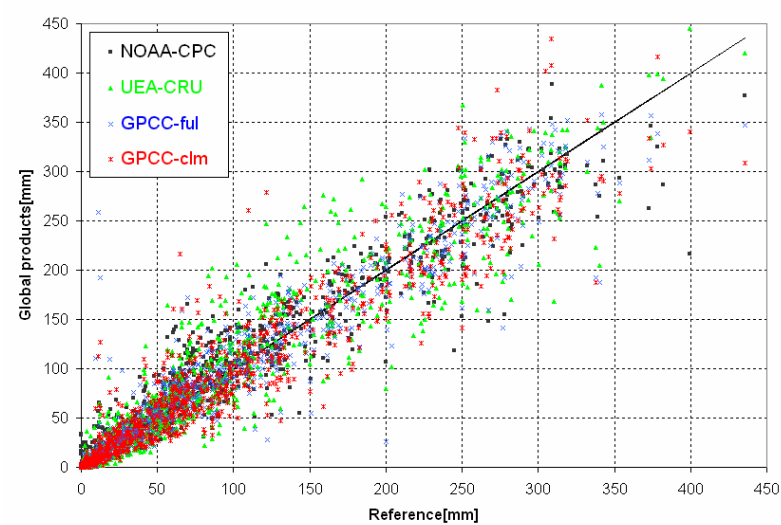
Figure 3. Comparison of the monthly total rainfall for different products at 2.5^o spatial resolution.

Table 7. Comparison of gridded gauge products at a spatial resolution of 2.5^o. N=number of data pairs.

N = 960	NOAA-CPC	UEA-CRU	GPCC-ful	GPCC-clm
CC	0.95	0.94	0.96	0.94
Eff	0.89	0.88	0.92	0.88
Bias	1.04	1.03	1.00	1.00
ME(mm)	4.4	2.9	0.5	-0.3
MAE(mm)	17.6	21.3	15.6	20.3

*Comparison of UEA-CRU, GPCC-ful and GPCC-clm at 1° and 0.5^o
Spatial Resolutions*

The NOAA-CPC product is available only at spatial resolution of 2.5^o, thus it was not compared with the other products in this section. Figure 4 and Table 8 compare the three products at a spatial resolution of 1°. Figure 3 shows a good agreement between the global products and the reference. However, the GPCC products overestimate low and high rainfall amounts, while UEA-CRU shows some overestimation at moderate rainfall amounts. The error statistics in Table 8 show that the performance of the three products is still very good: correlations are above 0.9 while Eff values are above 0.8, and bias is still very small. The GPCC products have a slightly better statistics.
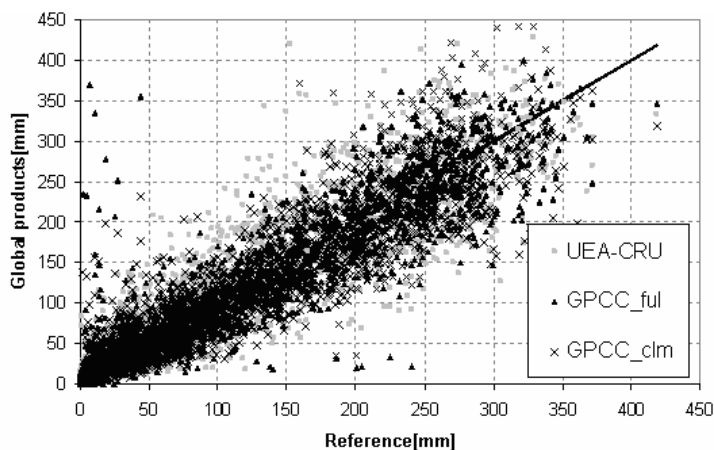
Figure 4. Scatter plot comparing the performance global gridded products with respect to the reference data at a spatial resolution of 1.0^o.

Table 8. Comparison of gridded gauge products at a spatial resolution of 1.0^o.

N=2640	UEA-CRU	GPCC-ful	GPCC-clm
CC	0.91	0.92	0.92
Eff	0.81	0.84	0.85
Bias	1.02	0.99	1.00
ME(mm)	2.5	-1.2	-0.2
MAE(mm)	28.3	21.9	24.9

The evaluations at 0.5° spatial resolution are given in Figure 5 and Table 9. The scatter in Figure 8 is similar to the scatters at 1.0° and 2.5° resolutions, except for the wider scatter owing to the higher spatial resolution. Thus, even at this relatively high resolution, the overall performance of these products is very encouraging. This is also evident from Table 9 where the correlations are still about 0.9, Eff values are close to 0.8, and the biases values are very small. Again the GPCC products have a slightly better statistics as compared to that of UEA-CRU.
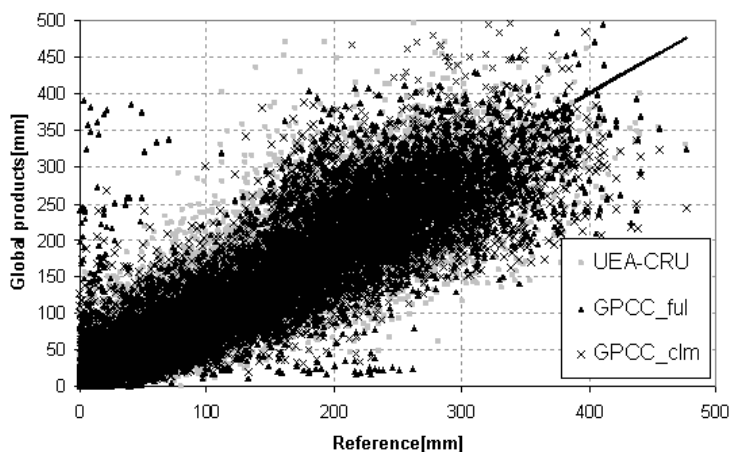
Figure 5. Scatter plot comparing the performance global gridded products with respect to the reference data at a spatial resolution of 0.5°.

Table 9. Comparison of gridded gauge products at a spatial resolution of 0.5°.

N = 13440	UEA-CRU	GPCC-ful	GPCC-clm
CC	0.89	0.90	0.90
Eff	0.78	0.80	0.81
Bias	1.01	0.99	0.99
ME(mm)	1.8	-0.7	-1.2
MAE(mm)	32.3	27.1	29.1

CONCLUSION

A relatively dense station network over the Ethiopian highlands has been used to evaluate satellite rainfall estimates and global gridded gauge products at different spatial and temporal resolutions. The evaluation of the satellite estimates was done for three groups of products. The first group consisted of GPCP, CMAP and TRMM-3B43, which were evaluated at monthly accumulation and a spatial resolution of $2.5^{o.}$ These products performed well with CMAP and TRMM-3B43 exhibiting a relatively better performance. The second of group of products included RFE, 1DD, 3B42, TAMSAT and CMORPH. These products are accumulated to 10-day total and are evaluated at spatial resolutions of 1°. Comparison of the previous (RFE1) and current (RFE2) \ versions of CPC-RFE has shown that RFE1 is much better than RFE2. This was attributed to the difference in dealing with orographic rain. Comparing the different products it was shown that 3B42, TAMSAT and CMORPH have a better accuracy, while that RFE was the least accurate. The third group of products were RFE, 3B42, CMORPH, PERSIANN and NRL. These were validated at daily accumulations and 0.25^{o} spatial resolution. These products performed reasonably well in detecting the occurrence of rainfall. The main shortcoming of these products was in estimating the amount of rainfall in each pixel. Five global gridded monthly rain gauge products from GPCC, NOAA-CPC and UEA-CRU are also evaluated. These products are compared at grid sizes of 2.5^{o}, 1.0^{o} and 0.5^{o}. There is a very good agreement between the global products and the reference data at all spatial resolutions. Comparison among products shows that there are some relatively small differences in the performance of the different products. The GPCC-ful has been found to be the best product for the current validation region, followed by NOAA-CPC, UEA-CRU, and GPCC-clm. The relative poor performance of GPCC-clm is related to the small number of stations included in this product. On the other hand, the UEA-CRU product employs a larger number of stations than do other products, but this is not reflected in its performance; this is mainly attributable to the use of elevation in constructing the climatological values used in this product.

REFERENCES

Adler, R.F., Huffman, G.H., Chang, A., Ferraro, F., Xie, P., Janowiak, J., Rudolf, B., Schneider, U., Curtis, S., Bolvin, D., Gruber, A., Susskind,J., Arkin, P., and Nelkin.,E,2003, the version-2 Global Precipitation Climatology Project (GPCP) monthly precipitation analysis (1979–present). *J. Hydrometeor.,* **4,** 1147–1167.

Beck C, Grieser J, and Rudolf B. 2005. A New Monthly PrecipitationClimatology for the Global Land Areas for the Period 1951 to 2000. *DWD, Klimastatusbericht* 2004, 181-190. Available online at: http://www.dwd.de/de/FundE/Klima/KLIS/prod/KSB/ksb04/28_precipitation.pdf

Chen M, Xie P, Janowiak JE, Arkin PA. 2002. Global land precipitation: A 50-yr monthly analysis based on gauge observations. *Journal of Hydrometeorology* **3**: 249-266.

Fuchs T, Schneider U, Rudolf B. 2007. Global precipitation analysis products of the GPCC. Available online at: (http://www.dwd.de/en/FundE/Klima/KLIS/int/GPCC/Reports_Publications/QR/GPCC-intro-products-2007.pdf)

Herman A., Kumar, V.B., Arkin P.A., and Kousky, J.V., 1997, Objectively determined 10-day African rainfall estimates created for famine early warning. *Int. J. Remote Sensing*, **18**(10), 2147-2159.

Huffman, G.H., Adler, R. F., Arkin, A., Chang, A., Ferraro, R., Gruber, A., Janowiak, J., McNab, A., Rudolf, B. and Schneider,U ,1997, The Global Precipitation Climatology Project (GPCP) combined precipitation data set. *Bull. Amer. Meteor. Soc.,* **78,** 5–20.

Huffman, G.J., Adler, R.F., Stocker, E.F., Bolvin, D.T., Nelkin, E.J., 2003, Analysis of TRMM 3-hourly multi-satellite precipitation estimates computed in both real and post-real time. *Combined preprints CD-ROM, 83rd AMS Annual Meeting, Poster P4.11 in: 12th Conf. on Sat. Meteor. and Oceanog.*, 9-13 Feb. 2003, Long Beach, CA, 6 pp.

Hsu, K. L., Gao,X., Sorooshian,S., and Gupta,H.V., 1997: Precipitation estimation from remotely sensed information using artificial neural networks. *J. Appl. Meteor.,* **36,** 1176–1190.

Joyce, R. J., Janowiak, J. E., Arkin, P. A., and Xie, P., 2004, CMORPH: A method that produces global precipitation estimates from

passive microwave and infrared data at high spatial and temporal resolution.. *J. Hydromet.*, **5**, 487-503.

Mitchell TD, Jones PD. 2005. An improved method of constructing a database of monthly climate observations and associated high-resolution grids. *International Journal of Climatology* **25**: 693-712. DOI:10.1002/joc.1181

New M.G., Hulme, M., Jones P.D., 2000, Representing twentieth-century space-time climate variability. Part II: development of 1901–1996 monthly grids of terrestrial surface climate. *Journal of Climate* **13**: 2217–2238.

Romero R., Guijarro, J. A., Ramis, C., and Alonso, S., 1998, A 30-year (1964-1993) Daily rainfall data base for the Spanish Mediterranean regions: First exploratory Study. *Int. J. Climatol,* **18**, 541-560.

Willmott, C.J. and Robeson, S.M., 1995, Climatologically aided interpolation (CAI) of terrestrial air temperature. *Intern. J. Clim.* **15**(2): 221–229.

Xie, P., and Arkin, P. A., 1997, Global precipitation: A 17-year monthly analysis based on gauge observations, satellite estimates, and numerical model outputs. *Bull. Amer. Meteor. Soc.,* **78,** 2539–2558.

RAINFALL ESTIMATION USING SATELLITE REMOTE SENSING AND GROUND TRUTH FOR HYDROLOGIC MODELLING OVER THE UPPER BLUE NILE REGION

Fiseha B.M.[a], Alemseged T.H.[b], Rientjes, T.H.M.[b] and Gieske, A. S. M.[b]

[a]Department of Irrigation Engineering, Arba Minch University,
P.O.Box 21, Ethiopia. E-mail: behulu13327@itc.nl
[b]Department of Water resources, ITC, P.O. Box 6, 7500AA,
Enschede, The Netherlands.

ABSTRACT

A major source of uncertainty in hydrologic modeling is the inaccurate specification of rainfall as a meteorological forcing term. Rainfall often shows high spatial and temporal variability and capturing such aspects over a given area is challenging. The objective of this study is to identify and retrieve image-based information relevant for rainfall estimation and evaluate the accuracy of the existing rainfall products using ground truth data.

In this study, the accuracy of two instantaneous rainfall products of the Tropical Rainfall Measuring Mission (TRMM), the Microwave Imager (TMI) and the Precipitation Radar (PR) are evaluated as well as the Infrared (IR) and Water Vapor (WV) channels of Meteosat Second Generation (MSG). From IR-10.8μm and WV-6.2μm, three primary indices namely: minimum Brightness Temperature (TBmin), Cold Cloud Duration (CCD) and Brightness Temperature Difference (BTD) of the IR and WV channels are identified. CCD is defined as the duration of clouds with brightness temperature lower than a predefined temperature threshold. The effectiveness of variable temperature threshold values is also assessed. For validation, reliable datasets are obtained from 10 automatic rain gauges over the Upper Blue Nile region (Gilgel Abay catchment). A space and time collocation has been made between the image-based estimates and products and ground-based observations. Such research is unprecedented for the study area.

A comparison between TRMM products and gauge observation over a spatial domain of 20×20 km showed better accuracy than 5×5 km resolution. However, the overall estimate from TMI and PR products is

unsatisfactory. Both overestimate the gauge measurements except at some high elevations (>3000m) where effects of orography are evident. Within the catchment, the CCD showed different performance when used at individual stations that shows a spatial variability in brightness temperature threshold. Regression equations are derived where possible for the relations between BTD and TBmin versus ground truth. A retrieval procedure based a regression equation that utilizes multiple indices is found superior as compared to utilizing single indices. Results from this study indicate that, even though rainfall can be estimated through satellite remote sensing data, caution is needed for application of rainfall estimations to hydrological modeling. However, it must be realized that assessments in this study focused on estimating rainfall from single events that are highly dynamic and non-linear.

Key Words: Rainfall, TRMM, MSG, CCD, Brightness Temperature, Upper Blue Nile

INTRODUCTION

A major source of uncertainty in hydrologic modeling is the inaccurate specification of rainfall as a meteorological forcing term. Rainfall often shows high spatial and temporal variability and capturing such over a given area is of great difficulty. Its observation can be through ground-based instruments or remotely sensed satellite images. Ground-based rainfall observations as obtained from ground radar and rain gauges are reported to have major limitations. Rain gauge observations are less accurate, unreliable and observation networks are sparse. Also rain gauge measurements are at point scale whereas most hydrologic studies require areal input. Even though it is possible to transform gauge scale to areal scale through spatial interpolation methods, the selection of the methods and the sparseness of the gauge networks are sources of error and uncertainty. Ground radar is found expensive, covers a limited space and its effectiveness for topographically non-uniform areas is questionable.

Gauges that measure rainfall at a point scale remain the most common approaches to ground-based observation. Large numbers of rain gauges have been established globally by meteorological and hydrological agencies in the past decades. These rain gauges are used to observe rainfall through direct measurement to produce "true" reading

for the duration of its occurrence. The meaning of true measurement only reflects the part of rainfall that reaches the gauge at some height above the ground. However the measurements have got some limitations that are either natural or artificially imposed. The natural limitations are caused by wind, vegetation and topography around the rain gauge stations that affect the observations. The man made limitations start from the design of the gauges to the reading of the recorded rainfall including their documentation. Thus such point observations are not directly representative for areal information but only provide point values limited to the aperture of the gauge. Moreover the observation is recorded as the accumulation of rainfall depth over a given duration ranging from few minutes to hours or even larger. The rain gauge records can be found either digitally or on written documents or charts.

Since the early 1960s, efforts have been made to estimate rainfall from remotely sensed satellite images which provide observations over large spatial scale where images can be obtained from orbiting and geostationary platforms. The rainfall estimation from images of geostationary satellites is based on the information provided through the Visible (VIS), Infrared (IR) or Water Vapor (WV) spectral bands. The estimation procedures using these images are commonly called VIS/IR-approaches. The underlying principle is that the radiation does not penetrate through the rain forming clouds and the precipitation falling from the bottom of the cloud is estimated indirectly from the radiation that is emitted or reflected from the top and/or side of the cloud, (Tsintikidis et al. 1999). However, the information pertaining to rainfall retrieval from images of geostationary satellites has an indirect relationship with the ground-based rainfall observations and causes that accuracy to be unsatisfactory. Even though there is weak physical relation between clouds top infrared brightness temperatures and rainfall, the high sampling frequency makes the geostationary satellites attractive in studying the temporal evolution of cloudiness and convection. According to Levizzani et al. (2002), rainfall estimation from VIS/IR images can be through any of the four techniques: cloud indexing, bi-spectral, life history, and cloud model. In this study the methods based on the cloud indexing techniques are used.

The orbiting satellites provide relatively direct information on cloud characteristics through microwave (MW) observations. The principle of precipitation estimation is based on the fact that the precipitation affects the emission and attenuation of radiation in the MW

frequencies. At higher frequency channels the scattering prevails due to ice while at lower frequency channels the emission is predominant from rain drops. The estimation procedure using the images from orbiting satellites is commonly referred to as MW-approaches. Though they have direct observation, they have poor temporal resolution of one or two observations per day. As such validation the products using ground truth data is important. As stated by Marks et al. (2000), four primary ground validation sites have been developed to evaluate the TRMM estimates that include: Darwin, Australia (DARW); Houston, Texas (HSTN); Kwajalein, Republic of the Marshal Islands (KWAJ); and Melbourne, Florida (MELB). But from rainfall variability point of view the applicability of the validation made in all these sites may not be representative for distant location. Some studies have also been conducted to validate TRMM rainfall estimates in some parts of Africa. Nicholson et al. (2003) conducted a study on validation of TRMM and other rainfall estimates for west Africa, Dinku et al. (2006) validated satellite rainfall products over east Africa and Adeyewa et al. (2003) performed validation of radar rainfall data over major African climatic regions. Some of these studies were dependent on the monthly products and large spatial domain 2.5^{o} by 2.5^{o}. It is mentioned that the approach is different when applied for estimation over land surface and ocean.

Considering the strength from either of the above, there is an approach to estimate precipitation combining images from geostationary and orbiting satellites. The estimation procedure in this case is referred to as combined IR/MW-based approach. Some studies that follow the combined approach include those by Brown (2006), Marzano et al. (2004), and Todd et al. (1995). For hydrological applications use of single channel and single sensor observations is not sufficient. Alemseged and Rientjes (2007) state that development and evaluation of the effectiveness of a 'multiple input-multiple outputs' type approach is a challenging research topic. They recommend the use of variable IR temperature threshold to identify clouds that produce rain and to add a physical basis to the existing rainfall retrievals.

The main objective of this paper is to identify and retrieve image based information relevant for rainfall estimation using multispectral images of Meteosat Second Generation (MSG) and to evaluate the accuracy of the existing instantaneous rainfall products that are obtained from Tropical Rainfall Measuring Mission (TRMM), Microwave Imager (TMI) and Precipitation Radar (PR). To achieve this objective, Gilgel

Abay catchment (4100 km^2) in the Lake Tana area is considered as study area. Figure 1.1 shows the rain gauge distribution over entire Ethiopia and the specific location of the study area. Ten automatic rain gauge stations were installed in May, 2007 those are also indicated in the Figure Elevation of the catchment ranges approximately from 1700 to more than 3000m. In addition to the high range of elevation, rainfall pattern in this region is affected by the movement of the ITCZ. This movement mostly takes place during the main rainy season that spans from early June to late September in the region.

In section 2, the data and methods used to estimate rainfall using MSG images and validate the TMI and PR products. Results from the validation of products and estimation are presented in section 3. Finally, the conclusion and recommendation based on the results are given in section 4 and 5 respectively.
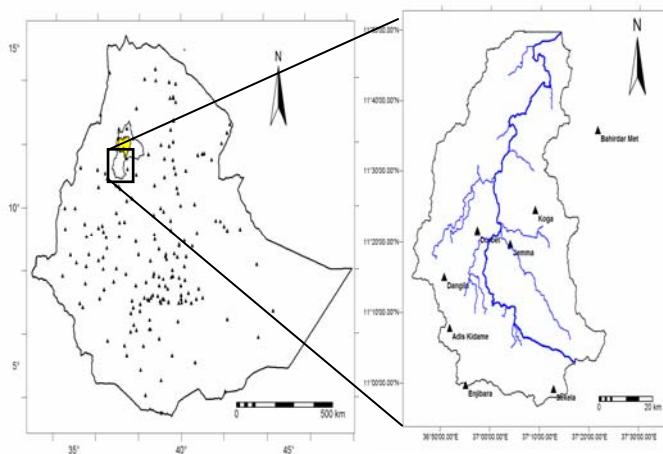

Figure 1.1. Location of study area with rain gauge distribution.

DATA AND METHODS

Data Source and Collection

For this study two basic data sources are identified: satellite data from MSG and TRMM, and ground observation from rain gauges. From the identified sources the study involves three basic stages: the first stage is to download remote sensing data for the area, the second stage is the collection of reliable ground observation from available sources and the third stage involves the arrangement of individual datasets for space and time collocation for further analysis.

Satellite Data

Descriptions of the remotely sensed satellite data used in this study as obtained from TRMM and MSG are given below. However, the reader is referred to the relevant publications for full information.

The MSG satellite is one of the geostationary satellites in the equatorial plane at an altitude of about 36,000 km above the earth's surface and performs sampling every 15minutes at nearly 3 km spatial resolution (http://www.eumetsat.int/Home/index.htm). There is MSG image receiver at ITC and these images can be retrieved free of charge for research purposes. Through the data retriever developed at ITC, it is possible to get synchronized multispectral data from all its channels. However, selection of channels is on the appropriateness of the information they delivered for rainfall estimation. Only the water vapor (WV 6.2μm) and Infrared (IR 10.8μm) channels are used in this study. From the temporal resolution, 96 images are expected per day per individual channel. However in some cases, images are missing or provide corrupted data showing zero readings. Hence these images are identified and consideration is given in the data processing stage. For instance, in the month of July, 2007 there were total of 95 missing images out of the expected 2976. In practice, the utilization of MSG images for rainfall estimation requires the conversion of digital numbers to radiance and then brightness temperature values (see Gieske et al. 2005). For this study such processing is handled in an automated fashion by the data retriever.

The TRMM is a non-sun synchronous orbiting satellite at an altitude of 402 km, inclination angle 35^0 and orbital period of 92 minutes that provides rainfall products through its three primary packages. The data from this source is also free of charge and hence the levels 2A12 (TMI) and 2A25 (PR) are collected for the duration of July to August. The orbit viewer software that shows the satellite pass line over the study area is used for identifying the period for which there is observation over an area. Figure 2.1 shows the TMI and PR over pass and the difference in their swath width over the study area.
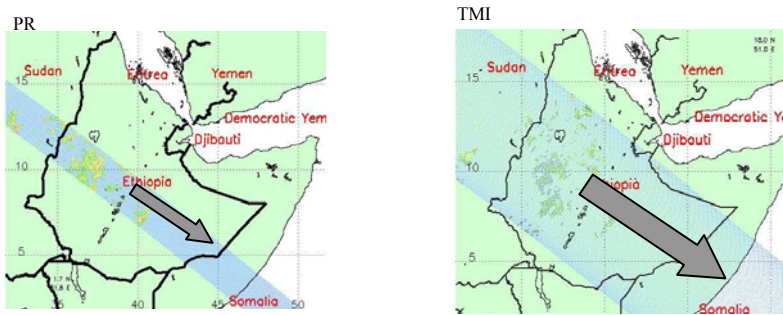
Figure 2.1. TRMM overpass over the study area on July 7, 2007 in descending path.

For this study only the instantaneous rainfall products were taken through the orbit viewer. Hence from TMI the only rainfall product called surface rain and from PR, the estimated surface rain is used.

Gauge Data

Out of the 10 automatic rain gauges in the study area, observations from eight gauges are analyzed as a reference data to assess the accuracy of the estimates from satellite data. Details of the gauging stations that are used in this paper are given in table 2.1. The latitude and longitude of the stations are according to WGS84 coordinate system.

234

Table 2.1. Selected rain gauge stations location in the
Gilgel Abay Catchment.

Station Name	Longitude	Latitude	Elevation (90m resolution)
Sekela	304828	1215253	2715.459
Bahirdar	321197	1282816	1798.421
Jemma	289034	1253171	1970.711
Enjibara	272644	1216262	2592.649

Data Processing

As stated by Grimes et al. (1999), the difficulty in comparing gauge data with those from satellites is that they provide two different kinds of information. The satellite estimates are averages over the area of the satellite pixel, whereas gauges provide measurements made at a point. For a meaningful comparison between the two data sets, either point values can be extracted from the satellite pixels or pixel areal averages from the rain gauge data can be calculated. The time scale is generally not representative when a comparison between satellite estimates and point measurement is made. This is due to the fact that a gauge observation represents an accumulated depth over several minutes to several hours while satellite estimates are instantaneous observation or simply "Snapshot". Based on the objectives, the data processing involves two major steps; the first is validation of TMI and PR and the second is estimation of rainfall from MSG images to assess the effectiveness of indices.

Rainfall Estimation from MSG Images

From MSG images the IR and WV channels are used for the derivation of indices at daily time step. Hence from the 96 daily raw images the daily minimum Brightness Temperature (TBmin), Brightness Temperature Difference (BTD) and CCD at different temperature threshold level are derived for each station and further analysis is carried out. Scatter plots of the values against the areal rainfall from ground observation at 3 km spatial resolution are shown in Figure 2.2a.

The CCDs are determined as the duration of clouds with brightness temperature lower than a temperature threshold. Different threshold values are considered for each station and their scatter plots are made with the observed daily rainfall. In deriving the CCD, missing observations are manually corrected by considering the values of consecutive images. Figure 2.2b shows the scatter plots of daily rainfall vs CCD in fraction of days at brightness temperatures threshold of 230K.
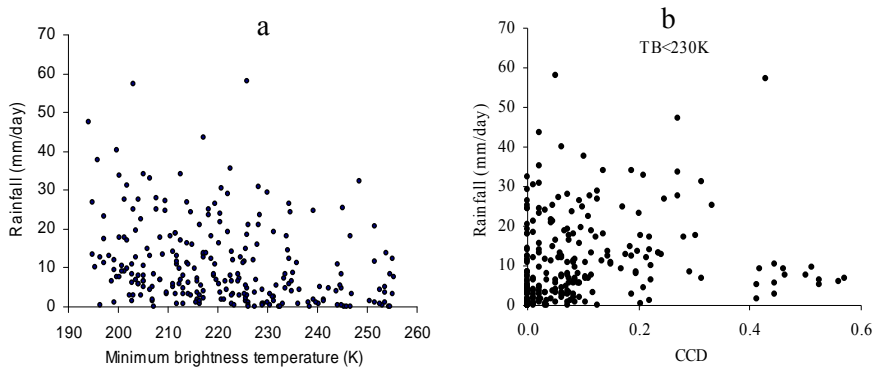
Figure 2.2. a) TBmin   b) Cold Cloud duration vs. daily rainfall observations in July, 2007

The WV (6.2μm) brightness temperature values are subtracted from IR (10.8μm) temperature for determination of BTD. The BTD is determined as the number of observations that shows the IR and WV differences below some threshold value. This threshold value is determined by trial and error procedure with the objective to find its relation with rainfall and found to be 9 for this study. However it should be noted that this value could be different for different time period and locations. In the same way as the TBmin and CCD the scatter plots (not shown) of daily rainfall vs BTD are made for further analysis.

After determining all the three indices for each day a single value of each index is calculated. These results are statistically combined with the gauge records interpolated daily rainfall and finally a single regression equation is determined in terms of the indices. The accuracy of the regression is then checked through error quantification analysis between the estimate and reference data.

236

Validation of TRMM Data for the Study Area

To understand the accuracy and limitations of TRMM estimation products, a comparison with the gauge observation is made. For validation purposes, the TMI and PR are compared independently with the rain gauge data collected over the area. After collecting the data for the time coincident with the satellite passes over the study area, the individual products are arranged for comparison. The analysis period is limited to the rainy season (June-August) for the year 2007, because it is the only period with full and reliable gauge data. The expected output is thus to answer the question, "What is the relation between satellite products and surface rainfall observation?" The answer to this question explicitly addresses how well TRMM products represent rainfall over the study area as compared to gauge observation. The accumulation of rainfall over hourly time period are compared to instantaneous rainfall products from TRMM assuming that the TRMM observation within the one hour window is comparable to the ground observation.

From TRMM the datasets are extracted using the orbit viewer and the resulting output tables are imported to ILWIS. Since TRMM is orbiting the earth at 35^0 inclinations it is not possible to get the data in normal LatLon arrangement. Even though, the products represent pixel value they are provided as a point value representing the pixel of nearly 5×5 km resolution. To overcome these problems a simple spatial interpolation using nearest neighbour is done for the whole products at spatial resolution in multiples of five in the same way as that of gauge data. The multiple 5 km spatial resolution is selected based on the fact that the TRMM instruments' horizontal resolutions are changed from 4.3 km to 5 km due to the August 2001 boost (e-mail communication with Dr. Zhong Liu from NASA). The TMI and PR are then independently compared with the gauge datasets for the all the stations. The overall validation results are presented through error quantification of each method under result and discussion section.

The rain gauge data from ground observations at the eight stations are used in two different ways. First, hourly rainfall intensities are arranged for the corresponding overpass time for TMI and PR. These hourly data are then converted into areal estimate using the Inverse Distance Weighted (IDW) method for validation of TRMM instantaneous products. Second, the daily rainfall data from the stations are used for comparison with the MSG estimates.

For quantitative comparison and performance assessment of the results, Root Mean Square Error (RMSE), and Coefficient of determination (R^2) are used with the target values of zero and 1 respectively. R^2 measures the degree of correspondence between the estimated and observed distributions. As it is impossible to present here the whole sets of results, only the most relevant results related to the objective of this study are described in the following sections and the full results of this study will be given on a paper under preparation for publication.

RESULTS AND DISCUSSIONS

Variability of Rainfall and Correlation Matrix

Table 3.1 shows the correlation matrix of the daily rainfall from four gauging stations in Gilgel Abay catchment for the month of July, 2007. The highest correlation values in each column appear in bold. The overall analysis shows that there is a poor spatial correlation between the gauge networks that indicates that there is high spatial variability of rainfall within the catchment. A qualitative investigation between the stations indicates that the station at Sekela with an elevation at about 2700m above mean seal level has the least correlation to the other stations. This is presumably due to the fact that the station at Sekela is most affected by orography. It may also indicate that the distribution of the gauges is non-uniform.

Table 3.1. Correlation matrix of selected rain gauge stations based on daily rainfall of July, 2007

Stations	Sekela	Bahirdar	Jemma	Enjibara
Sekela	1			
Bahirdar	-0.078	1		
Jemma	0.094	**0.281**	1	
Enjibara	**0.274**	0.187	**0.252**	1

Estimation Results from MSG

Estimation Results Using Minimum Brightness Temperature

For the stations in the study area, rainfall shows a decreasing trend for the minimum brightness temperature values between 190K and 260K. However, the scatter plot shows some clusters of data and these could be ruled out based on the principles of IR approaches. For this reason the scatter plot for all the stations are made and the clusters at individual stations are taken out considering the CCD <10% and the amount of rainfall below 2mm/day. One of these plots is shown in Figure 3.1 for station at Enjibar. The possible cause for this discrepancy in rainfall-TBmin relation is that some clouds produce higher rainfall rates for a very short duration that on its turn relates stage of cloud development. On the other hand, there are also clouds that stay in the system for longer duration with small amount of rainfall. It was also found that the there is no unique relationship between TBmin and rainfall. For instance, the station at Bahirdar has best performance (not shown in Figure) when polynomial function is used while for other station exponential function is related. Although preliminary analyses have been executed to assess each of these causes, results are not presented here.
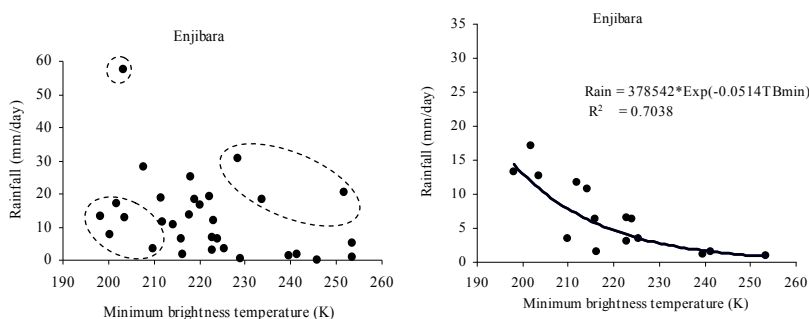
Figure 3.1. a) Daily rainfall vs. minimum brightness temperature and b) best fit for rainfall estimation at Enjibara station for July 2007.

Estimation Results Using CCD and BTD

The CCD derived using temperature threshold of 230K for the eight stations is shown in Figure 2.2. A qualitative assessment of the figure gives the information that there are clustered values for CCD>0.4. These clusters show clouds that have long duration in the system but produce small amount of rainfall which is nearly less than 10mm in this case. On the other hand there are values with very high rainfall amounts that reaches up to 50mm for CCD=0. Hence in the same manner as that of the TBmin this effect is ruled out to get the relationship between the CCD and rainfall which is found to be a linear relation. The station at Enjibara is again considered in this case and the result is shown in Figure 3.2. The CCD performance is different at the different gauging stations in the catchment. This is due to the spatial variability of the threshold values used for the derivation of CCD. For instance, the station at Bahirdar and Enjibara has shown better performances at threshold value of 220K and 240K respectively. The corresponding relationship between the rainfall and the BTD is also derived after the routine adjustment of the clustered values and the result for Enjibara station is given in Figure 3.2b.

Figure 3.2. a) Daily rainfall vs. CCD and b) Daily rainfall vs. BTD at Enjibara station in July, 2007.

Performance indices of two gauging stations are shown in table 3.2. In one station the performance of estimate through TBmin is less than the CCD and BTD while in the second station such is not observed. Although not indicated in the table, at all the stations the R^2 values for

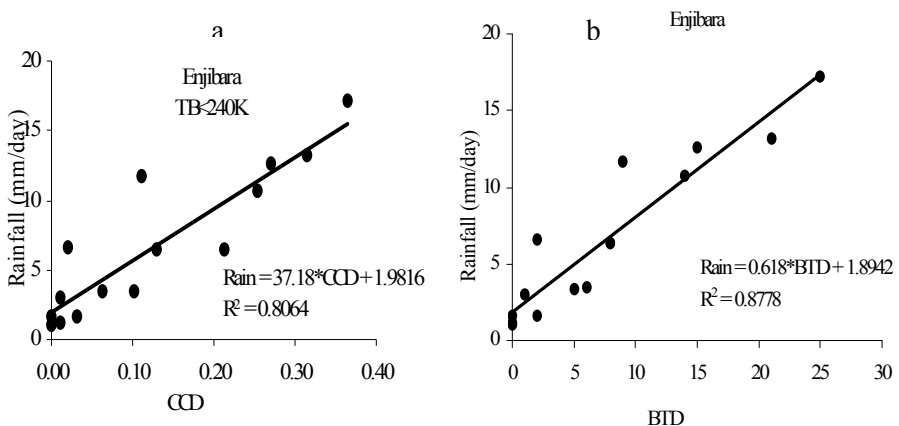TBmin based estimates are less than the CCD and BTD. Apparently, the relation between TBmin and station observations is poorest but possibly could be effected by false alarms from cloud tops. Such, however, although could not clearly be established in the image processing and further analyses are required.

Table 3.2. Performance estimation methods using TBmin, CCD and BTD.

Stations	Indices	Equation	Performance indicators	
			R^2	RMSE
Enjibara	TBmin	378542×Exp(-0.0514T×Bmin)	0.703	2.876
	CCD	37.18×CCD+1.9816	0.806	2.209
	BTD	0.618×BTD + 1.8942	0.878	1.755
	combined	10.259-0.0357×TBmin+0.7285×BTD-10.7374×CCD	0.885	1.703
Jemma	TBmin	3E+11×Exp(-0.113×TBmin)	0.748	4.576
	CCD	114.41×CCD+2.6284	0.704	5.357
	BTD	1.2459×BTD + 1.7987	0.727	5.142
	combined	73.552-0.308×TBmin+0.7686×BTD-5.497×CCD	0.798	4.362

The estimation procedures are repeated and equations are derived that combine indices. Comparatively, such results indicate better performance as when using the equation based on single indices. Although not shown in the table, the least value of the RMSE at all the stations is observed when the multi-variate regression equation is used as based on the three indices. The corresponding coefficient of determination R^2 is also better than the equation based on single indices at all the stations. A single best fit regression equation for stations at Enjibara is shown in Figure 3.3 and the performance assessment is given in table 3.2.
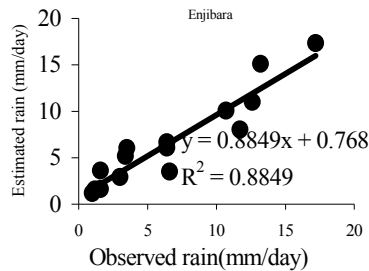
Figure 3.3. Observed vs. estimated rainfall using combined indices.

Preliminary Intercomparison of TMI and PR Rainfall Products

Due to the difference in scan geometry and capability of the instruments to capture different rainfall types, there is issue of mismatch between the different data. It is found that the number of cases where PR rain is detected while TMI does not detect rain is about 25% of the total coincident observations for the months of July and August. Also few cases are observed where TMI detects rain while PR does not detect. An example for these differences in coincidence of observation is shown in Figure 3.4 for TRMM observations of August 10, 2007.

a) TMI surface rain

b) PR estimated surface rain rates

c) Comparison of pixel values at gauge location (5km ×5km)

Figure 3.4. Preliminary comparison of TRMM rain rate on August 10, 2007 and 23:00 local time.

The mismatch in observation count indicates that the TMI instrument has weaknesses in capturing shallow rain irrespective of its wider scan geometry. However, the PR algorithms as described by Iguchi et al. (2000) and Meneghini et al. (2000) has the tendency to iterate for weak rain and apply surface reference technique when rain attenuation is high.

Figure 3.4 shows that the PR estimate is higher than the TMI over all the stations except at Sekela which is at high elevation. The possible cause for higher estimates at this station could be the tilting of the storm system due to higher elevation where TMI detects higher scattering signal from the ice in the cloud system in turn higher rain rate. On the contrary, PR detects no precipitation below the cloud system at that location that results in smaller rain estimate. The effect of tilting of storm system is described in Hong et al. (2000). The overall assessment of this result reveals that the rainfall for this specific date is dominated by convective type as the TMI underestimates convective rain over land, (see also Fur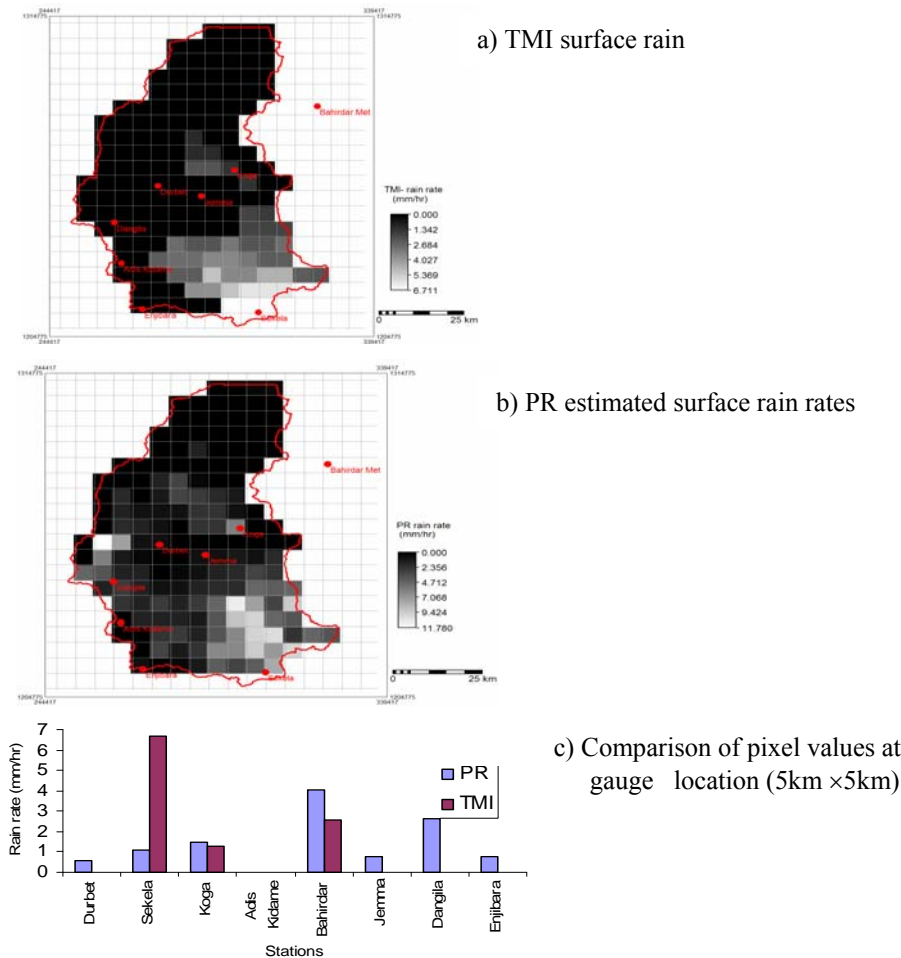uzawa and Nakamura, 2005). In some cases the PR rain rate shows lower estimation than the TMI rain rate. This brings a challenging issue in arriving at a conclusion whether one of the products clearly over- or under-estimates the rainfall. However, this ambiguity can be differentiated by visualizing the products through their dependences on local time. For instance, over our study area, all the PR rain rates are lower than the TMI rain rates for the duration between midday to midnight and higher for the remaining of the day in the month of July. This result holds true only for the observation values greater than zero in either rainfall products. For such analysis Furuzawa and Nakamura (2005) assumed a threshold of 0.7mm hr^{-1} as the minimum detectable rain rate for both.

Comparison of TRMM Rainfall Products with Ground Observation

The overall comparison shows that both the TMI and PR overestimate the reference gauge observations. Figure 3.5 shows the scatter plots of the TMI estimates with the gauge observations where 353 number of TMI estimates are found to be coincident with the reference. In case of PR only 137 coincident observations (not shown in figure) are found between the product and gauge observations.
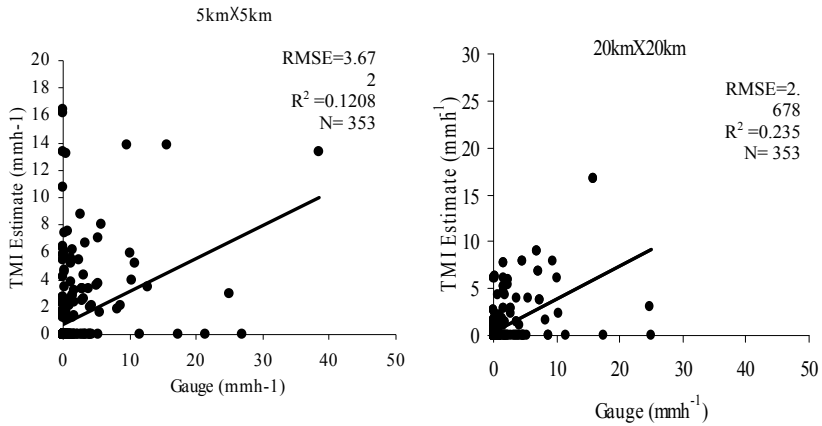
Figure 3.5. Comparison of TMI estimate with gauge observation

The comparison is made at different spatial resolution that shows exceedingly poor performances. The results resemble the findings of Nicholson et al. (2003) in western Africa. For instance, the coefficient of determination R^2 shows 12% at 5×5 km resolution and as high as 23.5% at 20×20 km resolution. The BIAS indicates that the PR overestimates by more than 10% of the TMI in all cases (see Figure 3.4). Another evaluation through the RMSE also shows larger error at 5×5 km and smaller error at 20×20 km that ranges from 3.672 to 2.678mm.

The performance indicators (RMSE and R^2) of both products are shown in Figure 3.6. The attractive nature of these performance indicators is that for the large pixel size of 20×20 km the performance increases in representing the reference gauge observation. However, from hydrologic modeling point of view this is somewhat disappointing since, hydrologic modeling requires areal rainfall at some model element that could be very much less than the 5×5 km. Though the TMI and PR can provide instantaneous products their usage in hydrologic model still remains questionable based on the results of this study.
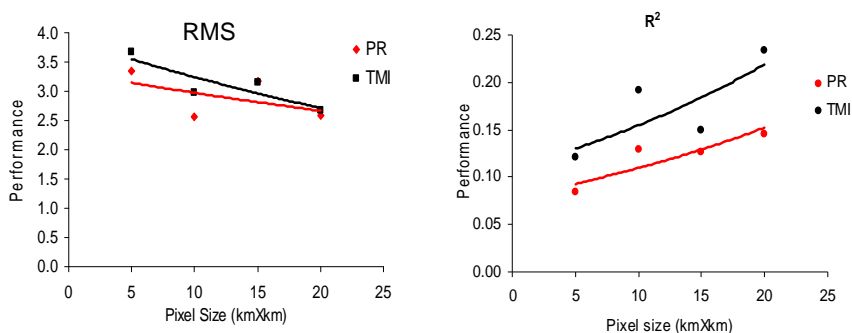
Figure 3.6. Performance of the TMI and PR estimates at different spatial resolutions

CONCLUSION

The aim of this study can be generalized into three as (i) the assessment of the effectiveness of indices for rainfall estimation from MSG; (ii) the validation of instantaneous rainfall products from TRMM; and (iii) the relation between ground-based observation and satellite products and/or estimates.

From the MSG estimates three different indices are derived for rainfall estimation over the study area. The effectiveness of those indices are highly affected by the multiple cloud system observed in the month of July. However by introducing a clustering procedure the required assessment is carried out. Based on the results obtained, a retrieval procedure based a multi-variate regression equation that utilizes three indices is found superior as compared to utilizing single indices. In this study it has been found that the stations have different performance for different temperature thresholds. This variation favors the spatial variability of temperature threshold.

From validation of TRMM instantaneous products, a diagnostic evaluation of the PR and TMI products has been performed for eight stations in Gilgel Abay catchment. The error of both products are relatively large and they overestimate the reference gauge data. However, based on this study, it is possible to conclude that accuracy of estimates increases when pixel size changes from 5×5 km to 20×20 km. As we have seen from the results the accuracy decreases as we opt for

245

higher resolutions and indicates that averaging effects over larger spatial domains is favarable. Obviously such compensates for the poor temporal resolution of TRMM.

Even though rainfall can reasonably be estimated through satellite remote sensing in the Gilgil-Abay catchment, caution is needed for application of rainfall estimations to rainfall-runoff modeling. First, for such applications the relation between the ground-based observations and satellite estimates should be stronger defined while secondly spatial scales of rainfall images are propably too course to simulate runoff production and catchment runoff in a spatially distributed fashion. Although much debate is in literature on grid size selection in distributed runoff modeling there is consensus that grid sizes of 25 km^2 or larger are not effective for catchments of regional or smaller scale when rainfall-runoff response times are much smalleer than 1 day as is observed in the Gilgel-Abay.

RECOMMENDATION

From the MSG channels only the 10.8 and 6.2 microns are used for derivation of indices, however the possibility of deriving indices from the other channels can be exercised in the future. As such the temporal variability of the brightness temperature threshold was not done due to the multiple cloud effects in the system. Hence further study should consider those effects due to the cloud types and cloud development stages that affect estimation accuracy. Another important and challenging research topic is the integration of the observations from microwave and infrared channels for regional scale rainfall-runoff and hydrologic studies.

The data analysis in this work is carried out for only two months of the rainy season in 2007 and thus further study is important to check the accuracy of satellite estimates by considering analysis from the dry season as well. In order to compare the satellite estimates with the ground-based observations different areal interpolation methods were used for ground observation and satellite estimates. This was done assuming that the effects of difference in interpolation methods are negligible, however consideration in future study is essential. On the other hand the area is limited to Gilgel Abay catchment and hence further study could be continued for the Upper Blue Nile region using the methodologies developed in this study.

ACKNOWLEDGEMENT

REFERENCES

Alemseged, T. H. and T.H.M., Rientjes. 2007. Spatio-Temporal rainfall mapping from space: Setbacks and strengths. ISDQ Workshop at ITC, Enschede, The Netherlands

Anagnostou, E. N. A. J. Negri and R. F. Adler. 1999. Satellite infrared technique for diurnal rainfall variability studies. Journal of Geophysical Research, Vol. 104(1999)D24, pp. 31,477-31,488.

Brown, J. E. M. 2006. An analysis of the performance of hybrid infrared and microwave satellite precipitation algorithms over India and adjacent regions. Journal of Remote Sensing of Environment 101: 63-81.

Furuzawa, F. A. and Nakamura K. 2005. Differences of rainfall estimates over land by Tropical Rainfall Measuring Mission (TRMM) Precipitation Radar (PR) and TRMM Microwave Imager (TMI) - Dependence on Storm Height. Journal of Applied Meteorology 44: 367-382.

Gieske, A. S. M, V. Retsios J, Hendrikse B, Van Leeuwen B, H. P. MaathuisM. Romaguera J, A. Sobrino W, J. Timmermans and Z. Su. 2005. Processing of MSG-1 SEVIRI data in the thermal infrared algorithm development with the use of the SPARC2004 dataset.

Iguchi, T, T. Kozu R. Meneghini J. Awaka and K. Okamoto. 2000. Rain-profiling algorithm for the TRMM precipitation radar. Journal of Applied Meteorology 39: 2038-202.

Levizzani, V, R. Amorati and F. Moneguzzo. 2002. A Review of Satellite-based Rainfall Estimation Methods.

Marzano, F, S.D. Cimmini, G. Giuliani and F. J. Turk. 2004. Multivariate Statistical Integration of Satellite Infrared and Microwave Radiometric Measurements for Rainfall Retrieval at the Geostationary Scale. IEEE Transactions on Geoscience and Remote Sensing 42 (5).

Meneghini, R, T. Iguchi, T. Kozu, J. Jones, L. Kwiatkowski, L. Liao and K. Okamoto, (2000). Use of the surface reference technique for path attenuation estimates from the TRMM precipitation radar. Journal of Applied Meteorology 39: 2053-2070.

Nicholson, S. E.B. SomeJ. McCollum D. Nelkin D. KlotterY. BerteB. M. Diallo and I. Gaye, (2003). Validation of TRMM and other rainfall estimates with a high-density gauge dataset for West Africa. Part II: validation of TRMM rainfall products. Journal of Applied Meteorology 42: 1355-1368.

Todd, M. C.E. C. Barret and J. B. Michael.1995. Satellite Identification of Rain Days over the Upper Nile River Basin Using an Optimum Infrared Rain/No-Rain Threshold Temperature Model. 34: 2600-2611.

Tsintikidis, D.K, P. Georgakakos, A. Artan and A. A. Tsonis. 1999. A feasibility study on mean areal rainfall estimation and hydrologic response in the Blue Nile region using METEOSAT images. Journal of Hydrology 221(3-4): 97-116.

CHARACTERISTICS OF MONTHLY AND ANNUAL RAINFALL OF THE UPPER BLUE NILE BASIN

Wossenu Abtew[1], Assefa M. Melesse[2] and Tibebe Dessalegne[3]

[1]Principal Engineer, South Florida Water Management District, West Palm Beach, USA; email:wabtew@sfwmd.gov
[2]Assistant Professor, Department of Environmental Studies, Florida International University
[3]Senior Engineer, BEM Systems

ABSTRACT

The Upper Blue Nile Basin is relatively wet with mean annual rainfall of 1423 mm (1960-2002) with standard deviation of 125 mm. The rainfall statistics is based on 32 rainfall stations with varying length of record. This mean rainfall is similar to a mean annual rainfall reported for a longer period of record (1900-1998). The annual rainfall has a normal probability distribution. The year-to-year rainfall variation is relatively small with a coefficient of variation of 0.09. The 100-year-drought basin annual rainfall is 1132 mm and the 100-year-wet basin annual rainfall is 1745 mm. The dry season is from November through April. The wet season runs from June through September with 74 percent of the annual rainfall and with low variation and skewness. October and May are transitional months. Monthly rainfall probability distribution varies from month to month fitting to Gamma-2, Normal, Weibull and Lognormal distributions. Monthly and annual rainfalls for return periods 2, 5, 10, 25, 50 and 100-year dry and wet patterns are presented. Spatial distribution of annual rainfall over the basin is mapped and shows high variation with the southern tip receiving as high as 2049 mm and the northeastern tip as low as 794 mm annual average rainfall.

INTRODUCTION

The Blue Nile Basin is the main source of the Nile River with a drainage area of 324,530 km^2 (Peggy and Curtis, 1994). Eighty six percent of the annual flow of the Nile comes from the Blue Nile Basin (59 percent) and 14 percent from the Barro-Akobo-Sobat sub-system and 13 percent from the Tekeze/Atbara/Gash sub-system (Degefu, 2003). The remaining 14 percent comes from the equatorial lakes after losses of evaporation in the Sudd region and Machar marshes (Degefu, 2003). The Upper Blue Nile River Basin (Figure 1) is 176,000 km^2 in area (Conway, 2000).The Upper Blue Nile Basin is relatively wet. Annual rainfall ranges from over 2000 mm in the Southwest to a 1000 in the northeast (Conway, 2000). Bewket and Conway (2007) reported mean annual point rainfall of 1445, 1665, 1542, 1349 mm rainfall at Bahir Dar, Chagni, Dangla and Debremarkos, respectively. Peggy and Curtis (1994) reported 1521 and 1341 mm long-term average annual rainfall for Bahir Dar and Debremarkos, respectively. Kebede et al. (2006) reported 1451 mm average annual rainfall for Bahir Dar based on observations from 1960 to 1992.

Rainfall is the most important hydrologic parameter in rain-fed agriculture. The frequency of low rainfall events determines the frequency of drought while the frequency of high rainfall events determines high stream flow occurrences. Point and regional rainfall frequency analysis characterize the temporal and spatial variation of rainfall over a region. Point rainfall frequency analysis is the temporal characterization of rainfall from a single gauge. Spatial mapping of the characteristics of all gauges in a region provides the spatial characteristics of rainfall. Regionally averaged rainfall frequency analysis characterizes rainfall over the region. Decent data length and quality is needed for temporal and spatial characterization of rainfall. Conway et al. (2004) studied the history of rainfall and temperature monitoring network and available records in Addis Ababa, Ethiopia and concluded that there are very few numbers of sites where continuous rainfall and temperature measurement records are available. In the absence of long term concurrent rainfall observations in a basin, efforts need to be made to make the most use of existing data as much as possible.

RAINFALL DATA ANALYSIS

The Upper Blue Nile Basin spatial average rainfall was generated by computing average values from 32 rainfall gauges. The period of record for each station varies and there are frequent data gaps. For each month of analysis, the average of all gauges with record was computed as an estimated basin-wide average monthly rainfall. Annual basin spatial average rainfall was computed as a sum of the monthly estimated basin rainfall. Figure 2 depicts the rain gauge network that was employed in the analysis.

Figure 1. Location of the Upper Blue Nile River Basin in Ethiopia.

Monthly Rainfall Data Statistics

Temporal statistical characteristics of monthly spatially averaged rainfall is shown in Table 1. Based on the mean (μ), January has the lowest rainfall and July has the highest monthly rainfall. The standard deviation (σ) is relatively high for the dry season and transitional months. The dry season months are November, December, January, February, March and April. The wet season months are June, July, August and September. May and October are transitional months, respectively from dry season to wet season and from wet season to dry season. The coefficient of variation, c.v. (σ/μ) of the wet season months is small indicating that these months have low variation. For

comparison, South Florida, a 46,400 sq. km basin has c.v. of 0.53, 0.46, 0.45 and 0.52 for the wet months of June, July, August and September (Ali et al., 2000). The dry season months have higher c.v. indicating that the year-to-year variation for these months is high. The degree of skewness is high in the dry season months relatively than in the wet season months. January, February, May, July, August, November and December are Leptokurtic (Kurtosis > 3). January, February, November and December have higher skewness and c.v. than the other months. Monthly rainfall and cumulative monthly rainfall is depicted in Figure 3 distinctly showing dry and wet seasons. The change in slope in May and October demonstrates that these months are transitional months.
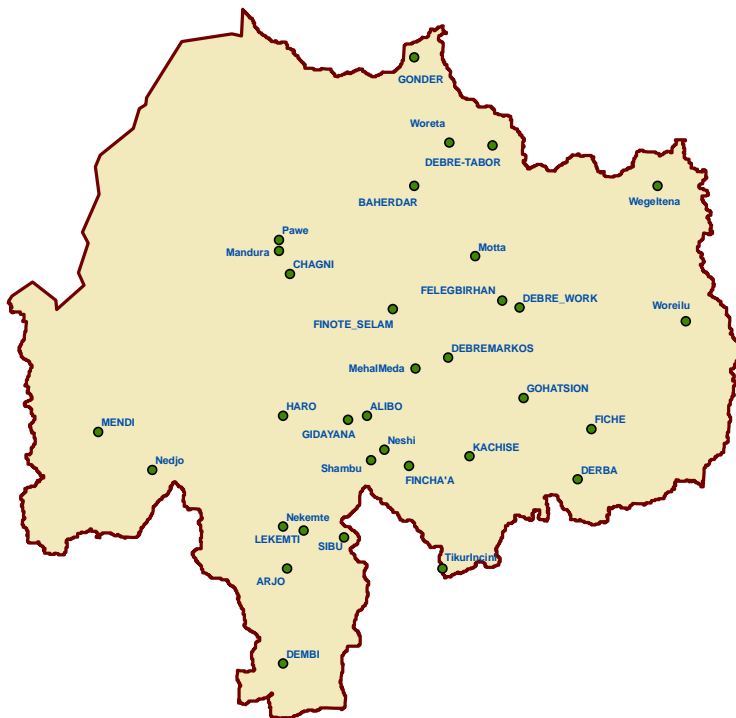
Figure 2. The Upper Blue Nile Basin rain gauge network used in this analysis.

Table 1. The Upper Blue Nile Basin monthly rainfall statistics and best-fit probability distribution.

Month	Mean mm	Standard Deviation mm	Coefficient of Variation	Skewness	Kurtosis	Distribution 90% C.I.
January	10.4	10.5	1.00	1.90	7.43	Gamma
February	15.0	12.3	0.82	1.14	4.31	Weibull
March	42.0	21.2	0.51	0.26	2.62	Normal
April	57.9	28.6	0.49	0.31	2.93	Normal
May	124.6	42.4	0.34	0.19	3.44	Normal
June	197.2	28.6	0.15	-0.10	2.58	Weibull
July	331.9	42.0	0.13	0.38	3.80	Gamma
August	320.2	42.7	0.13	-0.07	3.60	Normal
September	197.6	35.4	0.18	0.57	2.90	Lognormal
October	86.8	43.9	0.51	0.51	2.84	Gamma
November	26.9	20.6	0.76	1.09	3.58	Gamma
December	12.7	10.5	0.83	1.45	6.46	Weibull
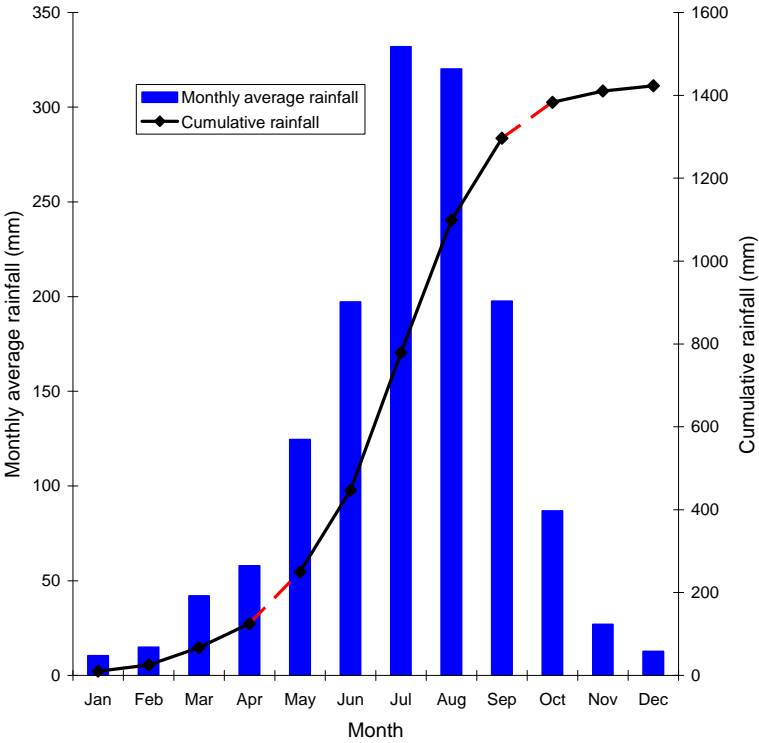
Figure 3. Monthly average and cumulative rainfall for the Upper Blue Nile Basin.

253

Frequency Analysis of Monthly Rainfall

Frequency analysis of monthly rainfall requires the selection of the best-fit theoretical probability distribution for each month's spatially average rainfall. A probability distribution is selected from a list of commonly applied statistical probability distribution models. The models were Normal, Gamma-2, Lognormal and Weibull. Each model was fitted to each month rainfall and the best-fit model was selected based on the ratio of computed Chi-square (χ^2) to the tabular χ^2.

$$\chi^2 ratio = \frac{\chi^2 computed}{\chi^2 table} \qquad (1)$$

When χ^2 ratio is less than 1, the model is accepted and greater than 1, the model is rejected at 90 percent confidence interval. Once selection of model is completed, a month's rainfall histogram and frequency is plotted. Figure 4a and 4b depict observed histogram and theoretical frequency distribution fitting for each month.

Figure 4a. January-June observed and theoretical distributions for the Upper Blue Nile Basin monthly rainfall.
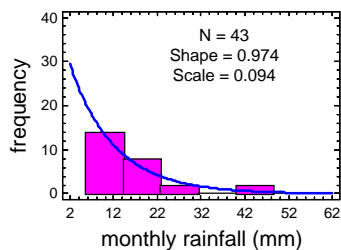
Gamma distribution fitting for July rainfall

Normal distribution fitting for August rainfall
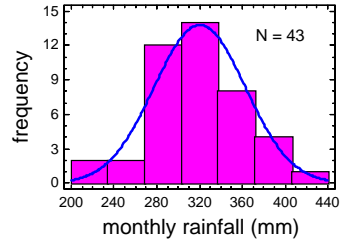
Lognormal distribution fitting for September rainfall
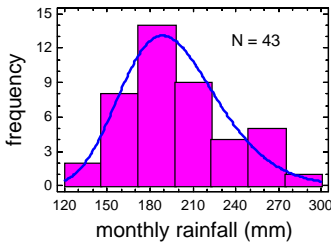
Gamma distribution fitting for October rainfall
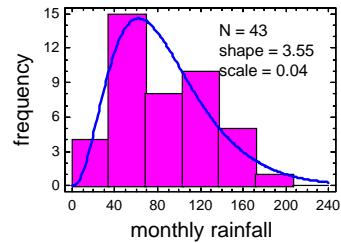
Gamma distribution fitting for November rainfall
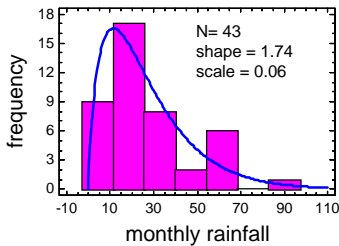
Weibull distribution fitting for December rainfall
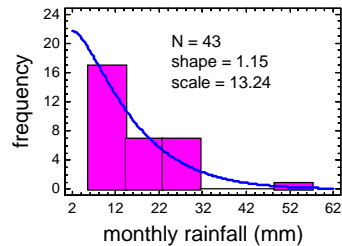
Figure 4b. July-December observed and theoretical distributions for the Upper Blue Nile Basin monthly rainfall.

Rainfall return period is a probabilistic measure of the likelihood of occurrence of a given amount of rainfall. Return periods for dry (below average) and wet (above average) rainfall patterns were computed for return periods of 2, 5, 10, 25, 50 and 100-year. Return periods in years were computed as follows from the Cumulative Density Function (CDF) for each month's respective distribution fitting.

$$DryReturnPeriod = \frac{1}{1-CDF} \quad \text{for CDF} \leq 0.5 \qquad (2)$$

$$WetReturnPeriod = \frac{1}{CDF} \quad \text{for CDF} \geq 0.5 \qquad (3)$$

Return period for dry and wet pattern rainfall for each month is depicted in Table 2. The 2-year values are the monthly mean values as estimated by the respective probability distribution model. Months fitted with Normal Distribution have means similar to the arithmetic means. The other model estimated means deviate from the arithmetic means due to the characteristics of the distributions (Table 1).

Table 2. Dry and wet return periods for monthly rainfall of the Upper Blue Nile Basin.

Month	Dry						Wet				
	100-yr	50-yr	25-yr	10-yr	5-yr	2-yr	5-yr	10-yr	25-yr	50-yr	100-yr
January	0.0	0.1	0.3	1.0	2.3	7.2	16.4	23.9	33.6	41.0	48.6
February	0.4	0.7	1.2	2.6	4.9	12.4	24.9	33.4	44.1	51.8	59.2
March	0.0	0.0	4.8	14.8	24.1	42.0	59.9	69.2	79.2	85.6	91.4
April	0.0	0.0	7.8	21.2	33.8	57.9	81.9	94.5	108.0	116.7	124.5
May	26.4	37.9	50.7	70.5	89.1	124.6	160.1	178.7	198.5	211.3	222.8
June	119.6	130.2	141.9	159.4	174.7	200.7	222.5	232.5	242.2	248.0	253.0
July	243.2	252.5	263.1	280.1	296.7	330.1	366.1	385.9	407.7	422.3	435.7
August	220.8	232.5	245.4	265.4	284.2	320.2	356.1	374.9	394.9	407.9	419.5
September	129.2	135.6	143.0	155.3	167.8	194.6	225.6	243.8	264.8	279.3	293.0
October	15.0	19.2	24.8	35.4	47.8	78.9	121.2	148.3	181.4	205.2	228.3
November	1.1	2.0	3.2	6.2	10.2	22.1	40.9	53.9	70.6	83.1	95.4
December	0.3	0.6	1.0	2.2	4.0	10.2	20.4	27.5	36.2	42.5	48.7

Annual Rainfall Statistics and Probability Distribution

The Upper Blue Nile Basin is relatively wet with annual mean rainfall of 1423 mm (1960-2002) with standard deviation of 125 mm (Figure 5). The rainfall statistics is based on 32 rainfall stations with varying length of record. Conway (2000) reported a mean annual basin rainfall of 1421 mm based on 11 gauges for the period 1900-1998. The Upper Blue Nile Basin annual rainfall probability fits normal distribution at a confidence level of 90 percent (Figure 6). Annual dry and wet return periods computed from normal probability cumulative density functions are shown in Figure 7 for dry and wet return periods of 2, 5, 10, 25, 50 and 100-year. The 100-year drought annual basin rainfall is1132 mm while the 100-year wet annual rainfall is 1745 mm.
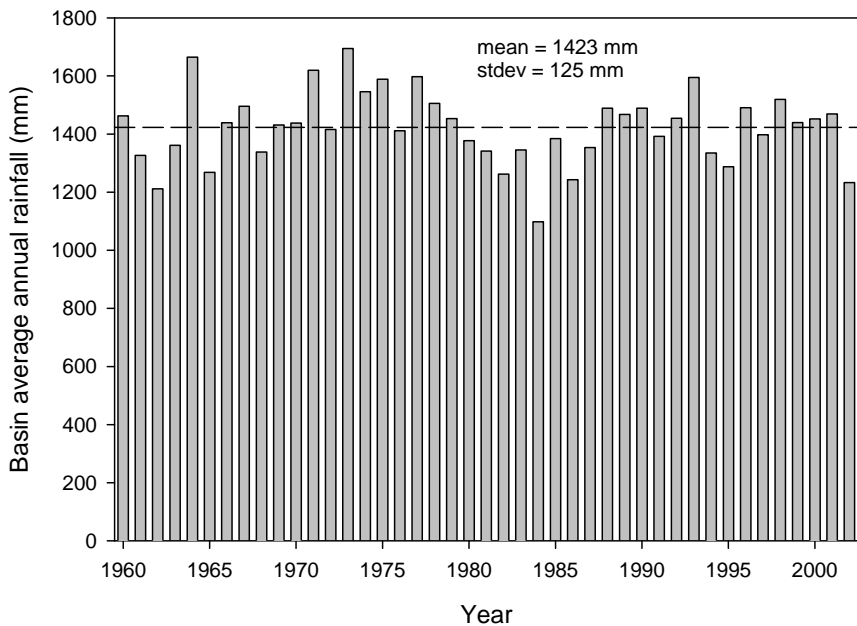
Figure 5. The Upper Blue Nile Basin average annual rainfall (1960-2002).
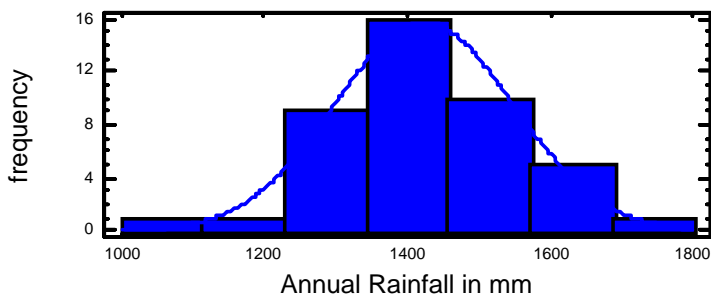
Figure 6. Observed and theoretical probability distributions for annual rainfall of the Upper Blue Nile Basin.
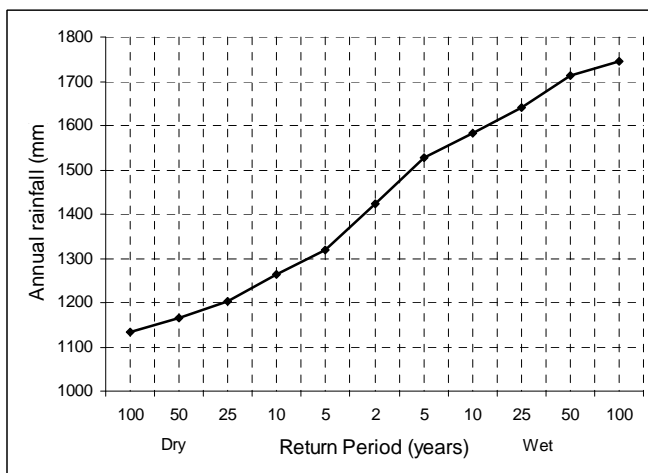
Figure 7. Dry and wet annual rainfall return periods for the Upper Blue Nile Basin.

Spatial Variation of Rainfall over the Upper Blue Nile Basin

Spatial variation of rainfall over the basin is high with a coefficient of variation of 0.25. Rainfall amount varies generally from the southwest to the northeast decreasingly. The highest annual average rainfall of 2049 mm is in the southern tip of the basin and the lowest average annual rainfall of 794 mm is in the northeast. Average rainfall

over the basin is spatially mapped using 28 rain gauge annual average records. Isohyetal map was generated using the Kriging interpolation package in SURFER Version 8 with linear variogram (Figure 8).
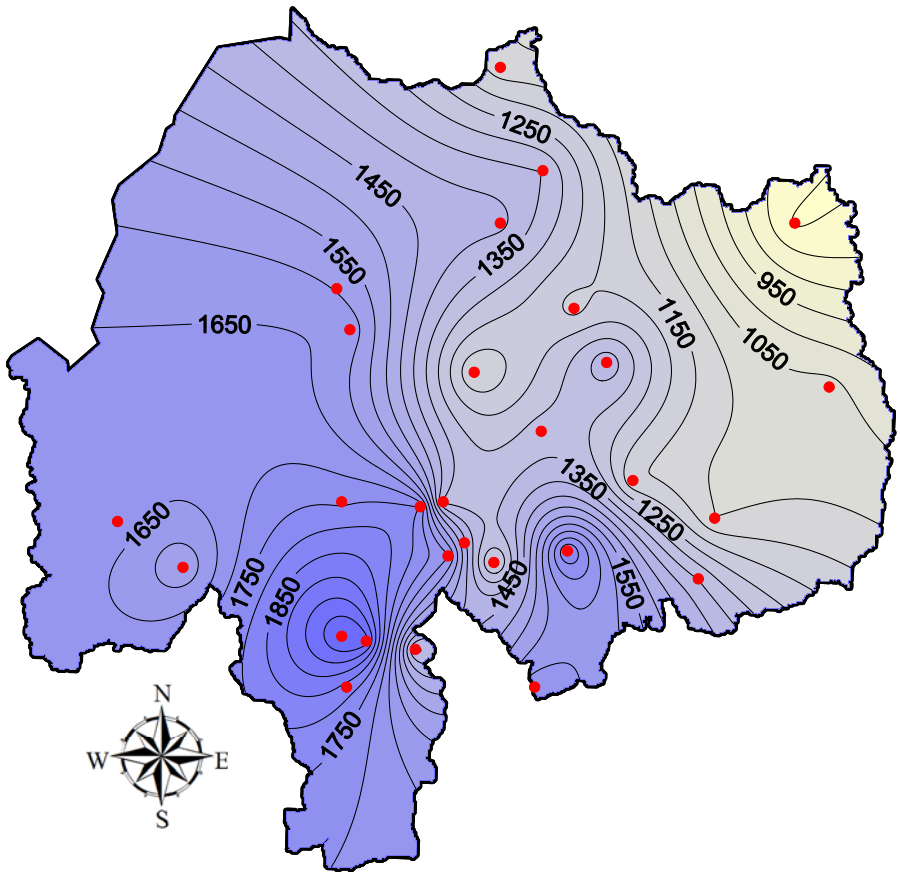
Figure 8. Spatial distribution of the Upper Blue Nile Basin average annual rainfall with rain gauge locations.

SUMMARY

The Upper Blue Nile Basin spatial average rainfall was analyzed to determine spatial and temporal statistical characteristics and derive applicable information. The Upper Blue Nile Basin is relatively wet with mean annual rainfall of 1423 mm (1960-2002) with standard deviation of

125 mm. The rainfall statistics is based on 32 rainfall stations with varying length of record. This mean rainfall is similar to a mean annual rainfall study for a longer period (1900-1998). The annual rainfall has a normal probability distribution. The year-to-year rainfall variation is relatively small with a coefficient of variation of 0.09. The 100-year drought basin annual rainfall is 1132 mm and the 100-year wet basin annual rainfall is 1745 mm. The dry season is from November through April. The wet season runs from June through September with 74 percent of the annual rainfall and with low variation and skewness. October and May are transitional months. Monthly rainfall probability distribution varies from month to month fitting to Gamma-2, Normal, Weibull and Lognormal distributions. Monthly and annual rainfalls for return periods 2, 10, 25, 50 and 100-year dry and wet patterns are presented. Spatial distribution of annual rainfall over the basin shows high variation with the southern tip receiving as high as 2049 mm and the northeastern tip as low as 794 mm annual average rainfall.

REFERENCES

Ali, A., W. Abtew, S.V. Horn and N. Khanal. 2000. Temporal and Spatial Characterization of Rainfall over Central and South Florida. Journal of the American Water Resources Association. Vol. 36(4):833-848.

Bewket, W. and D. Conway. 2007. A Note on the Temporal and Spatial Variability of Rainfall in the Drought-Prone Amhara Region of Ethiopia. International Journal of Climatology. Vol. 27:1467-1477.

Conway, D. 2000. The Climate and Hydrology of the Upper Blue Nile. The Geographical Journal. Vol. 166(1):49-62.

Conway, D., C. Mould and W. Bewket. 2004. Over one Century of Rainfall and Temperature Observations in Addis Ababa, Ethiopia. International Journal of Climatology. Vol. 24:77-91.

Degefu, G.T. 2003. The Nile Historical Legal and Developmental Perspectives. Trafford   Publishing. St. Victoria, B.C., Canada.

Kebede, S., Y. Travi, T. Alemayehu and V. Marc. 2006; Water Balance of Lake Tana and its Sensitivity to Fluctuations in Rainfall, Blue Nile Basin, Ethiopia. Journal of Hydrology. Vol. 316:233-247.

Peggy, A.J. and D. Curtis. 1994. Water Balance of Blue Nile Basin in Ethiopia. Journal of Irrigation and Drainage Engineering. Vol. 120(3):573-590.

SIMPLE MODEL AND REMOTE SENSING METHODS OF EVAPORATION ESTIMATION FOR RIFT VALLEY LAKES IN ETHIOPIA

[1]Assefa M. Melesse, [2]Wossenu Abtew and [3]Tibebe Dessalegne

[1]Assistant Professor, Department of Environmental Studies, Florida International University, Miami, USA; email:melessea@fiu.edu
[2]Principal Engineer, South Florida Water Management District
[3]Senior Engineer, BEM systems

ABSTRACT

In most arid regions of the world, evapotranspiration (ET) is a major component of the water budget. Accurate estimation of ET has been a challenge for hydrologist mainly because of the spatiotemporal variability and also most available models rely on intensive metrological information for ET estimation. Such data are not available at a desired spatial scale in less developed parts of the world. Measurement and estimation methods of ET usually provide different results as is the case for the Rift Valley Lakes of Ethiopia. Such limitations have necessitated the development of simple models that are less data intensive and also the use of remote sensing that can be applied to large areas where metrological data are not available. In areas like the Rift Valley regions of Ethiopia, the applicability of the Simple Method of lake evaporation estimation and surface energy balance approach using remote sensing was studied. The Simple Method of potential ET, lake evaporation and wetland ET estimation from a single parameter, solar radiation, has been successfully applied in South Florida. The Simple Method and a remote sensing evaporation estimates for Rift Valley Lakes were compared to the Penman, Energy balance, Pan, Radiation and CRLE methods. Results indicate a good correspondence of the model outputs to that of the Penman, Energy balance, CRLE and Radiation methods. Comparison of the 1986 and 2000 monthly ET from the Landsat images to the Simple and Penman Methods show that the remote sensing and surface energy balance approach is promising.

Key Words: evaporation, evapotranspiration, Simple Method, remote sensing, Rift Valley Lakes

INTRODUCTION

Evapotranspiration (ET) is one of the hydrologic parameters and has least variation on monthly and annual basis. It is a major component of the water cycle and important in water resource development and management. Measurement and estimation of this parameter usually provides different results. Evapotranspiration estimation models range from the complex as Penman Monteith to the simple, Pan method. Complex models require many meteorological measured and estimated input parameters which incur high monitoring cost. The error in measurement and estimation of input parameters increase the error in ET estimation. The adaptability of simpler methods especially in geographical areas where there is limited resource for monitoring is worth investigation. A Simple Method of potential ET, lake evaporation and wetland ET estimation has been successfully applied in South Florida (Abtew, 1996; Abtew, 2001, Abtew et al. 2003; Abtew, 2005). Preliminary analysis shows that this model can be applied at other locations. The coefficient, K_1, can be adjusted to the region if needed.

Lake evaporation (E_o) depends on the availability of energy and the mechanism of mass transfer, depth, and surface area of the lake. Evaporation is a function of solar radiation, temperature, wind speed, humidity, atmospheric pressure, and the surrounding environment. The most commonly used and the simplest method is the Pan method (Eq. 1) where evaporation from large surface area lake is related to evaporation from a small pan. The common problems with the pan method are errors caused due to difference in environment between the pan and the lake and errors in pan evaporation measurement. The use of pan data requires the development of a coefficient (K_p) to relate pan evaporation (E_{pan}) to lake evaporation. As the settings and operations of pans differ, different pan coefficients would be required for each pan to relate it to a single lake's evaporation. Abtew (2001) developed pan coefficients for seven pans in South Florida correlating monthly pan evaporation to evaporation from Lake Okeechobee and developed annual average pan coefficients ranging from 0.64 to 0.95.

$$E_o = K_p E_{pan} \tag{1}$$

Energy balance, mass and momentum transfer methods require measurement and estimation of several parameters and coefficients. The energy balance method requires input data of net radiation, sensible heat

flux and change of energy storage in the lake. Mass transfer and momentum transfer methods need differences in specific humidity, wind speed at different heights and mass and momentum coefficients. Combination methods as the Penman and Penman-Monteith methods are input parameter intensive. The Penman-Monteith method input requirements include measured parameters solar radiation, air temperature, humidity, wind speed and atmospheric pressure. The method also requires derived parameters as air density, canopy resistance, aerodynamic resistance, vapor pressure deficit, psychrometric constant, slope of saturation vapor pressure curve and heat storage. Additionally, estimated parameters as stomatal resistance, leaf area index, cover height, displacement height, aerodynamic roughness, momentum roughness and heat capacity are needed. Radiation and temperature based methods require fewer input data.

THE SIMPLE METHOD

A two-year lysimeter study of evapotranspiration in three wetland environments (cattails, mixed vegetation marsh, and open water/algae) was conducted in the Everglades Nutrient Removal Project, a constructed wetland in south Florida ($26^o\ 38^{'}$ N, $80^o\ 25^{'}$ W). The design of the lysimeter system is presented in Abtew and Hardee, 1993. The results of the study were applied to test and calibrate six evapotranspiration estimation models: Penman-Monteith, Penman-Combination, Priestly-Taylor, Modified Turc, Radiation/Tmax, and Radiation (Simple) methods. The performance of each method was compared. The Simple Method required a single measured parameter, solar radiation, and achieved comparable performance to the complex methods with numerous input requirements.

Input data requirements increase from the Simple Method to the Penman-Monteith Method. In south Florida, most of the variance (73 percent) in daily evapotranspiration is explained by solar radiation alone. The effect of humidity and wind speed in estimating ET is relatively minimal. The Simple Method (Eq. 2) requires a single measured parameter, solar radiation, and is less subject to local variations (Abtew, 1996). The Simple Method is also cited as Abtew Equation and Simple Abtew Equation in published literature.

$$ET = K_1 \frac{Rs}{\lambda} \tag{2}$$

Where ET is daily evapotranspiration from wetland or shallow open water (mm d^{-1}), Rs is solar radiation (MJ m^{-2} d^{-1}), λ is latent heat of vaporization (MJ kg^{-1}), and K_1 is a coefficient (0.53). The Simple Method was further cross validated by comparing the estimates to four years of Bowen-Ratio ET measurements at nine sites in the Everglades of South Florida (Abtew, 2005).

Comparative application of the Simple Method further demonstrates its usefulness. In an effort to identify the most relevant approach to calculate potential evapotranspiration for use in daily rainfall-runoff models, Oudin et al. (2005) compared 27 potential ET models for stream flow simulation from 308 catchments in France, United States and Australia. Each potential ET model estimate was applied to four continuous daily lumped rainfall-runoff models. Comparison of the Nash-Sutcliffe (Nash and Sutcliffe, 1970) efficiency (Eq. 3) in validation of various potential ET methods as applied in the HBV0 model is shown in Figure 1. The model efficiency (E) goodness-of-fit measure is based on the error variance and is, defined as:

$$E = \left[1 - \frac{\sigma_\varepsilon^2}{\sigma_o^2} \right] \tag{3}$$

The error variance σ_ε^2 is defined as

$$\sigma_\varepsilon^2 = \frac{1}{n-1} \sum_{i=1}^{n} (PE_{o,i} - PE_{p,i})^2 \tag{4}$$

The variance of the measured potential evapotranspiration (PE), σ_o^2 defined as

$$\sigma_o^2 = \frac{1}{n-1} \sum_{i=1}^{n} (PE_{o,i} - \overline{PE_o})^2 \tag{5}$$

Where $\overline{PE}_0$ is average measured PE.
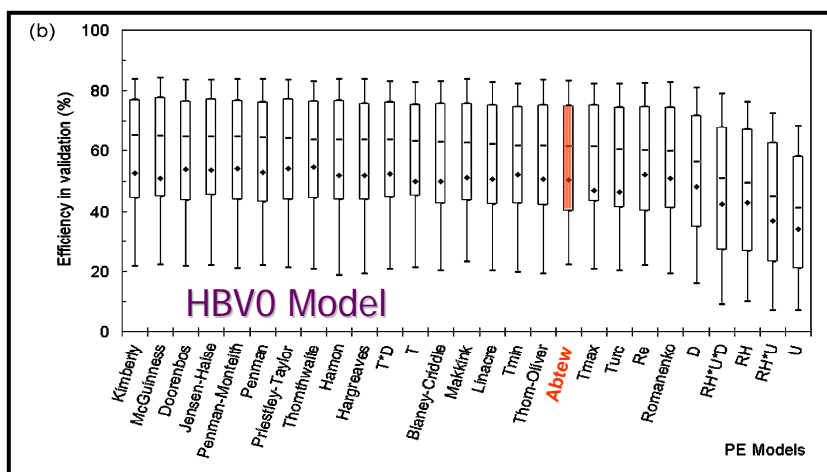
Figure 1. Average and 0.10, 0.25, 0.50, 0.75 and 0.90 percentile of
Nash-Sutcliffee (E) Criteria obtained by 27 PE models in validation
mode for HBV0 model (Oudin et al., 2005).

The simple method was applied to estimate evaporation from
Lake Titicaca, South America. Compared to eight evaporation models, it
was found to be the best evaporation estimation model (Delclaux and
Coudrain, 2005). Xu and Singh (2000) evaluated various radiation based
methods for calculating evaporation and concluded that the Simple
Method can be used when available data is limited to radiation data. The
Simple Method is applicable to remote sensing where the input, solar
radiation, is acquired through satellite observations (Jacobs et al., 2000).

LAKE EVAPORATION ESTIMATION METHODS
APPLICATION TO LAKE ZIWAY, ETHIOPIA

The Simple Method Application to Lake Ziway

Lake Ziway (Figure 2) is located in the Ethiopian Rift valley
with an average surface area of 490 km^2 at an elevation of 1636 m msl
(Coulomb et al., 2001). Monthly and annual average Lake Ziway
evaporation estimates have been published (Coulomb et al., 2001;
Ayenew, 2003). The estimates vary from method to method of
evaporation estimation. Annual lake evaporation estimates by Coulomb

et al. (2001) were 1777, 1875 and 1728 mm, respectively estimated with the Energy balance, Penman and Complementary Relationship Lake Evaporation (CRLE) methods. Estimates by Ayenew (2003) were 2022, 1599 and 1769, respectively estimated with Penman, Radiation and Pan methods (Table 1).
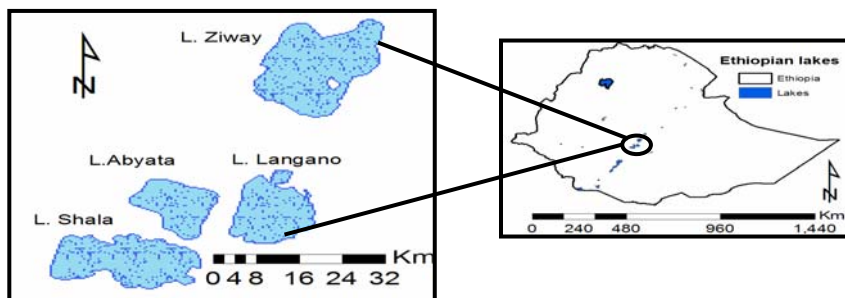
Figure 2. Ethiopian Rift valley lakes

Table 1. Lake Ziway evaporation estimations with various methods.

Month	Solar Radiation	Simple Method Lake Evaporation K=0.53	Coulomb et al. (2001) Lake Evaporation			Ayenew (2003) Lake Evaporation		
			Energy	Penman	CRLE	Penman	Radiation	Pan
	W/M^2	mm	mm	mm	mm	mm	mm	mm
January	245.8	142.4	143.2	153.8	132	150	135	159
February	250.1	130.9	149.1	162.2	135.3	128	120	144
March	249	144.3	151.7	166.1	149.2	148	142	192
April	252	141.3	155.5	165.6	154.6	188	138	142
May	259.2	150.2	163.2	170.3	159.9	188	138	156
June	243.4	136.5	147.4	167.6	154.6	135	107	137
July	208.3	120.7	127.7	135.8	146	139	115	126
August	219.2	127.0	136.3	137.1	136.3	135	115	123
September	225.5	126.4	141.1	136.4	137.4	164	124	112
October	260.3	150.8	158.9	162.4	140.6	200	151	170
November	262.7	147.3	159.6	161.1	143.8	223	157	178
December	249.4	144.5	143	156.5	138.5	225	157	130
Total		1662	1777	1875	1728	2023	1599	1769

Application of the Simple Method was tested with input of average monthly solar radiation data (Coulomb et al., 2001). With the original coefficient value (K = 0.53), the annual lake evaporation estimate by the Simple Method is 1662 mm (Table 1). The Simple Method estimate is 4 percent lower than the CRLE method estimates (Coulomb et al., 2001) and 3.8 percent higher than the Radiation method estimates (Ayenew, 2003). The coefficient of the Simple Method can be adjusted to much annual estimate of any of the methods as a way of calibration if it is believed those methods are more reliable. Monthly lake evaporation estimates by the Energy Balance and Penman Equation (Coulomb et al., 2001) were compared to the Simple Method with adjusted K values. Results are shown in Figure 3 and 4. Monthly lake evaporation estimates by the Simple Method with single measured parameter, solar radiation, has fitted well compared to estimates of the energy balance and Penman equation.
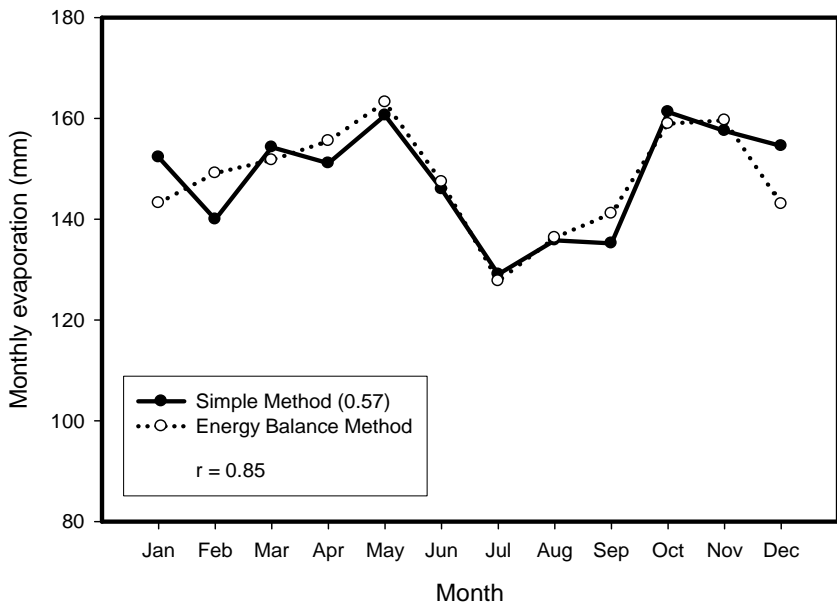
Figure 3. Comparison of Energy Balance and Simple Method estimates of Lake Ziway evaporation.
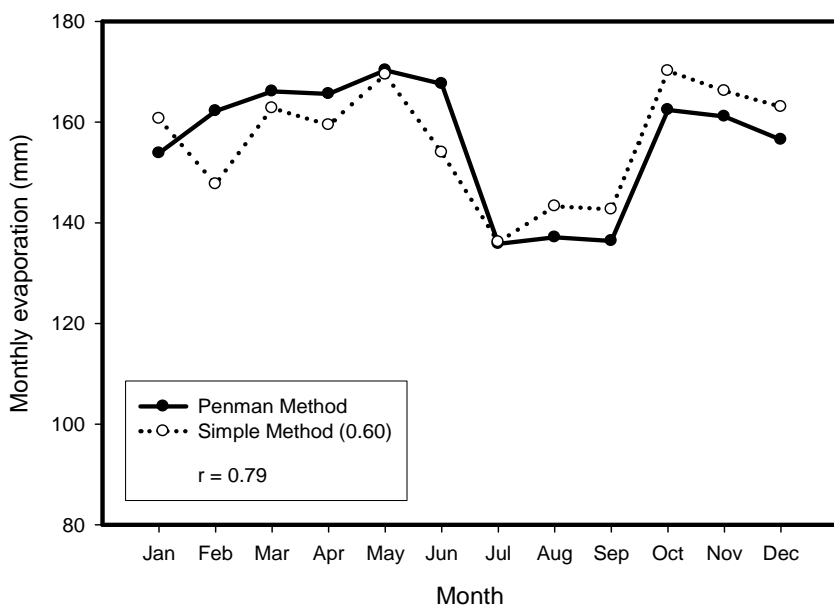
Figure 4. Comparison of Penman and Simple Method estimates of Lake Ziway evaporation.

Remote Sensing Application in ET Estimation

Remote sensing-based evapotranspiration (ET) estimations using the surface energy budget equation are proving to be one of the most recently accepted techniques for areal ET estimation covering larger areas (Morse et al. 2000). Surface Energy Balance Algorithms for Land (SEBAL) is one of such models utilizing Landsat images and images from others sensors with a thermal infrared band to solve equation (6) and hence generate areal maps of ET (Bastiaanssen et al. 1998a; Bastiaanssen et al. 1998b and Morse et al. 2000).

SEBAL requires weather data such as solar radiation, wind speed, precipitation, air temperature, and relative humidity in addition to satellite imagery with visible, near infrared and thermal bands. SEBAL uses the model routine of ERDAS Imagine, an image processing software, in order to solve the different components of the energy budget equations. In the absence of horizontally advective energy, the surface

269

energy budget of land surface satisfying the law of conservation of energy can be expressed as,

$$R_n - LE - H - G = 0 \qquad \text{(W/m}^2\text{)} \qquad (6)$$

where R_n is net radiation at the surface, LE is latent heat or moisture flux (ET in energy units), H is sensible heat flux to the air, and G is soil heat flux. Energy flux models solve equation (6) by estimating the different components separately. Net radiation is estimated based on the relationship by Bastiaanssen et al. (1998a),

$$R_n = R_{s\downarrow}(1-\alpha) + R_{L\downarrow} - R_{L\uparrow} - R_{L\downarrow}(1-\varepsilon_s) \quad \text{(W/m}^2\text{)} \qquad (7)$$

where $R_{S\downarrow}$ (W/m^2) is the incoming direct and diffuse shortwave solar radiation that reaches the surface; α is the surface albedo, the dimensionless ratio of reflected radiation to the incident shortwave radiation; $R_{L\downarrow}$ is the incoming long wave thermal radiation flux from the atmosphere (W/m^2); $R_{L\uparrow}$ is the outgoing long wave thermal radiation flux emitted from the surface to the atmosphere (W/m^2), ε_s is the surface emissivity, the (dimensionless) ratio of the radiant emittance from a grey body to the emittance of a blackbody.

The soil heat flux is the rate of heat storage to the ground from conduction. Studying irrigated agricultural regions in Turkey, Bastiaanssen (2000) suggested an empirical relationship for G given as:

$$G/R_n = 0.2(1 - 0.98NDVI^4) \quad \text{(W/m}^2\text{)} \qquad (8)$$

where $NDVI$ is the normalized difference vegetation index (dimensionless).

Sensible heat flux is the rate of heat loss to the air by convection and conduction due to a temperature difference. Using the equation for heat transport, sensible heat flux can be calculated as:

$$H = \frac{\rho C_p (T_a - T_s)}{r_{ah}} \quad \text{(W/m}^2\text{)} \qquad (9)$$

where ρ is the density of air (kg/m^3), C_p is the specific heat of air (1004 J/kg/K), T_a is the air temperature (K), T_s is surface temperature (K) derived from the thermal band of Landsat images and r_{ah} is the aerodynamic resistance (s/m).

With R_n, G, and H known, the *latent heat flux* is the remaining component of the surface energy balance to be calculated by SEBAL. Rearranging equation (4) gives the latent heat flux where:

$$LE = R_n - G - H \ \ (\text{W/m}^2) \tag{10}$$

The detailed technique for estimating latent and sensible heat fluxes using remotely-sensed data from Landsat and other sensors is documented and was tested in Europe, Asia, Africa, and in Idaho in the US and proved to provide good results (Bastiaanssen et al. 1998a; Bastiaanssen et al. 1998b; Wang et al. 1998; Bastiaanssen 2000; Morse et al. 2000; Melesse et al., 2006).

Surface energy balance and remote sensing application to Lake Ziway

In this study, two Landsat images (Landsat TM from December 1986 and Landsat ETM+ from January, 2000) were used for the computation of energy fluxes and lake evaporation estimation. Images wee processed based on the procedures outlined in SEBAL model. Based on the daily lake evaporation estimates from the SEBAL model, monthly estimates were generated for comparison to the Simple and Penman Models. Table 2 shows statistics of the results of the remote sensing-based lake evaporation estimates. It is shown that the monthly estimates correspond well with the long-term averages of the monthly evaporation values from the Simple and Penman Method for Lake Ziway. Comparison of Lake evaporation estimates among lakes shows that, Lake Langano, the mercky lake with high sediment loads has lower average monthly evaporation than the other three lakes, which have less sediment loads and are clearer. Figure 5 shows the spatial evpotranspiration estimates from the two Landsat images.

Table 2. Monthly lake evaporation (mm)

Ziway	1986	2000	Langano	1986	2000
Min	121	121.8	min	110	100.4
Max	204	201	max	194	199
Mean	145	138.7	Mean	116.9	115
STD	7.3	2.13	STD	1.6	4.1

Abiyata	1986	2000	Shala	1986	2000
Min	129.6	129.7	Min	131.2	130.5
Max	148.22	185	Max	192	196
Mean	140.9	141.8	Mean	135.5	143.7
STD	2.1	2.1	STD	1.3	7.8
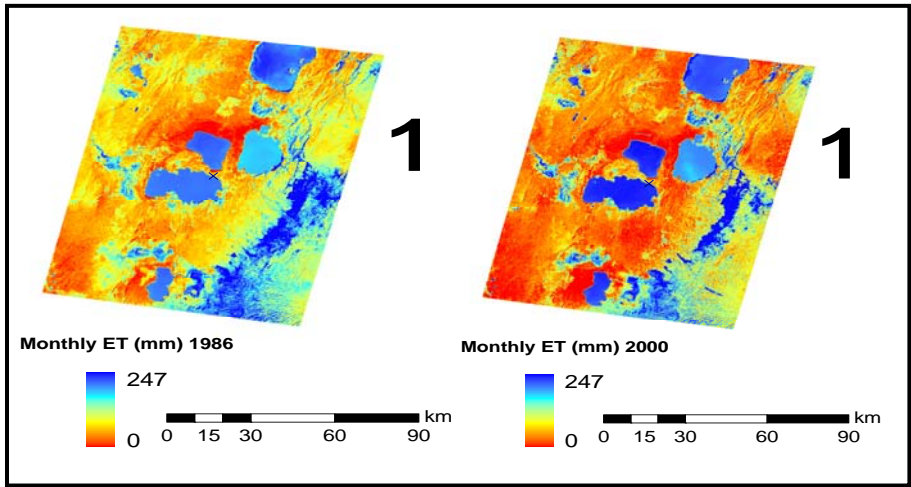
Figure 5. Spatial monthly evpoatranspiration map of Rift valley lakes, Ethiopia for December 1986 and January 2000.

SUMMARY

Evaporation from ponds, lakes and reservoir is a key hydrologic parameter and cost effective estimation method is desired specially in areas where monitoring resources are limited. Open water evaporation can be estimate of potential evapotranspiration. The Simple Method has been tested and applied in South Florida where it is currently the standard method for lake evaporation, wetland evapotranspiration and potential evapotranspiration estimation by South Florida Water Management District, a 47,000 square km complex water management system. Other applications are also cited. The method should do well in tropical and subtropical areas where humidity is high, wind speed is not high and temperature is correlated to radiation. In this study the Simple Method evaporation estimates with and without recalibration of the coefficient, K_1, are comparable to the estimate of the input data intensive methods.

The application of the Simple Method and surface energy balance approach using remotely-sensed data were applied to Rift Valley Lakes of Ethiopia, where other approaches are less effective due to limited observed metrological data and remoteness of the areas. The monthly lake evaporation estimates from the two approaches corresponds very well with Penman and energy balance approaches from previous studies.

REFERENCES

Abtew, W. 2005. Evapotranspiration in the Everglades: Comparison of Bowen Ratio Measurements and Model Estimates. Proceedings of the ASAE Annual International Meeting Technical Papers, July 17-20, 2005, Tampa, Florida.

Abtew, W., J. Obeysekera, M. Irizarry-Ortiz, D. Lyons and A. Reardon. 2003. Evapotranspiration Estimation for South Florida. P. Bizier and P. DeBarry (ed.). Proceedings of the World Water and Environmental Resources Congress 2003. ASCE.

Abtew, W. 2001. Evaporation Estimation for Lake Okeechobee in South Florida. Journal of Irrigation and Drainage Engineering, ASCE. Vol. 127(3):140-147.

Abtew, W. 1996. Evapotranspiration Measurements and Modeling for Three Wetland Systems in South Florida. Journal of the American Water Resources Association. Vol. 32(3):465-473

Abtew, W. and J. Hardee. 1993. Design of a Lysimeter for a Wetland Environment: Evapotranspiration of Cattails (*Typha domingensis*). Paper presented at the 1993 ASAE International Winter Meeting, Chicago, IL. Dec. 14-17. Paper No. 93-2553.

Ayenew, T. 2003. Evapotranspiration Using Thematic Mapper Spectral Satellite Data in the Ethiopian Rift and Adjacent Highlands. Journal of Hydrology, 279:83-93.

Coulomb, C.V., D. Legesse, F. Gasse, Y. Travi and T. Chernet. 2001. Lake Evaporation Estimates in Tropical Africa (Lake Ziway of Ethiopia). J. of Hydrology 245:1-18.

Bastiaanssen, W.G.M., 2000. SEBAL-Based Sensible and Latent Heat Fluxes in the Irrigated Ediz Basin, Turkey. Journal of Hydrology 229:87-100.

Bastiaanssen, W.G.M., M. Menenti, R.A. Feddes and A.A.M. Holtslag. 1998a. The Surface Energy Balance Algorithm for Land (SEBAL): Part 1Formulation, Journal of Hydrology 212-213: 198-212.

Bastiaanssen, W.G.M., H. Pelgrum, J. Wang, Ma Y., J. Moreno, G.J. Roerink and T. Van der Wal. 1998b. The Surface Energy Balance Algorithm for Land (SEBAL): Part 2 Validation, Journal of Hydrology 212-213: 213-229.

Delclaux, F. and A. Coudrain. 2005. Optimal Evaporation Models for Simulation of Large Lake Levels: Application to Lake Titicaca, South America. Geophysical Research Abstract, Vol. 7, 07710 266:53-65.

Jacobs, J.M., D.A. Myers, M.C. Anderson and G.R. Diak. 2000. GOES Surface Insolation to Estimate Wetland Evapotranspiration. J. of Hydrology. Vol. 266:53-65.

Melesse, A., J. Oberg, O. Beeri, V. Nangia, D. Baumgartner. 2006, Spatiotemporal Dynamics of Evapotranspiration and Vegetation at the Glacial Ridge Prairie Restoration, Hydrological Processes, Vol. 20(7): 1451-1464.

Morse, A., M. Tasumi, R.G. Allen and W. Kramber. 2000. Application of the SEBAL Methodology for Estimating Consumptive use of Water and Streamflow Depletion in the Bear River Basin of Idaho Through Remote Sensing. Final Report Submitted to the Raytheon Systems Company, Earth Observation System Data

and Information system Project, by Idaho Department of Water Resources and University of Idaho. 107pp.

Nash, J.E. and J.V. Sutcliffe, 1970. River Flow Forecasting Through Conceptual Models, Part I, A Discussion Of Principles. J. of Hydrology. Vol. 10(3), 282-290.

Oudin, L., F. Hervieu, C. Michel, C. Perrin, V. Andreassian, F. Anctil and C. Loumagne. 2005. Which potential evapotranspiration input for a lumped model? Part 2-Towards a simple and efficient potential evapotranspiration model for rainfall-runoff modeling. Journal of hydrology, 303:290-306.

Wang, J., W.G.M. Bastiaanssen, Y. Ma and H. Pelgrum,1998. Aggregation of Land Surface Parameters in the Oasis-Desert Systems of Northwest China, Hydrological Processes, 12: 2133-2147.

Xu, C.Y. and V.P. Singh. 2000. Evaluation and Generalization of Radiation-based Methods for Calculating Evaporation. Hydrological Process, 14:339-349.

WATER BALANCE DYNAMICS IN THE NILE BASIN

Gabriel B. Senay[1], Kwabena Asante[1] and Guleid Artan[2]

For presentation at a workshop on "Nile Basin Hydrology and Ecology
under Extreme Climatic Conditions";
June 16-19, 2008; Addis Ababa, Ethiopia.

[1]Research Scientist and Adjunct Professor; SAIC, contractor to the U.S.
Geological Survey (USGS) Earth Resources Observation and Science
(EROS) Center / Geographic Information Science Center of Excellence
(GIScCE) South Dakota State University, South Dakota, USA;
senay@usgs.gov. Work performed under USGS contract 03CRCN0001.
[2]Research Scientist; SAIC, contractor to USGS/EROS

ABSTRACT

Understanding the temporal and spatial dynamics of key water
balance components of the Nile River will provide important information
for the management of its water resources. This study used satellite-
derived rainfall and other key weather variables derived from the Global
Data Assimilation System to estimate and map the distribution of
rainfall, actual evapotranspiration (ETa), and runoff. Daily water balance
components were modeled in a grid-cell environment at 0.1 degree (~10
km) spatial resolution for 7 years from 2001 through 2007. Annual maps
of the key water balance components and derived variables such as
runoff and ETa as a percent of rainfall were produced. Generally, the
spatial patterns of rainfall and ETa indicate high values in the upstream
watersheds (Uganda, southern Sudan, and southwestern Ethiopia) and
low values in the downstream watersheds. However, runoff as a percent
of rainfall is much higher in the Ethiopian highlands around the Blue
Nile subwatershed. The analysis also showed the possible impact of land
degradation in the Ethiopian highlands in reducing ETa magnitudes
despite the availability of sufficient rainfall. Although the model
estimates require field validation for the different subwatersheds, the
runoff volume estimate for the Blue Nile subwatershed is within 7.0% of
a reported figure from an earlier study.

Further research is required for a thorough validation of the results and their integration with eco-hydrologic models for better management of water and land resources in the various Nile Basin ecosystems.

INTRODUCTION

Water balance studies of a river basin provide important information for the management of its water resources for efficient and equitable allocation to different users and economic sectors in a sustainable environment. Typical water balance studies for a basin include the determination of the inflows (rainfall and incoming streamflow) and outflows (evapotranspiration, diversion, and river discharge). Although several studies have documented the rainfall (e.g., Cheung et al., 2008; Seleshi and Zanke, 2004) and flow (e.g., Conway, 1997; Hurst, 1950) contributions of some subwatersheds in the Nile Basin, a lack of uniformity in the quality and distribution of weather and flow observation points have prevented rigorous analyses in determining the spatial and temporal distribution of the various water balance components in the basin. Senay and Verdin (2004) used satellite-derived rainfall to estimate runoff distribution for the entire African continent but did not include the distribution of estimated actual evapotranspiration (ETa).

The Nile River is known to be the longest river (6,850 km) in the world and flows from south to north, discharging into the Mediterranean Sea. Most of the Nile water is generated in an area covering 20% of the basin, while much of the downstream area consists of arid or semiarid regions with little contribution to the flow but with large evaporative losses (Karyabwite, 2000: [http://www.grid.unep.ch/activities/sustainable/nile/nilereport.pdf]). About 94 km^3 (94 billion cubic meters) of water flows annually to Lake Nasser of Egypt and only 0.4 km^3 are released into the Mediterranean (Varis, 2000; Nile Basin Initiative, 2002: [http://www.nilebasin.org]).

The main objective of this study is to apply uniformly acquired weather data and vegetation condition indicators across the entire Nile Basin and estimate the spatial and temporal distribution of key water balance components using an agrohydrological model. The modeling approach used satellite-derived rainfall and other weather parameters from the Global Data Assimilation System (GDAS) (Kanamitsu, 1989)

to estimate daily evapotranspiration and runoff on a 10- x 10-km grid cell. The results are presented as annual totals.

MATERIALS AND METHODS

Study Site

The Nile Basin is located in northeast Africa and is composed of watersheds from 10 countries, from Burundi in the south to Egypt in the north. The 10 countries contributing to or benefiting from the flow of the Nile River are Burundi, Democratic Republic of the Congo (DRC), Egypt, Eritrea, Ethiopia, Kenya, Rwanda, Sudan, Tanzania, and Uganda. These 10 countries constitute about 10% of the African landmass but contain about 40% of its population (about 300 million people). The majority (70%) of the population of these countries resides within the Nile Basin (El-Fadel et al., 2003).

The major tributaries of the Nile are 1) the White Nile that originates from the highlands of Burundi, 2) the Blue Nile that originates from the central highlands of Ethiopia, and 3) the Tekeze (Atbara) that originates from the northern highlands of Ethiopia. A major contributor to the While Nile also comes from the southwestern highlands of Ethiopia as Baro-Akobo (Sobat). The Nile River system includes one of the largest swamps in the world, called the Sudd, which is known to lose about 55% of the White Nile's contribution to evapotranspiration (Baecher et al., 2000). According to El-Fadel et al. (2003), the majority (about 80%) of the annual Nile flow to Lake Nasser originates from the Ethiopian highlands, with the Blue Nile alone providing about 53% (50 km^3) of the annual flow (Conway, 1997).

Data

The most important data for this study included daily satellite-derived rainfall estimates (RFE), daily global reference evapotranspiration (ETo), average dekadal (nominally 10 days) normalized difference vegetation index (NDVI), digital soil map of the world (FAO 1988) and Moderate Resolution Imaging Spectroradiometer (MODIS) Vegetation Continuous Field (VCF) data.

Seven years of daily RFE data (Xie and Arkin, 1997), produced by the National Oceanic and Atmospheric Administration (NOAA)

Climate Prediction Center, were used in this study at 0.1-degree spatial resolution. The daily reference ETo data are produced at EROS from 6-hourly GDAS climate parameters using the standardized Penman-Monteith equation, then downscaled to 0.1 degree for this study (Senay et al., 2008). Historical average (1982–2006) dekadal NDVI datasets, described by Tucker et al. (2005), from NOAA's Advanced Very High Resolution Radiometer (AVHRR) were used to characterize the land surface phenology (LSP) to estimate temporal water use dynamics for estimating evapotranspiration (ET) on a pixel-by-pixel basis at 0.1-degree resolution. The percent vegetation cover dataset from MODIS VCF (Hansen et al., 2003) was used to estimate canopy interception parameters. Water holding capacity of soils was derived from the digital soil map of the world (FAO, 1988).

Modeling Approach

Daily weather data (RFE and ETo) were used to estimate daily actual evapotranspiration using the VegET model (Senay, 2008), which is based on standard water balance principles comparable to those outlined in Allen et al. (1998) and Senay and Verdin (2003). The modeling approach in VegET includes the use of LSP to estimate ETa according to each pixel's unique LSP temporal profile in place of using a "crop coefficient," which is used in most agrohydrologic water balance models. The VegET model estimates runoff as the residual of daily rainfall minus both water holding capacity and interception losses. Thus, the yearly water balance terms of runoff and ETa generally do not add up to the total rainfall. The residual between rainfall and (ETa + runoff) is mainly attributed to canopy interception-evaporation. In VegET, the interception coefficient for each modeling unit varies from a minimum of 0% in bare cover types to a high of 35% in areas with a dense forest cover. According to Hörman et al. (1996), evaporation by forest canopy interception accounts for 10 to 40% of the total rainfall. Area weighted average interception losses were estimated for each modeling pixel using vegetation cover distribution from the MODIS VCF, which provides the percentage of bare, herbaceous, and tree cover for each pixel (Hansen et al., 2003). The interception losses are subtracted from the daily precipitation to determine the effective precipitation that is used in the VegET water balance calculation. Soil moisture storage change is negligible in annual water balance calculations.

Analysis Approach

Daily estimates of RFE, Eta, and runoff were summed to an annual value for each of the 7 years from 2001 to 2007. The spatial distribution of the major water balance components were represented using the median values from the 7-year annual totals on a pixel-by-pixel basis. The median values were chosen from the average to reduce the influence of some extreme values from the relatively short time-series dataset.

Temporal charts of two selected subwatersheds were produced using watershed-average values for each of the 7 years. Watershed boundaries were derived from the HYDRO1k (http://edc.usgs.gov/products/elevation/gtopo30/hydro/index.html) elevation dataset by the U.S. Geological Survey Earth Resources Observation and Science (EROS) Center (Verdin and Jenson, 1996).

RESULTS AND DISCUSSION

Figure 1a shows the spatial distribution of satellite-derived annual rainfall using the median value for the years 2001 to 2007. High rainfall values in excess of 1,000 mm are shown to occur in much of Uganda, as well as in western Kenya, southwestern Sudan, and much of western Ethiopia. Low rainfall totals (less than 300 mm) are generally seen in the lower part of the basin, north of the confluence of the White Nile and the Blue Nile. As expected, estimated ETa follows the spatial patterns of rainfall (Figure 1b). Areas with annual ETa greater than 400 mm can be considered well vegetated, while areas less than 200 mm ETa would require a substantial amount of supplemental irrigation to produce enough vegetation biomass to support a substantial animal community and human settlement.
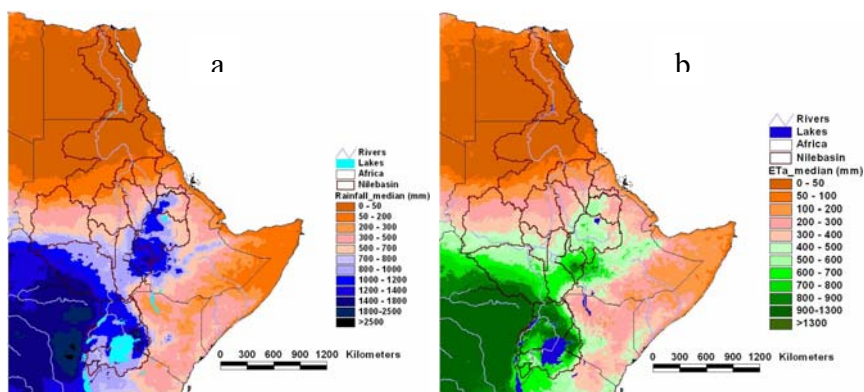
Figure 1. (a) Annual satellite-derived rainfall (median of 2001–2007) and (b) ETa estimate for the same time period.

The annual ETa distribution can be used to assess the integrated response of the landscape from the nature of its rainfall distribution and ability of the land cover to use the rainfall. In this study, we hypothesize that degraded landscapes will exhibit disproportionately lower ETa amounts despite good rainfall distribution. Figure 2a shows a ratio between annual ETa and rainfall totals. We used global water balance studies that show about 63% of terrestrial rainfall is lost to ETa (Peixoto and Kettani, 1973) as a reference to create three broad classes for the Nile Basin region. Areas where more than 80% of the rainfall is partitioned to ETa are shown to be in arid and semiarid regions of the basin. On the other hand, most agricultural lands of the Nile Basin fall in the broad region of 50–80% of ETa as percent of annual rainfall. Areas where the ETa is less than 50% can be interpreted in one of two categories: 1) the land is too degraded and does not support a dense vegetation to use rainfall for ETa processes, or 2) the rainfall is too abundant for areas in which vegetation ETa is controlled by the available energy instead of water supply. Three regions fall into this class: southwestern Sudan, northwestern Ethiopia (Blue Nile region), and eastern DRC (outside of the Nile Basin boundary). In most of these regions, annual rainfall exceeds 1,000 mm, except for areas in northern Ethiopia and parts of Eritrea. We believe that ETa values less than 50% of rainfall in the areas of northern Ethiopia and Eritrea may be attributed to land degradation. An analysis of the yearly minimum NDVI (Figure 2b) suggests that the same areas in Ethiopia show a much lower NDVI

281

(less vegetation) during the dry times than the other regions. A minimum
NDVI is chosen as an indicator of land degradation since higher NDVI
values, generally occurring in the rainy season, are less discriminating in
the degree of vegetation in the landscape. However, more investigation is
required to confirm if those areas in northern Ethiopia and Eritrea are
indeed unable to use the rainfall due to lack of vegetation, while the other
regions are receiving rainfall beyond the capacity of the landscape to use
it for vegetation growth.

(a)

(b)
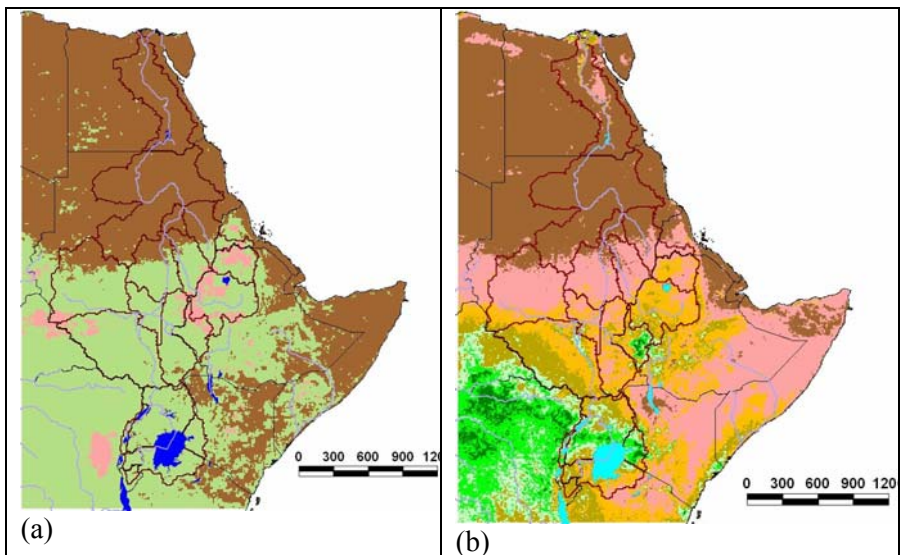
Figure 2. (a) Annual ETa estimate as percent annual rainfall
(ETa_Pct_Rainfall (%): both median of 2001–2007) and (b) average
minimum NDVI (AVHRR: 1982–2006) (NDVI_MN).

Generally, the balance between rainfall and ETa is considered
runoff, although some other losses, particularly interception-evaporation,
still account for some of the balance. Figures 3a and 3b show the
estimated annual runoff (Figure 3a) on a pixel-by-pixel basis, while
Figure 3b shows the runoff as a percent of the rainfall. Generally, high
rainfall areas (except for those in Uganda) show high runoff; moreover,
areas identified as low ETa fraction in Figure 2a show "high" runoff in
Figure 3a. Also, the runoff-rainfall percent map in Figure 3b shows
"degraded" areas in northern Ethiopia and Eritrea having among the

highest amounts of runoff as percent rainfall. The overall spatial pattern of the runoff depths is similar to runoff maps produced by Senay and Verdin (2004) in their Africa-wide water harvest potential assessment.
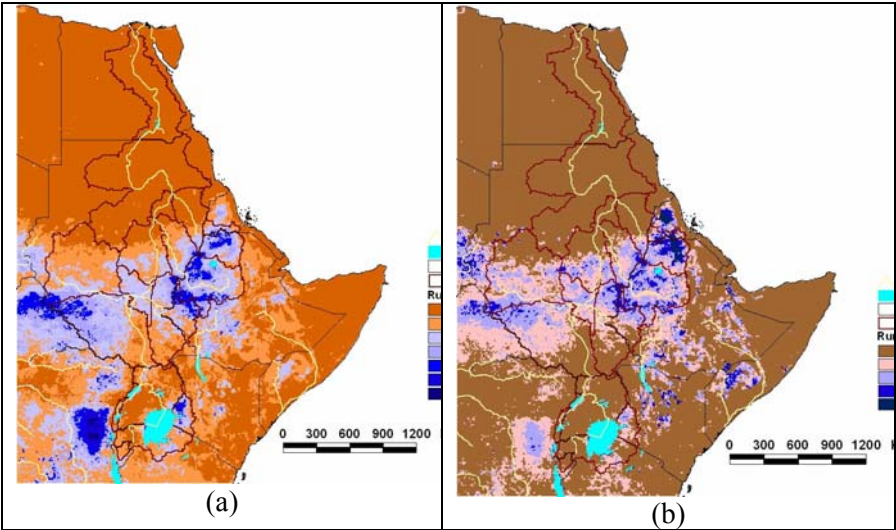
Figure 3. (a) Annual runoff estimate (median of 2001–2007) in mm and (b) annual runoff as percent annual rainfall.

A summary of the runoff volume estimate by subwatershed is shown in Figure 4. Note that the magnitudes of the various subwatershed volumetric estimations have not been validated with any discharge measurements. However, we are confident that the relative distribution of the volumetric values assists in understanding the relative runoff contribution of the different subwatersheds in the Nile Basin. The highest runoff generating subwatersheds are WN-1 (White Nile) at 50.5 km^3 and BN-1 (Blue Nile) at 41.4 km^3 in southwestern Sudan and northwestern Ethiopia, respectively. Other sizable contributions come from subwatersheds in Sudan, Ethiopia, Uganda, Tanzania, and Kenya. In relative terms, subwatersheds in Eritrea, DRC, Burundi, Rwanda, and Egypt generate lower runoff amounts (less than 5 km^3). Although these figures have not been independently verified, a paper by Conway (1997) reported an observed volumetric discharge of about 47.4 km^3 for the Blue Nile subwatershed using an area of 176,000 km^2, an average value for the time period between 1951 and 1987. Using an equivalent

watershed area to that used by Conway, the 41.4 km^3 reported in this study is equivalent to 44.0 km^3. Considering the differences in the period of study and the use of satellite-data sources, the closeness (within 7.0%) of the runoff volume estimate for the Blue Nile indicates the potential of the approach to depict the spatial and temporal patterns of the various water balance components. Furthermore, these estimates do not take into account evaporative losses in the various wetlands and lakes, particularly in the Sudd swamp of Sudan where an average of 55% of the water entering the Sudd is lost to ETa (Baecher et al., 2000).
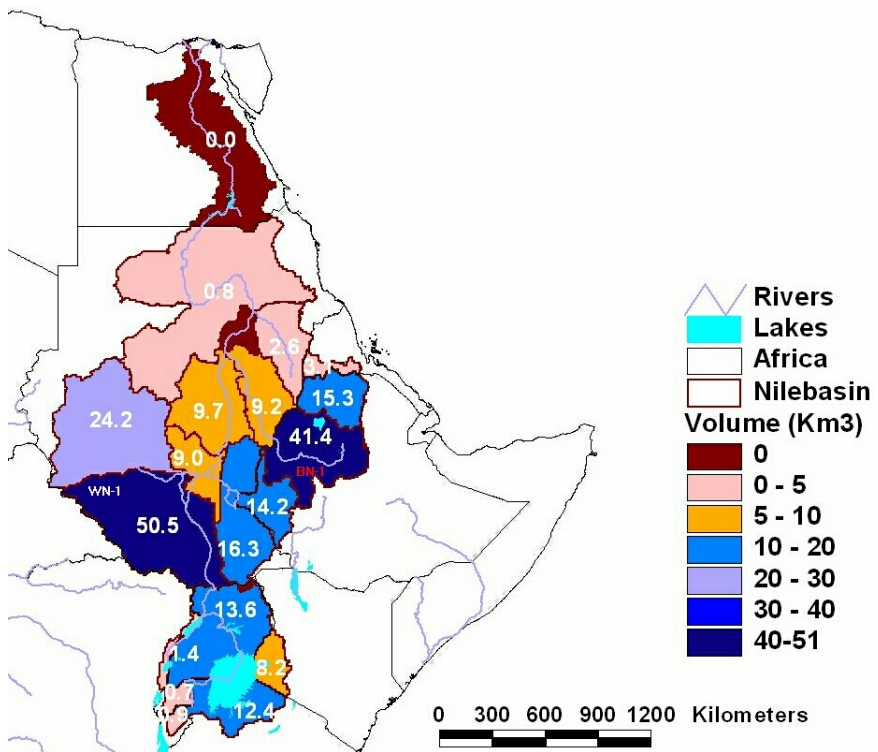
Figure 4. Annual runoff volume estimate by subwatershed in km^3 (median of 2001–2007).

The limited number of years in the satellite-derived rainfall estimates precludes a robust analysis of the temporal dynamics of the water balance terms in the Nile Basin. However, the major water balance components of the two subwatersheds with the greatest volumetric runoff estimates (WN-1 and BN-1) are shown in Figures 5 and 6. The White

Nile subwatershed in southwestern Sudan (WN-1) appears to be stable from year-to-year in that rainfall varied only between 1,000 mm and 1,200 mm in the 7-year period (Figure 5). The high rainfall in the WN-1 subwatershed produces a relatively high ETa (> 600 mm), indicating a healthy vegetation water use. On the other hand, the watershed-average runoff depth stayed under 200 mm in all years except in 2007. Despite the relatively high runoff generated in the WN-1 region, Conway and Hulme (1993) reported that most of the runoff from the Bahr El Ghazal subbasin that includes the WN-1 subwatershed does not contribute to the main Nile flow because of evaporation, with only 0.5 km^3 leaving the subbasin. The Blue Nile subwatershed (BN-1) appears to have a higher range of annual variability with minimum and maximum values around 800 mm (during 2004) and 1,300 mm (2006), respectively. The sum of runoff and ETa are generally less than the rainfall in both subwatersheds because the VegET model assumes the interception losses as percent of rainfall to be around 23% and 24% for BN-1 and WN-1, respectively, based on model parameterization using the MODIS VCF land cover distribution dataset.
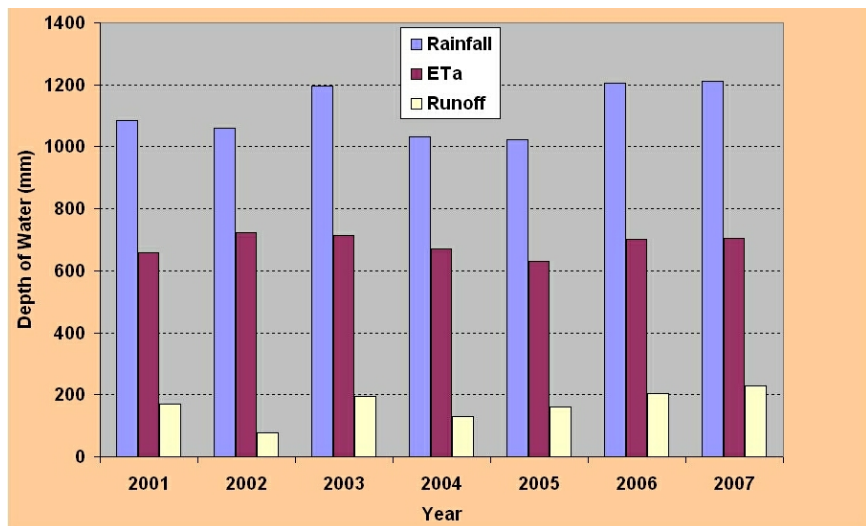
Figure 5. Major water balance components of the White Nile (WN-1, Figure 4) subwatershed.
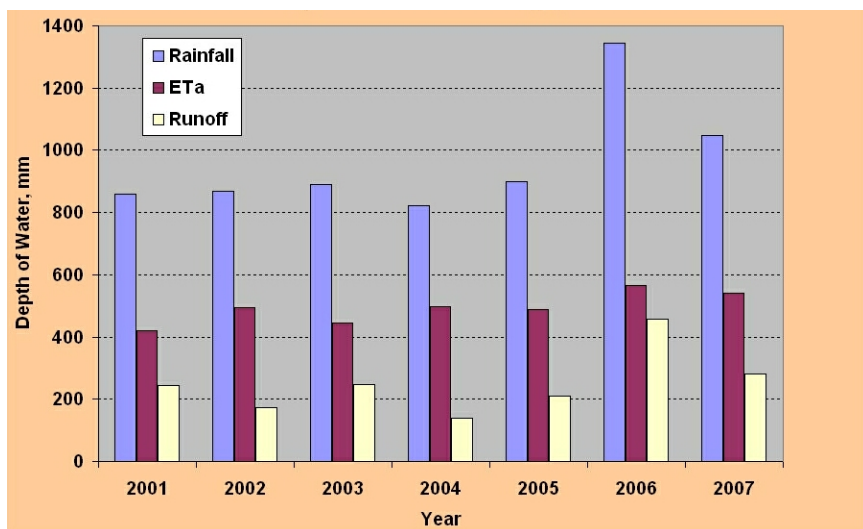
Figure 6. Major water balance components of the Blue Nile (BN-1, Figure 4) subwatershed.

The high rainfall of 2006 in the Blue Nile region resulted in several flood occurrences in the region, which can be noted from a marked runoff increase for the same year compared to the other years (Figure 6). This is also reported in the field report of Reynolds (2006 [http://www.pecad.fas.usda.gov/highlights/2006/09/eth_19sep2006]). Also, the average runoff for the Blue Nile (250 mm) is higher than the average runoff for the White Nile subwatershed (166 mm). The average ETa is about 700 mm for WN-1 and 500 mm for BN-1. In both watersheds a substantial change in rainfall generally affects the change in runoff more than the change in ETa. For example, during 2006 runoff, the Blue Nile subwatershed increased by 82% while ETa only increased by 14%.

CONCLUSION

The water balance dynamics of major water balance components were presented for the Nile River Basin. Satellite-derived rainfall data and VegET model output were used to assess the relative distribution of major water balance components on a pixel-by-pixel and subwatershed basis using 7 years of daily data and model output.

The spatial distribution of rainfall shows a higher magnitude in the upstream part of the Nile Basin, while a greater runoff percentage was observed in the Blue Nile subwatershed. The study suggests that the higher runoff-rainfall percentage exhibited in the Blue Nile subwatershed and surrounding regions could be partially attributed to land degradation.

Although the results of this study have not been validated using field-collected data such as stream discharge measurements, the volumetric estimate for the Blue Nile Basin corresponds closely to published values by other researchers. More research is recommended to validate and integrate these results with eco-hydrologic models.

A good understanding of the spatial and temporal dynamics of the Nile Basin hydrology will help design appropriate management scenarios for soil and water conservation, reservoir management, and agricultural development.

REFERENCES

Allen, R.G., L. Pereira, D. Raes and M. Smith. 1998. Crop Evapotranspiration. Food and Agriculture Organization of the United Nations. FAO publication 56. ISBN 92-5-104219-5. 290pp. Rome, Italy.

Baecher, G.B., R. Anderson, B. Britton, K. Brooks and J. Gaudet. 2000. Environmental trans-boundary opportunities and constraints for the Nile Basin, U.S. Agency for International Development, Washington, DC.

Cheung, W.H., G.B. Senay and A. Singh. 2008. Trends and spatial distribution of annual and seasonal rainfall in Ethiopia. International Journal of Climatology. DOI:10.1002/joc.1623.

Conway, D. 1997. A water balance model of the Upper Blue Nile in Ethiopia. Hydrological Sciences-Journal-des Sciences Hydrologiques. Vol. 42(2):265-285.

Conway, D. and M. Hulme. 1993. Recent fluctuations in precipitation and runoff over the Nile sub-basins and their impact on main Nile discharge. Climate Change. Vol. 25:127-153.

El-Fadel, M., Y. El-Sayegh, K. El-Fadl and D. Khorbotly. 2003. The Nile River Basin: A Case Study in Surface Water Conflict Resolution. J. Nat. Resour. Life Sci. Educ. Vol. 32:107- 117.

FAO. 1988. FAO/UNESCO soil map of the World: revised legend. Food

and Agricultural Organization of the United Nations. FAO
World Resources Report 60. Rome, Italy.

Hansen, M., R.S. DeFries, J.R.G. Townshend, M. Carroll, C. Dimiceli
and R.A. Sohlberg. 2003. Global Percent Tree Cover at a Spatial
Resolution of 500 Meters: First Results of the MODIS
Vegetation Continuous Fields Algorithm. Earth Interactions.
Vol. 7 (10):1-15.

Hörman, G., A. Branding, T. Clemen, M. Herbst and A.
Hinrichs.1996.Calculation and simulation of wind
controlled canopy interception of beech forest in Northern
Germany. Agric. For. Meteorol. Vol.79:131-148.

Hurst, H.E. 1950. The Nile Basin. Vol VIII. The hydrology of Sobata
and While Nile and the topography of the Blue Nile and Atbara.
Ministry of public works, Physical department,   Cairo, Egypt.

Kanamitsu, M. 1989. Description of the NMC Global Data Assimilation
and Forecast System. Weather and Forecasting. Vol. 4:335-342.

Peixoto, J.P. and M.A. Kettani. 1973. The Control of the Water Cycle.
Scientific American. Vol. 228:46-61.

Senay, G.B. 2008. Vegetation evapotranspiration (VegET) estimation
using vegetation index   enhanced water balance algorithm for
landscapes. In preparation.

Senay, G.B., J.P. Verdin, R. Lietzow and A.M. Melesse. 2008. Global
daily reference evapotranspiration modeling and evaluation.
Journal of American Water Resources Association. Vol. 44
(3):1-11.

Senay, G.B. and J. Verdin. 2004. Developing Index Maps of Water-Harvest
Potential in Africa. Applied Engineering in Agriculture. Vol.
20(6):789-799.

Senay, G.B. and J. Verdin. 2003. Characterization of yield reduction in
Ethiopia using a GIS-based crop water balance model. Canadian
Journal of Remote Sensing. Vol. 29(6):687-692.

Seleshi Y. and U. Zanke. 2004. Recent changes in rainfall and rainy days
in Ethiopia. International Journal of Climatology. Vol. 24: 973-
983, DOI:10.1002/joc.1052.

Tucker C.J., J.E. Pinzon, M.E. Brown, D. Slayback, E.W. Pak, R.
Mahoney, E. Vermote and N. El Saleous. 2005. An Extended
AVHRR 8-km NDVI Data Set Compatible with MODIS and
SPOT Vegetation NDVI Data. International Journal of Remote
Sensing.Vol.14:4485-   4498.

Varis, O. 2000. The Nile Basin in a global perspective: Natural, human,

and socioeconomic resource nexus. Water International. Vol. 25(4):624–637.

Verdin, K. and S. Jenson. 1996. Development of continental scale DEMs and extraction of hydrographic features, proceeding of the Third International Conference/Workshop on Integrating GIS and Environmental Modeling, Santa Fe, New Mexico, January 21-26, 1996, (CD-Rom).

Xie, P. and P.A. Arkin. 1997. A 17-year monthly analysis based on gauge observations, satellite estimates, and numerical model outputs. Bulletin of the American Meteorological Society. Vol. 78(11):2539-2558.

RAINFALL INTENSITY–DURATION-FREQUENCY RELATIONSHIP FOR SELECTED STATIONS IN EASTERN ETHIOPIA

Shimelis Birhanu and Tena Alamirew

Haramaya University, P. O. Box 138, Dire Dawa, Ethiopia
alamirew2004@yahoo.com

ABSTRACT

The rainfall Intensity-Duration-Frequency (IDF) relationship is a very useful site specific tool needed in the design and development of water resource systems. The information, however, has not been available due to absence of recording rain gauges in Ethiopia until very recently. In this study, rainfall Intensity-Duration-Frequency (IDF) relationships have been developed for six weather stations in eastern Ethiopia. The annual maximum rainfall data of varying duration were extracted from rainfall charts and fitted to theoretical frequency distribution and then extrapolation of values for larger return periods were made. The log Pearson type III distribution was applied to the annual maximum rainfall data sets generated in the six rainfall stations to estimate the parameters of general IDF mathematical forms for the study area. The chi-square test confirmed the appropriateness of the selected distribution. Log Pearson graphical plots and the computed confidence limits also showed that the log Pearson type III distribution fits the empirical distribution well. The IDF equations of the generalized mathematical form and families of curves have been generated for the station. The parameters of the equation were tested and found that they adequately describe the observed data showing that the method is reliable. The IDF relationship generated could be used for estimating peak runoff rates in water resource systems design and development.

HYDROLOGICAL WATER AVAILABLITY, TRENDS AND ALLCOATION IN THE BLUE NILE BASIN [1]

[1]Seleshi Bekele Awulachew, [1]Mathew McCartney,
[2]Yilma Seleshi Shiferaw, [1]Yasir Mohammed

[1]International Water Management Institute (IWMI)
[2]Addis Ababa University

ABSTRACT

The Blue Nile (known as the Abay in Ethiopia) is the principal tributary of the main Nile River providing 62% of the flow (approximately 50 billion m^3 per year) reaching Aswan. Ethiopia currently utilizes very little of the Abay water. In contrast, Sudan uses significant volumes both for irrigation (currently in excess of 1,1 million ha) and for hydropower production. However, there remains significant potential for additional exploitation and both Ethiopia and Sudan have plans to further develop the water resources of the river. In Ethiopia, several major irrigation schemes, with a total area of approximately 164,000 ha, are planned for completion by 2010. In addition several hydropower dams, including four located on the main stem of the river, are being contemplated. In the Sudan, no additional hydropower is being considered, but it is planned to develop an additional 889,000 ha of irrigation by 2025. In this study the Water Evaluation and Planning (WEAP) model was used to investigate both the current situation and future water demand scenarios. Time series of flows were generated (on a monthly time-step) to determine inter-annual and seasonal variability in water availability in the major tributaries. Existing water use, related to irrigation and hydropower, was estimated from actual data. Future development scenarios were based on information obtained from commissioned projects and the national water resource master plans. This paper illustrates the value of scenarios, and the application of a relatively simple model, to assess the implications of proposed water resource development.

Key Words: Abay, Blue Nile, Water Allocation, Water Use Potential, WEAP

BLUE NILE (ABAY) HYDROPOWER POTENTIAL, PRIORITIZATION AND TRADEOFFS ON PRIORITY INVESTMENTS

[1]Desalegn, D.T., [2]Awulachew, S.B., and [3]Moges, S.A.

[1]Arba Minch University P.O.Box 21, Arba Minch, Ethiopia,
der_tadesse@yahoo.com
[2]IWMI regional Representative, Sub-regional Officer for Nile Basin &
Eastern Africa, Addis Ababa, Ethiopia, s.bekele@cgiar.org
[3]Dean, School of Post Graduate Studies, Arba Minch University,
P.O.Box 21, Arba Minch, Ethiopia, semu_moges_2000@yahoo.com

ABSTRACT

Ethiopia is among countries which has very low modern energy sources. The topographic feature and the available water of Ethiopia permit to have a large hydropower potential. However, as the available runoff in rivers has very high hydrological variability, tapping in to this potential require investment on storage to smooth the temporal hydrological variability. In this paper, first the behaviour of this hydrological variability and implication of water resources development is discussed. Secondly, various documents and reports provide varying values of hydropower potential of Ethiopia and Abbay. To close the information gap, topographical and hydrological site evaluation for the selected hydropower potential sites have been carried out, for 129 possible potentials sites which are identified by WAPCOS in 1990 and having total capacity of 13,845 MW. After evaluations these sites 91 possible sites with potential of 12,148 MW are identified and mapped under various sub-basins. Dabus sub-basin stands first among the 16 sub-basins by 13 hydropower potential sites and these sites give 3524MW. In order to exploit the available hydropower potential in the country, it is crucial to rank these sites. The ranking of these sites have been carried out based on cost per kilowatt hour of the hydropower potential (HP) sites. Furthermore, the paper qualitatively discusses the benefits and tradeoffs for four priority development identified by ENTRO as Eastern Nile fast track projects.

Key Words: Hydrological variability, Abbay, hydropower, potential, tradeoffs

CRITICAL WATER RESOURCES MANAGEMENT ISSUES IN THE NILE RIVER BASIN

Muluneh Yitayew
Professor
Agricultural and Biosystems Engineering Department
The University Of Arizona
Tucson, Arizona 85721; email:myitayew@ag.arizona.edu

ABSTRACT

The central water management issue for the Nile River Basin, as in many other river basins throughout the world, is sustainability of water supply in the context of intense population growth, recurring drought, and increasing competition for water. The issue gets complicated as a result of global climate change that is taking place at an alarming rate. A serious discussion of these and other important water resource issues and the challenges in the basin is necessary and needs our attention to seek solutions and insure sustainability of the water supply. This paper will address the physical and hydrological conditions of the basin as a background and present the cross-cutting issues of concern in the basin. The challenges to obtain, protect, and manage the basin's water supply and ecosystem will also be discussed. Even though one cannot make a meticulous coverage of all the issues and challenges in the basin, a serious attempt will be made to present possible solutions at local and regional scale. The solution will be geared towards getting more of the water, using it as much, and making it sustainable.

INTRODUCTION

Sustainability of water supply in a given basin implies that the present water needs of the population in the basin are met without compromising the ability of the future generations to meet their needs. The situation with respect to Nile water need and supply is getting critical and growing worse. The demand for the water is increasing significantly as a result of increased population and the effect of global warming. Some of the basin states have already experienced critical water shortage as a result of some extreme events such as recurring drought while some had occasional flooding. Shortage of water occurs when the needed amount of quality water is not available at the right time and place of need. It can be due to drought or due to contamination

of the available water.   In the later case the water can become degraded to an extent it is not safe for human consumption.

Considering a threshold value of 1000 m^3 per person per year, it is projected that some of the Nile Basin countries: Burundi, Rwanda, Egypt, Ethiopia, and Kenya will be considered as water "scarce" by 2025. This is based on a continuous population growth at the present rate. If the present trend of water shortage continues, which is likely to happen, the result will be that socio-economic development will be restrained and the potential for water conflict will be increased. What this also means is that hydrologists, engineers, sociologists, politicians, water resources managers, decision makers, and other water resources interest groups would have to be knowledgeable about the river water to develop, protect, keep, share and use it in an efficient and equitable manner. This may require a shift in paradigm, developing and adopting new ways of technically, legally, and administratively handling the Nile water. There may be a need to think regionally and act locally. Most of the Nile water issues today transcend one country, and the basin. In many cases even the region. Yet, a great portion of the solution must be attained at the country level. It is the author's belief that most of the basins problems are not result of the people living in the basin countries rather more and more of the basin's future water issues and problems will be driven out of a more regional and global environment. To this end this paper will discuss some of the critical issues in the management of the water resources of the Nile Basin that need attention and need to be addressed at this point in time.   There are many issues such as water scarcity, water quality, water policy, good governance, institutional and financial capacity, poverty reduction, food security etc. that affect management of the basin's water directly or indirectly and needs to be considered seriously in any discussion of the basin's water resources management.   Recognizing that it is very hard to make a meticulous coverage of all the issues, this paper only addresses three of the most critical ones and will suggest possible solutions for achieving sustainable water resources development and management in the basin. The physical and hydrological conditions are described first.

The Nile Basin Geography

The Nile River Basin (Figure 1) with its diverse ecosystem is one Africa's largest and most important river basin. It is located in a region with varied geographical, topographical, climatological,

hydrological, political, and physical characteristics. It extends through 35 degrees of latitude of the north-eastern African quadrant as it flows from the south highlands through alluvial plains and desert sands into the eastern Mediterranean to the north. It starts from its headwaters at elevation 1135 meters above sea level in Lake Victoria and above 1800 meters above sea level in the Ethiopian highlands resulting in a drainage area of about 3,007,000 km². This area spans over ten countries: Burundi, Egypt, Ethiopia, Eritrea, Kenya, Tanzania, Rwanda, Sudan, and the Democratic Republic of Congo. The total drainage area is nearly 10% of Africa's landmass.   From the headwater source the river flows 6700 kilometers to end up in the Mediterranean Sea. This makes the Nile the longest river in the world.

There are three major tributaries to the Nile: the Blue Nile, the White Nile, and the Atbara Rivers. The Blue Nile is the main tributary and starts in Lake Tana, Ethiopia before it travels northwest and joins the White Nile in Khartoum, Sudan. The Atbara drains also from Ethiopia as Tekeeze before it joins the main Nile about 300 kilometers north of Khartoum.   The White Nile originates from the Equatorial Lakes region and joins the Blue Nile at Khartoum. The Ethiopian headwater contributes about 85% of the Nile water through the Blue Nile, Atbara, and Baro-Akobo (Sabot) rivers (Table 1) with the remaining 15% coming from the Equatorial lakes headwater.
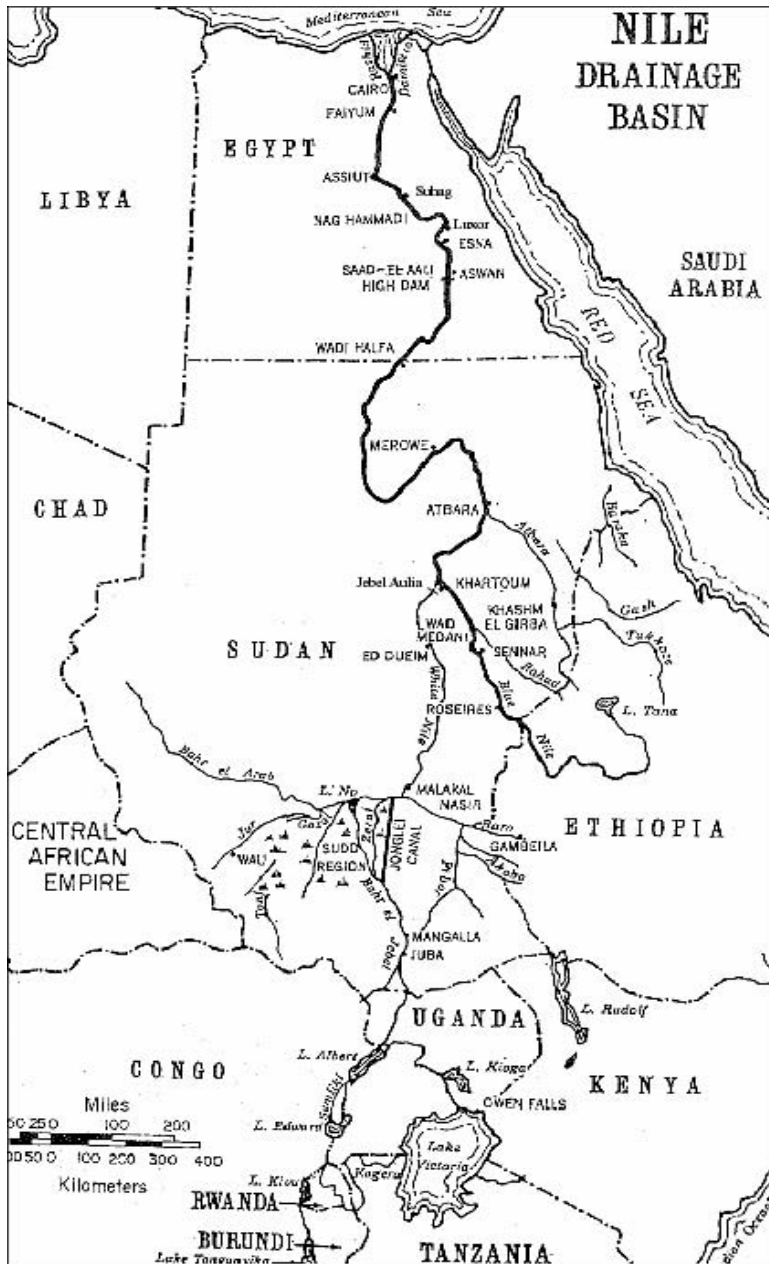
Figure 1. Map of the Nile River Basin

Table 1. Ethiopia's three rivers contributing to the Nile River system

No	River Basin	Catchment Area(Km^2)	Annual Runoff (BM^3)	Specific Discharge ($l/s/Km^2$)
1	Abbay	199,800	52.6	7.8
3	Baro-Akobo	74,100	23.6	9.7
8	Tekeze	90,000	7.6	3.2
	Total	363900	83.8	

Source: Compiled from Various river basin master plan studies and river basin surveys. Ministry of Water Resources, Ethiopia, 1999. Water Sector Strategy Document.

The Nile Basin can be divided into two main sub-basins, the White Nile and the Blue Nile. The White Nile sub-basin consists of catchment areas in Burundi, Ethiopia through Baro-Akobo drainage areas, Kenya, Rwanda, Sudan, Uganda, and Congo while the Blue Nile sub-basin consists of catchments from Ethiopia and Sudan (Figure 1).

The Nile Basin ecosystem has the two lakes i.e., Lake Victoria and Tana, the three major tributaries: Blue Nile, White Nile, Atbara, the Sudd, the largest freshwater swamp in the world, and the dams, mainly the Aswan high dam. Lake Victoria is the second largest freshwater lake in the world.

Nile Hydro-Climatology

The Nile hydrology shows a high degree of temporal and spatial variation. There is abundant rainfall in the headwaters and very low practically zero rainfall in the arid Sudan and Egypt. Although the watershed is large, the portion contributing to stream flow is almost half of the entire basin (only $1.6x\ 10^6\ km^2$) due to the fact that north of 18°N latitude, rainfall is almost zero (Teodoru et al., 2006). Precipitation increases towards the headwaters to over 1200 to 1600 mm yr^{-1} on the Ethiopian Plateau and in the region of the Equatorial lakes: Victoria, Albert, Kayoga, and Edward (Mohamed et al., 2005). The seasonal pattern of rainfall follows the Inter-Tropical Convergence Zone (ITCZ), where the dry northeast winds meet the wet southwest winds and are forced upward causing water vapor to condense. The ITCZ follows the

area of most intense solar heating and warmest surface temperature and reaches the northern part of the Ethiopian Plateau by late July. The southward shift of the ITCZ results in the retreat of the rainy season towards the central part of the basin after October. Therefore, the monthly distribution of precipitation over the basin shows one single but long wet season over the Ethiopian Plateau and two rainy seasons over the Equatorial Lakes Plateau (Mohamed et al., 2005).

Nicol (2003) identified three major hydrological characteristics of the Nile River. These are first its two major origins: in the highlands of Ethiopia and in the Nile equatorial lakes region. The former provides the major flow of the Nile north of Khartoum – the Blue Nile – and the latter the far lower and slower flows of the White Nile. The second major feature of the hydrological system is the huge seasonality of the Blue Nile's flows. A third major feature of the river system is caused by virtue of the river's situation in hot, arid areas where evaporation losses are high.

Subject to seasonal variations, about 80% of the total annual discharge of the River Nile occurs during the summer rainy season (July to October) mainly with the Blue Nile and the Atbara River (Woodward et al., 2001). Atbara River runs dry at times of the year while the White Nile maintains the flow in the Nile over the entire year. Without the discharge of the upper White Nile the Nile River would probably run dry in May. The annual flow distribution and suspended sediment budget is shown in Figure 2.
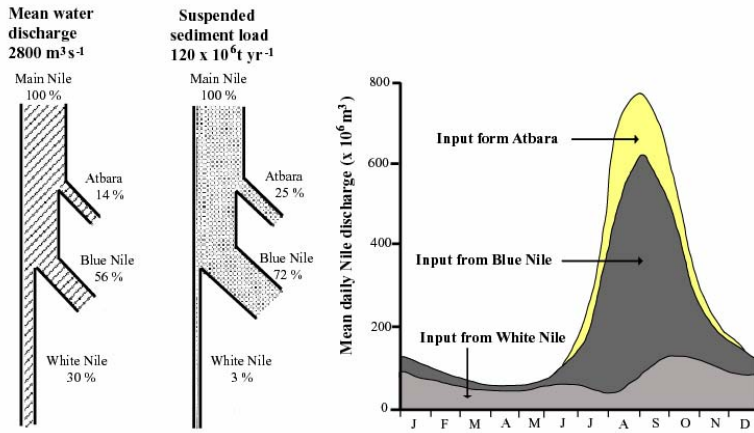
Figure 2. The water and suspended sediment budget of the present Nile basin (after Woodward et al., 2001)

More than 95% of the mean annual suspended sediment load of the Nile River upstream of the Aswan High Dam (120x106 t yr-1, Woodward et al. 2001) comes with the Blue Nile (72%) and the Atbara River (25%) whereas the White Nile contributes only 3% of the total load. Apart from seasonal variations, the total annual discharge of the Nile River is subject to intense annual variations with the highest annual flows of 154 km^3 yr^{-1} recorded in 1878 (Abu Zeid, 1987) and 120 km^3 yr^{-1} measured in 1984 (Woodward et al., 2001). The lowest annual flow on record was observed in 1913 with only 42 km^3 yr^{-1} (Abu Zeid, 1987).

As a result of increased water surface area being exposed to arid climate conditions, the evaporation from the lake behind the Aswan High Dam (AHD) was estimated to vary between 18 and 21% (19% in average) of the total river input (Aly et al., 1993). A review of earlier literature established a large range for evaporation from Lake Nasser between 1.7 m yr^{-1} and 2.9 m yr^{-1} (Sadek et al., 1997). Based on water balance, energy budget and modeling, narrower range of 2.1 m yr^{-1} to 2.6 m yr^{-1}, with an average of 2.35 m yr^{-1}, was calculated by Sadek et al., (1997). It was estimated that the annual evaporation from the AHD Reservoir varied between 12 and 12.6 km^3 yr^{-1} which correspond to an evaporation rate of 2.0 to 2.1 m yr^{-1} (Roskar, 2000). Compared to the reservoir volume of 162 km^3, the evaporation represents about 8% per year but more than 15% of the river inflow of 84 km^3 yr^{-1}.

The hydro-climatology studies show the variability in flow of the Nile both in time and space. Unless there is a way to regulate this flow condition it is difficult to plan a meaningful sustainable water resources development and management program. It is also apparent that in a basin as big as the Nile basin, a concerted effort to gather data that can be used to forecast the hydrologic and climatologic variables is absolutely necessary. Integrated basin-wide hydraulic cooperation must go parallel with the rest of the effort to bring the riparian countries to work together with a shared vision of benefiting socio-economically and politically. With this as a goal the next section addresses three of the critical issues that need to be considered in the basin immediately.

CRITICAL WATER ISSUES

Hydropolitics

With the basin comprising areas from ten countries: Burundi, Ethiopia, Egypt, Kenya, Uganda, Rwanda, Tanzania, Congo, Sudan, and Eritrea, and claims for the portion of the river water by most of these countries increasing, it is easy to see the complexity of dealing with sharing of the water in an equitable manner. For the most part, the hydropolitics of the Nile has been dominated by a single country, Egypt that is totally dependent on the Nile water that is generated in the upstream countries. It is by far the most powerful both militarily and economically of all the riparian countries. On the other hand, the upstream countries though they may have geographic advantage, are some of the least developed and poorest countries in the world facing poverty, recurring drought, and famine. This disparity between the upstream and the downstream countries lead to an unbalanced level of development within the basin as reflected by the gross domestic product (Table 2).

Table 2. The Nile Basin countries

Country	Percent of NRB (%)	Percent of country in NRB (%)	Population Total (mln)	GDP per capita (2005)	Renewable Water Resources, (m³/person)
Sudan	63.6	79	31.7	2,100	1,981
Ethiopia	11.7	32.4	65.8	900	1,666
Egypt	10.5	32.6	65.2	3,900	830
Uganda	7.4	98	22.8	1,800	2,663
Tanzania	2.7	8.9	34.4	700	2,472
Kenya	1.5	7.9	30.7	1,100	947
Eritrea	0.8	20.5	4.2	1,000	1,578
DR Congo	0.7	0.9	52.4	700	23,639
Rwanda	0.7	75.5	7.9	1,500	638
Burundi	0.4	47.6	6.9	700	538

In the nineteenth to the middle of the twentieth century the hydropolitics was also influenced by colonial power with the British Empire as the major player. Most of the agreements on the Nile Basin were made either between colonizers or bilateral agreement between Sudan and Egypt. With the blessing of the British, Egypt was able to dictate most of the treaties and bilateral agreements that are still in the books ratified by Sudan but never been accepted by the other riparian countries.   Most importantly, Ethiopia has never been a party to most of these agreements.

In the 1990s greater effort was invested by the riparian countries, the World Bank, and donor agencies, to forge a cooperative approach to the Nile water development and management. With the formation of the Nile Basin Initiative in 1999, the hydro-political environment has changed.   This came about as a result of the realization by the major players that the status quo is neither in their best interest nor is sustainable. It is also the result of their willingness to move from "unilateralism" to "multilateralism" in resource development (Nicol, 2003). With the formation of the Nile Basin Initiative, representatives of the riparian countries have been negotiating to develop a regional partnership for the cooperative development of the water resources in the Nile Basin with the goal of the initiative being "To achieve sustainable socioeconomic development through the equitable utilization of, and benefit from the common Nile Basin water resources" (NBI-www.nilebasin.org). The future for such cooperation in the basin will depend on the acceptance of benefit sharing over water sharing as guiding principle by the countries in the basin and also in recognizing "equitable and reasonable" allocations along with historical precedence of water usage.

As stated above over the last three decades, cooperation over the Nile water management has been the focal point for most of the riparian countries and the international community.   This cooperation to develop and manage the river water will become even more important as the basin face uncertain but increasingly evident challenges that the global climate change will bring. The recurring drought in most of the countries is a likely harbinger of tough times ahead making sustainable water management more difficult.   The increasingly stressful environmental and demographic conditions will require much more cooperative action now than has been delivered thus far.

These challenges the basin face present a strong rationales for working together cooperatively to assure adequate water supplies. All the individual countries interest for the Nile water need to be treated in a pragmatic manner. Most people take cooperation to have a positive value, on its face. To argue against would seem a crazy thought. The issue is to what extent individual countries influence the decision making about sharing the water resources. It is also important to clearly understand the value and the limits of cooperation for the individual countries such as Ethiopia that contributes 85 percent of the river water. One should not stretch cooperation to a point where it does lose its meaning. The question is what should the role of the upstream and downstream countries be in this cooperation and how can the countries maximize the value of their involvement and reach the best and informed decisions for the sake of their own population? At some point in the near future each country has to see if cooperation is working for it. There got to be some measure of success in cooperative outcomes. This will help each decide on future investment in cooperative management of the natural resources. It will also help continue to put a sustained effort by the riparian countries.

NBI brought the countries together which for a long time were not in talking terms at all. While they were able to work out their differences and reach some win-win consensus agreements, it has not changed the basic equation of equitably sharing of the Nile water. The most important challenge in this case is establishing the legal and institutional framework. To this end there has to be some mechanism to bring qualified members of each of the countries at the table and draw the expertise of the international community as the third party. This is the sticking point in the hydropolitics of the Nile basin and of all the pillars of the shared vision which may derail the movement towards continued cooperation and might even reverse the situation back to upstream and downstream squabble with the "zero-sum game" position back at work.

Climate Change

Global climate change as a result of increased carbon dioxide and other greenhouse gases is an accepted reality by many scientists around the world. Increase in temperature by several degrees is expected over the next century (Mitchell et al. 1995, Wigley and Raper 992, Houghton et al. 1992). Some believe global climate change as a

result of the effect of greenhouse gas concentration is already evident (Thomson 1995). The twentieth century's ten warmest years all occurred in the last fifteen years of the century (Colby et al., 2005).

The Intergovernmental Panel on Climate Change (IPCC, 2000) summarized hydrologic changes that can be expected as a result of global warming to include changes in precipitation levels, seasonal patterns of regional precipitation, and flood frequencies. Specifically their analysis suggested that a projected increase in the average temperature will have the effect such that the frequency and severity of droughts could increase in some areas as a result of decrease in total rainfall, more frequent dry spells, and higher evaporation. They also pointed out that the hydrology of arid and semi-arid areas is particularly sensitive to climate variation such that small variations in temperature and precipitation in these areas can result in a large percentage changes in runoff, increasing the likelihood and severity of droughts and floods.

The point is that climate change in the basin will occur and will shift and reshape the annual and seasonal climate patterns. It is inevitable that runoff and water supply will change. More important is also the fact, in the Nile basin, climate variability is amplified by the complexity of the hydrology of the basin. For example precipitation varies from close to about 2000 mm/year in the Ethiopian highlands and valley lakes to almost zero in the Egyptian deserts. Climate variability can bring large changes in the reliability of the existing reservoirs yield from small changes in precipitation and runoff. Climate changes can also reduce the productivity of hydroelectric dams by causing fluctuations in hydroelectric generation. The challenge is thus developing basin wide strategies to minimize the adverse effects of climate change and implementing it before it occurs. This is a serious consideration as the whole basin heavily depends on hydroelectricity and drought will affect the availability and cost of electricity.

Climate change has also a serious implication on sharing of the Nile water. It should be considered in all the negotiations and decision making regarding the equitable water allocation. There should, for example, an anticipation of droughts and prepare for it. Climate forecasting, monitoring and evaluating hydrologic variables will also help the parties adapt changes that will address water allocation in wet and dry years. It will help negotiate priorities of deliveries of the available river water especially during dry years.

The challenge is responding to the anticipated climate change to minimize the adverse effect of such changes. To this end, both structural and non-structural measures have to be considered. Flexible anticipatory adaptation policies with full consideration to the uncertainties of predicting the different types of climate change must be put in place. Climate change should be incorporated in long-term basin water management planning.   Use of inter-basin water transfers should be considered. Water conservation practices should be put in place. Changes in design and construction of hydraulic structures and proper dam sites selection should be adapted.

Information Sharing

Solutions to water management problems in the basin start and end with reliable data and information. Data gathering on the flow of the Nile, the quality of the water, control, and distribution it is absolutely a prerequisite for any cooperation in managing shared water resources. Information provides power to whoever owns it. This sometimes can create an apparent sense of control and advantage for the owner but can also create unnecessary suspicion for those who do not have it. Sharing data and information enable people to think together in solving problems, in building trust essential for cooperative efforts towards sustaining shared vital natural resources and in avoiding conflict. Naff (1999) summarized advantages of sharing data and information in that it enables people to think together in solving problems, to build trust, and avoid conflict. Sharing is the foundation of good neighborliness.   The ideal of peaceful, cooperative use of water and the environment cannot be achieved in the absence of sharing. Shared data is the most productive and efficiently used data. Solutions to water problems must be commensurate with their complexity; this is not possible without adequate, shared data. Equitable distribution of water among the users of transboundary water is not possible without shared data. Cooperative data collection and sharing prevents unnecessary duplication and reduces costs for all involved parties.

The Nile water resource management requires that the countries share data that is useful for planning, modeling, and management of a shared resource. This includes collecting relevant data, conducting water availability, and sustainable yield analysis. The challenge is to establish a protocol for collecting and analyzing data, managing, and sharing information among the ten riparian countries without a single country

dominating and taking advantage of the others. To this end the priority should be to identify and acquire the necessary technology for information and data gathering, build capacity and skills of the manpower needed in each country, and create the incentives for local data collection and data sharing. As an example, at a basin level, countries upon recognizing or anticipating specific water resources problem or combination of problems should initiate information and data gathering to determine the exact nature and extent of the water problems (including quantification of availability of the water resource and the past, present and projected water demands) and determine whether those problems warrant basin wide or local attention.

CONCLUSION

The Nile water is critical for long-term economic development, health and social welfare of the population in the basin. Any shortage in the future is likely to restrain socio-economic development and to become a potential source of conflict between the basin countries. Solutions to existing and potential problems of the Nile water resources sustainability therefore should be viewed with the desire to minimize such possibilities.   The way forward for the basin is to focus on benefit sharing rather than water sharing, multilateralism instead of unilateralism, and enhancing more cooperative approach. Establishing the NBI legal and institutional framework agreement with full consideration of the hydropolitics of the basin is urgently needed if the countries are to overcome their differences and attain a sustainable water development and management system. Improving the understanding of past climate conditions based on a collaborative information and data sharing system with the goal of improving the ability to predict the future effect of global climate change is also necessary. One should be optimistic and hope that the constructive measures suggested would be put to work to respond to the crucial issues of sustainable water resource development and management in the basin with a shared vision of developing and managing the Nile water fight poverty, advance socioeconomic development, and promote peace and stability in the region.

BIBLIOGRAPHY

Abu Zeid, M. 1987. Environmental Impact Assessment for the Aswan
High Dam. Water Research Center, Ministry of Irrigation. In:
Biswas A. and Q. Geping (Eds) Environmental Impact
Assessment for Developing Countries (pp 168-190). London

Aly, A.I.M., K. Froehlich, A. Nada, M. Awad, M .Hamza & W.M.
Salem. 1993. Study of Environmental Isotope Distribution in
the Aswan-High- Dam Lake (Egypt) for Estimation of
Evaporation of Lake Water and Its Recharge to Adjacent
Groundwater. Environmental Geochemistry and Health 15:37-49

Colby, G.B., J.E. Thorson, and S. Britton. 2005. Negotiating Tribal
Water Rights Fulfilling Promises in the Arid West. The
University of Arizona Press, Tucson, Arizona.

Houghton, J.T, B.A. Callander, and S.K. Varney.   1992. Climate change
-1992- the supplementary report to the IPCC Scientific
assessment. WMO/UNEP intergovernmental panel on climate
change. Cambridge University Press, Cambridge.

Intergovernmental Panel on Climate Variability and Change (IPCC).
2000. Water: The Potential Consequences of Climate Variability
and Change for the Water Resources of the United States.
National Assessment of the Potential Consequences of Climate
Variability and Change, IPCC, Geneva, Switzerland.

Mitchell, JFB., T.C. Johns, J.M. Gregory, and S.F.B. Tett. 1995.
Climate response to increasing levels of greenhouse gases and
sulphate aerosol. Nature 376:501-504.

Mohamed, Y.A., B.J.J.M Van der Hurk, H.H. Savenije and W.G.M.
Bastiaanssen. 2005. Hydroclimatology of the Nile: results from
a regional climate model. Hydrology of earth System Sciences 9:
263-278

NBI- www.nilebasin.org

Naff, T.   1999. Data sharing for international water resource
management: Eastern Europe, Russia and the CIS. Kluwer
Academic Publisher, The Netherlands.

Nicol, A. 2003. The Nile: Moving beyond cooperation. UNESCO-IHP-
WWAP IHP-VI Technical Documents in Hydrology PC-CP
Series No. 16.

Roskar, J. 2000. Assessing the water resources potential of the Nile
River based on data, available at the Nile forecasting center in
Cairo. Hidrometeorological Institute of Slovenia UDC: 556.53

(282.263.1) 36. Ljubliyana, http://www.zrc-sazu.si/giam/zbornik/roskar_40.pdf

Sadek M.F., M.M. Shahin and C.J. Stigter. 1997. Evaporation from the reservoir of the High Aswan Dam, Egypt: A new comparison of relevant methods with limited data. Theoretical and Applied Climatology 56: 57-66

Teodoru, C., A. Wuest, and B. Wehrli. 2006. Independent Review of the Environmental Impact Assessment for the Merowe Dam Project (Nile River, Sudan) Eawag, Seestrasse 79, 6047 Kastanienbaum, Switzerland

Thomson, D.J. 1995. The seasons, global temperature, and precession. Science 268:59-68.

Wigley, T.M.L. and S.C.B. Raper. 1992. Implementation for climate and sea level of revised IPCC emissions scenarios. Nature 357: 293-324.

Woodward, J.C., M.G. Macklin and D.A. Welsby 2001. The Holocene fluvial sedimentary record and alluvial geoarchaeology in the Nile Valley of northern Sudan. In: Madday D, at al. (Eds) River Basin Sediment Systems: Archives of environmental change (pp 327-355). Rotterdam, Balkema

BUILDING RESILIENCE IN WATER POLICY AND MANAGEMENT:
INTEGRATED STRATEGIES TO MEET THE CHALLENGE OF CLIMATE CHANGE

Robert Wilkinson, Ph.D.

Director, Water Policy Program
Donald Bren School of Environmental Science and Management
University of California, Santa Barbara
Email: Wilkinson@es.ucsb.edu

ABSTRACT

Global warming poses a serious threat to economic well-being, security, public health, natural resources, and the environment. The potential impacts of climate change and variability are serious. Integrated policy, planning, and management of water resources systems can provide important opportunities to respond effectively to challenges posed by climate change. Both mitigation (i.e. reducing greenhouse gas emissions) and adaptation (dealing with impacts) strategies must be developed. While both energy and water managers have used integrated planning approaches for decades, the broader integration of water and energy management in the context of climate change is a relatively new and exciting policy area. Opportunities and approaches will be outlined, using California as a case study.

ENHANCING WATER PRODUCTIVITY IN CROP-LIVESTOCK SYSTEMS OF THE NILE BASIN: IMPROVING SYSTEMS AND LIVELIHOODS

Tilahun Amede[1,2], Katrien Descheemaeker[1,2], and
Seleshi Bekele Awualchew[2]

[1]International Livestock Research Institute and
[2]International water Management Institute,
Addis Ababa, Ethiopia. Contact address T.amede@cgiar.org

ABSTRACT

The Nile Basin countries, particularly Ethiopia and Sudan, own the highest number of livestock in Africa. About half of all the cattle and more than a third of all sheep and goats in Africa are found in this basin. Besides direct contribution of livestock to the national economy and household livelihoods, they perform multiple socio-economic functions for small scale farmers. They produce food, provide security, enhance crop production, generate cash income and produce value added goods which can have multiplier effects and create a need for services. Different livestock production systems have evolved as the results of spatial and temporal diversity in climate; population density, economic opportunities and cultural practices. Those evolutions in livestock production system are highly associated with amount, distribution and access to water resources. The mixed crop-livestock systems are the most apparent systems in the Nile basin. Despite these important roles, the livelihood strategy of livestock-dependent farmers and communities is endangered by declining the resource-base and water scarcity, which is unable to support the increased demand for livestock feed and human food. This is aggravated by increasing human population, land degradation and increased demand for more cereal production through expanding crop fields to grazing areas, hillsides, wetlands and protected forests. This expansion is also putting a huge pressure on the livestock systems by competing for labour, water and land resources. As a result of this competition, there is now an increased global concern on the potentially negative effect of livestock on the environment, particularly in terms of livestock-related water depletion. Livestock-environment interaction varies with production systems and stages of intensification. When thinking about livestock and water, most people visualize the voluntary intake. Drinking water is small compared to the water required

to produce feed for animal. Evidences suggest that voluntary water intake ranges between 25-50 liter TLU^{-1} day^{-1}. Volume wise, the most important interaction of water and livestock is through transpiration process in producing animal feed, which is up to 100X more than drinking water.

This paper will display proven and potential interventions developed by collaborative work of the International Livestock Research Institute (ILRI) and International Water Management Institute (IWMI) that would help communities to improve water productivity, minimize the negative impacts and magnify the economic and social values of livestock. These interventions include targeting models that would help development actors at local, national, regional scales to disseminate livestock, water and land management interventions across production systems and socio-economic niches, forage technologies that would increase feed availability without competing with crop lands, water management strategies enhancing water productivity and minimizing water depletion through livestock, collective action schemes for enabling improved governance of livestock and water resources and policy suggestion for creating incentive mechanisms for livestock-keeping communities to invest in natural resources management. These interventions will be exemplified by case studies from Ethiopia, Kenya, Uganda and Tanzania.

WIND POWER-WATER EQUIVALENCY FOR THE WESTERN US REGION[1]

J. Doyle, D. Macuga, T. McTighe, M. Salazar and G. L. Toole
Los Alamos National Laboratory, Los Alamos, NM.

ABSTRACT

This paper describes a screening study performed in 2007 to identify the potential equivalency of wind power and water resources in the 14-state Western Electric Coordinating Council (WECC). The WECC comprises the entire electric Western Interconnection. With a footprint of 1.8 million square miles within the US, two Canadian provinces, and Baja Norte, Mexico, WECC offers significant but widely dispersed potential for farming wind resources. Provided that power produced in either the areas of abundant water resources or using generation technologies that are inherently low water consumers (wind, solar, dry cooled thermal), it can be efficiently transported to areas with limited water resources and substitute for locally produced power. Hence, local water demand may be decreased by improving the ability to reliably import electricity into water constrained areas. Using resource maps of greatest wind potential, electric generation is incrementally increased to reach a regional 25% penetration target. This approach allows overloaded transmission corridors to be identified and investments made to reliably ship power to the areas of greatest demand growth. Explicit consideration is given to reserve transmission capacity to estimate WECC's ability to move power from remote sites. Wind resource assumptions are based on National Renewable Energy Laboratory wind maps, Class 3 or higher (mean annual wind speeds = 6.9 m/s at 80 m). Limits are placed on distance to load centers to avoid transmission congestion and to implicitly acknowledge an economic break-even towards lower speeds and closer distance.

This presentation will be placed in the context of energy-water issues relevant to East Africa, specifically Ethiopia and the Upper Nile Basin.

Contact:
J. Doyle, 505-667-2954, jcd@lanl.gov, MS K488
D. Macuga, 505-667 3872, dmacuga@lanl.gov, MS C331
T. McTighe 505-665 2369, mctighe@lanl.gov, MS D452
M. Salazar, 505-667-9929, marvin@lanl.gov, MS K488
G.L. Toole, 505-667-9180, ltoole@lanl.gov, MS K488

Mailing address:
Los Alamos National Laboratory, PO Box 1663, Los Alamos NM 8754

IMPACTS OF IRRIGATION ON SOIL CHARACTERISTICS IN SELECTED IRRIGATION SCHEMES IN THE UPPER BLUE-NILE BASIN

Mekonnen Getahun[1], Enyew Adgo[2] and Asmare Atalay[3]

[1]Pedologis, Bureau of Water Resource Development, [2]Lecturer at Bahir Dar University, Amhara Regional Agricultural Research Institute, [3]Associate Professor, Virginia Tech University, USA

ABSTRACT

The study was conducted in five selected irrigation schemes which have been constructed before 20 years in the Upper Blue Nile Basin. Farmers' perception of changes in crop yield as a result of changes in soil characteristics and water logging problems were compared with soil physical and chemical analyses. Results were also interpreted along with irrigation water quality data. Soil profile pits were opened from selected representative sites in the respective irrigation command areas and from non-irrigated fields adjacent to the irrigated area for the purpose of comparison. Soil infiltration tests, soil pH, electrical conductivity, texture, different plant nutrient contents, CEC, base saturation, sodium etc., were analyzed.

Preliminary findings show that the soil pH at Mendel and Tikurit schemes ranges mildly alkaline to moderately alkaline in both irrigated and non-irrigated sites and increased with depth due to the corresponding increase in carbonates. Moreover; the pH in water at Jedeb, Fetam and Mendel were generally higher than in other sites, therefore, potential impacts on crop yields may result from the exceedence of this irrigation guideline. However, water quality analysis showing that low ranges of electrical conductivity values of irrigation water according to FAO guidelines. Obviously, irrigation water coming from the highlands of Western Amhara in the Upper Blue Nile Basin which are dominated by basaltic rocks is not carrying salts that might cause soil salinity. Measured infiltration rate and bulk densities in all schemes showed some variation between irrigated and non-irrigated sites.

Farmers perceive changes in land productivity as a result of irrigation activities compared with non irrigated plots especially onion crops decreased from time to times. Furthermore, seasonal water logging

was observed in some of the schemes during the rainy season as a result of flat topography and vertic nature of the soils of the command area. Total nitrogen, organic carbon and to some extent available phosphorus contents are generally found to be in the range of low to very low status while potassium is found to be more or less enough for the current low yield levels.

INTRODUCTION

When compared to neighboring countries, Ethiopia is endowed with significant amount of water resources, with a mean annual flow of about 110 Billion m^3 (BCM) that drain in to 12 drainage basins. Among these river basins Blue Nile (201,000 km^2), Tekeze (82,000 km^2), Baro-Akobo (74,104 km^2), Mereb-Gash (23,900 km^2) make up Ethiopia's contribution to the Nile waters (in which they cover more than 381,000 km^2 geographical area and more than 86% of the total Nile water). Its groundwater resources are insignificant with an estimated annual renewable potential of only 2.6 BCM when compared to surface water potential (MoWR, 1998).

In developing countries like Ethiopia, population growth often exceeds growth in food production; this deficit in food production is usually balanced by annual food aids donated by developed nations. Such dependency occurred because of natural causes, where conventional rain fed agriculture has become unreliable and the return from inputs applied is highly influenced by the moisture constraints that crop are facing at different growth stages. In order to have, sustainable development and to alleviate food insecurity, irrigated agriculture is going to play a vital role in agricultural development in Ethiopia and specifically Amhara Region.

The Amhara Region is dominated be rain-fed agriculture of the country where the mean annual rainfall exceeds at an average 1200mm in the highlands and middle altitudes. Blue Nile, Tekeze and Awash are the major river basins found in the region. About 80% of the region is drained with Blue Nile and the remaining (slightly less than 20%) is drained by Tekeze-Angerb and Awash main Basins and very few portion of the region is drained by the Afar Drainage Basins.

The region constitutes the major source of water in the country and Africa. Some studies indicate that the regional surface water potential is estimated to be 35 BCM, of which less than 2% is utilized for irrigation (ILRI, 2000).

In the Eastern part of the region moisture is relatively scarce and hence storage mechanisms shall be used to develop the available land potential through small-scale irrigated agriculture. Though moisture deficit is the major problem in the area there are more than 200 small streams flowing perennially and can be utilized for small-scale irrigated agricultural development (WWDSE, 1999).

Irrigation represents an alteration of the natural conditions of the landscape by extracting water from an available sources, adding water to fields where there was none or little before, and introducing man-made structures and features to extract, transfer and dispose of water. Irrigation projects and irrigated agriculture practices can impact the soil and water in a variety of ways.

The region has got considerable land potential for the development of both small-scale and medium and large scale irrigation agricultural developments. Land and Water Resources Inventory Report (Irrigation sub-sector 2004/5) indicate that there is well over 657,500 hectares of land suitable for irrigated agriculture; however, the area of land under irrigation so far is less than 12 percent of the potential.

Quality of irrigated agricultural land in Ethiopia and in particular in Amhara Region is deteriorating due to inappropriate planning, implementation and management of agricultural water. Desertification, salinization and water logging are reducing productivity and jeopardize in long-term sustainability. Wise management of the soil and water requires ability to forecast, monitor, measure and analyze environmental trends and the capabilities of land and water resources at different levels ranging from small-irrigated plots to large catchment's development. Generally any irrigation project, supply of excess irrigation water more than what is required, not only leads to wastage and leaching losses but also cause erosion and water logging, while crop growth is severely restricted if water supply is in sufficient.

As obtained from former Commission for Sustainable Agriculture and Environmental Rehabilitation in Amhara (Co-SAERA)

study reports, more than 10 earth dam and 45 diversion weir and traditional schemes were done in the region. However, as confirmed during field visit and gathering information from beneficiary farmers, resulting in non-sustainability of irrigation and drainage schemes are degradation of irrigation land (alkalinization, water logging and soil acidification), increased incidences water related disease, poor water quality (former Co-SAERAR socio-economic report, 1999, Bahir Dar). Therefore the purpose of the study was, to provide the necessary information to predict the soil and water related problems as consequences of irrigation practices undertaken at various irrigated command areas within Amhara region.

Therefore the study had the following objectives: Firstly we want to investigate main physical and chemical properties of soils of selected irrigation schemes. Secondly to assess the quality of irrigation water used in comparison with national and international water quality standards and finally the study would like to forward possible options to improve water management practices.

MATERIAL AND METHODS

Description of the study sites: The studies were conducted at three different administrative zones in the Amhara National Regional State, namely, West Gojjam, East Gojjam and Awi Zones. The study sites are Mendel and Tiqurit irrigation sites in West Gojjam (Tis-Abay woreda[1]), Jedeb is found in Machakel woreda 7 km West of Amanuel town at a distance of 23 km from Debre Markos to the way of to Bahir Dar and Geray is found in Jabi-tsehnan woreda 7 km from Finoteselam town. Fetam is located in Guangua woreda 5 km of Tilili town in Awi Zone.

Table 1. The study sites and their environment

Details	units	schemes				
		Geray	Jedeb	Fetam	Mendel	Tikurit
Command areas	Planned irrigated, ha	770	268	210	100	100
	Actual irrigated, ha	235(30.8%)	45(16.8%)	50(23.8%)	64(64%)	30(30%)
Rain fall	mm		850		900-1400	900-1400
Temperature	ºc		19		20	20
Altitude	masl	1875	2175	2321	1700	1750
Year of construction	In E.C.	1971-72	1985	1977	1979	1977
Number of beneficiaries	Family head	660	572	400	130	301

E.C= Ethiopian Calendar, Woreda[1] is equivalent to district

The sites are positioned on flat topography with moderate to imperfect drainage. The main parent materials were presented to be basalt, volcanic ash materials and some erosional deposits. The major crops grown are include, teff, wheat, Sugar cane, maize, onion, Garlic, potato, etc.

As it is mentioned on the above Table 1, in all command areas that had been planned to develop irrigation agriculture were 770, 268, 210, 100 and 100 hectares in Geray, Jedeb, Fetam, Mendel and Tiqurit respectively, however actual command areas are being irrigated are 30.4, 16.8, 23.8, 64 and 30 percents in Geray, Jedeb, Fetam, Mendel and Tiqurit respectively, therefore, it is clear that actual irrigated areas are being by far lower that what was actually planned. The reason for this could be planning problems as well as water management problems in the respective irrigation schemes.

The main factors that could have contributed to the problems why these schemes were lowered are: water shortage for dry season irrigation, seepage or percolation losses at head work and main canals and have no good irrigation performances, poor water management of the schemes (water logging and drainage problems), lack of awareness how to manage and control the schemes by beneficiary farmers and Yewuha Abat committees, etc.

Description of the soil profiles: Two representative pedons were dug on irrigated and non-irrigated areas adjacent to irrigated areas. The site was selected based on similarity of their topographic position, slope and soil type. Soil samples were collected depth-wise on the basis of observable differences.

Field observations, soil profiles (freshly dug pits) were described and the horizons were designated according to the guideline of FAO (1990). Soil color notation was according to Munsell color chart (KIS, 1994). Soil samples were collected from each genetic horizon of freshly dug pits. In general, disturbed and undisturbed soil samples were collected at all selected areas for laboratory analyses. The soil sampling started from the bottom of the pits up the profiles.

Physical and chemical analyses: Physical and chemical properties were determined on samples that were air dried, crushed, and sieved to pass ≤ 2mm. particle size was determined by hydrometer method (Boyuoucos,

1951); pH in 1:2.5 soil-water solution; organic carbon by wet digestion (Walkley- Black, 1934) and total N by Kjeldahl method (cottony, 1980). The available phosphorous content of the soil was determined by 0.5M sodium bicarbonate extraction solution (pH 8.5) method of Olsen as outlined by Van Reeuwijk (1993). Exchangeable cations content and the cation exchange capacity (CEC) of the soils were determined by the 1M ammonium acetate (pH7) method according to the percolation tube procedure (Van Reeuwijk, 1993) Base saturation was calculated by sum of exchangeable bases divided by the CEC and multiplied by 100. The CEC of clay was calculated by dividing the CEC by the clay% and multiplied by 100.

The infiltration rates were determined using the double ring infiltrometer method described in FAO soil Bulletin No.42 (1979). At each location the measurement site was pre-wetting on the afternoon preceding each test. This is normal procedure to avoid unrealistically high initial infiltration rates that can result from a test began on dry soils and to fill the cracks on soils with vertic properties. The bulk densities of the soils were determined using undisturbed cores samples collected. Samples were collected from the topsoil and subsoil and at approximately 50 cm and 100 cm depths.

RESULT AND DISCUSSION

Physical Properties

Soils of the study sites: All the studied soils except that of Fetam irrigation scheme have very deep profiles (>200 cm). As a whole, the soils in Mendel and Tiqurit manifested a high degree of similarity in morphology and physical characteristics. Invariably, they were clay in texture greater or equal to 58%, very deep, and uniform through the major part of the profiles which is attributed to marked pedoturbation resulting from the characteristic shrink-swell properties of the soils, with changes in moisture content, very hard, firm, very sticky and very plastic. The soils crack widely during the dry season, but the cracks close up again on rewetting. The resulting expansion and contraction is responsible for the formation of grooved shiny faces (slickenside) and wedge shape structures at depth (Photo1).

At Mendel and Tiqurit both at irrigated and non-irrigated command areas calcium carbonate nodules and concretions were

distributed throughout the profiles. The intensity of carbonates, whereby, increases with depth throughout the profiles. It was interesting to observe that at Mendel and Tiqurit sites carbonate precipitation were observed (Photo 2 & 3) along with the profile while Fe & Mn nodules were apparent in all profiles of Jedeb and Fetam schemes, which may be explained by intermittent anaerobic conditions caused by water logging as is evident from the imperfect drainage of the soils (Photo 4). By both bacterial and chemical action Fe and Mn and reduced to ferrous and managanous forms and become soluble and more mobile, where seasonal drying allows the re-oxidation of these materials, they are re-deposited as yellow and rusty' spots and streaks of ferric iron or as black manganese concretions (Crompton, 1967).

Photo 1. showing the nodules deep crack (Tiqurit)   **Photo 2**. Salt crystals (Tiqurit)   **Photo 3:** Calcareous (Mendel)

The soils in Jedeb, Geray and Fetam irrigated areas also have very deep and uniform profiles, however, the soils have different morphological characteristic which have not visible shrink-swell properties as compared Mendel and Tiqurit. As showed from Photo 4 the soils at Jedeb Having plinthite (Iron rich-it commonly occurs as red mottles) within 125 cm of the surface, showing gleyic and stagnic properties within 100 cm and 50 cm of the surface respectively, and showing ferric properties (Photo 4).

Photo 4: A soil profiles the Jedeb irrigation
site (visible Iron and Mn nodules)

Photo 5: profile description of Alisols

As presented above in Photo 5, soil profiles were dug at Alisols
have a brown ochric (to light in color) A-horizon, the surface soil
structure is rather weak, particularly where the organic matter content of
the A-horizon is low, the structure of the Bt (accumulation of clay)-
horizon is clearly more stable than that of the surface horizon(s), are
characterized by the presence of an argic B-horizon, a mixed clay
assemblage that is in a state of transition high aluminum levels in the
subsoil, & a general paucity of bases, for a description of the processes
of clay dispersion, clay transport and clay accumulation in an illuviation
horizons (Table 2).

As we have observed the irrigation schemes a water logging and drainage are the main problems in all study areas. The main causes of water logging in all schemes are flat topographic position, more clayey soils, poor drainage systems, and others management.

As shown below in Table 2, particle size distribution, on irrigated and non-irrigated command areas have not variations except Jedeb, Fetam and Mendel which shows minor differences. However, these variations are not strong enough to be emphasized here. Infiltration tests were carried out in the major soil units in the Mendel, Geray and Jedeb command areas and the result in irrigated sites were smaller than non-irrigated whereas measured bulk densities at irrigated command areas become larger and this shows more of compaction problems.

As indicated in Table 2, at Geray, Mendel and Tiqurit sites the infiltration tests results at irrigated command become slower than at non-irrigated command areas, this is might be due to clay texture however, at Jedeb infiltration result at irrigated site become faster and this is also related with soil textures. Generally optimum basic infiltration rates for surface irrigation are considered to in the range of 0.7 to 3.5 cm/hr, although an acceptable value normally rages from about 0.3 to 6.5cm/hr.

The bulk densities of at Geray, Jedeb, Fetam, Mendel and Tiqurit top soils at both irrigated and non-irrigated sites rages 1.02 g/cm^3 Tiqurit and 1.37 g/cm^3 at Mendel. Show variations between irrigated and non-irrigated schemes at irrigated areas the bulk density values become larger than non-irrigated sites this is might be due to effects of cultivation and other physical works.

Table 2. Some physical properties of the selected Schemes

Site name	Depth (cm)	Texture, %		Infiltration rate, cm/hrs		Bulk densities, g/cm^3	
		Irrigated	Non-irrigated	Irrigated	Non-irrigated	Irrigated	Non-irrigated
Geray	0-19	C	CL	1.3	2.3	1.14	1.1
	19-45	C	C				
	45-95	C	C				
	95-145	C	C				
	145-200	C	C				
Jedeb	0-15	SCL	C	3.6	2.1	1.21	1.29
	15-45	CL	C				
	45-95	SCL	C				
	95-145	SCL	-				
	145-200	CL	-				
Fetam	0-20	SL	L	-	-	1.26	1.2
	20-50	C	C				
Mendel	0-15	C	CL	1.1	1.4	1.37	1.22
	15-50	C	CL				
	50-110	C	CL				
	110-150	C	-				
	150-200	C	-				
Tikurit	0-20	C	-	1.3	2.5	1.1	1.02
	20-60	C	-				
	60-112	C	-				
	112-160	C	-				

Chemical Properties

Soil reaction (pH): As showed in Table 2, the soil pH increasing trends at all schemes at irrigated and non-irrigated sites. However, higher soil pH values at Mendel and Tikurit schemes ranges mildly alkaline to moderately alkaline and increasing trends along with the soil profile both irrigated and non-irrigated sites were observed, due to the corresponding increase in carbonates. While, other schemes showed that, Fetam become medium acid to slightly acidic, and Jedeb become very strong acid to slightly acidic. As indicated at Fetam and Jedeb acidity trends decreasing along the profiles.

Salinity (ECe, mmho/cm): As shown in Table 3 the electrical conductivity of the soils in all study schemes were very low and shows increasing tendency along the profile for Geray, Fetam, Mendel and

Tiqurit irrigated sites. The low EC values indicate that the total soluble salt content of the soils of the area is generally very low. It is therefore can concluded that a salinity effect is not critical problems for the time being in all irrigation sites.

Organic Carbon and Total Nitrogen: Total nitrogen contents in the cases of Geray and Tiqurit found to be in the range of low to very low in both irrigated and non-irrigated sites and shows decreasing trends along with the soil profiles (source: Booker Tropical soil Manual). In the case of Jedeb, and Fetam the nitrogen contents changes from low to very low at irrigated sites and medium to low at non-irrigated sites, however, the amounts N have decreasing trends along with the soil profiles, while in the case of Mendel even though the N content in irrigated site have very low and decreasing trends along with profiles in the case of non-irrigated site the trends become increased along with depth from medium to very high concentration (Table 3).

As indicated in Table 3, the results of OC at Geary showed low at irrigated and very low in non-irrigated sites and decreasing trends along with the profiles. In the case of Jedeb and Mendel the concentration at both irrigated and non-irrigated sites become very low at the surface and decreasing down with the profiles; however Fetam and Tiqurit decreases from low to very low for both irrigated and non-irrigated. As showed in the result Table 3, Fetam and Tiqurit are rich in organic carbon. Generally the organic carbon content of the schemes showed at regular decrease along with increasing soil depth.

Phosphorus content: As presented in Table 3, available P concentration is more in irrigated than non-irrigated sites, this might be P transported from the upper catchment along with sediments. In the case of Tiqurit since pH increases along with the profile the available phosphorus content decreases accordingly, this is may the presence of Ca, phosphate tends to be converted to calcium phosphate, and availability of P to plants is reduced, while the tendency in Mendel is the same regarding pH increases P content increases also along the depth, this can not be explained from our parts. In general the soils of Geray have high phosphorous contents as compared to soils in other soils such as Mendel, Tiqurit and Fetam. As observed P at Mendel especially at irrigated site and Jedeb at non-irrigated site become very low as stated by Olsen if P<5 ppm fertilizer responses are very important.

Table 3. Chemical characteristics of the schemes

Site Name	Depth (cm)	pH H2O 01:02.5		EC dS/m		T.N %		O.C %		C/N		Av. P. PPm (Olsen's	
		Irr.	N-irr.	Irr.	N-irr.	Irr.	N-irr	Irr.	N-irr.	Irr.	N-irr	Irr.	N-irr.
Geray	0-19	7.1	7.1	0.09	0.196	0.155	0.08	2.301	1.001	15	13	16.4	11.48
	19-45	6	7	0.055	0.054	0.069	0.077	0.897	0.624	13	8	0.44	0.6
	45-95	5.9	6.8	0.079	0.048	0.066	0.074	0.78	0.897	12	12	2.58	2.06
	95-145	6.5	6.9	0.064	0.038	0.06	0.033	0.39	0.293	7	9	3.58	2.04
	145-200	6.6	6.5	0.078	0.04	0.049	0.029	0.371	0.291	8	10	3.76	0.78
Jedeb	0-15	6.5	4.9	0.05	0.231	0.136	0.241	0.987	1.872	7	8	6.54	2
	15-45	6.5	5.9	0.04	0.075	0.105	0.175	0.722	1.307	7	7	5.58	1.54
	45-95	6.7	6.1	0.03	0.067	0.088	0.095	0.761	0.78	9	8	7.62	0.74
	95-145	6.4		0.04		0.072		0.56		8		7.02	
	145-200	6.5		0.05		0.034		0.237		7		7.7	
Fetam	0-20	6.1	5.9	0.02	0.015	0.17	0.349	2.75	3.179	16	9	11.28	7.1
	20-50	6.3	6.1	0.03	0.018	0.129	0.102	1.541	1.19	12	12	16.52	18.9
Mendel	0-15	6.7	7.1	0.121	0.471	0.066	0.644	0.936	0.644	14	9	3.32	10.44
	15-50	7	7.6	0.06	0.096	0.049	0.839	0.791	0.839	16	13	2.62	13.1
	50-110	7.6	7.9	0.089	0.086	0.042	1.443	0.429	1.443	10	10	6.56	16.3
	110-150	8.1		0.155		0.033		0.39		12		4.76	
	150-200	7.8		0.273		0.035		0.351		10		16.4	
Tikurit	0-20	7.5		0.278		0.149		2.243		15		11.36	
	20-60	8.1		0.151		0.057		0.878		15		4.38	
	60-112	8.8		0.598		0.04		0.585		15		3.32	
	112-160	9.4		0.907		0.034		0.488		14		trace	

324

Table 3. continued

Site Name	Depth (cm)	Na Irr	Na N-irr	K Irr	K N-irr	Ca Irr	Ca N-irr	Mg Irr	Mg N-irr	CEC Irr	CEC N-irr	Sum Ir.	Sum N-ir	BS % Irr.	BS % N-irr.	CEC of Clay Irr.	CEC of Clay N-irr.
		Exchangeable cations ----------------C mol(+)/Kg----------------															
Geray	0-19	0.39	0.89	0.9	1.29	5.51	6.08	2.71	2.55	21.4	31.8	9.51	10.8	44	34	48.64	88.33
	19-45	0.72	1.71	0.31	0.41	3.94	3.97	1.77	1.69	25	24.8	6.74	7.78	27	31	32.05	29.52
	45-95	2.32	2.1	0.31	0.61	3.23	4.43	1.73	1.69	24.2	23.6	7.59	8.84	31	37	31.03	27.44
	95-145	0.85	0.61	0.37	0.61	4.12	4.53	2.34	1.73	21.8	23.2	7.68	7.48	35	32.2	27.25	27.62
	145-200	2.21	1.87	0.31	0.63	3.23	3.33	2.81	1.4	20.4	19.4	8.56	7.22	42	37.2	24.29	23.1
Jedeb	0-15	0.01	0.12	0.63	0.36	2.18	10.1	4.86	4.28	28.4	42.8	7.68	14.84	27	34.68	101.43	91.06
	15-45	0.2	0.36	0.54	0.26	1.97	15.3	5.59	5.1	28.4	31.8	8.3	21.04	29.2	66.16	83.53	50.48
	45-95	0.34	0.36	0.5	0.27	14.92	24.8	5.76	9.13	29.4	39.2	21.52	34.56	73.2	88.16	105	60.31
	95-145	0.35	-	0.52	-	14.52	-	5.43		33.6	-	20.82	.	62	-	120	-
	145-200	0.21	-	0.58	-	14.47	-	5.84	.	31.8	-	21.1	.	66.5	-	106	-
Fetam	0-20	0.91	0.59	0.7	0.24	7.45	6	1.4	1.03	38.4	37.4	10.5	37.4	27	21	213.33	143.85
	20-50	1.65	0.39	0.52	0.29	6.32	5.19	1.44	1.03	35.6	29.2	9.93	29.2	28	24	74.17	48.67
Mendel	0-15	0	0.12	0.5	0.58	50.05	36.9	21.8	20.23	64.1	52.4	72.3	57.91	113	111	110.5	158.79
	15-50	0	0.12	0.61	0.63	51.9	36.9	17.3	20.07	68.6	50.6	69.8	57.7	102	114	114.3	174.48
	50-110	0.22	0	0.67	0.76	63.67	38	21	11.51	70	56.6	85.5	50.29	122	89	106.1	152.97
	110-150	0.54	-	0.78	-	55.74	-	16.9	-	71.6	-	73.9	-	103	-	108.5	-
	150-200	0.56	-	0.93	-	55.89	-	10.7	-	70.6	-	68.1	-	96	-	113.9	-
Tikurit	0-20	0.07	-	0.95	-	38.7	-	32.1	-	66	-	71.76	-	27	-	213.33	-
	20-60	1.54	-	0.6	-	35.1	-	32.1	-	71.6	-	69.29	-	28	-	74.17	-
	60-112	5.4	-	0.67	-	26.2	-	34.4	-	67.1	-	66.7	-	21	-	143.85	-
	112-160	9.11	-	0.72	-	5.64		46.1	-	58.1	-	61.52	-	24	-	48.67	-

325

The CEC and Exchangeable Cations

As indicated in Table 3 below, the Cations Exchangeable Capacity (CEC) of the schemes has the same trends in general. The CEC at Geray on irrigated ranges 21.4-24.2 $cmol_ckg^{-1}$ and non-irrigated ranged 31.8-19.4 $cmol_ckg^{-1}$. As indicated the distribution of CEC on irrigated site first increased from the surface down with the soil depth and decreased thereafter, however, at non-irrigated site shows decreasing trends along with the profile. The same is true for all other schemes (Table 3).

Exchangeable K ranged between 0.3-0.9 and 0.63- 1.29 $cmol_ckg^{-1}$ for irrigated and non-irrigated site at Geray, 0.5-0.63 and 0.27-0.36 $cmol_ckg^{-1}$ for irrigated and non-irrigated at Jedeb, 0.52-0.7 and 0.24-0.29 $cmol_ckg^{-1}$ for irrigated and non-irrigated at Fetam, 0.5-0.67 and 0.58-0.76 $cmol_ckg^{-1}$ for irrigated and non-irrigated at Mendel and 0.72-0.95 $cmol_ckg^{-1}$ for irrigated at Tiqurit. As shown in Table 3, it is clear that in Geray, Jedeb, Fetam and Tiqurit exchangeable K shows decreasing trends along with soil profiles both irrigated and non-irrigated sites except Fetam at non-irrigated shows increase trends along with soil depth. All schemes exhibited higher levels of exchangeable K than the range of 0.25-0.5 $cmol_ckg^{-1}$, which was indicated as a medium level by Metson (1956).

As obtained from the result, the exchangeable Ca in Geray irrigated (5.51-3.23 $cmol_ckg^{-1}$) and non-irrigated (6.08-3.33 $cmol_ckg^{-1}$), Fetam irrigated (7.45-6.32 $cmol_ckg^{-1}$) and non-irrigated (6.00-5.19 $cmol_ckg^{-1}$) and Tiqurit (38.7-5.64 $cmol_ckg^{-1}$) schemes were decreasing trends with along the soil profiles, whereas, at Jedeb in irrigated (2.18-14.92 $cmol_ckg^{-1}$) and non-irrigated (10.1-24.8 $cmol_ckg^{-1}$) as well as Mendel in irrigated (50.05-63.67 $cmol_ckg^{-1}$) & (36.9-38.0 $cmol_ckg^{-1}$) in non-irrigated sites exchangeable Ca shows that increasing trends along with the soil profile while as shown in Table 3, at Tiqurit exchangeable Ca at lower depth decreasing very much, on the other hand the exchangeable Na increase, the reason may be fixation of Ca with P and more soluble Na in the soil. The distribution of exchangeable Ca at Geray decreased from the plough layer to the third horizon and increases thereafter.

The exchangeable Na content of the soils regularly increases with increasing soil depth in irrigated and non-irrigated sites with some

inconsistency. This indicates that exchangeable Na is concentrated in the subsurface soils. However, the very low exchangeable sodium (Na) content of the soil at the surface in both irrigated and non-irrigated sites indicates that there is no sodicity problem in these soils.

Exchangeable Mg ranged between 1.73-2.71 and 1.69-2.55cmol$_c$kg^{-1} for irrigated and non-irrigated site at Geray, 4.86-5.43 and 4.28-9.13 cmol$_c$kg^{-1} for irrigated and non-irrigated at Jedeb, 1.40-1.44 and 1.03 cmol$_c$kg^{-1} for irrigated and non-irrigated at Fetam, 17.3-21.8 and 11.51-20.23 cmol$_c$kg^{-1} for irrigated and non-irrigated at Mendel and 32.1-46.1 cmol$_c$kg^{-1} for irrigated at Tiqurit. As shown in Table 3, it is clear that in Geray and Mendel shows decreasing trends from plough layer to the third horizon and increased afterward. At Jedeb, Fetam and Tiqurit exchangeable Mg shows increasing trends along with soil profiles both irrigated and non-irrigated sites except Jedeb exch. Mg on non-irrigated site shows decreasing trends along with soil depth. All schemes exhibited higher levels of exchangeable Mg than the range of 0.28-0.51 cmol$_c$kg^{-1}, which was indicated as a medium level by Metson (1956).

Generally the range of critical values (points above which crop response is not extracted and no fertilizer is recommended) for K, Ca and Mg is from, 0.25 to 0.5, 1.25 to 2.5, 0.25 to 0.5 and 0.28 to 0.51cmolc.kg^{-1} soils respectively (Sims, 2000).

The exchange complex of the soils is almost fully saturated with Ca and Mg as they are the main absorbed cations. In Mendel case, the sum of exchangeable cations is greater than the CEC within the soil profile, where as in Tiqurit case; the sum of exchangeable cations is greater only at the surface. This could be due to Ca and Mg extracted from free carbonates during determination. The presence of carbonate has been observed by dilute hydrochloric acid test in the field.

Percent base saturation (PBS) was very high at Mendel and Tiqurit. Its values decreased along with soil profile with few minor inconsistencies. The PBS values exceeding 100% in these studies indicates inflated condition. It could be due to underestimated CEC's of the soils which are calcareous. As has been discussed by Chapman (1965), calcareous soils present a problem with ammonium acetate method as a consequence of the solubility of $CaCO_3$, in the ammonium acetate solution giving lower values of CEC. This is because the dissolved Ca present in the NH_4OAC solution prevents complete saturations of the exchange positions with

ammonium. The above explanations, therefore, suggest for trying methods other than NH_4OAC to estimate the CEC of calcareous soils. The PBS at Fetam, Geray and Jedeb however, lower at the surface and increased down with soil profiles (Table 5).

 Irrigation Water Quality

As obtained from lab result electrical conductivity measurements of all samples areas are showed low salt concentration. As per of guideline for water quality for irrigation and drainage paper, FAO 29 showed that electrical conductivity of all sites is found within the low range, hence, salinity problems are not expected in the area for the time being. The study showed pH results at Jedeb, Fetam and Mendel were generally higher than in other sites. Potential impacts on crop yields may result from the exceedence of this irrigation guideline.

Table 4. Water quality analyses

S/No	Parameters	Site Names						
		Geray	Jedeb			Fetam	Mendel	Tikurit
			On diversion	Proposed Fish pond	Existing Fish pond			
1	Temp.0c	21.84	19.77	24.28	22.81	23.12	25.12	24.25
2	EC(mS/cm)	290.1	174.7	232.9	216.5	263.7	860.8	613
3	TDS, g/l	202.6	114	152.6	147.4	181.4	558.2	404.4
4	pH	6.52	7.75	8.56	9.45	8.61	8.65	8.11
5	DO, %	142.7	133	115.9	129.5	128.7	116	122.1
6	ORP	149.5	71.9	158.6	53.2	39.3	155.2	106.2

CONCLUSIONS

1. All the studied soils except that of Fetam irrigation scheme have very deep profiles (>200 cm). As a whole, the soils in Mendel and Tiqurit manifested a high degree of similarity in morphology and physical characteristics; they were clay in texture and calcium carbonate nodules and concretions were distributed and the intensity of carbonates, whereby, increases with depth throughout the profiles. These areas are located on the flat plain and receive water containing basic cations (Ca, Mg, K, Na), resulting in higher amount of cations compared with other schemes. Especially, in these schemes drainage, seasonal flooding as well as water logging problems were common,

the reason could be poor infiltration capacity of the soil due to clayey textured and flat topographic position of the areas.

2. Higher soil pH values at Mendel and Tikurit schemes and increasing trends along with the soil profile at both irrigated and non-irrigated sites were observed. The major effect of basic pH is to reduce the solubility of micronutrients like Fe, Zn, Cu and Mn. Also as shown in Table 3, phosphate at Tiqurit decreasing along with the soil profile and is often not readily available to some plants this is might be its precipitation in the soil solution by calcium or precipitation on solid calcium carbonate, while the exchangeable Na become increasing. While the pH measurement at the surface become acidic reaction at Jedeb and Fetam.

3. From the results discussed so far, it can thus be concluded that the studied areas have low to very low organic matter, total nitrogen, and low available phosphorous for high demanding crops.

RECOMMENDATIONS

1. Close follow-up and water management practice in the case of Mendel and Tiqurit and vertisols management, appropriate ploughing, and planting early and lately according to moisture requirement of crops is important to use vertisols and to improve their suitability for irrigated and rain-fed agriculture.

2. Introduction of appropriate deep drainage ditches and salt tolerant crops selection to control salinity problems in the case of Mendel and Tiqurit, whereas in the cases other schemes salinity would not be a problem rather acidity may be a problem so that close control and follow-up will be important.

3. Applications of organic and inorganic as well as nitrogen fertilizer are very crucial for plant growth in all schemes.

REFERENCES

Bouyoucus, C.J. 1951. A recalibration of the hydrometer method for making mechanical analysis of soils, Soil Science 59: 434-438
Cottenie, A. 1980. Soil and plant testing as a basis of fertilizer recommendations, FAO, Rome.

Crompton, E. 1967. Soil formation. In: Drew, J.V. 1967. Selected papers in soil formation and classification. Soil science society of America, Inc. Madison, Wisconsin, USA, pp3-15

Co-SAERAR socio-economic report on problem identification and need assessment, August, 1999. Bahir dar

Guidelines for water management and irrigation development, FAO water resources, development and management service, 1996

Metson, A.J. 1956. Methods of chemical analysis for soil survey samples. N.S.I.R. Bureau Bulletin 12

Martin L. Vander Schans, training consultant and Philippe Lemperiere, project coordinator. Manual on participatory rapid diagnosis and action planning of irrigated agricultural system (PRDA) - APPIA project, IWMI sub-regional office for the Nile Basin and Eastern Africa, Italy, Rome. FAO2006

Mitiku Haile. 1987. Genesis, characteristics and classification of soils of the Central highlands of Ethiopia. Volume I and II. Ph.D. thesis state university, Ghent. Belgium.

MunSell soil color charts, Macbeth Division of Kollmorgen instruments corporation 405 little Britain road, New Windsor, NY12553, 1994 revised edition

Raymond W. Miller/ Roy L. An introduction to soil and plant growth by Donahue prentice. Hall of India private limited New Delhi-110001, 1992

Regional Land and Water Resources Inventory (irrigation sub-sector 2004/5), March 2005, Bahir dar.

Soil- the Resources Base for survival, proceeding of second conference of ESSS 23-24 Sep,1993. AA, Ethiopia.

Technical problems identification and need assessment study for Geray irrigation project.

Unpublished study document on Employment generation in conservation based irrigation development, Co-SAERAR, 2002, Bahir dar

Walkley, A and C. A. Black. 1934. An examination of the Degtjareff method for determining soil organic matter, and a proposed modification of the chromic acid titration method. Soil Science 37: 29-38.

Water Works Design & Supervision Enterprise (WWDSE), V-4, sub-sector reports on irrigation development (draft final), Dec., 2001, Addis Ababa

FLOOD HAZARD AND RISK ASSESSMENT IN FOGERA WOREDA USING GIS & REMOTE SENSING

Dagnachew Legesse and Woubet Gashaw
Addis Ababa University (AAU), Earth Sciences Department, GIS and
Remote Sensing Program; P.O.Box: 150309, Addis Ababa, Ethiopia;
email: alem21st@yahoo.com

ABSTRACT

Fogera plain is one of the most severely flood affected areas in Northwest Ethiopia in general and the Lake Tana Catchment in particular. An attempt has been made to apply modern techniques of GIS and Remote Sensing for the assessment of flood hazard and risk in this plain. The flood causative factors were developed in the GIS and Remote Sensing environment and weighted and overplayed in the principle of pair wise comparison and Multicriteria Evaluation (MCE) techniques in order to arrive at flood hazard and risk mapping. Land use/cover change detection was done for the catchment using 1985 and 1999 Landsat images. Comparison between long year (1974-2006) annual maximum daily rainfall and annual maximum daily gauge levels (1971-2005) data of Ribb and Gumara rivers showed that rainfall slightly decreases while gauge level increases, and this can be attributed to land cover removal especially in the upper catchment. Flood frequency analysis was done using Ribb and Gumara Rivers annual maximum daily gauge levels by Gumbel's and Log-Pearson Type III methods, and the likely flood levels in different return periods were found. CHI square test showed that Gumbel's method was best fitted with observed data and therefore, DEM and the 100 year return period base flood from Gumbel's method were combined in the GIS environment in order to produce flood inundation maps. The major findings of the study revealed that most of the Peasant Associations (PAs) in the downstream part of the catchment and the different land uses in these areas are within high to very high flood hazard and risk levels. The presence of risk assessment mapping will help the concerned authorities to formulate their development strategies according to the inherent risk to the area.

Key Words: Flood Risk, MCE, GIS, Remote Sensing, Flood Frequency, Land use/cover Dynamics

INTRODUCTION

Topographically, Ethiopia is both a highland/mountainous and lowland country. It has nine major river basins, the drainage systems of which originate from the centrally situated highlands and make their way down to the peripheral or outlying lowlands. Especially during the rainy season (June-September), the major perennial rivers as well as their numerous tributaries forming the country's drainage systems carry their peak discharges.

The country experiences two types of floods: flash floods and river floods. Flash floods are the ones formed from excess rains falling on upstream watersheds and gush downstream with massive concentration, speed and force. Often, they are sudden and appear unnoticed. Therefore, such floods often result in a considerable toll; and the damage becomes especially pronounced and devastating when they pass across or along human settlements and infrastructure concentration. The recent incident (summer of 2006) that most of the country the Country experienced was typical of flash flood. On the other hand, much of the flood disasters in Ethiopia are attributed to rivers that overflow or burst their banks and inundate downstream plain lands. The flood that has recently assaulted Southern Omo Zone and South Gondar (mainly Fogera Woreda) Zone was a typical manifestation of river floods.

Therefore, owing to its topographic and altitudinal characteristics, flooding, as a natural phenomenon, is not new to Ethiopia. They have been occurring at different places and times with varying magnitude. Some parts of the country do face major flooding. Most prominent ones include: extensive plain fields surrounding Lake Tana and Gumara and Rib Rivers in Amhara Regional State; areas in Oromia and Afar Regional States that constitute the mid and downstream plains of the Awash River; places in Somali Regional State that fall mainly along downstream of the Wabishebelle, Genalle and Dawa Rivers; low-lying areas falling along Baro, Gilo and Akobo Rivers in Gambella Regional State; downstream areas of Omo River in the outhern Nations, Nationalities and Peoples Regional State (DPPA, 2006).

Fogera Woreda, which is located between $11^0 57'$ N and $12^0 30'$ N latitude & $37^0 35'$ E and $37^0 58'$ E longitude, is traditionally identified as one of flood prone areas of Ethiopia. This Woreda has an aerial extent of 1110 square kilometer and a total population of about 246541 of

which over 90% has rural setting. Elevation in the study area ranges from 1780 m to 2510 m and it has an average elevation of 1937 meter above mean sea level. The Woreda is drained by two major rivers, namely Ribb and Gumara. It totally lays in Ribb-Gumara Catchment, which is part of the Blue Nile Basin. This Catchment encloses big flat to gently sloping plains located in the administrative Zone of South Gondar, east side of Lake Tana. Fogera Woreda is particularly found in the downstream part of the above mentioned catchment.

Flood is probably the most devastating, widespread and frequent natural hazard of the world. This problem is more acute in highland areas like Ethiopia under strong environmental degradation due to population pressure. According to UNEP (2002), the major environmental disasters in Africa are recurrent droughts and floods. Their socio-economic and ecological impacts are devastating to African countries, because most of them do not have real time forecasting technology or resources for post-disaster rehabilitation. Although flood events are not new to Ethiopia, the country, in the 2006 main rainy season, was threatened by quite unprecedented flooding of abnormal magnitude and damage. Apparently, this is, for the large part, due to torrential or heavy rains falling for long days on the upstream highlands. The rains have caused most rivers to swell and overflow or breach their courses, submerging the surrounding 'flat' fields or floodplains, which are mostly located in the outlying pastoralist regions of the country. It is evident that the problem of river flooding in Ethiopia is getting more and more acute due to human intervention in the fragile highland areas at an ever-increasing scale. According to United Nation Office for the Coordination of Humanitarian Affaires (UNOCHA) (2006), across Ethiopia, the number of people affected by the floods of 2006 was 357,000, including 136,528 forced to abandon their homes. Ethiopia's northern Amhara region was the worst hit in the giant Horn of Africa nation, with 97,000 people affected, of which 37,000 lost their homes. The floods swamp large areas of cropped land in this region. Another survey conducted by the Joint Government and Humanitarian Partners Flash Appeal for the 2006 Flood Disaster in Ethiopia showed that in Amhara Region 40500 people were vulnerable, 47100 affected, and 5 were died by this year flood.

Geographic information system (GIS) is a computer-based system that provides the capabilities for input, data management (data storage and retrieval), manipulation and analysis, and output to handle georeferenced data (Aronoff, 1995). GIS provides a broad range of tools

for determining area affected by floods and for forecasting areas that are likely to be flooded due to high water level in a river. GIS was extensively used to assemble information from different maps, aerial photographs, satellite images and digital elevation models (DEM). Census data and other relevant statistical abstract was also used to make the risk map more oriented to need of the local inhabitants.

Remote sensing is the science and art of acquiring information (spectral, spatial, and temporal) about material objects, or area, without coming in to physical contact with the objects or areas, under investigation (Lillesand, 2004). Remote sensing technology along with GIS has become the key tool for flood monitoring in recent years. The central focus in this field revolves around delineation of flood zones and preparation of flood hazard and risk maps for the vulnerable areas. River flooding in the developing countries of Africa is very acute because of their heavy dependence on agriculture but any flood estimation or hazard mapping attempt in this region is handicapped by poor availability of high resolution DEMs. Flood Hazard Mapping is a vital component for appropriate landuse planning in flood-prone areas. It creates easily read, rapidly accessible charts and maps, which facilitates the administrators and planners to identify areas of risk and prioritize their mitigation/response efforts.

Overflow of Ribb and Gumara Rivers and backflow of Lake Tana has affected and displaced 43127 and 8728 people respectively in Fogera Woreda in this summer (UNOCHA, 2006). Some people said that several months of excessive rain has flooded rivers and stranded families in low-lying areas. While others said it is severe environmental degradation of specially the highlands that cause floods of this Woreda. This issue needs research in order to design long-lasting solutions for the safety of the population and the natural environment as well.

The regulation of flood hazard areas coupled with enactment and enforcement of flood hazard zoning could prevent damage of life and property from flooding in short term as well as in long term. Flood management and control are necessary not only because floods impose a curse on the society, but the optimal exploitation of the land and proper management and control of water resources are of vital importance for bringing prosperity in the predominantly agricultural based economy of this highly populated Woreda. This cannot become technically feasible without effective flood hazard and risk mapping. Flood risk mapping is

the vital component in flood mitigation measures and landuse planning. This study attempts to synthesize the relevant database in a spatial framework to evolve a flood risk map for Fogera Woreda in particular and flood hazard map of Ribb and Gumara Catchment in general with the application of MCE technique. Basic aim of this effort is to identify the area chronically suffering from flooding and creates a flood hazard and risk maps based on topographical, meteorological, hydrological, and socioeconomic data. The study has also focused on the identification of factors controlling flood hazard in the study area. A flood risk map based on administrative units is particularly handy for the planners and administrators for formulating remedial strategy. It also makes the process of resource allocation simple resulting in a smooth and effective implementation of the adopted flood management strategy.

MATERIALS AND METHODS

Study Area

Ribb-Gumara Catchment, drained by Ribb and Gumara Rivers, is located between $11^0 43$'N & $11^0 53$'N Latitude and $37^0 47$' E & $37^0 54$' E Longitude (Figure 1). This catchment is part of the Nile Basin and more particularly part of that of the Lake Tana Basin located on the Northeastern side of Lake Tana. It has an areal extent of about 3320 square kilometers. Fogera Woreda, which has an area of 1110 square kilometers, totally lies in this Catchment. This Woreda is found in the down stream part of the Catchment where Ribb and Gumara Rivers join to Lake Tana. Overflow of these rivers and back flow of Lake Tana frequently flooded this Woreda than other woredas in the Catchment, and therefore selected for detailed flood risk study.

Gumara River, which is found at 13 km from Woreta Town (headquarter of Fogera Woreda), has its source in Mogishe Kidane Mihiret kebele, Farta Woreda. Guna Mountain in Farta Woreda is the source of Ribb River which crosses the main Bahir Dar-Gondar road at 10 km from Woreta Town. As explained above, in their lower reaches, these rivers flow through a large flat to very gentle sloping plain which is exposed to serious floods.
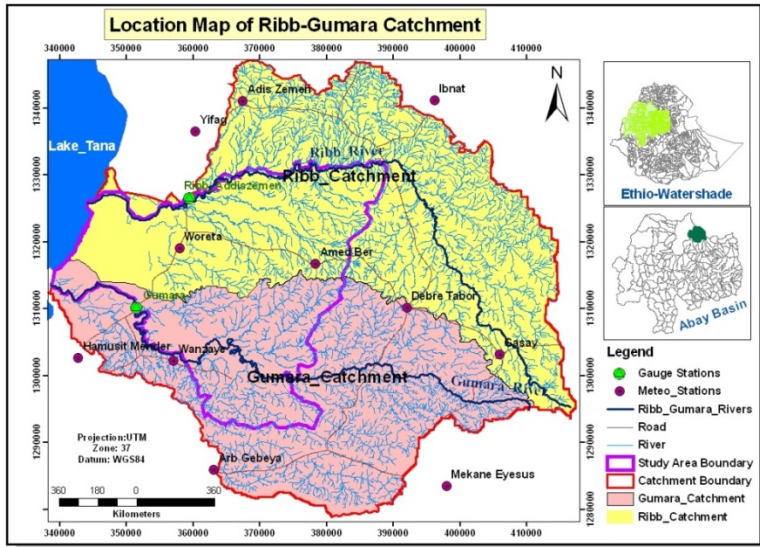
Figure 1. Location Map of Ribb-Gumara Catchment

Fogera Woreda lies to the south-eastern shore of Lake Tana on the road from Bahir Dar to Gondar, 625 km from Addis Ababa and 55 km north of the Regional capital of Bahir Dar. It is one of the 105 woredas in the Amhara National Regional State of Ethiopia and located at its center. The major towns in Fogera Woreda are Woreta and Amed Ber, the former being the head quarter of the Woreda and it has twenty-five Peasant Associations (PAs) or Kebeles and 1 urban Kebele. The area is located between 11° 57' N and $12^0 30$' N latitude and 37° 35' E and $37^0 58$' E longitude (Figure 1). The study area has a very flat land, which is known by the Fogera plane, adjacent to the eastern coast of Lake Tana. Altitude ranges from 1780 m to 2510 m. Total annual rainfall ranges from about 1100 mm to 1530 mm/year. The spatial distribution of rainfall showed that Eastern and Central part of the Woreda receive highest rainfall while the northern portion receives the lowest. The seasonal rainfall has a Unimodal distribution with peak in July. This is the 'Meher' season and it receives about 70% of the annual rainfall. The mean annual rainfall is 1430 mm and mean monthly values varies between 0.6 mm (January) and 415.8 mm (July), which indicate poor temporal distribution of rainfall. The mean monthly temperature of the area is about 19 ^{0}C, monthly mean maximum temperature is about 27.3 ^{0}C, and monthly mean minimum temperature is 11.5 ^{0}C. The major soil types in Fogera Woreda exhibit a general relationship with altitude and

336

slopes. Vertisols and Fluvisols are generally dominating the Woreda and particularly the lowland flat plains, valley bottoms and river terraces. Texturally these soils are sandy clay and sandy loam respectively. Shallow Leptisols are the dominant soil types found in the mountain and hills of the study area. Luvisols dominate the southern and central part of the Woreda. There have been many destructive floods in Fogera Woreda, including very severe floods of 1996, 1998, 1999, 2000, 2001, 2003 and 2006 (Shiferaw and Wondafrash, 2006). The 1996 flood set a new record for flooded area, while 2006 flood was unprecedented with its long duration and damage.

Data Collection and Software Used

Contour (20m interval) was digitized from 1:50000 scale Topographic map obtained from Ethiopian Mapping Authority (EMA). Drainage networks were also digitized from this topographic map. Annual maximum daily gauge level data (1971-2005) of Ribb and Gumara rivers at Ribb-Addiszemen and Gumara Gauge Stations respectively was obtained from Ministry of Water Resources (MoWR). Annual maximum daily rainfall records (1974-2006) from eleven meteorological stations in and around the catchment were collected from National Meteorological Agency (NMA). Soil type shape file was obtained from Endaweke (2007), and Fogera Woreda boundary was obtained from Ethiopian Livestock Research Institute (ELRI) and converted to digital format by digitization. The 1999 Population record of the Woreda was gathered from Fogera Woreda office of Agriculture and Rural development (FWOARD). Landsat images of November 23, 1985 and October 09, 1999 were downloaded from American Global Land Cover Facilities (GLCF) website. Finally, ground truths of the 2006 flood damage and accuracy assessment points were collected with GPS in the field.

Software used in this study was selected based on the capability to work on the existing problems in achieving the predetermined objectives. First and for most, Arc Hydro 9 software, which works as an extension on ArcGIS 9.0 and above version software, was used to delineate the watershed for which flood hazard analysis was done. MS Excel was used for the flood frequency analysis. ERDAS 8.7 was used for image processing activities on satellite images. ENVI 4.2 was used to compute change detection analysis on Landuse/Landcover map of classified images and to do accuracy assessment. The factor map

development was carried out using ArcGIS 9.1 software package. The factors that are input to for multi-criteria analysis should be pre-processed in accordance to the criteria set to develop flood hazard and risk analysis. So, using Spatial Analyst, 3D Analyst and Geostatistical Analyst extensions, some relevant GIS analyses were undertaken to convert the collected shape files. Eigen vector for the selected factor was computed using Weight module in IDRISI 32 software.

Methodology

Landcover mapping requires the use of other interpretation elements than just reflectance, particularly positioned in the landscape, with size and association. In addition, knowledge of the landuse systems and their extent is essential for attributing spectral reflectance curves to landcover types.

Since the same spectral reflectance curve can represent a variety of landcover types, ground information is essential. Ground information is also needed to determine other landcover characteristics (interpretation elements) such as associations, landscape position, etc. Field visits were consequently undertaken as early as possible in the mapping of the study sites. The principal aim of the field visit was to understand the image representation of the ground information; to learn what all the image and patterns represent, although areas of uncertainty will always be discovered later. This method was previously used to interpret aerial photography – rather than the black box approach whereby ground information is only recognized from specific training areas.

Flood risk of the Woreda was analyzed from the following general risk equation (Shook, 1997).

Risk = (Elements at risk) * (Hazard * Vulnerability)...………..equation (1)

The flood hazard analysis was computed using MCE. To run MCE, the selected flood causative factors such as slope, soil type, elevation, landuse/cover, drainage density, and rainfall were developed and weighted. Then weighted overlay technique was computed in ArcGIS 9.1 Model Builder to generate flood hazard map. Considering the degree of loss to be total for the study area, the vulnerability is assumed to be one. Finally to generate flood risk map of the Woreda, elements at risk layer (population density and landuse) and the flood

hazard map were overlaid using weighted overlay analysis technique in ArcGIS 9.1 environment.

Flood frequency analysis is one of the important studies of river hydrology. It is essential to interpret the past record of flood events in order to evaluate future possibilities of such occurrences. The estimation of the frequencies of flood is essential for the quantitative assessment of the flood problem. The knowledge of magnitude and probable frequency of such recurrence is also required for proper design and location of hydraulic structures and for other allied studies. The gauge data which are random variable follow the law of statistical distribution. After a detailed study of the distribution of the random variables and its parameters such as standard deviation, skewness etc. and applying probability theory, one can reasonably predict the probability of occurrence of any major flood events in terms of discharge or water level for a specified return period.

Flood frequency analysis was done in this study by selecting annual maximum daily gauge levels at Ribb-Addiszemen and Gumara gauge site located in the catchment area. Two methods of statistical distribution i.e. Gumbel's extreme value distribution and Log Pearson type III distribution were attempted by selecting peak gauge level data for 35 years (1971-2005) at the two catchments above.

Gumbel's Method:

This extreme value distribution was introduced by Gumbel (1954) and is commonly known as Gumbel's distribution (R. Suresh, 2005). It is one of the most widely used probability analysis for extreme values in hydrologic and meteorological studies for prediction of flood, rainfall etc.

Gumbel defined a flood as the largest of the 365 daily flows and the annual series of flood flows constitute a series of largest values of flows. This study attempt to find out water levels at different return period using the Gumbel's equation:

$$x_T = x + k * SDV, ,\ldots\ldots\ldots\ldots\ldots\ldots\ldots\ldots\text{equation (2)}$$

where

x_T = Value of variate with a return period 'T'

x_{avg} = Mean of the variate

SDV = Standard deviation of the sample

k = Frequency factor expressed as

$$k = (y_T - 0.577) / 1.2825 \ldots\ldots\ldots\ldots\ldots\text{equation (3)}$$

y_T=Reduced variate expressed by

$$(y_T) / (T - 1) = -(LN*LN)\ldots\ldots\ldots\ldots\text{equation (4)}$$

T =Return period

Log Pearson Type - III Method:

This method is extensively used in USA for project sponsored by US Government. In this method, the variate is first transformed into logarithmic form (base10) and the transformed data is then analyzed (Chow, 1988). If 'X' is the variate of a random hydrologic series, then the series of 'Z' variates where z = log x are first obtained. For this 'z' series, for any recurrence interval "T", the equation is:

$$z_T=z_{avg}+Kz* SDV\ldots\ldots\ldots\ldots\ldots\ldots\ldots\ldots\text{equation (5)}$$

Where,

K_z = Frequency factor taken from table with values of coefficient of skew "Cs" and
    recurrence interval 'T'.

SDV = Standard deviation of the 'Z' variate sample.

Cs = Co-efficient of skew of variate 'Z'

$$=\{ N \Sigma (z - z_{avg})3 \} / \{ (N - 1) (N - 2) (SDV)3 \}\ldots\ldots\text{equation (6)}$$

z_{avg} = Mean of the 'z' values

N = Sample size = Number of years of record

After finding 'z_T' with the equation above, the corresponding value of 'x_T' is obtained by

$$x_T = \text{Antilog}(z_T)\ldots\ldots\ldots\ldots\ldots\ldots\ldots\ldots\ldots\text{equation (7)}$$

After obtaining gauge levels by the above two methods for different return period flood, Chi
Square test was carried out for "goodness of fit".

Recurrence Interval can be calculated as $(n+1)/m$,…………equation (8)

where
        n is number of samples (years), and
        m-rank of a given gauge level.

Data Processing and Analysis

Database Design

The geographic database (geodatabase) is a core geographic information model to organize a spatial data in to thematic layers and spatial representations. Two types of geodatabase architectures are available under ESRI's ArcGIS package: Personal Geodatabase and Multiuser Geodatabase. In this study, personal geodatabase was implemented to store the necessary data that could be applicable to the final analysis for the designed objectives.

Landuse/Landcover Analysis

The 1973 MSS, 1985 TM and 1999 ETM Landsat images were used "to define the different classes of land cover types (WBISPP, 2004)" and there by for the landuse/cover change detection.

Supervised image classification which is a widely used technique (Sluiter, 2005); (Nangendo, 2005) was applied in this study. Accordingly, the three landuse/cover maps of the year 1973 (Figure 2(a)), 1985 (Figure 2(b)) and 1999 (Figure 2 (c)) were generated using the widely used maximum likelihood classifier algorithm (Lillesand et al.,2004).
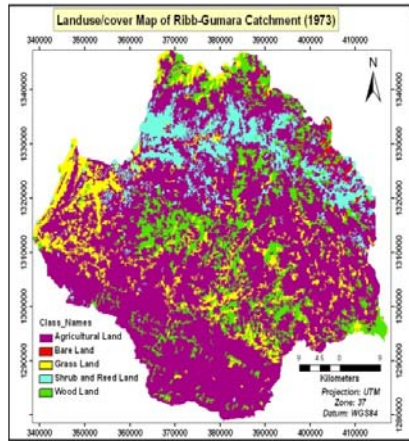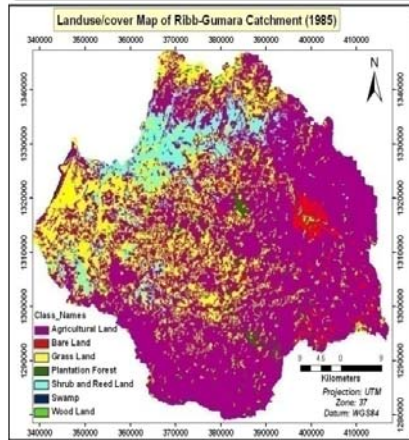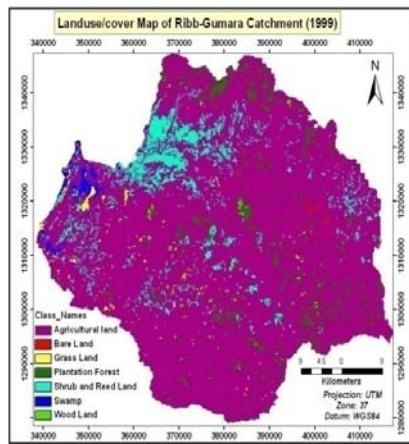
Figure 2. Landuse/cover Maps of Ribb-Gumara Catchment (a=1973; b=1985; & c=1999)

ACCURACY ASSESSMENT

The ground truth data were utilized in the maximum likelihood report as the independent data set from which the classification accuracy was compared. The accuracy is essentially a measure of how many ground truth pixels were classified correctly. An overall accuracy of *87.63% was* achieved with a Kappa coefficient of *0.8402* for Landsat 1999 ETM image. The overall accuracy is a similar average with the accuracy of each class weighted by the proportion of test samples for that class in the total training or testing sets. Thus, the overall accuracy is a more accurate estimate of accuracy. The Kappa coefficient represents the proportion of agreement obtained after removing the proportion of agreement that could be expected to occur by chance (Leica Geosystem, 2000). This implies that the Kappa value of 0.8402 represents a probable 84.02% better accuracy than if the classification resulted from a random, unsupervised, assignment instead of the employed maximum likelihood classification. Kappa values are characterized into 3 groupings: a value greater than 0.80 (80%) represents strong agreement, a value between 0.40 and 0.80 (40 to 80%) represents moderate agreement, and a value below 0.40 (40%) represents poor agreement (Leica Geosystem, 2000). Therefore, the classification in this study meets the specified requirement.

Factor Development

Flood causative factors particularly in the study area were identified from field survey, and literature. Accordingly slope, soil type, elevation, landuse type, drainage density, and rainfall were listed in order of importance. The factors were developed in the following assumptions. Slope has a great influence on flood hazard. The flatter the slope, the higher will be the probability of the area to be inundated. Soils of the catchment were converted to raster format and reclassified based on their water infiltration capacity. The lower the elevation, the higher will be its vulnerability to flooding. Landuse/cover types of the catchment were reclassified into a common scale in order of their rainwater abstraction capacities for the flood hazard analysis, while that of the Woreda were reclassified in order of their vulnerability to flooding. Drainage density was reclassified in the assumption that the denser the drainage network in a given area the higher will be the flood hazard. Flood hazard and risk assessment requires an areal rainfall intensity data. However, NMA only provides point rainfall data. In addition, even though rainfall intensity

was the best data for flood hazard analysis, this type of data was not available for most of the Meteorological stations in Ethiopia; and therefore annual maximum daily rainfall was used. This data was changed in to rainfall surface using ordinary kriging in the Geostatistical extension of ArcGIS 9.1 environment. Rainfall surface was reclassified in to common scale in the assumption that the higher the annual maximum daily rainfall amount the higher the flood hazard will be. Population density was reclassified in the assumption that the denser the population the more vulnerable it will be to flood hazard. Standardized values of each factor in the reclassification process were listed in Table 1 and 2 below.

Flood Hazard Analysis

MCE technique was used to assess flood hazard of the Catchment using GIS. MCE is a procedure which needs several criteria to be evaluated to meet a specific objective. It is most commonly achieved by one of two procedures. The first involves Boolean overlay whereby all criteria are reduced to logical statements of suitability and then combined by means of one or more logical operators such as intersection (AND) and union (OR). The second procedure which was used in the study is known as weighted linear combination (WLC) where continuous criteria (factors) were standardized to a common data model that was raster layer with a resolution of 30 m cell size, and then combined by means of a weighted overlay. The result is a continuous mapping of flood hazard and finally thresholded to yield a final decision.

The standardized raster layers were weighted using Eigen vector that is important to show the importance of each factor as compared to each other in the contribution of flood hazard. Accordingly, the Eigen vector of the weight of the factors was computed in IDRISI 32 software in Analysis menu Decision Support/Weight module. The Weight module was fed with the pair wise comparison matrix file of the factors in a Pair wise comparison 9 Point continuous scale. And the principal eigenvector of the pair wise comparison matrix using the factors affecting flood hazard was calculated. It was found that the Consistency Ratio to be 0.02, which is acceptable. The computed Eigen vector was used as a coefficient for the respective factor maps to be combined in Weighted Overlay in ArcGIS environment.

Table 2. Scaled and waited flood hazard inducing factors

Factor	Weight	Sub-Factor	Scale (Hazard)
1. Slope (Percent)	0.2690	0 –0.9	5 (Very High)
		0.9 – 6.4	4 (High)
		6.4 – 12.8	3 (Moderate)
		12.8 – 22.8	2 (Low)
		22.8 – 88.9	1 (Very Low)
2. Soil (based on drainage capacity)	0.1793	Eutric Vertisols	5 (Very High)
		Eutric Fluvisols	4 (High)
		Haplic Luvisols	3 (Moderate)
		Chromic Luvisols	2 (Low)
		Eutric Leptosols	1 (Very Low)
3. Elevation (meter)	0.0860	1780 – 2240	5 (Very High)
		2240 – 2700	4 (High)
		2700 – 3160	3 (Moderate)
		3160 – 3620	2 (Low)
		3620 - 4080	1 (Very Low)
4. Land use (Level of flood abstraction)	0.0562	Swamp	5 (Very High)
		Agriculture/Bare land	4 (High)
		Grass Land	3 (Moderate)
		Wood & Shrub land	2 (Low)
		Plantation Forest	1 (Very Low)
5. Drainage density (Km/Sq. Km)	0.3712	0 – 0.7	5 (Very High)
		0.7 – 1.4	4 (High)
		1.4 – 2.1	3 (Moderate)
		2.1 – 2.8	2 (Low)
		2.8 – 3.5	1 (Very Low)
6. Daily Max Rainfall (mm)	0.0383	76.9 - 70.5	5 (Very High)
		70. 5-64.0	4 (High)
		64. 0 -57.5	3 (Moderate)
		57.5 -51.1	2 (Low)
		51. 1 -44.6	1 (Very Low)

Flood Risk Analysis

As the flood hazard result of the catchment revealed in the next section, all of the very high and high hazard areas of the Catchment fall in Fogera Woreda. Therefore, it is found important to do the flood risk assessment for this Woreda. Flood risk assessment was done for Fogera Woreda using the flood hazard layer and the two elements at risk, namely population and landuse. Vulnerability was assumed to be one. These three factors remained to be equally important in the Weighted Overlay process (Table 2).

Table 2. Scaled and weighted flood risk analysis factors

Factors	Weight	Sub-factors	Scale (Risk)
1. Flood hazard	0.3333	very high high moderate low very low	5 (Very High) 4 (High) 3 (Moderate) 2 (Low) 1 (Very Low)
2. Population density (person/Sq. km)	0.3333	2396-400 400-225 225-200 200-175 175-149	5 (Very High) 4 (High) 3 (Moderate) 2 (Low) 1 (Very Low)
3. Land use types (based on their sensitivity to flooding)	0.3333	Agriculture Grass Land/Bare land Swamp Plantation Forest Wood & Shrub land	5 (Very High) 4 (High) 3 (Moderate) 2 (Low) 1 (Very Low)

Flood Frequency Analysis

Hydrologic systems are sometimes impacted by extreme events, such as severe storms, floods and droughts. The magnitude of an extreme event is inversely related to its frequency of occurrence, very extreme events occurring less frequently than more moderate events. According to Chow (1988), the probability of occurrence of an event in any observation is the inverse of its return period; $P(X>=X_T) = {}^1/_T$.

The objective of frequency analysis of hydrologic data is to relate the magnitude of extreme events to their frequency of occurrence through the use of probability distributions. The hydrologic data analyzed are assumed to be independent and identically distributed, and the hydrologic system producing them (e.g., a storm rainfall system) is considered to be stochastic, space-independent, and time-independent (Chow et al., 1988). The hydrologic data employed should be carefully selected so that the assumptions of independence and identical distribution are satisfied. In practice, this is often achieved by selecting the annual maximum of the variable being analyzed (e.g., the annual maximum discharge, which is the largest instantaneous peak flow occurring at any time during the year) with the expectation that successive observations of this variable from year to year will be independent. The result of flood frequency analysis can be used for many engineering purposes: for the design of dams, brides, culverts, and flood control structures; to determine the economic values of flood control projects; and to determine flood plains and determine the effect of encroachments on the flood plain.

Flood frequency analysis in this study was done using annual maximum daily gauge level data at Ribb-Addiszemen and Gumara gauge stations (1971-2005). Ribb-Addiszemen gauge station is located at $12^00'$ N latitude and $37^043'$ E longitude, and has elevation 1795 m amsl, while that of Gumara is $11^050'$ N latitude and $37^038'$ E longitude, and 1800m amsl. Flood frequency calculations were done using the Gumbel's and Log-Pearson Type III methods. CHI Square Test was conducted to test the best fit method to observed data. Using the 100 year base flood level of the best fit distribution, areas that are likely to be inundated in case of embankment failure of the two rivers were mapped. All the neighborhood pixels in the DEM which has an elevation lower or equal to the specified flood levels were marked likely to be inundated using the

Spatial Analyst (Map Calculator) extension of ArcGIS 9.1 software. This result was compared with the result of the flood hazard map done through overlay process of other topographic and meteorological flood causative factors.

RESULT AND DISCUSSION

Flood Hazard

The flood hazard maps (Figure 3 (a and b) below shows that 192.8, 502.7, 547.2, 1099.7, 974.3 square kilometer of Ribb-Gumara Catchment, and 141.6, 178.8, 324.3, 355.7, 108.8 square kilometer area of Fogera Woreda were subjected respectively to very high, high, moderate, low and very low flood hazards.

About three-fourth of areas of the catchment under very high flood hazard fall in Fogera Woreda while this Woreda is only one-third of the catchment. PAs with more than three-fourth of their areas fall under high and very high flood hazard include Wagtera (100%), Nabega (99.6%), Kidiste Hana (98.9%), Shina (93.1%), and Shaga (92.2%). All of these areas lie in the downstream part of Ribb and Gumara Rivers where they join to Lake Tana. Further analysis revealed that 99.7% swamps, 93.8% grass lands, 27.9% shrub lands, and 24.1% Agricultural lands fall under high to very high flood hazard.
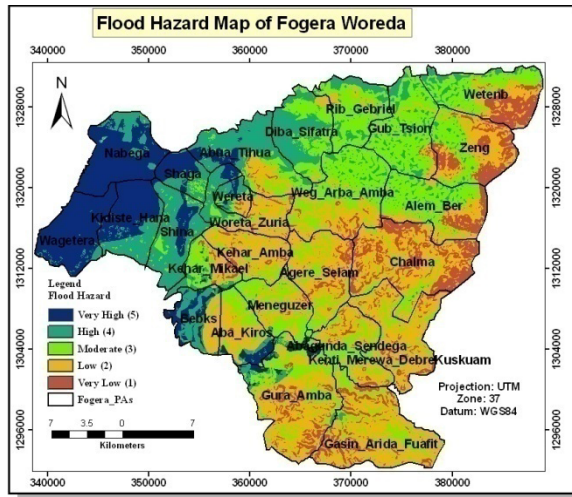

(a)

Flood Hazard Map of Fogera Woreda

(b)
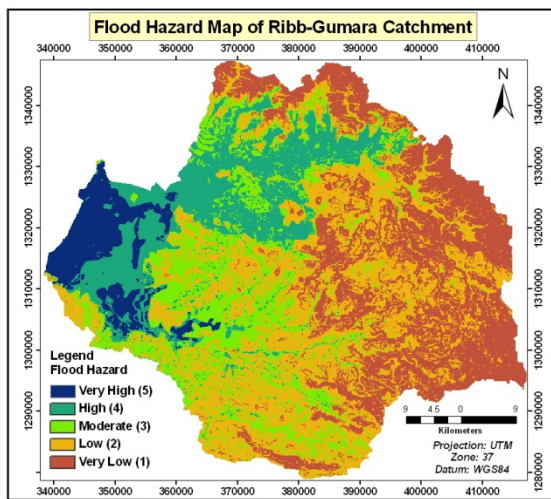
Figure 3. (a) Flood Hazard Map of Ribb-Gumara Catchment,
and (b) Fogera Woreda

Flood Risk

Flood risk assessment and mapping was done for Fogera Woreda
by taking population and landuse/landcover elements that are at risk
combined with the degree of flood hazards of the Woreda.

According to the flood risk map (Figure 4), it was estimated that
40.1, 165.5, 331.3, 385.8 and 186.4 square kilometre areas of Fogera
Woreda were subjected respectively to very high, high, moderate, low,
and very low flood risk.

Elements at risk considered in this study show different levels of
risk. PAs that are about half of their area under flood risk include
Wagtera (96.1%), Shaga (90.3%), Nabega (87.5%), Woreta (65.2%),
Bebks (55.8%), Kidiste Hana (53.3%), Shina (49.4%), and Abua Thua
(47.15). With regard to the other element at risk, landuse/landcover,
81.8% swamps, 81.6% grass lands, 12.8% agricultural lands are under
high to very low flood risk.

The 2006 flood worst hit PAs of Fogera Woreda are among the
above PAs that are under flood risk. Therefore, the result was in

349

agreement with the reality that is going on in the study area. Specifically, results were compared with ground truth data of the 2006 flood disaster damaged areas which were collected with GPS during field survey. All these damaged schools, water pumps, crops, and so on fall in the high to very high flood risk areas of the flood risk map of this study. In addition, the above PAs have been traditionally identified as flood prone areas.
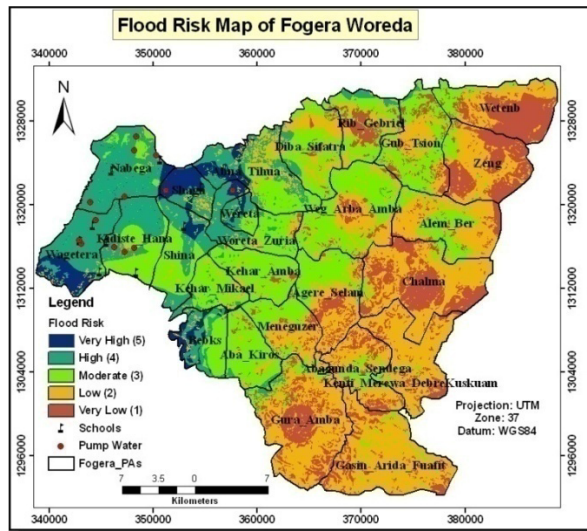

Figure 4. Flood Risk Map of the Study Area

Flood Frequency

By using Gumbel's Method, the calculated Gauge levels of Gumara River for 2, 10, 25, 50 and 100 year return period flood were 5.900 m, 7.091 m, 7.685 m, 8.147 m, and 8.582 m respectively while that of Ribb-Addiszemen were 6.806 m, 7.714 m, 8.166 m, 8.518 m, and 8.85 m respectively. The same gauge data was then analyzed by Log-Pearson Type III Method and gauge levels obtained for 2, 10, 25, 50 and 100 year return period flood for Gumara are 6.075 m, 7.06 m, 7.369 m, 7.553 m, and 7.706 m respectively, while that of Ribb are 7.016 m, 7.604 m, 7.731 m, 7.793 m, and 7.836 m respectively.

The Chi square test comparing computed values with observed values was carried out to find the best fit method and Gumbel's method was found to be the best fit for both rivers. That is, this method was with

the lower CHI Square value than the Log-Pearson Type III method (0.081 Vs 0.519 for Gumara River, and 0.055 Vs 0.860 for Ribb). Therefore, inundation area mapping was done using the Gumbel's method 100 year return period base flood result.

An 8.582 m gauge level in Gumara River is expected to occur in every 100 year while that of the Ribb is 8.850 m. In other words, the probability of occurrence of an 8.582 m gauge level in Gumara River in a given year is 1/100 or (1%), while with this probability, an 8.85 m gauge level is expected in Ribb River. In Gumara, a 5.900 m gauge level has a 50% probability to occur in any year while in Ribb 6.806 m gauge level is expected with the same probability.

From the Gumbel's distribution result, given the same return periods, gauge levels for Ribb River were found to be a bit greater than that of Gumara (Table 3). This is because, river density in the Ribb catchment is relatively greater than that of Gumara and again Ribb has more perennial tributaries than that of Gumara.

Table 3. Gauge Levels for Selected Return Periods

Return Period	Gauge Level (m)	
	Gumara	Ribb-Addiszemen
2	5.900	6.806
5	6.616	7.352
10	7.091	7.714
25	7.685	8.166
50	8.147	8.518
100	8.582	8.850

As discussed previously, in times of embankment failure, inundation will occur in the areas that have an elevation lower than the gauge level and that are connected with the location of the embankment failure. In this study, the 100 year gauge level, which is considered as base flood or project flood, from Gumbel's method for the Ribb and Gumara rivers were taken to map the likely inundation areas in the two respective catchments (Figure 5a and 5b). These flood maps were merged in the GIS environment so as to see their aggregate effects in the Ribb-Gumara Catchment in general and Fogera Woreda in particular. This map was crossed with the maps of elements at risk in Fogera

Woreda to see its impact on the elements at risk. The quality of the DEM highly limited the inundated area mapping for other return periods. The difference in gauge level between the two year and hundred year return periods was calculated as 2.682 m (Gumara) and 2.044 m (Ribb), while the DEM was developed from a 20 m interval contour, therefore failed to show different inundated area maps for different return periods.
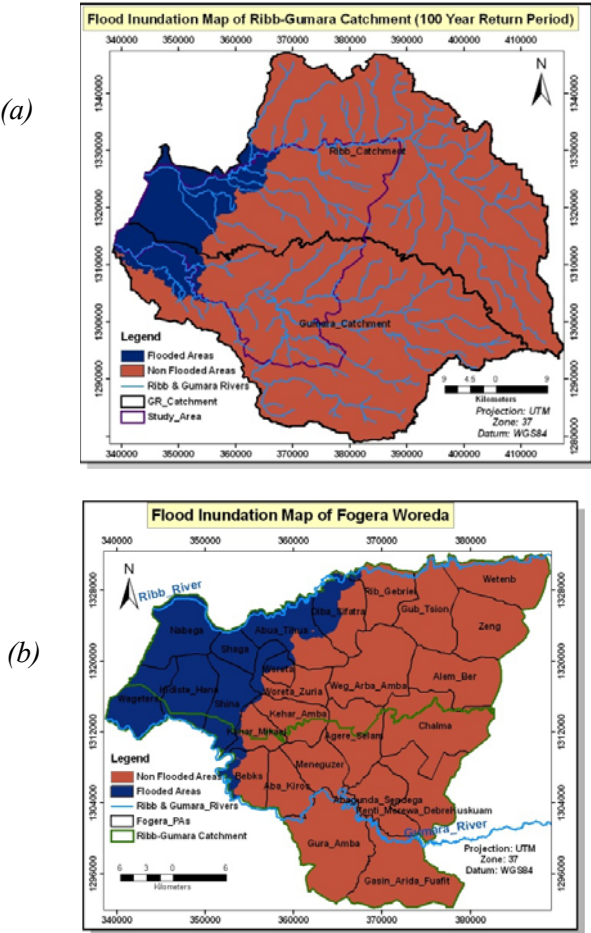
(a)

(b)

Figure 5. Flood Inundation Map of Ribb-Gumara Catchment (a) and Fogera Woreda (b) (100 Year Return Period)

For a 100 year return period flood which gage level was calculated as 8.582 m (Gumara) and 8.850 m (Ribb), the total area of the

catchment inundated by the flood will be 352 square kilometers. This area is about 12% of the total catchment area, and that of Fogera Woreda is 256 square kilometers (23% of the Woreda). As the above maps show, almost all the area likely to be inundated by a 100 year return period flood fall in Fogera Woreda. Important to mention here is that the identified areas likely to be flooded by the flood frequency analysis fall in the high and very high hazard areas identified by the overlay analysis of the flood hazard assessment. Thus, the result from the frequency analysis soundly agreed with that of the overlay analysis.

The areal comparison above shows that about three-fourth of the inundated area of the catchment (72.7%) fall in Fogera Woreda while this Woreda is only one-third of the catchment.

With regard to landuse classes, with the above mentioned return period flood, 99.8% swamps, 94.0 grass lands, 30.6% shrub land, and 13.9% agricultural lands were found likely to be inundated. 100% of Wagtera, Kidiste Hana, Nabega, Shaga, and Shina and 64.7% of Abua Tihua are likely to be flooded. Most parts of these PAs were actually inundated by the last year (2006) flood and the people were displaced from their residence. Moreover, agricultural crops including grazing lands of the pastoralist people of these areas were severely damaged by the 2006 flood. As explained before, these areas have been affected by flood almost every year and therefore traditionally identified as flood prone areas.

The return period T of major flood is the expected value of recurrence interval (τ), $E(\tau)$, its average value measured over a very large number of occurrences. For the Ribb-Gumara Rivers data, there are six recurrence intervals covering a total period of ten years between the first and last occurrences of major flooding, so the return period of major flooding of the Ribb-Gumara rivers is approximately $\tau_{av}=10/6=1.67$ years (Table 4). Thus the return period of an event of a given magnitude may be defined as the average recurrence interval between events equaling or exceeding a specified magnitude (Chow et al., 1988). As discussed in the previous chapter, in Fogera Woreda major flood peaks occurred in 1996, 1998, 1999, 2000, 2001, 2003 and 2006.

Table 4. Years of Major Floods with their
Corresponding Recurrence Intervals

Major flood year	1996	1998	1999	2001	2003	2006	Average
Recurrence Interval (years)	2	1	1	1	2	3	1.67

Therefore, from the flood frequency analysis, the calculated two year return period gauge level is expected in Ribb-Gumara catchment in general and Fogera Woreda in particular. That is, 6.806 m and 5.90 m gauge levels are expected approximately in every two year in Ribb and Gumara Catchment respectively. In other words, these gauge levels have a 60% probability of occurrence in every year in the two respective rivers.

Dynamics in Landuse/Landcover Types

Changes in land cover driven by land use can be categorized into two types: modification and conversion. Modification is a change of condition within a cover type; for example, unmanaged forest modified to a forest managed by selective cutting. Conversion is a change from one cover type to another, such as deforestation to create cropland or pasture.

The most important change from 1973 to 1985 was observed in the clearance of wood land for agricultural lands, and that of the 1985 to 1999 was observed in the expansion of swamps and agricultural lands at the expense of grass lands (Table 5 and Figure 6). Even bare lands were changed in to agricultural lands. The reason of areal increment of grass land from 1973 to 1985 was that the 1973 MSS image was taken in February 01 (dry season) while that of the 1985 TM image was taken in October 09 (just after the rainy season). Decrement in wood, grass, and shrub and reed lands was observed from 1973 to 1999 while there is increment in agricultural land and plantation forest.   Note that, most plantation forests during the field survey (May 2007) were cleared for additional agricultural lands and for firewood and construction. These have impacts on the past flooding hazards by decreasing surface roughness which retards the peak flow down stream. Table 5 shows areal extent of the different landuse/cover classes in three different periods, (1973, 1985 and 1999). It also incorporates the change of the Landuses/covers between the given years and their percent change.

Table 5. Landuse/cover changes in Ribb-Gumara Catchment Between 1973 to 1985, 1973 to 1999, and 1985 to 1999.

| LULC Type	Area Coverage (Sq. Km)			Change					
				1973 & 1985		1985 & 1999		1973 &1999	
				Sq. Km	%	Sq. Km	%	Sq. Km	%
	1973	1985	1999						
Agriculture	2205.6	2229.7	2855.8	24.1	1.1	626.1	28.1	650.2	29.5
Shrub	292.2	271.8	239.2	-20.4	-7	-32.6	-12	-53	-18.1
Plantation	0	47.3	160.1	47.3		112.8	238.5	160.1	
Swamp	0	4.3	30.4	4.3		26.1	607	30.4	
Grass	349	699.4	24.9	350.4	100.4	-674.5	-96.4	-324.1	-92.9
Wood	464.5	11.9	7.4	-452.6	-97.4	-4.5	-37.8	-457.1	-98.4
Bare	16.9	59.3	6	42.4	250.9	-53.3	-89.9	-10.9	-64.5
Total	**3320.2**	**3320.2**	**3320.2**						
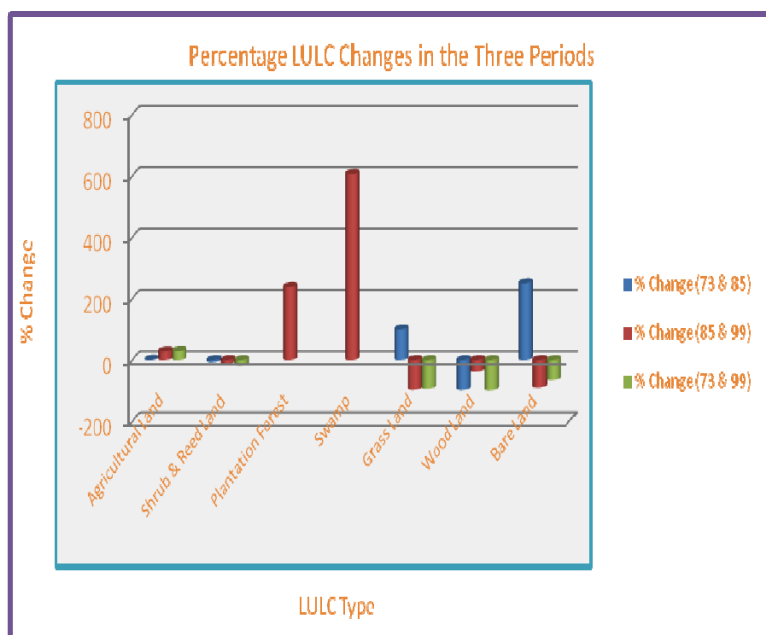
Figure 6. LULC Percentage Changes between the Periods 1973 & 1985, 1985 & 1999, and 1973 & 1999.

Landuse/cover Change and Flood Hazard and Risk

The land covers (shrub land, wood land, grass land) of the upland sites and the flood plain area have been decreased. Therefore, there is high soil erosion in the upstream and sediments and dissolved substances cumulatively called river load deposited in the river channels and on adjacent flood plains in down stream of the major rivers.

According to Shiferaw and Wondafrash, sediments deposited in Ribb and Gumara rivers have changed the rivers gradient, cross-sectional area, average velocity of water flow and discharge of rivers. Therefore, overflow of rivers occurred and flooded the local communities. The cross sectional area of Gumara and Rib rivers have been decreasing from time to time as a result of sediment deposition. In some areas the depth of Rib River diminished from 35 meter to 11 meter. Deep rooted and tall grasses that had been grown along river banks have been buried by soil sediments, which are transported by rivers. Some agricultural land crops have been buried by the deposited sediments. Overall, the river channels depth and width decreased and the water discharging capacity of the major rivers (Gumara and Rib) and their tributaries minimized in which it leads to overflow of water and flooding consecutively. All this indicates that the rate of erosion and soil loss in the upstream is high due to lack of flood water abstraction.

The long year daily maximum rainfall trend (Figure 7 (a)) shows that there is a slight decrease in daily maximum rainfall from 1974 to 2006. There were high daily maximum rainfall peaks in the middle of 1970s and around 1990 even though the severe flood in Ribb-Gumara Catchment occurred last summer (2006 Ethiopian main rainy season). Here, one can judge that the resent floods in the catchment in general and Fogera Woreda in particular were not caused mainly from rainfall.
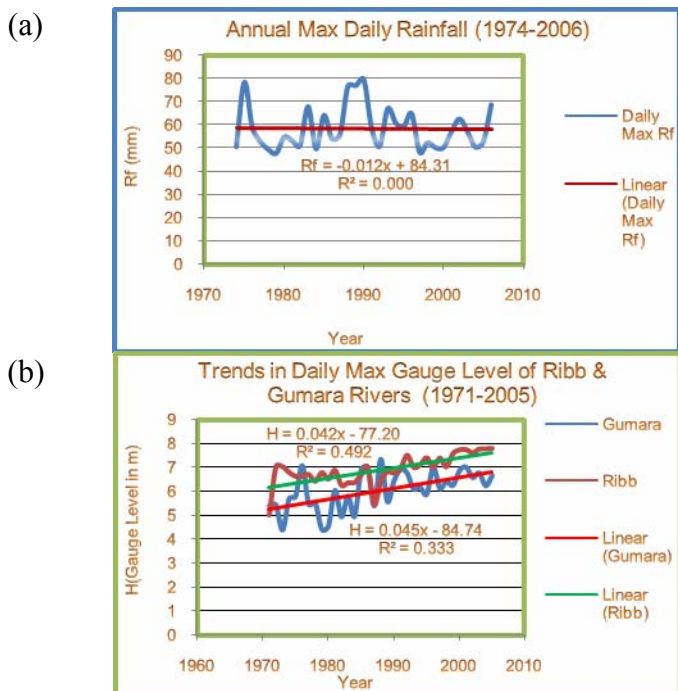
Figure 7. Trends in (a) Annual Maximum Daily Rainfall (1974-2006) from Ten Meteorological Stations in & around Ribb-Gumara Catchment, and (b) Annual Maximum Gauge Levels (1971-2005) of Gumara and Rib Rivers

As discussed in the previous section, overflow of Ribb and Gumara rivers causes flooding in Ribb-Gumara catchment. Vast areas that lie below the point where there is a sharp decline in slope (2200 m) are prone to flooding in the main rainy season. Almost all such areas are found in the so called Fogera Plain   just adjacent to Lake Tana where the two rivers empty their water.

According to Fogera Woreda disaster prevention and preparedness office (FWODPP) flooding in the Woreda has a short history. Flooding, which is the first in its kind in the area occurred some ten years ago, in 1996. The flooding of that year affected eight PAs of the Woreda, namely, Wagtera, Nabega, Kidiste Hana, Shaga, Shina, Woreta Zuria, Kuhar Michael, and Abatihua. From this year onwards, flooding has a regular incidence in some areas especially those PAs adjacent to Lake Tana. Such frequency of the flooding is related to high

gauge levels of the two rivers (Figure 7 (b)). Analysis of gauge level data of more than thirty years shows a general increase in daily maximum gauge level. As indicated on Figure 7 (b), daily maximum gauge level of Ribb and Gumara rivers were increasing at a rate of 0.042 and 0.045 per annum respectively. A relatively higher rate of increase in the daily maximum gauge level is observed in the 1990s and onwards. The 2006 flood was the most severe of all the flood events experienced in the area so far. During this time (1990s and onwards) flood incidence was very high as discussed previously. Therefore, the patterns of gauge level in the catchment reflect the contributions of changes in the physical characteristics particularly landuse/landcover changes which is discussed previously. This can be evident from the comparison of trends in the rainfall and gauge level in the catchment. While rainfall was relatively high in the middle of the 1970s and around 1990 (Figure 7 (a)), gauge level was not that much high compared to that of the middle of the 1990s and onwards. This implies that small proportion of the rainfall turns in to runoff thereby increasing the gauge level which can possibly held by some abstractions such as vegetation and infiltration in to the ground water table.

CONCLUSION

The basic idea of flood hazard and risk assessment and mapping as undertaken in this study is to regulate landuse and population distribution by flood plain zoning in order to restrict the damages. In the light of above discussion, it can be said that flood risk mapping, being an important non-structural flood management technique, will go long way in reducing flood damages in areas frequented by flood.

Pair wise comparison method of flood hazard map generation is a good approach to deduce a sound decision for a forthcoming flood disaster, provided the required data are standardized to a common scale in personal geodatabase. This study confirmed that the method used was capable to integrate all the flood hazard causative factors and the components of flood risk as well in a GIS environment. In this fashion, composite maps were generated to assess flood risk of Fogera Woreda. One of the Multi Criteria Evaluation techniques known as Weighted Overlay in GIS environment was shown to be useful for delineating areas at different rating in terms of flood hazard and flood risk. Moreover, factor weight computation in Weight module, that is developed by providing a series of pair wise comparisons of the relative importance of

factors to the suitability of pixels for the activity being evaluated, has generated valuable information. This could be useful for disaster studies in the future. Therefore, it has been shown that MCE–GIS based model combination has potentiality to provide rational and non-biased approach in making decisions in disaster studies.

Satellite images were shown to be very important for Landuse/Landcover change studies with certain limitations like cloud cover and striping. The change statistics of landuse/landcover of Ribb-Gumara Catchment showed that clearance of landcover for agricultural expansion has been aggravating flood hazard in the downstream areas of Ribb and Gumara Rivers, Fogera Woreda.

Flood frequency analysis of peak hydrological data yielded the return periods of each major peak discharges and the magnitude and probability of occurrence of flood peaks of specified return periods so as to help preparedness to cope with such peaks. Flood frequency analysis combined with GIS was found very important to map the likely inundated areas of a given catchment. In this study, the likely inundated areas mapped using the 100 year return period base flood and DEM, and the flood hazard map obtained from the overlay analysis of flood causative factors in the study area soundly agree to each other. And therefore, the combination of the two results would be a step forward for flood management and mitigation strategies.

Although flooding is a natural phenomenon, we can not completely stop it; we can minimize its adverse effects by better planning. The study has shown that automatic flood map delineation can be produced for big river system in short time with the support of GIS and Remote Sensing.

and Rural Development, and all the staffs for their unforgettable cooperation in my field- and post-field work.

REFERENCES

Alexander, D. (1993) Natural Disasters. London, UCL Press Limited.

Aronoff, 1995 Geographic Information Systems: A Management Perspective; WDL Publications; Ottawa, Canada.

Congalton, R.G. and K. Green (1999) Assessing the Accuracy of Remotely Sensed Data: Principles and Practices. Boca Raton FL: Lewis   Publishers.

DPPC, (1978) Flood Risk and Vulnerability in Different Regions of Ethiopia, Draft for Discussion; Addis Ababa, Unpublished.

DPPC, (1996) Flood Risk Areas in Ethiopia; Addis Ababa, Unpublished.

DPPC, (1997) Worst Case Scenarios: Drought, Flood, Influx of refugees and Epidemics and the Present Response System; Vol. I-Summary, Addis Ababa, Ethiopia.

DPPA, (2006) Joint Government and Humanitarian Partners: Flash appeal for the 2006 flood disaster in Ethiopia. http://www.dppc.gov.et/downloadable/reports/appeal/2006/Flood%20Appeal%20II%20MASTER%20Final.pdf. Access Date: March, 2007.

Endaweke Assegid, (2007) Suitability Analysis of the Proposed Upland rice Production using GIS and Remote sensing in Fogera Woreda; Post Graduate Thesis, AAU, Addis Ababa

FAO, (2006) World Reference Base for Soil Resources: A Framework for International Classification, Correlation and Communication, Rome; http://www.fao.org/docrep/W8594E/W8594E00.htm. Access Date: May, 2007.

FWOARD, (2006) Short Description of the 2006 summer flood in Fogera Woreda

J. Ronald Eastman (2001) IDRISI Guide to GIS and Image Processing, Volume 2, www.gyml.unibas.ch/go/17/pdf2/Guide2, on January 2007; Clark University Version 32.20. Version 32.20. Clark University.

Kefyalew Achameyeleh (2003) Integrated Flood Management: Case Study in ETHIOPIA: Integrated flood management, WMO and Global Water Partnership, Editor: Technical unit; Unpublished.

Keith Smith & Roy Ward, (1998) Floods: Physical Processes and Human Impacts; England

Ken Granger, 2002. Community Risk Assessment in Mackay: A Multi-
        Hazard Risk Assessment,
        http://www.ga.gov.au/image_cache/GA4177.pdf . Access Date:
        April, 2007.
Leica Geosystem, (2000) ERDAS Field Guide^{TM}; Sixth Edition, Atlanta
        Georgia.
Lillesand, M. Thomas and W. Ralph Kiefer (2004) Remote Sensing and
        image Interpretation: 5th ed. John Wiley & Sons, Inc.
Malczewski, J. (1999) *GIS and Multicriteria Decision Analysis*, John
        Wiley and Sons, New York, NY.
Manuela da Gloria Muianga, (2004) Flood Hazard Assessment and
        Zonation in the Lower Limpopo,
        Mozambique; ITC Dissertation, Netherlands;
        http://www.itc.nl/library/Papers_2004/msc/wrem/da_gloria_mui
        anga.pdf . Accessed on March, 2007.
Nangendo, G. (2005) Changing Forest-Woodland-Savanna Mosaics in
        Uganda: With Implication for Conservation. Wageningen,
        Wageningen University, 2005. ITC Dissertation 123,
        Netherlands.
P. Sarma, (2006) Flood Risk Zone Mapping of Dikrong Sub Basin in
        Assam;GISdevelopment, A.E.E, Brahmaputra Board, Assam, In
        dia;http://www.gisdevelopment.net/application/natural_hazards/f
        loods/nhcy0006.htm. Accessed on February 2007
R.Suresh, (2005) Watershed Hydrology: Principles of Hydrology; Lomus
        Offset Press, Delhi
Shiferaw and Wondafrash, 2006 Causes and Effects of Flooding in the
        Amhara National Regional State: A Case Study in Fogera
        Woreda, Addis Ababa, unpublished
Shook, G. (1997) An assessment of disaster risk and its management in
        Thailand.
Sluiter, R. (2005) Mediterranean land cover change: Modeling and
        monitoring natural vegetation using GIS and remote sensing.
        PhD Thesis, Universiteit Utrecht, the Netherlands
UNEP (2002) Africa Environmental Outlook: Past, Present and Future
        Perspective. Nairobi, United Nations Environmental Program.
UNOCHA, (2006) Flood Affected Woredas in Ethiopia,
        http://www.ochaeth.org/Home/downloadables/FD_0014_Recent
        Flood_WWW.pdf. Accessed on March, 2007.
Ven Te Chow et.al, (1988) Applied Hydrology; McGraw-HILL
        International Edition, Civil Engineering Series, Singapore.

TECHNICAL AND INSTITUTIONAL EVALUATION OF GERAY IRRIGATION SCHEME IN WEST GOJJAM ZONE, AMHARA REGION

Gashaye Checkol and Tena Alamirew
Haramaya University, P. O. Box 138, Dire Dawa, Ethiopia.
Email: alamirew2004@yahoo.com

ABSTRACT

The technical and institutional performance evaluation of Geray Irrigation Scheme was made in order to identify management practices that should be implemented to improve the system operation and the general health of the irrigation system. The technical evaluation was made by looking into the selected performance indicators such as conveyance efficiency, application efficiency, water delivery performance, and maintenance indicators. Moreover, availability of institutional and support services were also investigated through a questionnaire administered to beneficiary farmers and other stakeholders.

The results obtained showed that the main and tertiary canal conveyance efficiencies were 92 and 82 percent, respectively. Many of the secondary and tertiary canals are poorly maintained and many of the structures are dysfunctional. Application efficiency monitored on three farmer's plots located at different ends of a given secondary canal ranges from 44 to 57 percent.

Water delivery performance was only 71 percent showing a very substantial reduction from the design of the canal capacity. Maintenance indicator evaluated in terms of water level change (31.9%) and effectiveness of the infrastructures shows that the scheme management was in a very poor shape. Dependability of the scheme evaluated in terms of duration and irrigation interval shows that the scheme is performing below the intended level.

The 47 percent of the land initially planned is currently under irrigation while there was no change in the water supply indicating that the sustainability of the scheme is in doubt. The scheme was managed by four year old WUA despite the fact that it was commissioned 27 years ago. The overall rating of the WUA in terms of managing the scheme was very poor.

Support services rendered to the beneficiaries were minimal. There were very few indicators that production was market oriented. Ironically, farmers didn't recognize market as their problem. Conflict resolution has been the duty of the *Kebele* Council, and WUA has no legal authority to enforce its bylaws.

In conclusion, the overall technical adequacy of the scheme is rated as very poor requiring tremendous mobilization of community to sustainably manage it. Proper institutional setup need to be in place and WUA need to be empowered more in order to enforce its bylaws.

THE BLUE NILE PUB:
KNOWLEDGE GAPS IN THE BLUE NILE HYDROLOGY

Y. A. Mohamed[1,2] , T.S. Steenhuis[3]; S. Uhlenbrook[2,4]

[1]IWMI NBEA, P.O.Box 5689, Addis Ababa, Ethiopia.
[2]UNESCO-IHE, P.O. Box 3015, 2601 DA Delft, The Netherlands
[3]Department of Biological and Environmental Engineering, Riley Robb Hall Cornell University Ithaca NY 14853, USA
[4]Delft University of Technology, Stevinweg 1, 2628 CN Delft, The Netherlands

EXTENDED ABSTRACT

The Abbay/Blue Nile Basin with a catchment of 330,000 km^2 at the White Nile confluence, has an average flow of 50 km^3 per year, constituting approximately 60% of the total Nile flow. The river water originates from the Ethiopian Plateau, and travels a distance of 1500 km from Lake Tana up to the confluence with the White Nile at Khartoum. Rainfall varies from above 1200 mm/year over the Ethiopian Plateau to less than 200 mm/year on the downstream end at the confluence. The Blue Nile basin is characterized by rugged topography on the upper parts, and flat plains downstream the Ethiopian Sudan border.

Intensive rainfed agriculture is practiced over the upper parts on the Plateau, while large irrigation and hydropower dams have been built on the Blue Nile and Main Nile downstream of the Ethiopian Sudan border (e.g., Gezira Scheme, Roseires dam, etc.). However, ambitious development plans for dams exist in Ethiopia (e.g., Tana Beles Scheme, Karadobi dam, etc.), but none has been built on the Abbay/Blue Nile yet. The large temporal and spatial variability of rainfall (and thus discharges), poses significant challenges towards optimum utilization of the Blue Nile basin resources. Droughts and floods are interchangeably hit the production systems of the vulnerable communities living in the basin.

The identification of research questions pertinent to the Blue Nile hydrology and water resources is part of ongoing efforts of the Blue Nile PUB committee (Prediction in Ungauged Basins) with the task to characterize the hydrology of the Blue Nile. The PUB committee has been established recently (June 2007) and is hosted by the International

Water Management Institute Sub-Regional Office in Addis Ababa. The committee is specifically interested in predicting the seasonal and long term variability in discharge and associated constituents (sediments, nutrients, etc) in un-gauged catchments in the upper parts of the basin where hydrological data are extremely scarce.

In addition the PUB group is concerned about the implications of natural and anthropogenic land use changes on water and sediment fluxes at different spatio-temporal scales. To characterize main land-atmosphere feedbacks for better understanding of the regional water cycle and to assess the implications on water and sediment yields is also targeted by the PUB group.

Water uses and demands by different systems (rainfed, irrigation, hydropower, environment, etc.) are not accurately identified in the Blue Nile basin. The upstream downstream interdependencies at catchment as well as at basin levels are not clearly understood. These pose additional challenges for optimal water resources management at different spatial scales from watershed up to sub-basin and basin levels.

In the presentation we will address the ongoing work on identification of the hydrology of the Abbay/Blue Nile. Specifically we will address innovative methods for data generation (remote sensing, isotopes, data assimilation, etc) to fill in the data/knowledge gaps and to review existing and new methods and models to predict the hydrology and sediment fluxes in ungauged watersheds. We will give a review of the recent and ongoing research on climate variability and climate change and the impact on hydroclimatology. Key research questions and knowledge gaps will be assessed. Similarly, we will review research work on land use changes and main challenges in this field.

The current research efforts in the Abbay/Blue Nile in which the authors are involved will be summarized briefly (i.e. integrated research project, hydrological modeling studies). The presentation will conclude discussing optimal paths to implement hydrological studies in the Blue Nile Basin to validate the existing models.

Key Words: Blue Nile; PUB; hydrology; research questions

POTENTIAL AND RELIABILITY OF SMALL HYDROPOWER IN THE NILE BASIN

Kwabena Asante, Gabriel Senay, Eugene Fosnight, Guleid Artan and Hussein Gadain

SAIC/USGS Center for Earth Resources Observation and Science, Sioux Fall, SD 57198

ABSTRACT

The Nile River is a potentially significant source of renewable energy in the form of hydropower. Several countries in the basin have initiated efforts to develop this resource through the construction of hydropower dams. Small hydropower plants with minimal capabilities to store water are generally less harmful to the environmental than larger plants. However, smaller plants are also less reliable since they are more susceptible to climatic variability and associated impacts on river flow. In this paper, an assessment of small hydropower potential in the Nile basin is carried out. Daily streamflow on each river reach is computed over a 10 year period from 1998 to 2007 using a geospatial hydrologic model. The potential head along each river reach is also computed using high resolution elevation data from the Shuttle Radar Topography Mission (SRTM). By combining the flows and head, hydropower potential is computed for a specified length of penstock running over the land surface. A power generation reliability analysis is conducted over the 10 year period for different scenarios of installed plant capacities. The results of the analysis are expressed in terms of estimates of the optimal run-of-river hydropower plant capacity that could be adopted for river reach if it a specified reliability of power generation. The results are also aggregated to show the small hydropower potential by administrative units.

Key Words: Nile, streamflow, hydroelectric, SRTM, geospatial hydrological model